

# ANALYSIS OF HYDROLOGICAL IMPACTS DUE TO SEDIMENTATION VARIABILITY ON ALLUVIAL STREAM- AQUIFER SYSTEMS

By

Beason M. L. Mwaka

B.Sc., M.Sc.

NEWCASTLE UNIVERSITY LIBRARY

-----  
094 51527 3  
-----

Thesis L5395  
-----

A thesis submitted to the Department of Civil Engineering  
of the University of Newcastle Upon Tyne,  
in the candidacy for the degree of  
Doctor of Philosophy.

December, 1994

"We could feed every one with existing technology, if we go on mining the soil and water. But when we run out of those, we will not be able to feed anyone"

*(Klaus Lampe, in Mackenzie, 1994)*

## ABSTRACT

Alluvial streams re-shape their own geometry in response to changes imposed by nature or by humanity. Such adjustments may induce landscape and water surface elevations that are not compatible with the natural environment or existing activities. Therefore, for the purpose of planning, design and management, it is necessary to evaluate the variation of the levels, their effect on water and sediment movement and their general impacts to project developments. Both fieldwork and modelling techniques have been developed for assessing the hydrological impacts of such changes.

In-stream sand quarry pits on alluvial rivers provide classic examples where streambed elevations are significantly affected by sedimentation changes, which occur concurrently with variation of water surface elevations. The hydrological impacts of a sand mining location on the River Kibos in Kenya are demonstrated by the aid of a simple improvised technique based on rating curve analysis, showing, for example, that due to sand mining the river bed and the corresponding low flow levels fell by about 0.8 m between 1977 and 1982.

Noting the desire to make such assessments in advance so as to avoid the repair costs, a modelling procedure has been developed to enable a priori assessments. The dynamic equations describing the one-dimensional open-channel water and sediment flows, and the equation for the two-dimensional transient groundwater flow are solved simultaneously, and linked through a time-dependent interface boundary layer between the alluvial stream-aquifer systems. Considering the scarcity and uncertainty of data sets in this subject, the model has been applied to conceptual hydrologic systems to delineate interrelationships among individual hydrologic components as well as to determine the degree of influence of various parameters on the system behaviour

Results by numerical experiments have suggested that baseflow recession curves for aggrading channels deviate steeply from the theoretical logarithmic recession curve as the river becomes more and more influent, while in a degrading reach the baseflow recession curves flatten, deviating from the theoretical recession curve as the river becomes more and more effluent. The hydrologic and fluvial impacts of in-stream sand borrow pit schemes have also been analysed. On the basis of some set-up options, the model allows for realistic predictions of changes to the water and sediment yields, and for the final selection of quarry schemes with least negative impact on the environment.

## ACKNOWLEDGEMENTS

I wish to express my gratitude to my main supervisor, Professor P. E. O'Connell and my second supervisor, Dr. C. Nalluri of the Department of Civil Engineering at the University of Newcastle, who supervised this work throughout the study period. Their valuable comments and counselling during the preparation of this thesis is greatly appreciated. I am also indebted to Dr. P. Younger for helpful suggestions of specific literature which contributed considerably to this work. Much thanks are also extended to Dr. A. Purnama who contributed significantly through critical but encouraging comments during the early stages of this study, and to Prof. P. Misiko of Egerton University, who helped a great deal during the organisation of fieldwork in Kenya. Discussions with the following at various stages of the study have also been helpful: Dr. S. White and Dr. M. Onanda at the University of Newcastle, Mr. A. Kola, the Provincial geologist in Nyanza province of Kenya, and Mr. Openji, the officer in-charge of the Nyando Flood Protection Unit in Kenya.

This study program was funded by Rank Xerox through the British Council. The assistance by both is gratefully acknowledged. Egerton University supported the fieldwork expenses, and their assistance is also appreciated.

Lastly, I wish to express my appreciation to all of my family members, especially my wife Mary, and our children, Khayanje and Awinja, for their patience during my absence from home at a tender stage of our family life.



# **TABLE OF CONTENTS.**

<b>1. INTRODUCTION</b>	<b>1</b>
1.1 Prelude	1
1.2 Objectives and Scope	3
<b>2. HYDROLOGY OF ALLUVIAL STREAM SYSTEMS</b>	<b>8</b>
2.1 A General Historical Overview.	8
2.2. Computational Hydrology on Alluvial River Systems	11
2.2.1 Background	11
2.2.2 Water and sediment routing in channels	19
2.2.3 Stream-aquifer interaction	22
2.2.4 The transient nature of the interface boundary between alluvial stream-aquifer systems	30
<b>3. FIELDWORK ASSESSMENTS OF THE EFFECTS OF STREAMBED ADJUSTMENTS ON THE RIVERS KIBOS AND NYANDO (KENYA)</b>	<b>40</b>
3.1 Introduction	40
3.2. The General Hydrogeology of the Nyando Basin	42
3.3 The Hydrological Impacts due to Sand Mining in River Kibos	48
3.3.1 Introduction	48
3.3.2 Assessment of the variation of bed elevations based on the theory of rating curve analysis	54
3.4 A Review of Flood Mitigation Alternatives on the Nyando	63
3.4.1 Introduction	63
3.4.2 Embankment and flood warning systems	65
3.4.3 Drainage and training	72
3.4.4 Storage reservoirs	75
3.4.5 Difficulties and conflicts in flood control projects	79

<b>4. ANALYSIS AND MODELLING OF ALLUVIAL STREAM-AQUIFER INTERACTION</b>	<b>84</b>
4.1 Introduction	84
4.2 Streamflow Routing	87
4.3 Riverbed Sedimentation	99
4.3.1 Introduction	99
4.3.2 Residual transport capacity	100
4.3.3 The sediment mixing layer	104
4.3.4 Sediment routing	108
4.4 Groundwater Flow on Flood Plains	113
4.5 Linkage of Alluvial Stream-Aquifer Systems	116
<b>5 MODEL VERIFICATION, CALIBRATION AND APPLICATIONS</b>	<b>127</b>
5.1 Introduction.	127
5.2 Verification of the Model	128
5.2.1 Water routing in a trapezoidal irrigation canal	129
5.2.2 Water and sediment routing in hypothetical channels	131
5.2.3 Flood wave modifications due to stream-aquifer interaction	144
5.3 Model Calibration and Test of Predictive Uncertainty	147
5.3.1 Calibration	147
5.3.2 Test of predictive uncertainty	166
5.4 Application of the MASAI for Predictive Analysis of the Hydrological Responses Due to the Proposed Cut-Off Works on the River Nyando near the Ahero NIB Village	169
<b>6. CONCEPTUAL ANALYSIS OF THE EFFECTS OF SEDIMENTATION ON STREAMFLOW HYDROGRAPHS</b>	<b>176</b>
6.1 Introduction.	176
6.2 Effects of System Parameters on Baseflow Hydrographs	178

6.3	Effects of Sedimentation on Baseflow Hydrographs	186
6.3.1	Introduction	186
6.3.2	Simulation of the effects of sediment yield on baseflow hydrographs	187
6.3.3	Sensitivity analysis of Baseflow to sediment yield	192
6.4	Evaluation of Riverine Land Degradation and Conservation Applications	194
6.4.1	Introduction	194
6.4.2	Simulation of the effects of sediment yield on baseflow recession	196
6.4.3	Simulation of the hydrological and fluvial impacts due to in-stream sand mining schemes	205
6.4.4	Evaluation of the impacts of weir controls in Soil and water conservation practices	219
7.	<b>DISCUSSION, CONCLUSIONS AND SUGGESTIONS FOR FURTHER RESEARCH</b>	<b>223</b>
7.1	Discussion	223
7.2	Conclusions	228
7.3	Suggestions for Further Research	230
 <b>APPENDICES</b>		
Appendix 1	A1. SOLUTION OF THE NON-LINEAR ALGEBRAIC EQUATIONS BY NEWTON'S ITERATIVE METHOD	232
Appendix 2	A2. SOLUTION OF THE SYSTEM OF EQUATIONS DERIVED FROM THE FULLY IMPLICIT SCHEME BY FREAD'S (1971) TECHNIQUE	239
Appendix 3	A3. SEDIMENT TRANSPORT CALCULATION BY THE ACKERS-WHITE PROCEDURE	245
Appendix 4	A4. AN ECOLOGICAL VALUATION METHOD FOR CHANNEL SYSTEMS WITH IN-STREAM SAND MINING ACTIVITIES	247

	A4.1 Ecological Valuation on the Kibos	247
	14.2 Generalisation of the Valuation Method	252
Appendix 5	A5. AN EXAMPLE OF THE COMPUTER PROGRAM FOR THE MASAI	256
	<b>REFERENCES</b>	<b>258</b>

## LIST OF FIGURES

Figure 2.1	Channel aggradation of two sections on River Thiba, upstream of the Kamburu dam (Kenya)	36
Figure 2.2	Channel degradation on the Warujayeng-Kertosono canal (Indonesia)	37
Figure 3.1	Map of Kenya showing the location of the Nyando Basin	43
Figure 3.2	The Nyando Basin showing the main rivers, gauging stations and proposed dam sites	45
Figure 3.3a	Sand harvesting near Kibos bridge.	49
Figure 3.3b	Bare ground with arid-looking conditions around Kibos bridge	49
Figure 3.4	Particle size distribution of sediment materials obtained from the River Kibos at Nyamasaria.	51
Figure 3.5	Cross-sectional bed elevation profiles of the River Kibos at Nyamasaria	51
Figure 3.6a	Downstream section reach viewed from Nyamasaria bridge, showing dredged river bed material deposited on the banks.	52
Figure 3.6b	Upstream section reach viewed from Nyamasaria bridge, showing the rich riparian vegetation cover	52
Figure 3.7	The rating curves at the gauging station 1HA16 (Kibos bridge) showing the falling trend of the "effective zero" flow level	56
Figure 3.8a	Downstream section reach viewed from Kibos bridge, showing degraded riparian land.	58
Figure 3.8b	Upstream section reach viewed from Kibos bridge, showing land slide problems on the river banks.	58
Figure 3.9a	Cows being guided into River Kibos for water	61
Figure 3.9b	Degraded riverine land near Kibos bridge, showing goats negotiating into the river.	61
Figure 3.10a	Discharge measurement on the River Nyando, on the, upstream side of the Ahero bridge.	66



Figure 3.10b	Downstream section reach of the Nyando viewed from the Ahero bridge, showing the proximity of the flood plain to flooding	66
Figure 3.11	Annual maximum flood discharges at the gauging station 1GD3 near Ahero on the River Nyando	69
Figure 3.12	Variation of the water levels in the bore hole at the Ahero Catholic Mission and in the River Nyando at Ahero bridge	73
Figure 3.13	Daily discharge hydrographs at the gauging station 1GD3 and at Ahero bridge on the River Nyando	74
Figure 3.14	Variation of flood discharge contribution from the Nyando and Ainobngetuny Basins	77
Figure 4.1	A sketch for the definition of the weighting factors	91
Figure 4.2	Line mesh on the (x,t) plane for describing the implicit method	92
Figure 4.3	Network for describing the sediment routing implicit method	110
Figure 4.4	A typical relationship between flow from aquifers to rivers, and groundwater potential	117
Figure 4.5	Grain size versus depth for alluvial sediments of the Missouri, Arkansas and Mississippi River Valleys	117
Figure 4.6	Hydraulic conductivity versus mean grain size of alluvial sediments for the Missouri and Arkansas Rivers	119
Figure 4.7	A general pattern of hydraulic conductivity increase with depth for the Rivers Missouri and Arkansas sediment data	119
Figure 4.8	A schematic sketch of a groundwater recharging river	122
Figure 4.9	Flow chart showing the major steps of computation of the Model for Alluvial Stream Aquifer Interaction (MASAI)	125
Figure 5.1a	Comparison results of water routing in a canal at a distance 475 m from the upstream section	130
Figure 5.1b	Comparison results of water routing in a canal at a distance 1575 m from the upstream section	130
Figure 5.2	Bed elevation profiles upstream of a dam, after 30 minute of sediment laden flow through the reservoir	134
Figure 5.3a	Variation of water flow depth with time and distance, in a unit-width channel	138

Figure 5.3b	Degradation of the bed of a channel when upstream sediment input is zero	138
Figure 5.4a	Computed downstream rating curve using the Alam and Kennedy (1969) method	141
Figure 5.4b	Computed Manning's n using the Alam and Kennedy (1969) method	141
Figure 5.4c	Simulated results of river bed degradation below a structure, using the Ackers-White (1973) bed material load and Lee and Odgaard (1986) size loading functions	142
Figure 5.4d	Change in bed material size distribution caused by the degradation	142
Figure 5.5a	Flood wave attenuation at a distance 15240 m from the upstream boundary for a stream with and without leakage into the aquifer	146
Figure 5.5b	Flood wave attenuation at a distance 42672 m from the upstream boundary for a stream with and without leakage into the aquifer	146
Figure 5.6	The stage-discharge relationship at the Ahero road bridge on the Nyando River	152
Figure 5.7	Sediment particle size distribution at the gauging station 1GD3 and Ahero bridge on the River Nyando	152
Figure 5.8	Comparison of computed and measured bed material load	159
Figure 5.9	Simulated and observed discharge hydrographs on the River Nyando, at the Ahero road bridge	164
Figure 5.10	Observed and simulated streamflow discharges at the Ahero road bridge	168
Figure 5.11	Predicted discharge and flow depth hydrographs, before and after training alterations on the Nyando River near the NIB village	173
Figure 5.12	Predicted sediment yield distribution, before and after training alterations on the Nyando River near the NIB village	173
Figure 6.1	A plot of the flood wave hydrograph used in the modelling	181
Figure 6.2a	Baseflow hydrographs at the downstream station for varied hydraulic conductivity of the aquifer	182
Figure 6.2b	Baseflow hydrographs at the downstream station for varied specific yield of the aquifer	183

Figure 6.2c	Baseflow hydrographs at the downstream station for varied hydraulic conductivity of the river bed	184
Figure 6.3a	Baseflow hydrographs at the downstream station for varied concentration of input sediments	189
Figure 6.3b	Baseflow hydrographs at the downstream station for varied particle size distribution of input sediments	190
Figure 6.4a	Baseflow recession curves resulting from variation of the hydraulic conductivity of the river bed	198
Figure 6.4b	Baseflow recession curves resulting from variation of the input sediment load	199
Figure 6.5	Predictions of bed and water surface elevations after a flood has passed through a quarry pit	209
Figure 6.6a	Cumulative sediment yield of 1 week, along a reach with quarries of varied length	212
Figure 6.6b	Water yield after 1 week from bank storage in a reach with quarries of varied length	212
Figure 6.7a	Cumulative sediment yield of 1 week, in a reach with quarries of varied depth	215
Figure 6.7b	Water yield after 1 week from bank storage in a reach with quarries of varied depth	215
Figure 6.8a	Cumulative sediment yield of 1 week, in a reach with varied number of quarries	217
Figure 6.8b	Water yield of 1 week from bank storage in a reach with varied number of quarries	217
Figure 6.9a	Sediment yield of 1 week, in a reach of varied downstream control levels	221
Figure 6.9b	Water yield of 1 week from bank storage in a reach of varied downstream controls levels.	221
Figure A4.1	Relative ecological valuation for five section reaches on the River Kibos	251
Figure A4.2	Conceptual ecological values of various flood flow levels	253
Figure A4.3	A conceptual distribution of ecological values against the average flood flow levels derived from Figure A4.2	253



## LIST OF TABLES

Table 2.1	Selected regime equations for straight sand-bed streams or canals	13
Table 2.2	Field cases exemplifying annual sediment deliveries in some major river systems	35
Table 3.1	Annual maximum discharges at the gauging station 1GD3 on River Nyando.	67
Table 5.1	Characteristics of the initial conditions for the channel in Chang and Richards (1971) model.	132
Table 5.2	Characteristics describing the initial conditions for the channel applied by Chen (1973)	136
Table 5.3	Sediment particle size distribution for the example of bed armouring	139
Table 5.4	Characteristics of the Nyando River channel near Ahero	149
Table 5.5	A form of current meter gauging records ( used during fieldwork on the Nyando River	151
Table 5.6	Observed hydraulic properties of River Nyando near Ahero.	154
Table 5.7	Sediment particle size analysis of a sample from the Nyando River near Ahero.	156
Table 5.8	Infiltration test results for the Nyando flood plains near Ahero.	163
Table 5.9	Computation of the statistical properties of observed and predicted discharges	166
Table 5.10	Statistical properties comparing the observed and predicted hydrographs	167
Table 5.11	Distance between sections of a reach on the Nyando, before and after cut-off works near the Ahero NIB village	171
Table 6.1	Results of sensitivity analysis of the model's baseflow output	193
Table A4.1	Attribution criteria for ecological valuation along River Kibos.	249
Table A4.2	Ecological valuation of 5 locations on a reach along the River Kibos	250

## LIST OF SYMBOLS AND ABBREVIATIONS

A	cross sectional area of water flow
$A_b$	cross sectional area of the channel which results from accumulated erosion or deposition
$\alpha$	gauge height for zero flow
b	width of channel
biotic	of or related to living organisms
BBC	British Broadcasting Corporation
BC	(period) Before Christ
$\beta$	slope of stage-discharge rating curve on semi logarithmic graph paper
C	discharge when the head $(h - \lambda) = 1$
$C_a$	an empirical constant relating hydraulic conductivity with depth for alluvial sediments
$c_i$	sediment load of a particular class interval i
$C_s$	coefficient relating the height of a sediment layer with the dune height
d	depth of the channel
$d_i$	particular size of sediment material of a particular class interval i
$D_{50}$	mean diameter of sediment material
ecotone	the zone between two major ecological communities
EMP	Environmental Management Program
Eq.	Equation
$\xi$	specific sediment seepage resistance
$f_{si}$	fraction of grains in a particular class interval i
F	depth-width ratio of a channel



$F_i$	notation for the water continuity function
Fig.	Figure
$g$	gravitational acceleration
$G_i$	notation for the water momentum conservation function
$h$	gauge height of the surface of water
$H$	depth of water flow
HEC	Hydrologic Engineering Centre (of the corps of engineers of USA)
$H_s$	dune height
$I$	vertical infiltration of water into the ground
JKCAT	Jomo Kenyatta College of Agriculture and Technology
$k$	a factor for velocity head loss of a flood
$k_1$	coefficient of hydraulic conductivity to thickness of a sediment layer
$k_2$	coefficient of hydraulic conductivity of thickness of aquifer material
$K$	geometric mean conveyance of a channel
$K_1$	hydraulic conductivity of a streambed's sediment layer
$K_2$	hydraulic conductivity of aquifer material
LBDA	Lake Basin Development Authority (of Kenya)
$m$	percent of silt clay in a channel
$m_i$	fraction of grains in a class interval $i$ in the mixing layer at the beginning of the time interval $\Delta t$
$m_i'$	fraction of grains in a class interval $i$ in the mixing layer at the end of the time interval $\Delta t$
$m$	saturated thickness of the aquifer
MASAI	Model for Alluvial Stream Aquifer Interaction
m.a.s.l	meters above sea level
MOWD	Ministry of Water Development (of Kenya)

NIB	National Irrigation Board (of Kenya)
$n$	Manning's roughness coefficient
$\Omega$	the remaining fraction of the transport capacity to transport additional sediment material
$\phi$	time weighting factor
$P$	wetted perimeter of the channel
$\rho_s$	Density of sediments fraction
$p_{si}$	fraction of grains in a particular class interval $i$ of parent bed material
$q$	lateral discharge per unit length
$q_s$	lateral inflow rate on sediment material per unit length
$Q$	water discharge flow rate
$Q_a$	mean annual discharge of a channel
$Q_b$	baseflow at a time $t$
$Q_o$	baseflow at the start of the time period
$\Delta Q_s$	weight of material eroded from the mixing layer
$Q_{fs}$	weight per unit width of the mixing layer
$R$	hydraulic radius
RGS	River Gauging Station
$S_c$	Storativity of aquifer
$S_g$	specific gravity of sediments
$S_y$	specific yield of aquifer
$S_o$	channel bed slope
$S_f$	energy gradient
$T$	water surface width

$T_i$	potential sediment transport capacity for a particular class interval $i$
$T_{ri}$	residual transport capacity for a particular class interval $i$
$T_B$	total potential bed material transport capacity per unit width
$T_s$	thickness of streambed mixing layer
$\tau$	bed shear stress
$\tau_{cr}$	critical bed shear stress
$u_l$	velocity component of lateral inflow
UNEP	United Nations Environmental Programme
$\omega$	space weighting factor
WRE	Water Resources Engineering
$x$	distance along the discharge centreline
$Z$	bed elevation
$Z_{b1}$	thickness of the streambed's sediment layer
$Z_{b2}$	distance between riverbed and reference point in the aquifer

## **1. INTRODUCTION**

### **1.1 Prelude**

Natural alluvial rivers normally involve the flow of soil and water, both of which are vital resources for maintaining life and nature. However, with time they are becoming more limited and strained because of the increasing and changing needs of humankind. And given that they are finite and already under intensive use, the need for their sustainable development has now become more routine and necessary than ever before.

To make use of the rivers, people have applied various river engineering works such as river training, water transfer, grade control, dredging, dam construction, etc. In upstream catchments, cultural practices as agricultural cultivation, livestock grazing, deforestation, urbanisation, etc. are also changing, thereby affecting the sediment yield and the amount of water flowing over and through the soil mass into the rivers. But unlike rigid channels, natural alluvial rivers are self-regulatory in that they adjust their characteristics in response to these development changes. Both river engineering works and varying sediment yield distort the natural quasi-equilibrium of the rivers, and in the process of restoring the equilibrium, either scouring or deposition or both, occur in the river channels. Many case histories of stream adjustments involving substantial aggradation and degradation changes can be found

in the literature (e.g. Schumm, 1968; Gregory, 1976; Garde and Ranga Raju, 1985; Chang, 1988a)

Brooks (1988), for example, has addressed most of the dramatic aspects of people's impact on river channels. He has discussed in detail some of the conventional river engineering works, their physical and biological impacts on rivers, and how the impacts have led to new or revised legislation intended to protect the environment. Walling (1983) has demonstrated the problem of sediment delivery in some major rivers, and how the channel elevation can be adjusted through aggradation or degradation. On the other hand, Petts and Foster (1992) have addressed the river systems in even wider perspectives. They have discussed how the catchment hydrology and fluvial systems interact and vary in space and time, and how they can be adjusted by developments within the catchment. In Calow and Petts (1994), detailed articles have been presented with regards to the sensitivity of river systems to environmental perturbations. They have also described the changes that have occurred within river ecosystems, and also elucidated the complex interactions between physical, chemical and biological components.

Therefore, the use of fundamental principles of river and sedimentation engineering is necessary in the analysis of new conditions of every river project, because the establishment of every river development project, in fact, means the beginning of another "war" with the river as it "fights" back towards its pseudo-equilibrium conditions. Although the domain of the river development works may be limited to the river channel, and the time scale is of interest to the project in question, the subsequent hydrologic behaviour is, nevertheless, affected by the fluid and fluvial system as a whole, thus entailing the geologic space and time scales. In other words, river development changes involve responses that are not only limited within the river's channel, but also the adjoining geologic formations.



With the advancements in water resources engineering, considerable efforts have been directed towards gaining a physical understanding of the various processes and components which comprise the hydrologic systems. This has led to an investigative approach of applied hydrology, which consists of the analysis of hydrologic systems for the purpose of establishing quantitative or graphical relationships for describing the behaviour of various components of the hydrologic cycle. This is because the increasing developments on alluvial river systems are greatly changing the behaviour of both surface and subsurface hydrology, like flood levels/frequencies, sediment transport/yield, groundwater recharging potential, etc., thereby necessitating a wide spectrum of planning, design and operation analyses. For example, the following quote by Brown (in Mackenzie, 1994) indicates the extent of human impacts to hydrological systems: "And the water level under India's vital Punjab wheat fields is sinking by a metre a year, according to the World Resources Institute in Washington DC. With runoff from the Himalayas feeding it, we thought that was the aquifer least at risk".

These analyses need basic understanding and ingenuity, not only of the development system in its given state, but also of the responsive behaviour of the system and of the processes connected with it. It is therefore with regards to these that this study is directed towards the development of techniques that will enhance the ability to understand and analyse the physical hydrologic behaviour resulting from sedimentation variation in alluvial stream-aquifer systems.

## **1.2 Objectives and Scope**

In-stream sand mining provides a good example of the conflicting humanity requirements from alluvial rivers. Besides the expected economic benefits, river sand mining also causes riverine land degradation because of its disturbances to the

natural river processes of sediment transport, streamflow, stream-aquifer water interchange, etc. What makes it even worse is that the time scales involved for the degradation effects to be noticed are very large, compared to the time taken for the economic benefits to be realised from the same practice. This obscures the need to reflect upon the extent to which the mining activities disrupt nature and its surroundings, especially in the eyes of the benefits being accrued from the same. However, it has been perceived that provision of simple illustrations based on practical field cases can aid in the understanding and increase awareness about the destructive tendencies. When such destructive practices and/or corrective interventions are derived from local historical cases and targeted for the local communities, they can be more perceptible to the people and therefore supportive of the need for change of habits and cultural practices towards those that are suitable for sustainable usage of the rivers.

However, before changing and adapting a new practice, or impose a new system on a river, it is advisable that the hydrological responses to the new morphological conditions are perceived in advance because once they have been induced, it may be very expensive, both time-wise and money-wise, to re-adjust or stop them. Mathematical models have been proved as useful tools for this kind of predictive analysis (Gregory, 1976; Hey, 1988; Chang, 1988b; Gambolati and Galeati, 1990)

Application of mathematical models to analyse stream-aquifer interacting systems has previously been confined to regime boundary river channels. The models are normally simulated with the channel beds as pre-defined stable boundary profiles, (e.g. Pinder and Sauer, 1971; Cunningham and Sinclair, 1979; Younger, 1990). On the other hand, erodible channel flow and sediment routing models are simulated assuming a value for the lateral groundwater seepage as a pre-defined calibrated parameter (e.g. Chen, 1973; HEC-6, 1977, Chang, 1990). Physically, representation of these modelling procedures are a bit oversimplified, at least in performance for

alluvial stream-aquifer interacting systems with erodible boundary channels, realising how many natural fluvial processes have been altered in one way or another. In the process of adjusting to restore the dynamic equilibrium disturbed by the alterations, scour or fill or both are usually induced, together with the corresponding variation in the bed elevation profiles and hydraulic gradient between the river and groundwater levels. Considering that many case histories have shown that physical hydrologic processes for stream-aquifer interacting systems are more sensitive to the river channel characteristics than to the aquifer parameters (Pogge and Chiang, 1977, Cunningham and Sinclair, 1979, Bathurst, 1986, Younger, 1990), enhancement of modelling procedures reflecting the time-dependent variation of streambed elevations is worthwhile.

Consequently, the following objectives have been conceived for this study:

1. while noting the lack of data necessary for evaluation of hydrological impacts due to in-stream sand mining activities, seek a practical case in the field and derive a simple assessment method which can be applied to demonstrate the tendency of the activities to degrade the surrounding environment,
2. develop a solution procedure involving the physical equations governing streamflow, streambed sedimentation and groundwater flow and link them through a time-dependent interface boundary - referred to herein as Model for Alluvial Stream-Aquifer Interaction, or simply abbreviated as MASAI,
3. considering that upstream land use changes lead to variation in soil erosion, sediment yield and sediment delivery in river channels, assess the influence of such sedimentation variability on baseflow hydrographs,



4. observing that conservation of nature does not mean hoarding of natural resources, address a criterion for the selection of in-stream sand quarrying schemes with least negative impacts to the environment.

The results of this work are presented in this text, starting with chapter 2, which is an overview of the background and developments in the subject of river hydrology.

Objective 1 is addressed in chapter 3. This was achieved through a fieldwork exercise, which resulted in the development of an improvised solution procedure for analysing the hydrologic and fluvial impacts of in-stream sand harvesting on the River Kibos in Kenya. The theory of rating curve analysis was applied to demonstrate trends in the general streambed and low flow levels of a river section undergoing in-stream sand mining. This chapter also contains a review of the alternatives for flood mitigation on the Nyando River, which is hydraulically connected to its underlying aquifer.

Objective 2, which is addressed in chapter 4, was accomplished by drawing on previous contributions by other researchers. The conceptual setting of the individual modules of alluvial stream-aquifer interaction model do not represent a completely original effort by the writer. Rather, the different mathematical models were noted but with a sizeable gap existing between them, and therefore limiting their performance for alluvial stream-aquifer systems. Those concepts put forth by both streamflow and sediment routing modellers on the one hand, and stream-aquifer interaction modellers on the other hand, have been synthesised to form the linked model, without having to derive all the basic equations contained in the MASAI. Notable contributions followed closely include those of Chen (1973) and Chang (1988b) for channel water and sediment routing, Pinder and Sauer (1971) and Cunningham and Sinclair (1979) for stream-aquifer interaction, and Rovey (1975) for the linkage mechanism. This is how objective 2 was achieved, which provides a

linkage mechanism of streamflow to groundwater through a time-dependent boundary system. Physically, this is a more realistic modelling procedure for alluvial stream-aquifer systems that are undergoing development changes, yet it does not require different data that has not been adopted in hydrologic modelling before, save for the amount.

Because the concepts of the primary models, streamflow-sediment routing and stream-aquifer interaction, have been adopted from well established literature, verification here has only been made to validate the working of the computer program for the synthesised overall framework of the algorithm developed. The mathematical and structural properties of the primary models have been analysed elsewhere, and readers interested are referred to the relevant literature, like the ones given in the previous paragraph. The computation algorithm was accepted to be working, at least for the purpose of this study, on the basis of producing simulation results comparable to those obtained by published models. The procedure for calibration and testing for predictive uncertainty of the MASAI is presented in chapter 5

Considering the scarcity and uncertainty of the necessary data (Walling, 1988; Bathurst and Wicks, 1991; Petersen, 1993) the hypothetical hydrologic system based on that of Pinder and Sauer (1971) has been used to derive baseflow hydrographs and address objectives 3 and 4, as presented in chapter 6. The baseflow so derived is applied to assess the influence of sedimentation on the theoretical streamflow recession curve relationship of alluvial stream-aquifer systems. Based on the baseflow hydrographs and sediment yield curves, the MASAI concept was applied to derive methodologies for evaluating the hydrologic and fluvial impacts due to in-stream sand mining, and soil and water conservation by check-dam interventions.

Conclusions and suggestions for further research are given in chapter 7.



## **2 HYDROLOGY OF ALLUVIAL STREAM SYSTEMS**

### **2.1 A General Historical Overview**

Long before civilisation people lived a nomadic life depending on hunting wildlife and gathering plants for their food. But even by then, they had already perceived the significance of water resources - noting from the Holy Bible, itself with origins in prehistoric times, that water was held in high esteem (Psalms 1: 1-3; Psalms 104: 10-13), whereas its extremes, floods and droughts, were regarded with great fear (Genesis 7: 17-24 and Jeremiah 14:1-6). Likewise, myths explaining the beginning of human settlement also reveal how they largely depended upon hydrological elements and knew from experience the connection between these quantities and the phenomena of fauna and flora. For instance, in the Eastern Mediterranean, it is believed that settlement began around 6000 BC, when the receding ice in Northern Europe and increasing aridity of the Savannah in North Africa and Near East compelled people to retreat into the river valleys (Garbrecht, 1985).

With the convergence of populations in the valleys, the water resources in their natural conditions soon became over-stretched. This is probably when civilisation was realised, when ownership and manipulation of land resources was started, particularly for flooding irrigation in order to increase acreage for food production. And when the population expanded beyond the borders of the river plains, the idea of

waterworks was conceived to direct some streamflow from its natural courses to artificial systems in order to convey and have the water where and when it was needed for agriculture, animal husbandry and other uses. This was presumably the beginning of Water Resources Engineering (WRE). The earliest large scale water resources engineering works are attributed to Menes, the founder of the first Egyptian dynasty, around 3100 BC (Linsley and Franzini, 1979). Along the River Nile in Egypt are some of the earliest flood level marks existing on projecting rocks or structures on the river banks, as well as calibrated scales to quantitatively determine the water levels. Such early waterworks were not designed and built by engineers in the modern sense of the word, but must be considered as art which presupposed the ability to intuitively understand the behaviour of water in nature, and based on good manual technical skills.

Advances in civilisation, especially water use in sanitary and dietary practices reduced mortality rates and increased life expectancy. The increasing population required expanded acreage for agriculture and animal husbandry, water supply, energy, transport, drainage and pollution control, and industrialisation. Civilisation thus progressed until it became apparent that development had become more dependent on water than it was in the past and further river-works could no longer be solved by the rule of thumb alone. Engineering hydrology describing the major processes of streamflow was required for any further development on the river systems.

Hydrology itself is defined as the science that deals with the occurrence and movement of water on earth. And so the hydrology of streamflow begins when part of precipitation as well as any other flow contribution appear as total water runoff confined in a natural channel. The streamflow is collected from a drainage basin, and as it circulates through the earth's crust forms a primary adjunct to chemical weathering of rocks and other earth formations. Precipitation detaches surface

particles by rain drop impact, and runoff transports the particles and other eroded soil minerals to points of deposition, some on the river banks along its course and the rest into the river delta. These alluvial plains, with good water, rich fertile soils and a diversity of fauna and flora, provided people with favourable conditions for settlement and agriculture. That is why it is no wonder that most early civilisation began developing near river valleys, like Egypt on the Nile, and Mesopotamia between Tigris and Euphrates, among others.

In this regard it should also be noted that people were not always blessed by the life-giving streams when under control. They were also alternately plagued by their destructive nature when out of control. In addition to the rivers' natural stresses, people's increased dependency on streamflow disrupted their natural hydrological behaviour, making the rivers to respond to their interventions, and with impacts on the ecosystems in very many ways. As such, reclamation of waste water and wastelands, new soil and water conservation techniques and other land and water management practices became issues of increased concern. In this way, methods of solution for positive water resources development evolved as topics of interest for further studies and research.

Because of its broad based nature, documentation of data, experiences and principles about water resources was important for effective transfer and sharing of knowledge so that practical field problems could be approached with concerted efforts and in a wider perspective. Given its demand, documentation picked up and increased fast such that today it can be said the subject of water resources has a vast and varied body of literature dealing with various aspects of its topics.

It is not possible to list all of these texts in this chapter, but contribution by Chow (1964), is a good example to note as a reference text which introduces almost all topics in water resources. The other notable authorities, but with a tendency to

specialise, are, among others, Chow (1959), Linsley and Franzini (1979), Chen, (1979), Garde and Ranga Raju (1985), Wilson (1990), Novak et al (1990), on the one hand treating surface flows, and Bear (1988) and Freeze and Cherry (1979) on the other hand treating groundwater flows. However, all of this literature is not relevant to the present work. Therefore, the review that follows is only focused on the hydrological aspects of alluvial river systems.

## **2.2 Computational Hydrology on Alluvial River Systems**

### **2.2.1 Background**

The growing concern for the preservation of the natural environment as well as enhancing the existing land and water resources potential suggests that a careful analysis of the impacts of development projects on drainage systems is necessary. And given that the objectives for conservation, reclamation and many other river development projects are often meant to induce changes that would increase the quantity or quality of water delivered in certain reaches, it is in order to find with them river engineering measures that include some or all of the following:

- (i) interception or exclusion of sediments from reaching downstream reaches,
- (ii) mining or dredging sediment material for building or improvement of channel capacity,
- (iii) stabilisation or grade-controls to reduce scour and/or fill,
- (iv) detention of excess water to reduce flood damage and/or recharge groundwater,
- (v) storage/diversion of water for agriculture, water supply or power production,
- (vi) adjustments of river conditions in order to enhance environment



values and/or navigation transport.

In other words, the interventions are meant to heal the degenerating drainage systems or exploit the river's potential, and yet route out safely the drainage flows. This requires the ability to predict the morphological changes due to the interventions, and how the hydrological behaviour will respond to the new changes.

In all cases, economic constraints exist as well as physical limitation. That is, minimum excavation and structural costs, compatible with physical stability, are desirable. For such problems involving stable channels, methods of channel design based on the "tractive force theory" and the essentially empirical "regime theory" would be appropriate (Richards, 1982). According to the tractive force theory, a channel is designed to carry a given maximum discharge of clear water without scour by ensuring that the tractive force exerted by the flow on the perimeter is everywhere equal to or less than the threshold for initiation of particle motion. But, noting from the applications listed above, and the nature of unsteady sediment yield/storage in alluvial rivers, it is unlikely for channels of this kind of application to be maintained at threshold, which limits use of the theory.

Regime theory, on the other hand, provides the basic design criteria for stable sediment bearing channels. A channel "in regime" has a sediment transport capacity which matches the input sediment rate, so that although local temporary scour and fill occur, over a period of years the morphology and the "specific gauge" are on average constant. Therefore, regime theory has normally been used to develop empirical equations to predict geomorphologic and hydrologic processes in quasi-stable channels. A review of all of them is not necessary in this context, but it is hoped that the few presented below will suffice to highlight the major variables concerned, and update the general developments in the subject.



In the last half of the last century, it was noticed that Punjab canals constructed after 1950 had arbitrarily selected width and slope, and often suffered severe sedimentation problems during self-adjustment (Richards, 1982). It is no wonder then that the regime theory is said to have been originated by engineers working on the irrigation canals in India and Pakistan as they gradually observed certain correlation among the variables for stable sand-bed canals. The classic regime equations developed by Kennedy, Lindley, Lacey and Blench, based on data from the Indian canal systems, mainly applicable to sand-bed channels, are given in Table 2.1.

**Table 2.1 Selected regime equations for straight sand-bed streams or canals. (Source: Richards, 1982)**

Kennedy (1895)	Lindley (1919)	Lacey (1930)	Blench (1952)
A. Manning-type resistance equation, $v_o = 0.55 d^{0.64}$	A. Manning-type resistance equation $B. V_o = 0.57 d^{0.57}$	A. $P = 4.84 Q_a^{0.5}$ B. $R = 0.47 Q_a^{1/3} f_L^{-1/3}$ C. $V = 0.44 Q_a^{1/6} f_L^{-1/3}$ D. $S = .0003 Q_a^{-1/6} f_L^{5/3}$	A. $b = (F_b / F_s)^{0.5} Q_a^{0.5}$ B. $d = (F_s / F_b^2)^{1/3} Q_a^{1/3}$ C. $S = \frac{F_b^{5/6} F_s^{1/12} v^{1/4}}{1.11 g Q_a^{1/6} (1 + \frac{C_b}{2333})}$ D. $F_b = 1.9 D_{50}^5 (1 + .012 C_b)$ E. $F_s = 0.009$ (sandy loam) to 0.028 (clay loam) $F_s = F_b^2 / 8$ (gravel bed)
	C. $V_o = 0.28 b^{0.36}$ D. By combining B and C, $b = 7.2 d^{1.61}$	E. $f_L = 1.76 D_{50}^{0.5}$	

where b is the width of channel, d is depth of channel,  $Q_a$  is discharge of channel, P is wetted perimeter, S is slope of the surface of water in channel,  $D_{50}$  is the median grain diameter,  $V_o$  is Kennedy's non-silting velocity;  $f_L$  is Lacey's silt factor;  $F_b$  and  $F_s$  are Blench's bed and side factors

Since then, different methods reflecting increasing knowledge and greater

sophistication on canal design have evolved. For example, Leopold and Maddock (1953), on the basis of numerous studies of channel morphology and stability, demonstrated the following relationships:

$$b = kQ_a^{0.5} \quad (2.1)$$

$$d = CQ_a^{0.4} \quad (2.2)$$

where  $b$  = width (ft),  $d$  = depth (ft),  $Q_a$  = mean bankfull discharge (cfs) and  $k$  and  $C$  = coefficients which vary for each stream channel.

Moreover, Schumm (1960) noted with interest that with downstream increase in the amount of water discharge, channel width or depth could also decrease. This led him to emphasise that besides water, there was another major factor contributing to channel morphological changes, which he attributed to the type of sediments in the channel. The depth-width ratio ( $F$ ) of quasi-stable channels was hence found to be related to the percentage of silt-clay ( $m\%$ ) in the channel as:

$$F = 255m^{1.08} \quad (2.3)$$

$$F = 55Q_a^{-1.0} \quad (2.4)$$

But in this area of channel morphological and hydrological changes, it can be said that it was Lane (1955) who made the initial major breakthrough when he developed a function which could be used to predict the effects of humanity on channel system responses. From various field observations, he established that:

$$Q_a S_0 = f(Q_s D_{50}) \quad (2.9)$$

where  $Q_s$  = sediment discharge and  $D_{50}$  = median grain size.

White et al (1982) have made an analytical approach to the regime theory, but it is Chang (1988a) who has gone further and quantified Lane's relationship, and developed a method for river channel's adjustment of its equilibrium, and illustrated the method by examples. The method is based on the quantitative relationship among the variables of water discharge, bed material discharge, slope, sediment size, and channel width and depth for sand-bed rivers under dynamic equilibrium. In response to changes of certain variables, the direction and magnitude of adjustment for the others may be determined using the Chang's method. The adjustments refer to changes of river channels from one quasi-equilibrium state to the other, but without necessarily having to show regard to the intermediate processes.

These empirical relationships, when derived from a large set of data that is also of high variability, are useful in prediction of the effects of development projects on channel system responses. But good engineering designs must invariably seek to enhance the natural tendency of the channel system towards expected equilibrium conditions. To do so, an understanding of the direction and magnitude of change in the system characteristics caused by the action of people and nature is required, a condition which limits the application of empirical equations and brings in rational arguments. This is because a good understanding cannot be obtained from historical data alone, but in addition, by studying the channel in natural conditions, having knowledge of the sediment and water discharges, being able to fore-see people's future activities, and applying to them a sense of environmental awareness.

In addition, considering that alluvial channels, as drainage systems, are subject to changes in response to any activity on their regime, it is essential to carry out calculations accounting for the time sequence in which discharge amounts are delivered, and people's activities within the reach so as to assess the resulting

geomorphic and hydrologic impacts. Here, it must be emphasised that the resulting changes and development successes are not just the result of the constructions alone, but also of the interactions between the discharge, the quantity and character of the sediment discharge, and the composition of the bed and bank materials. In alluvial channel development, therefore, the major challenging task is not just the design of the controls for the channel in its present state, but also the prediction of the system responses to the works. This kind of problem can be solved by hydrologic models, which are defined as simplified versions of the real hydrologic system that approximately simulate the hydrologic phenomena that are considered as processes.

Whereas hydraulic models for river engineering tend to concentrate on more detailed description and accurate simulation of particular streamflow phenomena, hydrologic models assume simplification, of different degrees, of the streamflow phenomena (Todini, 1991). This is because hydrology is not a science in the same way as are its constituent parts: meteorology, soil physics, etc. Hydrology is a kind of "scientific conglomerate", grouping together a large number of otherwise rather separate sciences extracting material from these sciences and combining this material according to objectives which are usually quite other than the objectives of the individual sciences themselves (Abbott, 1991). In general, hydrologic modelling has gained from application of the experiences acquired during the development of hydraulic modelling.

Hydrologic modelling may be divided into two broad categories, of physical (scale) models and mathematical (abstract) models (Chow et al, 1988). Physical models represent the system on a reduced scale, such as analogue and prototype models, whereas mathematical models describe the system operation by a set of equations linking the input and output variables. However, physical modelling these days is less favoured unless sufficient sets of governing equations are not available, because of the large expenditure involved and the time consumed in model construction and



experimentation. But the major setback which limits its accuracy is the scale of distortion, which is almost unavoidable whenever it involves sedimentation, as is the case here.

In mathematical modelling, the variables may be functions of space and/or time, and they may also be probabilistic or random variables which do not have a fixed value at a particular point in space and time but instead are described by probability distributions. Stochastic models are those that consider randomness and are subject to error. They are generally used for the generation of artificial or synthetic data sets considering a random field, which is a region of space and time within which the value of a variable at each point is dependent on a probability distribution. This dependence of stochastic methods on randomness is in this context a limitation because the alluvial streamflow hydrology in question here is subject to changes, which need to be tracked down and their effects to be reflected in the system output. Furthermore, in water resources developments, very often each project encounters a unique set of physical conditions to which it must conform. Hence, standard designs which lead to simple hand book solutions can rarely be used. Besides, human alterations of natural flow conditions are normally governed by legal riparian regulations and/or market forces which may not necessarily follow any pattern, making it difficult for statistical analysis.

Deterministic models are those that do not consider randomness. Their relationships are developed among physical variables so that a given input always produces the same output. Deterministic modelling of alluvial channels has been advanced with the progress in the physics of fluvial processes and computer techniques. Since the actual size of a river channel is employed, there is no scale distortion. The applicability and accuracy of the model output depends on the physical foundation and numerical techniques employed.

According to spatial variability, the hydrological models can be classified as lumped or distributed models. Deterministic lumped models rely primarily on comparison between observed and simulated catchment outflows for calibration of the model parameters, and may in fact be based solely on the technique of system analysis in relating input to output without reference to the internal mechanism of the channel. The system is spatially averaged or regarded as a single point in space without dimensions. In contrast, deterministic distributed models are physically-based, and thus descriptive in the sense that the main objective is to represent the behaviour of a physical process, often with the object of gaining a better understanding of the processes (Beven and O'Connell, 1982). They consider the hydrologic processes taking place at various points in space and defines the model variables as functions of the space dimensions. The advantage of using distributed models is that they have parameters that are in principle measurable in the field, and therefore the relationships used may be validated by process measurements, and improved over time as a result of experiments in the same way as other scientific laws.

Another method of classifying hydrologic models depends on time variability. Models for which the flow rates do not change with time are classified as steady flow models, unlike unsteady flow models whose flow rates vary with time.

With regard to the variability of alluvial stream-aquifer systems, in both time and space, therefore, this study has considered the deterministic-distributed-unsteady modelling approach. The study is based on partial system synthesis, which consists of structuring system components in such a way as to preclude the necessity of full system synthesis. The main components followed are the three phenomena of alluvial stream-aquifer systems, comprising: (1) water and sediment routing in channels; (2) stream-aquifer interaction and (3) the interface boundary between alluvial stream-aquifer systems. A review of the components is briefly outlined in the following sub-sections.

### 2.2.2 Water and sediment routing in channels

Simulation of streamflow routing in alluvial channels is in this context concerned with gradually varied unsteady flow. Furthermore, it is limited to the one-dimensional partial differential equations, which include the Saint-Venant's equations of water continuity and momentum, (Eqs. 2.10 and 2.11), as presented by Chow (1959), Strelkoff (1969) and Chang (1988a), among others:

$$\frac{\partial Q}{\partial x} + \frac{\partial A}{\partial t} - q = 0 \quad (2.10)$$

$$\frac{\partial Q}{\partial t} + \frac{\partial}{\partial x} \left( \frac{Q^2}{A} \right) + gA \frac{\partial H}{\partial x} - gAS_0 + gAS_f - qU_l = 0 \quad (2.11)$$

where  $Q$  is the discharge,  $A$  is the cross-sectional area of flow,  $t$  is the time,  $x$  is the distance along the discharge centreline,  $H$  is the depth of flow,  $q$  is the lateral discharge per unit length,  $u_l$  is the velocity component of lateral inflow in the  $x$ -axis direction,  $g$  is the acceleration due to gravity,  $S_f$  is the energy gradient and  $S_0$  is the bed slope.

Analytical solutions to these equations are not available, except for very oversimplified special cases. Solutions are usually accomplished through numerical techniques, which may be appropriately put into one of the four classifications (Strelkoff, 1969):

- (i) Development of a network of characteristics,
- (ii) Explicit finite-difference of characteristics,
- (iii) Direct, explicit finite-difference,
- (iv) Direct, implicit finite-difference.

Advantages and disadvantages of application of the various methods to field problems can be found in the literature, (e.g. Amein and Fang, 1970 and Fread, 1971). For instance, methods of characteristics network can be limited because the channel cross-sections are surveyed at fixed locations such that the analyst cannot apply them to his/her own points of interest along the reach. On the other hand, explicit methods require very short computation time steps because of a stringent stability condition. In this respect, implicit schemes are advantageous in that they can provide computational results, even with large time steps, and the analyst can apply them to his/her own points of interest along the channel reach.

Streamflow in natural alluvial channels normally involve sediment discharges as well. To include these in the routing, Chang and Richards (1971) added a sediment discharge function to the differential equations for simulating gradually varied unsteady flow in alluvial channels, but restricted the application of the model to rectangular channels. Natural alluvial channels are not necessarily rectangular in shape; and even artificial channels of rectangular shape in alluvial channels are subject to deform unless the channel conveys only steady water and sediment discharges. This restriction to rectangular channels limited the application of Chang and Richards (1971) method.

Chen (1973) made a major advancement when he added the partial differential equation for sediment continuity, Eq. 2.12, to the Saint Venant equations, Eqs. 2.10 and 2.11, and developed a mathematical model for simulating water and sediment routing for gradually varied unsteady flow in natural alluvial channels:

$$\frac{\partial Q_s}{\partial x} + (1 - \lambda) \frac{\partial A_b}{\partial t} - q_s = 0 \quad (2.12)$$

where  $Q_s$  is the bed material discharge,  $\lambda$  is the porosity of bed material,  $q_s$  is the



lateral inflow rate of sediment per unit length, and  $A_b$  is the cross-sectional area of the channel which results from accumulated erosion or deposition.

His simulations of the time-dependent river degradation and aggradation, channel development response problems, and the demonstration of the channel bed scouring during the period when the flood wave was rising, and filling when the flood was receding, are all of notable interest to the current study. Other models simulating the fluvial processes through alluvial channels have since then been developed (e.g. HEC-6, 1977, Borah et al, 1982, Rahuel et al, 1989, etc.). These efforts which involve numerical simulations of the time dependent river bed profiles are noteworthy because of the influence of the changes to the hydrological aspects being studied herein. However, application of the models focused on the simulation of longitudinal and vertical variations alone. The transient nature of lateral phenomena of alluvial rivers have not been considered.

Chang's (1982) contribution advanced further the subject of mathematical modelling for predicting morphological changes of erodible channels. The significant feature of his model is its ability to account for changes in both channel width and channel bed profiles of aggrading and degrading streams. The model employs the techniques for water and sediment routing, and an additional condition based on the concept of minimum stream power as the width predictor.

Through applications of the model, for example, he was able to demonstrate the substantial changes that occurred in the bed profiles of the San Diego River near Highway 67 in Lakeside, California, during the March 1978 flood. The natural channel configuration had been altered primarily by sand mining before the flood. The two large borrow pits created on each side of the bridge left a sand ridge between them. The model simulation results illustrated how, during the flood period, deposition took place in the upstream pit first, and after filling the pit, the accelerated

flow over the ridge started scouring the ridge section, advancing towards upstream while filling the downstream pit. At the end of the flood event, the river bed in the reach had been reshaped to have a more or less continuous slope, with some points in the sand mining sections filling by up to about 5 m while those over the ridge scouring by up to 3 m.

Chang's (1982) approach has an advantage over the others because of its ability to simulate the width of aggrading or degrading channels, which in turn has effects on water movement over and across the bed. In a way it represents an extension of the above models which consider only aggradation and degradation. Nevertheless, this study is focused on the limitation that the models cannot be applied to track the transient nature of seepage flow from groundwater. Given the significance of bank storage and baseflow to streamflow, the limitation is a set-back in applications where the model is used to solve flood routing in alluvial rivers that are hydraulically connected to their underlying aquifers.

### **2.2.3 Stream-aquifer interaction**

Considering that the other hydrologic systems that adjoin alluvial rivers are also susceptible to variation in the rivers' conditions, it is necessary to advance the channel routing models so that they can simulate not only the in-channel hydrologic processes but also their interaction with the other adjoining systems. The other adjoining hydrological systems in mind are the flood plain aquifer and the corresponding riverine land conditions.

A complete review of groundwater modelling is not attempted here because this study is only concerned with the interaction between alluvial streams and their flood plain aquifers. A full literature on the mathematical modelling of groundwater can be

obtained, for example, in Bear and Verruijt (1987) and Dillon (1983). Other useful texts for practical numerical methods in groundwater modelling include those by Wang and Anderson (1982), which covers both finite difference and finite element techniques, and the report by Prickett and Lonquist (1981) of the Illinois State Water Survey which includes listings of programs and worked examples.

Early mathematical methods for studying stream-aquifer interactions (SAI) had been confined to changes in river elevations, with the assumption that the river elevations changed only as a function of time and that horizontal groundwater flow occurred only normal to the stream, (Hantush, 1964). However, analysis of the modification of a flood hydrograph due to groundwater from the surrounding aquifer requires the time and space distribution of stream elevations to be determined by solving the differential equations which describe the open channel flow and which include the effects of groundwater flow normal to the channel through the wetted perimeter. The flow through the wetted perimeter of the channel is a function of the hydraulic head in the aquifer as well as the streamflow elevations. Computation of the head in the aquifer below a permeable alluvial river channel has been accomplished by numerical schemes for the transient two-dimensional confined groundwater equation, Eq. 2.13 (Cunningham and Sinclair, 1979).

$$T\left(\frac{\partial^2 \Psi}{\partial x^2} + \frac{\partial^2 \Psi}{\partial y^2}\right) = S_c \frac{\partial \Psi}{\partial t} + \frac{q}{P} \quad (2.13)$$

and elsewhere, where the aquifer is unconfined,

$$T\left(\frac{\partial^2 \Psi}{\partial x^2} + \frac{\partial^2 \Psi}{\partial y^2}\right) = S \frac{\partial \Psi}{\partial t} + I \quad (2.14)$$

where  $\psi$  is the hydraulic head,  $T = K_2 m$  is the aquifer transmissivity,  $K_2$  is the hydraulic conductivity of the aquifer,  $m$  is the saturated thickness of the aquifer,  $S_c$  is

the aquifer storativity,  $S_y$  is the aquifer specific yield,  $q$  is the lateral seepage flow,  $P$  is the channel wetted perimeter and  $I$  is the vertical infiltration into the unconfined aquifer.

The interdependence of the open channel and the groundwater systems necessitated coupling the solutions of the differential equations describing each system (i.e. Eqs. 2.10, 2.11, 2.13, and 2.14). This means that when modelling alluvial stream-aquifer systems that are hydraulically connected, another expression describing the movement of water between the two is required. The stream-aquifer exchange flux  $q$ , can be represented by an expression based on Darcy's law (Pinder and Sauer, 1971; Cunningham and Sinclair, 1979):

$$q = PR_c(H - \psi) \quad (2.15)$$

where  $R_c = K_2 / Z_2$ ,  $K_2$  is the effective hydraulic conductivity of the aquifer,  $Z_2$  the thickness of the stream-aquifer interface boundary material,  $P$  is the wetted perimeter bordering the river,  $H$  is the pressure head in the river and  $\psi$  is the potential head in the aquifer immediately below the river.

When the differential equations for both systems are solved simultaneously at each time step, the solution scheme is said to be internally coupled. However, since groundwater flows are much slower than the channel water flows, the two systems' solutions can be obtained independently and then the output of one system applied as an input to the other system without necessarily satisfying any condition on the internal boundary connecting the two systems. This type of scheme is referred to as external coupling. Although the external coupling scheme requires relatively less computer storage capacity and time for computation, there seem to be no obvious advantage in accuracy gained by using either method. The accuracy of the results is primarily a function of the type of problem which is being solved. A concise review



of the various models for stream-aquifer interaction has been presented by Younger (1987).

Significant modelling techniques of physically based stream-aquifer interaction schemes seem to have started evolving in the early 1970's. Pinder and Sauer (1971), developed a numerical scheme that could calculate the modification of a flood wave due to bank storage effects. The dynamic equations describing the one-dimensional open channel flow and the two-dimensional transient groundwater flow were solved simultaneously, coupled by an expression for flow through the wetted perimeter of the channel. Through numerical experiments, they were able to demonstrate that bank storage attenuates flood waves, and the modification increased with distance towards downstream such that it may be considerable in the lower segment of a long reach. It was also shown that the extension of the hydrograph base time by bank storage effects may generate a recession curve similar in appearance to the one due to regional groundwater. In their experiments, they found that the hydraulic conductivity of the flood plain aquifer had considerable influence on the modification of the flood wave, and the response of the aquifer to the propagation of the flood wave decreased rapidly with distance from the stream. Cunningham and Sinclair (1979) generalised Pinder and Sauer (1971) method and addressed questions regarding the application of such a model to both real and hypothetical hydrologic systems in terms of parameter sensitivity, prediction uncertainty and the uniqueness of model solution.

The coupling equation applied by Pinder and Sauer (1971) and Cunningham and Sinclair (1979), Eq. 2.15, has the capability to account for the transient nature of the potential head driving the seepage flows, and it accounts for the thickness of the sediment layer at the bottom of the river. It does not, however, simulate the water flow as seepage through two media, of a sediment layer over aquifer materials, occurring in series. The hydraulic resistance across one layer is different from the

hydraulic resistance across two media arranged in series (Bear and Verruijt, 1987). If the hydraulic conductivity of the river bottom layer is higher than that of the aquifer, the limiting factor for the water interchange is the seepage resistance of the aquifer itself. Whereas if the conductivity of the sediment layer is lower than that of the aquifer, the limiting factor of the seepage flow is the hydraulic resistance of the sediment layer. This difference cannot be tracked by the coupling relationship in Eq. 2.15. The lack of the equation to represent the combined effect of the two media limits its application to field conditions that are patchy.

However, Cunningham and Sinclair applied the equation to link the stream-aquifer systems and produced some notable analyses. In carrying out the model sensitivity analysis, they obtained an initial model solution based on some given input values. Parameter sensitivities were then computed with respect to various model output variables by raising each parameter first by 10% and then by 100% while keeping all other parameters at their original values. Results of output variables in this analysis were river discharge, river stages, stream-aquifer water interchange and water-table elevations. With the help of these results they managed to demonstrate that the hydrologic processes were more sensitive to changes in Manning's roughness coefficient and the channel bed slope for virtually all types of output considered. At the 10% level of parameter change, river stage, discharge and stream-aquifer water exchange were most sensitive to Manning's  $n$ , while water-table elevations were most influenced by channel slope. The results differed only slightly at the 100% level of change in that the river-bottom conductivity becomes the most sensitive parameter in terms of the computation of stream-aquifer interaction.

In overall, they noted that the river parameters were dominating as the most sensitive factors. For example, they observed by comparison of sensitivities, that Manning's  $n$  was from about 50 to 200 times more sensitive than aquifer parameters when modelling fluctuations in the water table. These results are of interest to this study

because in alluvial river developments, it is the channel that has variables that are most vulnerable to the changes. The aquifer properties, the hydraulic conductivity and storativity, are themselves less dynamic and least likely to be changed by the interventions, at least during a given engineering period.

Further developments in stream-aquifer water resources have been contributed by Younger (1990). In his study on the stream-aquifer systems of the Thames Basin, he developed a modelling procedure to simulate water flow through a system of different aquifer formations, including the water interchange between the Thames River and the surrounding aquifers. His model represented the thickness of the sediment layer below the Thames, and simulated the combined effect of the layer and the other aquifer formations to the water interchange between the river and the aquifers. However, because he was dealing with a more or less stable river system, his model did not simulate the sediment routing effects (or aggradation and degradation), but he did recognise the hydrological significance of the spatial and temporal variation of the sediment layer at the bottom of the river. For example, he illustrated the influence of the streambed variables to the flow and transport between the river and aquifer systems, and highlighted the sensitivities of the flow and transport simulations to the streambed parameters. He also pointed out the need for further work considering spatial and temporal variations in the thickness of the streambed sediment, and the desire for the hydraulic conductivity of the streambed sediments to be determined in-situ.

The SHE (by Abbott et al 1986), a physically-based, distributed catchment modelling system is another good example linking the hydrological processes of the land and river systems. With respect to the patchy nature of channel beds, the SHE is formulated to simulate the stream-aquifer interaction for four different cases:

- (i) phreatic surface in direct contact with a flowing stream,



- (ii) phreatic surface in direct contact with a dry stream,
- (iii) phreatic surface lying below a flowing stream,
- (iv) phreatic surface below a dry stream.

In addition, the channel boundary can be assigned a hydraulic conductivity different from that of the surrounding aquifer. This is in order to account for the higher or lower conductivity which may characterise the sediments in the immediate vicinity of the channel. However, the SHE does not describe the variation with time, from one of the cases to another, which is possible for erodible alluvial channels.

Storm (1991) also acknowledged the significance of groundwater in the hydrological cycle, and reviewed some of the modelling efforts which have been made to analyse and understand the role of saturated flow in the hydrological cycle in recent years. He noted that although the three-dimensional (3-D) modelling of unsaturated-saturated transient flow has been developed since early 1970's, application of these rigorous 3-D approaches in water resources engineering has been handicapped, for example, by computer technology, in terms of memory requirement. Therefore, studies have been mainly concerned with the description of two dimensional (2-D) subsurface flow models. In many cases, he noted, the purely 2-D approach was inadequate when the interaction between the surface and the subsurface water was important. He observed that the 2-D model can conveniently be extended to a quasi-3-D model by including a vertical component. He demonstrated, using the SHE model as an example, how the subsurface flow regime is a coupled 1-D unsaturated and a 2-D saturated system. Although he demonstrated the variation of the saturated zone both seasonally and during rainstorms, especially around river systems, he did not consider the possibilities of seasonal variation of channel beds.

In the recent past, the awareness on the environmental issues has also increased and stimulated research interests in issues relating riverine ecosystems to hydrological



phenomena. Ecologists are spearheading this course, especially while concerned with the effects of water quality on the river's ecosystem. Although their considerations are generally biased towards biological effects, nevertheless, knowledge of the interdependence of the biological observations with the hydrological behaviour is an added advantage especially while addressing the ecological impacts of river engineering systems. In fact, most practical problems encountered on river systems need a joint understanding by both hydrologists and ecologists since the phenomena concerned are inseparable. For instance, regarding riverine ecosystems, it may not be obvious whether the effects are of biological vegetation on hydrological flow, or of hydrological flow on biological vegetation.

Developments in this direction can be seen from the example by Pinay and Decamps (1988), demonstrating the interdependence of the hydrological and biological processes on river systems. They encountered the case whereby they proposed various conceptual models to explain the dynamics of nitrogen in the riparian wood on the River Lange in France. Their study was with regard to the influence of the frequency, intensity and duration of flooding to the functioning of the riparian woods. The outcome of their study made it apparent that water logging conditions are important for the maintenance of riparian systems and the dynamics of the nitrogen cycle. Groundwater flow through a distance of about 30m under the riparian woods studied was enough to remove all the nitrate, and de-nitrification rates of up to 50 mg of nitrogen per square metre per day were observed in the field.

From the foregoing review, therefore, it is seen that sedimentation variability in river systems plays a significant role in the processes of alluvial stream-aquifer interaction. It is also noted from the stream-aquifer interaction models outlined (Younger, 1990; Storm, 1991; Abbott et al, 1986) that considerable developments have been made in order to account for the spatial variability of the streambed conditions. However, the modelling techniques have not addressed the transient nature and effects of the

sedimentation processes of alluvial stream-aquifer systems. This is the endeavour of this study, but restricted to the interface boundary between alluvial rivers and groundwater systems.

#### **2.2.4 The transient nature of the interface boundary between alluvial stream-aquifer systems**

Groundwater modelling had been representing rivers as lines of fixed head acting as impermeable no-flow boundaries for groundwater (Wang and Anderson 1982). Such fixed river head boundaries are conceptually equivalent to rivers which fully penetrate the aquifer. In nature this is a rare case. Usually, alluvial rivers partially penetrate the aquifer such that there is the possibility for the exchange of the flow between the portions of the aquifer systems on either side of the river, and the river stage is subject to changes, which may affect the bank storage.

In most cases the water interchange is affected by the condition of the interface sediment layer along the wetted perimeter of the river. This sediment layer is also itself subject to transformation through scour/fill, due to sediment transport/storage in the channel reach. The sedimentation layer generally has a different hydraulic conductivity from the surrounding aquifer material, and can drastically affect the rate of seepage between the two systems.

A study of the behaviour of silt layers in natural channels has been conducted by Matlock (1965), who conducted both field observations of natural streams and experiments in a laboratory flume to determine the effects of silt on infiltration rates from the river. The general conclusions from his observations were that seepage from a stream carrying a silt laden water is restricted by a silt layer deposited on the wetted perimeter of the channel. For instance, he observed that a silt layer of only one

or two millimetres thickness could reduce the seepage rate to as little as one-hundredth of the seepage rate prior to the formation of that silt layer. He also observed that a break in the silt layer caused by some local disturbance results in an increased seepage rate, but only for a short period of time in most instances. The high local seepage rate brings about the rapid accumulation of fine sediments in the break, and the silt layer reforms almost immediately.

Rovey (1975) took these observations into consideration when he developed the equation describing seepage from a stream to a hydraulically connected aquifer through a silt layer as:

$$q = P \frac{K_1 K_2}{Z_{b1} K_2 + Z_{b2} K_1} (H - \Psi) \quad (2.16)$$

where  $K_1$  is the hydraulic conductivity of the interface boundary sediment material between the river and the aquifer,  $K_2$  is the hydraulic conductivity of the aquifer medium,  $Z_{b1}$  is the thickness of the interface sediment layer,  $Z_{b2}$  is the distance between the river and reference point in the aquifer, and the rest are as previously defined.

His coupling equation was based on local conditions on a reach in the Arkansas Valley of south-eastern Colorado, which was assumed to be stable. The coupling equation (Eq. 2.16) takes account of the combined effects of the sediment layer and the aquifer materials, and is more general and applicable to other systems with a sediment layer at the bottom of a river. But because the equation was developed for a stable system, it cannot simulate the temporal variation of the sediment layer. The formulation may be adequate for calibration and application to quasi-stable river systems, but under certain conditions, like in tropical conditions where storm floods are of short duration and with intense magnitudes, and the river channel boundaries



are of loose sand materials, prediction of the hydrologic behaviour using this expression may suffer from lack of dynamism to keep track of the time-dependent interface boundary variation. In channels having interventions, the extent and rate of aggradation/degradation may be even more variant, requiring both spatial and temporal representation of the fluvial and hydrological processes in order to produce valid simulations. It is also observed that in the event of the whole sediment layer being eroded away, the coupling equation would be indeterminate because the value of  $K_1$  would be zero.

Channel aggradation and degradation are defined as the respective bed filling and cutting that occur over a relatively long river reach and long period of time, say several years. Channel scour and fill apply to similar processes within a shorter river reach during a shorter period of time, say minutes, hours, days or even seasons.

An example to demonstrate the transient nature of river systems is seen on the upper Rhine in Europe. In order to mitigate flood damage and associated diseases, a "Rhine correction" was performed in the middle of the last century, by training the river into a straight bed, thereby increasing the bed slope by about 30%. This in turn gave rise to an erosion process that even today has not yet come to an equilibrium state (Novak, 1991). Also, the width of the natural river channel and bars were changed into a normalised cross-section, thus reducing the diversity of its habitat. As a result, the Rhine water levels have dropped steadily due to the erosion and the normalisation.

Furthermore, the construction of a French shipping canal system in Northern France, diverted a large portion of the river discharge. In consequence, groundwater levels dropped severely with drastic impacts on the vegetation in the Rhine valley. The reduction of the habitat damaged the resilience of the river ecology and the self purification ability of the river. In the 1970's, the groundwater problems led to the



construction of special weirs on the river, which serve the purpose of raising the water levels at very low discharges, and consequently to elevate and stabilise the regional groundwater levels.

The problems associated with the hydrology, sediment transport and ecology of alluvial river systems can also be exemplified by past observations on the Danube River. The Danube is Central Europe's largest river, with a large underground water reservoir and sustains a large flooded forest. However, due to past "mistakes", its fluvial processes were disturbed, which suddenly caused the river to cease deposition, but increased its ability to erode. The erosion has been so intense that the level of the river bed has been lowered by up to 2.5 m over 30 years. The mistakes made were: (1) river dredging by the Slovaks for flood protection and sediment material for building, (2) straightening and narrowing the river for navigation, and (3) construction of a dam in Austria, which held back an estimated 600000 m<sup>3</sup> of gravel every year. All of these led to the erosion that progressively cut the Danube from its wetlands.

As a result, over 30 years, fish stocks diminished, the native wild carp came close to extinction, and the water table under the flood plain forest fell fast, losing a tenth of its trees (Pearce, 1994). The decline in the fish stock and native carp was because of reduced flooding levels and frequency on the flood plains, which are important for spawning and rearing for the aquatic animals (Large and Petts 1994). The loss of trees can be related to the falling water table.

These examples are highlighted to illustrate cases in which it may be necessary to make predictive analyses of the hydrological impacts due to impending land use and/or river engineering developments. This is particularly important in cases where the streamflow is the main source of groundwater recharge, or acts as the base-level for the surrounding groundwater levels. The examples do not mean to highlight the

bad side-effects and discourage flood plain developments, knowing that most general river developments, whether for river regulation to prevent flooding, sand mining for construction materials, land drainage for agriculture and deforestation of riparian forests for firewood and construction, will lead to the decrease, or even to the disappearance, of the buffer capabilities of the riparian zones. They have been introduced to demonstrate the importance and efficiency of the riparian vegetation as natural filters vis a vis water quality, and add interest to the ecotones as components of dynamic fluvial landscapes and bank storage hydrology.

In line with this, the study by Large and Petts (1994) is noted to be of significant contribution. They have demonstrated the importance of rehabilitating the river margins, and also illustrated the processes influencing the margins. They have explained, for example, how the degree of heterogeneity is an important feature of the riparian ecotone. In natural situation, such heterogeneity is determined mainly by flow variability, topography, sediment permeability, and the frequency of destructive events such as flood plain erosion. Furthermore, they have described how progressive sedimentation due to erosion, deposition and other flood disturbances may eventually change the wetland habitats. Morphological and physiological adaptations directly related to stream-aquifer interaction occur in riverine plants and collectively these adaptations determine a species' success in different moisture conditions.

Other examples of river systems with notable time-dependent bed elevations are, for instance, River Huang in China which as a result of the weak slope in the middle and lower courses, has up to 40% of the sediment settling in the river plain between the dikes on either side of the river, thereby increasing the bed elevations over the years. As such, water levels between the dikes are often 5-8 m higher than the surrounding alluvial plains (Garbrecht, 1985). In lakes and reservoirs in the Mississippi river valley, sediment accumulation rates exceeding 3 cm per year have been measured at

individual sites (Ritchie et al 1986). The average rate for 328 sediment profiles collected was 2.49 cm per year for the 1954 - 1964 time period, and 1.74 cm per year for the time period since 1964. A case of a single flood event scouring and filling to cause drastic changes in the river bed profile has already been exemplified previously while explaining Chang's (1982) model.

Finally, some cases are given in tabular and graphical form in order to give a picture of the problem in the field. The first example, Table 2.2, shows the amount of sediment delivered in channels of some major rivers, which can cause river bed adjustments. Figures 2.1 and 2.2 are presented to exemplify field cases of streambed elevations that vary with time. The examples also show that the streambed adjustments can be recorded so that empirical (or statistical) functions can be derived for estimating the variation of the elevations with time.

**Table 2.2 Field cases exemplifying annual sediment deliveries in some major river systems,**  
*(source: Walling, 1983)*

River	Station	Area (km <sup>2</sup> )	Total suspended sediment load (t/yr.)	Loss between stations (%)
Nile (Sudan -Egypt)	Kajnarty Cairo	1850000 3000000	133700000 111000000	17
Wisla (Poland)	Zawichost Plock	50543 168857	1990000 1180000	41
Lech (Germany)	Fussen Feldheim	1422 2124	329433 192489	42
Po (Italy)	Becca Piacenza	30170 35430	4374650 3791010	13.3
Menan (Thailand)	Tha Pia Pitsannloke	12790 25491	4999355 3252201	35
Atrak (Iran)	Shirrin-Darrah Reza-Abad	1500 5430	92510 31406	66
Nazus (Mexico)	El Palmito Canon Fernad	18321 33468	2451129 1813094	25

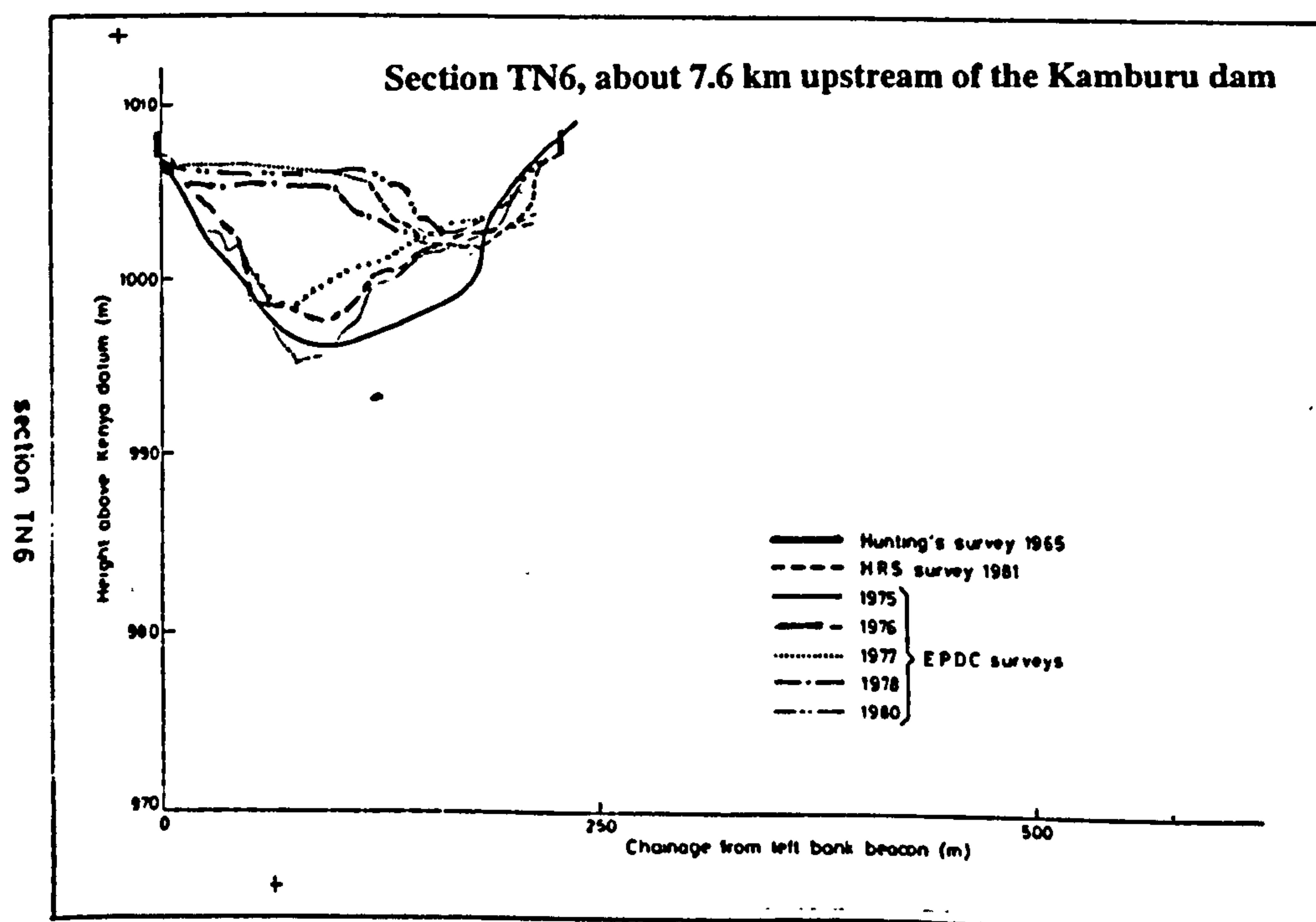
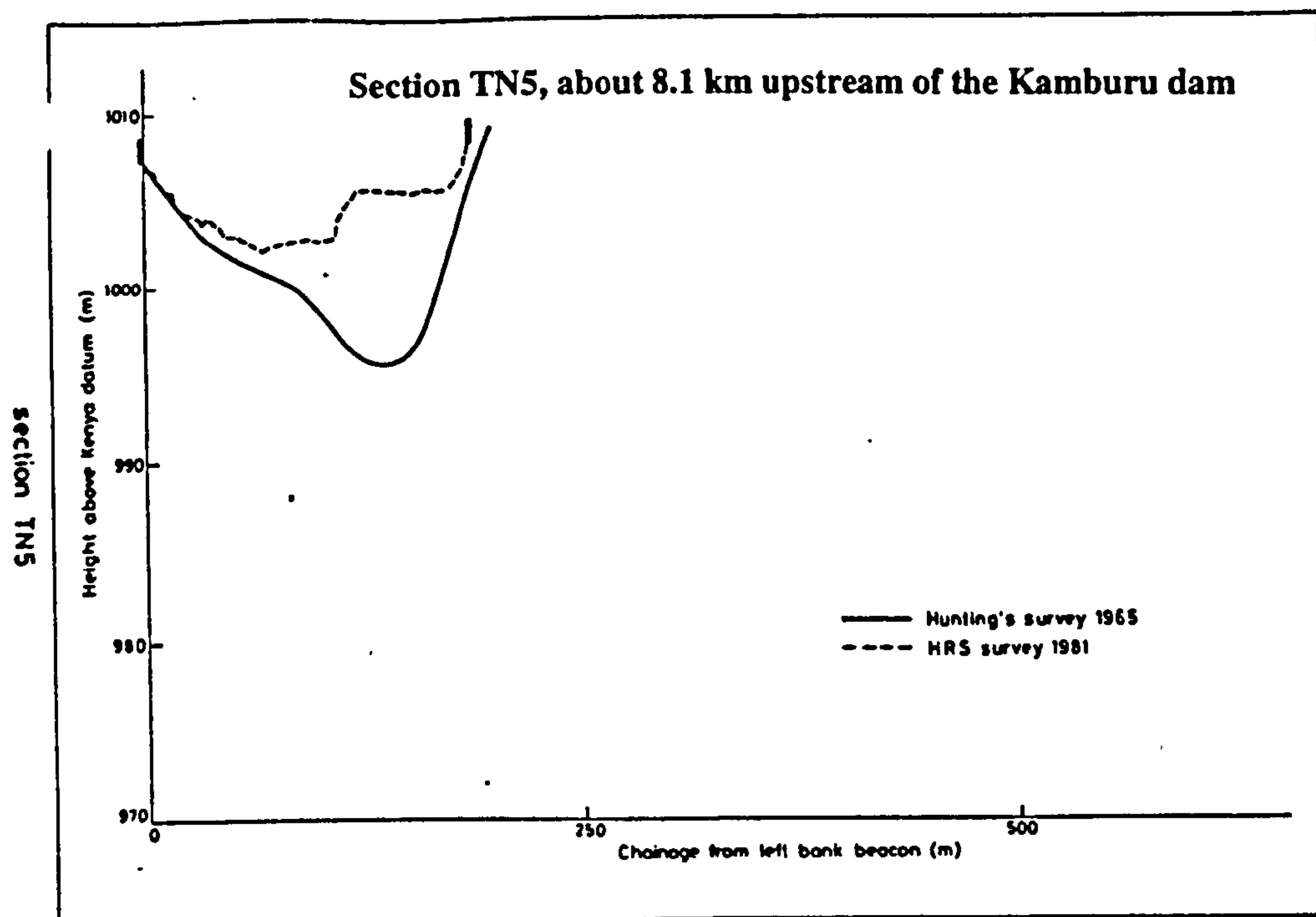


**Fig. 2.1 Channel aggradation of two sections on River Thiba, at about 7.6 km (TN6) and 8.1 km (TN5) upstream of the Kamburu dam (Kenya), (Source: Wooldridge, 1983)**



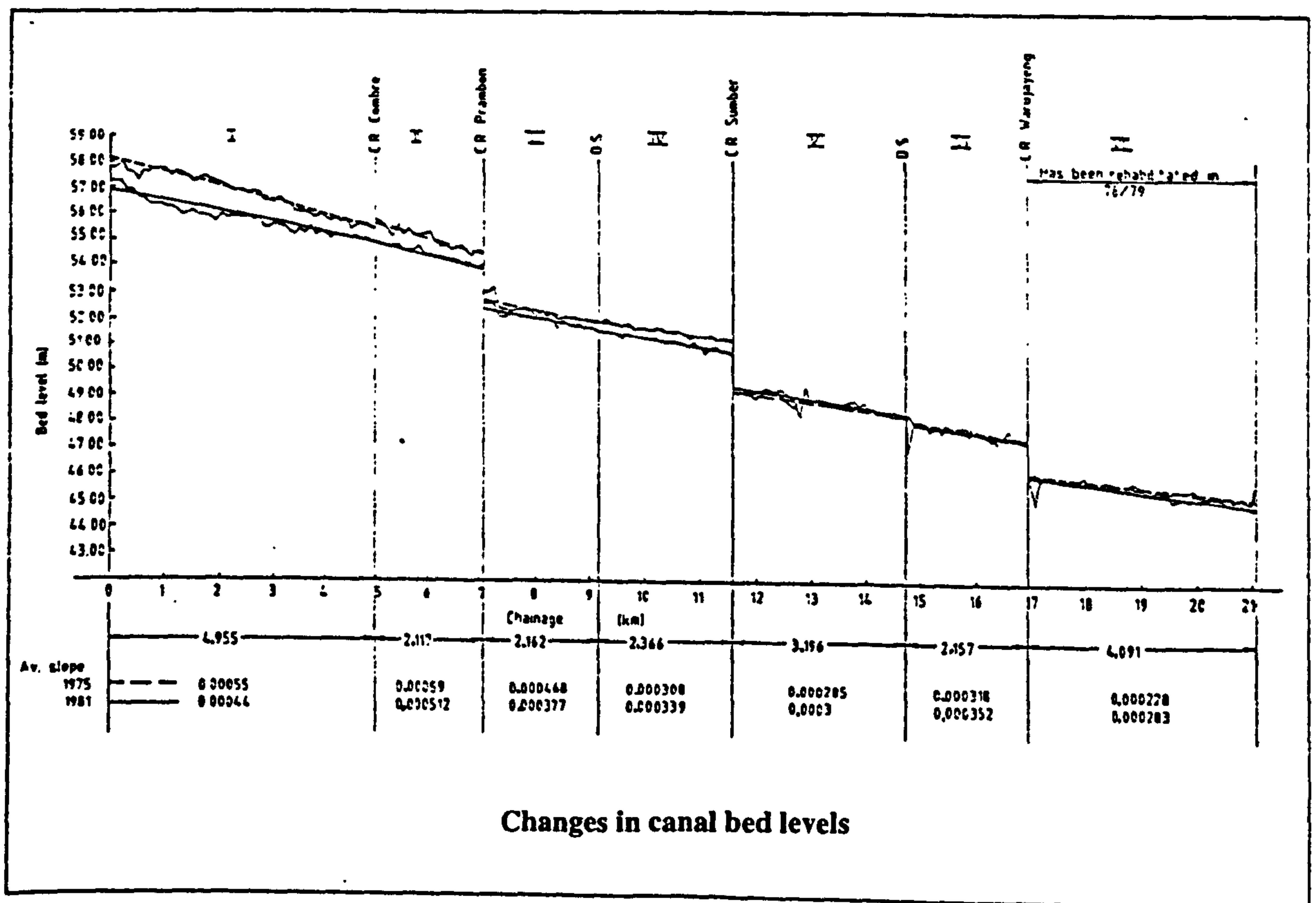
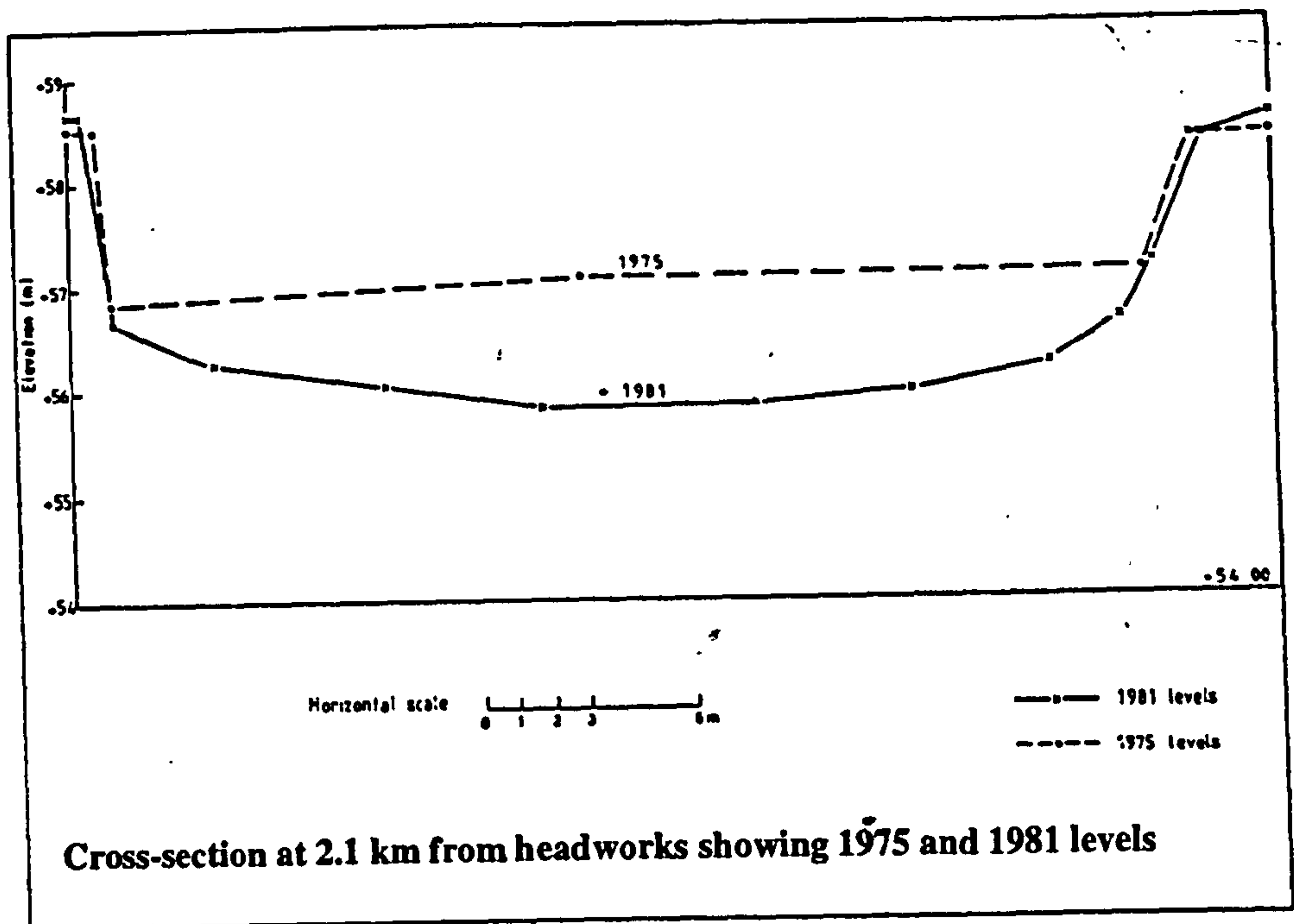


**Fig. 2.2 Channel degradation on the Warujayeng-Kertosono canal (Indonesia),**  
*(Source: Kadiro and Santoso, 1982)*

In artificial groundwater recharge, close inspection has revealed that success depends on the permeability of the river bed and this is the weak link in the system (Huisman and Olsthoorn, 1982). Artificial groundwater recharge is defined as the planned activity of people whereby surface water is made to infiltrate the ground, commonly at rates and in quantities many times in excess of natural recharge, giving a corresponding increase in the magnitude of the safe yield. Many alluvial rivers carry appreciable amounts of sediment load and other clogging agencies, which are filtered out as the water enters the aquifer. After some time, the bed of the river will be covered by a less pervious layer, a so-called filter skin, with a large resistance against the inland flow of river water. With a constant rate of abstraction the groundwater table will drop, impeding the process of recovery and adversely affecting other groundwater users. In the past, this was not a serious problem as most rivers in their natural state do not have a stable bed. In this condition, sand and gravel are deposited in periods of low to normal flow and are picked up again when the river is in spate. Clogged areas of the riverbed are thus removed by scouring after which the clogging process can start all over again. Today, on the other hand, intervention systems are being developed on many rivers. High river velocities and their scouring effects no longer occur in certain sections and as with reservoirs, persistent clogging of the river bed takes place. The clogging of the channel bed is a limitation not only in the process of groundwater recharge but also poses a threat to aquatic environments throughout the river valleys.

From this review, it is perceived that considerable progress has been made in the area of regime stream-aquifer interaction. However, it has also been highlighted that many alluvial rivers have unstable channels that are subject to changes. The significance of the stream-aquifer interface sediment layer to the water interchange between linked stream-aquifer systems has also been highlighted. This means that the assumption of regime channel beds in modelling of alluvial stream-aquifer interaction is a limitation. Therefore, the need for a modelling procedure which

includes sedimentation processes and river bed elevation adjustments is justified. More field examples, with respect to the situation in Kenya, exemplifying the need for the development and application of the MASAI approach, are discussed in the next chapter.

### **3. FIELDWORK ASSESSMENTS OF THE EFFECTS OF STREAMBED ADJUSTMENTS ON THE RIVERS KIBOS AND NYANDO (KENYA)**

#### **3.1 Introduction**

Although the main aim of the fieldwork had been to define and go through the procedures of collecting the necessary data for model calibration, nonetheless, the exercise also undertook to relate practical problems in the field to which the concept of stream-aquifer interaction modelling can be applied. Therefore, besides fieldwork experimentation and computation of quantitative parameters for calibration purposes, fieldwork in this context also involved assessments and reviews of some field problems associated with local development changes on alluvial river systems. Such assessment studies have been lagging far behind, especially in developing countries where the severity of riverine development impacts could be even more serious, given their prevalent land degradation and arid characteristics - and Kenya is no exception.

In Kenya, two thirds of its land is arid or semi-arid, implying that availability of water resources is critical for its development and growth. Faced with a rapidly expanding population, of about four per cent per annum, and with limited alternative means for economic growth, there is an urgent need to increase output from its



natural resources, but on a sustainable basis. River systems are among the few natural resources that are exposed to the public and offer a variety of economic options, ranging from irrigation agriculture, fishing, livestock watering, domestic and industrial water supply, building sand material, dams for hydropower production, and many others. As a result, the rivers are now under the threat of over-exploitation by the encroaching populations of people from all walks of life. Guidelines to proper utilisation of the river systems, therefore, are basic to this endeavour, and promotion of knowledge and understanding of what is happening, and of what can happen is part of this exercise.

In the past (in Kenya) water resources conservation has been more of a trial and error exercise, sometimes at the expense of those dwelling near the water resources systems. For instance, in an effort to protect the riparian land and conserve water resources, it is stipulated in the Agriculture Act CAP 318 of the laws of Kenya, that "cultivation is limited to within two metres from the water course or, in case the water course is wider than two metres, to within a distance equal to the width of the water course but not exceeding 30 m". This is among the so-called cultural or biological measures of soil and water conservation. Elsewhere, in the same light, dams, grade control weirs, gabbions and river training works, generally referred to as structural measures of soil and water conservation, are being recommended for the purpose of storm water management by way of reducing flood magnitudes, promoting groundwater recharge, bank storage, and harvesting river sand for building materials or sand dams.

However, there is now a continuing debate about the relative merits of structural measures of conservation as opposed to cultural or biological measures. Although it is clear that both have a role to play, greater attention is needed for those implementations that would lead to improved bank storage and stability, and improved riparian plant cover which would eventually lead to enrichment of the

surrounding land potential. But overall, the identification of appropriate and acceptable measures for the different hydro-ecological and farming units is a major undertaking that demands the attention and co-operation of both the research scientists and the local farming/business communities. It was on this basis that the need for development of a scientific approach for evaluating soil and water conservation through investigation, research and testing was conceived.

Therefore, fieldwork exercises were conducted in Kenya so as to experience some of the local problems in the country. The exercise was done in two terms of three months each, that is, in December 1991 - March 1992 and February 1993 - May 1993. Based on the objectives of the study, the fieldwork was limited to alluvial river channels that were subject to some physical changes. In particular, study sites were identified on the Rivers Kibos and Nyando, largely because of their easy access. The section reaches identified on the River Kibos were undergoing changes through sand mining for building material, while the River Nyando is being considered for flooding mitigation. The fieldwork was executed under three main topics, namely: (1) the general hydrogeology of the Nyando basin; (2) evaluation of impacts due to sand mining on the River Kibos, (3) a review of flood mitigation alternatives on the River Nyando.

### **3.2 The General Hydrogeology of the Nyando Basin**

The River Nyando catchment is one of the seven that form the Lake Victoria basin of Kenya, whose rivers drain into the lake. The other six are Sio, Nzoia, Yala, Sondu, Kuja and Mara catchments. The Kibos is a relatively small river, falling within the Nyando basin (Figure 3.1).



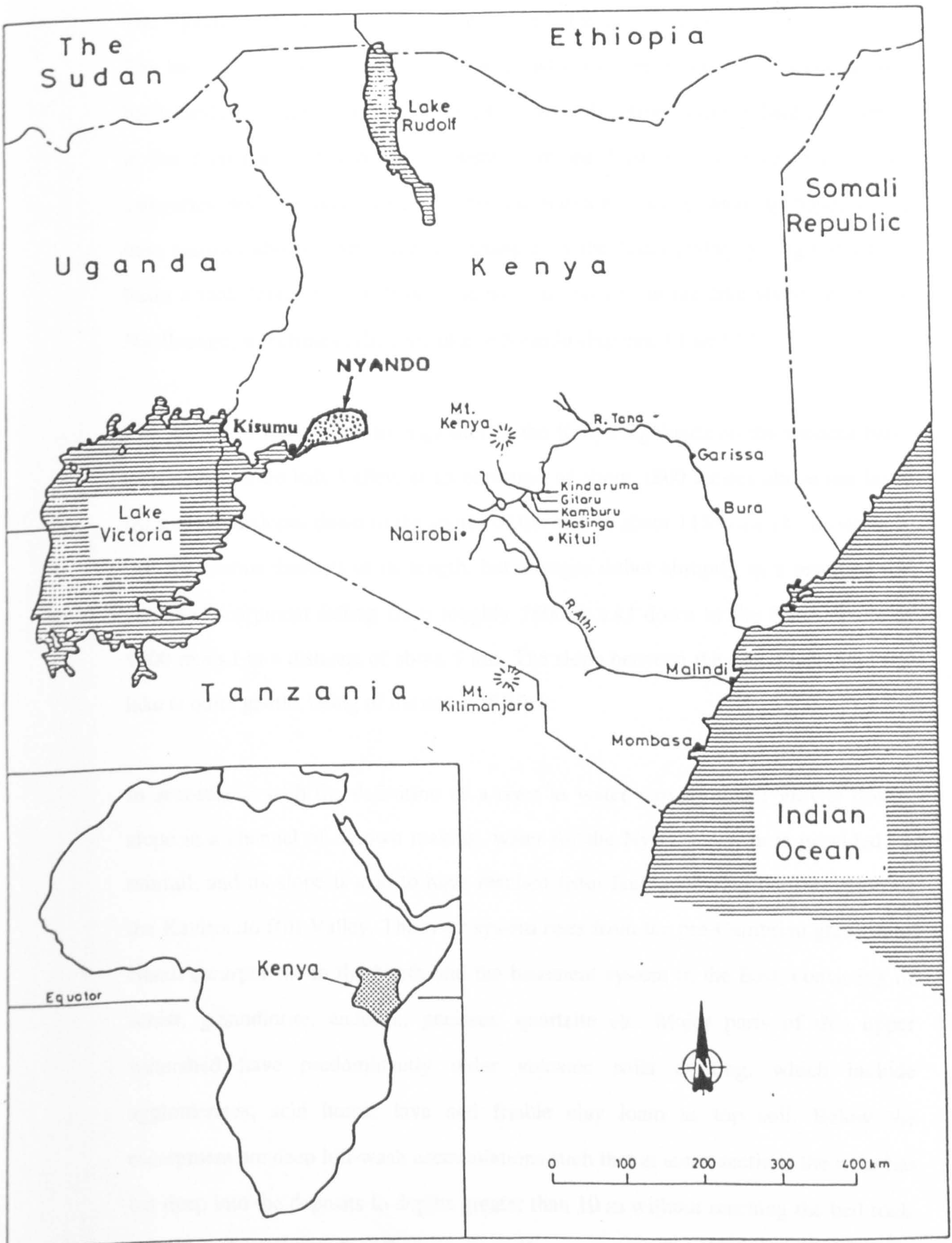


Fig. 3.1 Map of Kenya showing the location of the Nyando Basin



The Nyando catchment is approximately astride the equator and the longitude 35 °E. The basin has an area of about 3450 km<sup>2</sup>, which is about 6% of the Kenyan lake basin land mass, traversing in a general East-West direction from the Timboroa forest in the North and Mau forest of Kericho in the East. It falls into two general categories, with the major part in the highlands in a roughly rectangular shape, which then narrows abruptly into another rectangle on the Kano plains, giving the whole basin a table-tennis racket shape. The basin terminates in the lake shore swamp of Nyalbiengo, sometimes called Miruka or Nyando (Figures 3.1 and 3.2).

The system of River Nyando originates in the Kenya highlands on the western bank of the Kavirondo Rift Valley, at an elevation of about 1800 metres above sea level (m.a.s.l), and slopes down to the shores of the lake at about 1135 m.a.s.l. Its slope is not continuous throughout its length, but changes rather abruptly as a result of the Nyando escarpment falling from roughly 1800 m.a.s.l down to the Kano plains at 1200 m.a.s.l in a distance of about 5 km. The slope between the escarpment and the lake is quite gentle, being of the order of 0.3%.

In accordance with the definition of a river as water moving under gravity down-slope in a channel of its own making, water for the Nyando system is provided by rainfall, and its slope is said to have resulted from faulting during the formation of the Kavirondo Rift Valley. The river system rises from the pre-Cambrian granites of Nandi escarpments in the North and the basement system in the East, consisting of schist, granodiorite, andesite, gneisses, quartzite etc. Major parts of this upper watershed have predominantly older volcanic soils existing, which include agglomerates, acid humic lava and friable clay loam as top soil. Below the escarpment are deep hill-wash accumulations such that at some sections the river has cut deep into the deposits to depths greater than 10 m without reaching the bed rock. The plain is composed of Quaternary to Recent sedimentary formations consisting mainly of clay, sand, gravel, sandstone and tuffs accumulated in a tectonically



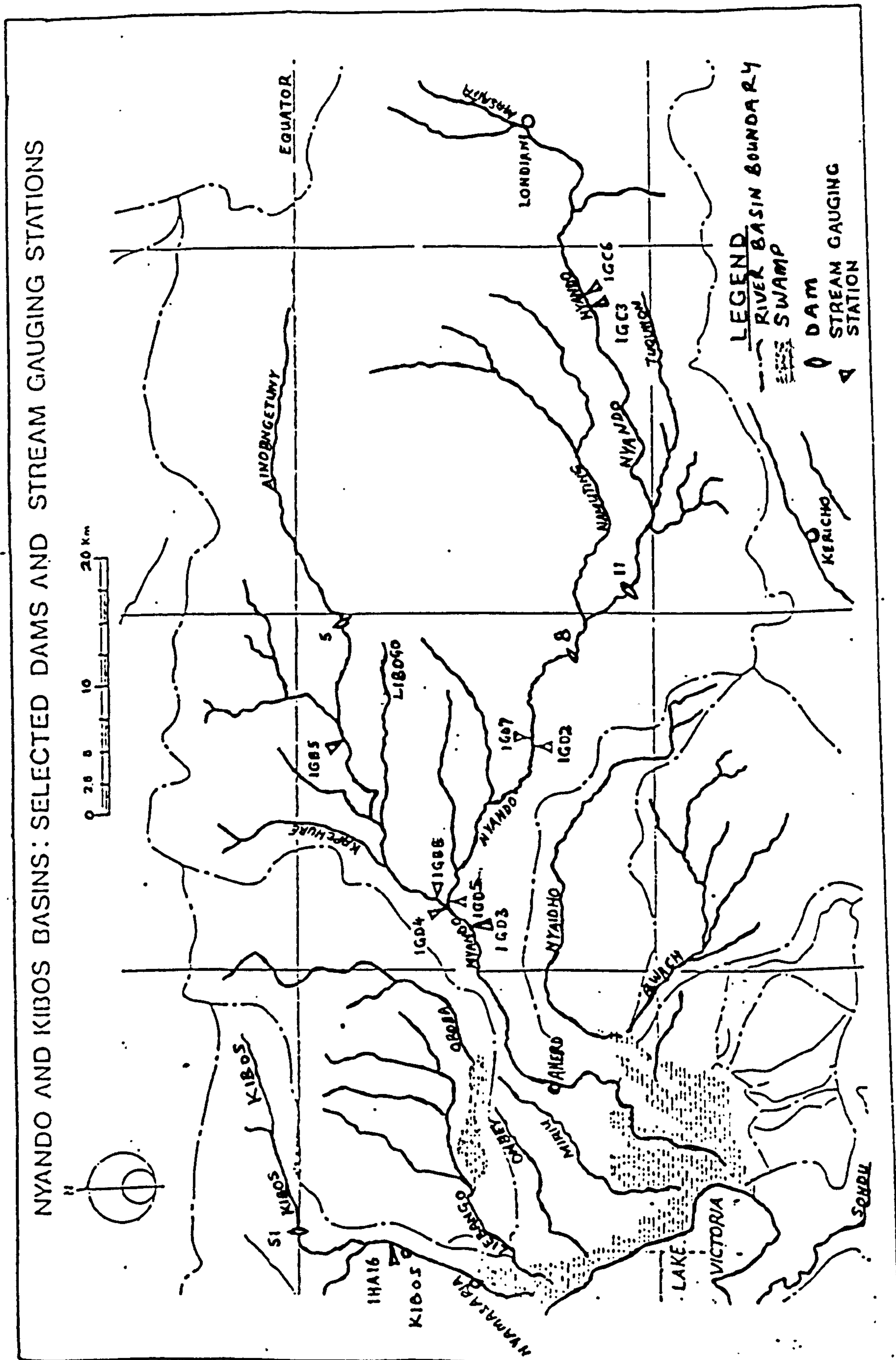


**Fig. 3.2 The Nyando Basin showing the main rivers, gauging stations and proposed dam sites**

preformed graben system. The alluvial accumulations were probably formed as a result of frequent changes of courses by the streams of the area, and constitute the main source of parent material of the Kano plain soils. The deposits, on the basis of well records, reach a maximum thickness of over 400 m, but nothing much can be stated about the total thickness distribution owing to lack of detailed information. An average thickness of 75 m has been considered as a working hypothesis since most wells reaching bedrock are between 50 and 100 m deep (Italconsult, 1983).

Overall, the plain aquifer can be considered as unconfined. Analysis by Italconsult (1983), from 97 wells spread over the plain showed that the depth of the water table ranged from a minimum of 8 m in the western part of the plain to an absolute maximum of 50 m in the central part. They also did bimonthly measurements of standing water-table levels between June 1979 and January 1980, from a network of 29 observation wells, which showed a fluctuation of 0.5 - 2 m in the water table levels. But these records may not be true representations of the regional annual water table fluctuations, because the observations did not run through the complete hydrologic cycle of the region, having missed the wettest season in April - May, and the driest period in January - February. Analyses of the water table elevations have also indicated a depletionary trend, implying that the aquifer has a low potential for development and needs detailed studies in order to balance its water abstraction with the recharge capabilities.

The source of recharge for the aquifer is mainly linked to runoff from the escarpment and infiltrating flood waters. But its capacity is dependent on the volume, duration and distribution of the flood hydrographs and the volume storage-space available in the banks/plain aquifer. The volume and distribution of the flood hydrographs determine the amount of water available in a given reach, and the duration of the floods determine the opportunity time available for the water to infiltrate/seep into

the aquifer. Infiltration itself will take place only when there is room (free void volume) in the ground for the water to flow into.

Soils are generally of black or grey clay, distributed in soil-groups related to altitude and slope. In the highlands the soils are mainly of light clay with good drainage and often good moisture holding capacity. The land is of high fertility rating with occasional large areas of rock and rock-outcrops. The steep escarpments are dominated by shallow and stony soils. Combined with the numerous rock-outcrops, the escarpments are poor for cultivation purposes and are responsible for the high sediment input onto the flood plains downstream. The plains have gentle slopes and are dominated by heavy clay soils with low drainage capacities. Cultivation is better than on the steep escarpments, but the occasional swampy conditions are a limitation.

Most of the precipitation over the catchment is of convective type. The rains are characterised by late afternoon thunderstorms that develop from day-long heating of the moist air mass over the lake, causing it to rise and cool into towering anvil-shaped clouds in the Nandi and Mau hills. The rains therefore start falling in these highlands and spread westwards into the lake. The mean annual rainfall for the catchment is not uniform, varying from about 1000 mm on the lake shore to more than 2000 mm in the highlands. The bulk of the storms occur over short duration but with intense capacities. Runoff concentration time is short in the upstream sub-catchments, but the flows are retarded when they arrive on the plains. The daily temperatures fluctuate between 18 °C and 26 °C, with an average day time temperature of about 22 °C, and the average daily sensible sunshine hours range from 8 in wet seasons to 12 in dry seasons.

After this preliminary information, the two specific problems on the Rivers Nyando and Kibos were studied more closely. Specific hydrological limitations of the projects were sought during the fieldwork, from which the conditions of specific



river reaches, in their present state, possible development solutions, and their hydrological impacts were studied as outlined in the following sections.

### **3.3 The Hydrological Impacts Due to Sand Mining in River Kibos**

#### **3.3.1 Introduction**

River sand is one of the resources obtained from alluvial rivers as a principal ingredient for construction concrete. But because alluvial river banks are erodible and unstable, the difficulty of moving the sand along the channels may lead to intensive use of quarries dug in channel sections close to the vicinity of a road. Since such sections provide good sites for marketing and transportation, sometimes commercial interests may overshadow conservation requirements and lead to sand mining rates that exceed limits for sustainable exploitation.

The River Kibos in the Nyando Basin of Western Kenya has been selected to illustrate this case (Figure 3.2). It rises from the pre-Cambrian granites and porphyritic-granites of the Nandi escarpment north-east of Kisumu town. With an average low flow of about  $1.0 \text{ m}^3/\text{s}$ , which may rise to more than  $20.0 \text{ m}^3/\text{s}$  during rainy seasons, the river flows for about 25.0 km before descending onto the Kano plains and eventually into the Lake Victoria. The effect of reduction in the general surface gradient can be seen along its course on the plains, where it has failed to transport most of its input sediment yield. Deposition of the sediment has resulted in a gradual growth of sand harvesting spots along the river, (Figures 3.3a and 3.3b), with significant mining practices at two sections, near the Kibos road bridge and the Nyamasaria (Nakuru) road bridge. These sections have two other river works; side bank lining gabbions at the Kibos road bridge and a grade control weir at the Nyamasaria road bridge. Although these structural measures may not have been





**Fig 3.3a** Sand harvesting near Kibos bridge.



**Fig 3.3b** Bare ground with arid-looking conditions around Kibos bridge. The road track is leading to one of the sand collection points.



initially intended for soil and water conservation purposes, they are nevertheless used here to define, on the basis of qualitative analysis, a set of possible realistic solutions for river sand harvesting and preservation, taking into account the economic and geographic constraints as well as the hydrogeologic features of the area. The particular solutions under consideration are:

- (i) in-stream sand mining with side bank lining preservation,
- (ii) in-stream sand mining with grade control preservation,
- (iii) in-stream sand mining without any preservation

Because of the economic limitations and the relative ease of working through the alluvial deposits in the river, the sand harvesting is done manually. Spades are used to scoop the sand from the river bed, which is then moved by wheelbarrows and pails into heaps at collection points (Figure 3.3a and 3.3b). Also, because of the high variation in the river discharges during wet and dry seasons, mining operations cannot be continued during rainy seasons, when the workability on the river bed is hindered by high river stage, stronger flood waves and deposition of poor quality bedload material. The location of the urban centres, Kibos and Nyamasaria, are shown in Figure 3.2, along the River Kibos. Field experiments for measuring cross-section profiles, and collecting bedload samples at the Nyamasaria road bridge section, during both rainy and dry seasons were made for comparison purposes. The sand mine stretched for about 1 km along the river, and the samples were taken at three locations in a section somewhere in the centre of the mine. An auger was used to sample the bed material from the river bed, to a depth of about 30 cm. Because the experiments were meant to compare the materials of the wet and dry seasons, sampling was done only twice. The first one was done towards the end of the dry season in March, 1993, and the other one was during the rainy season in May, 1993. The results are illustrated in Figures 3.4 and 3.5, with Figure 3.4 showing the variation of the particle size distribution, and Figure 3.5 showing the variation of the depth of fill in the cross section.

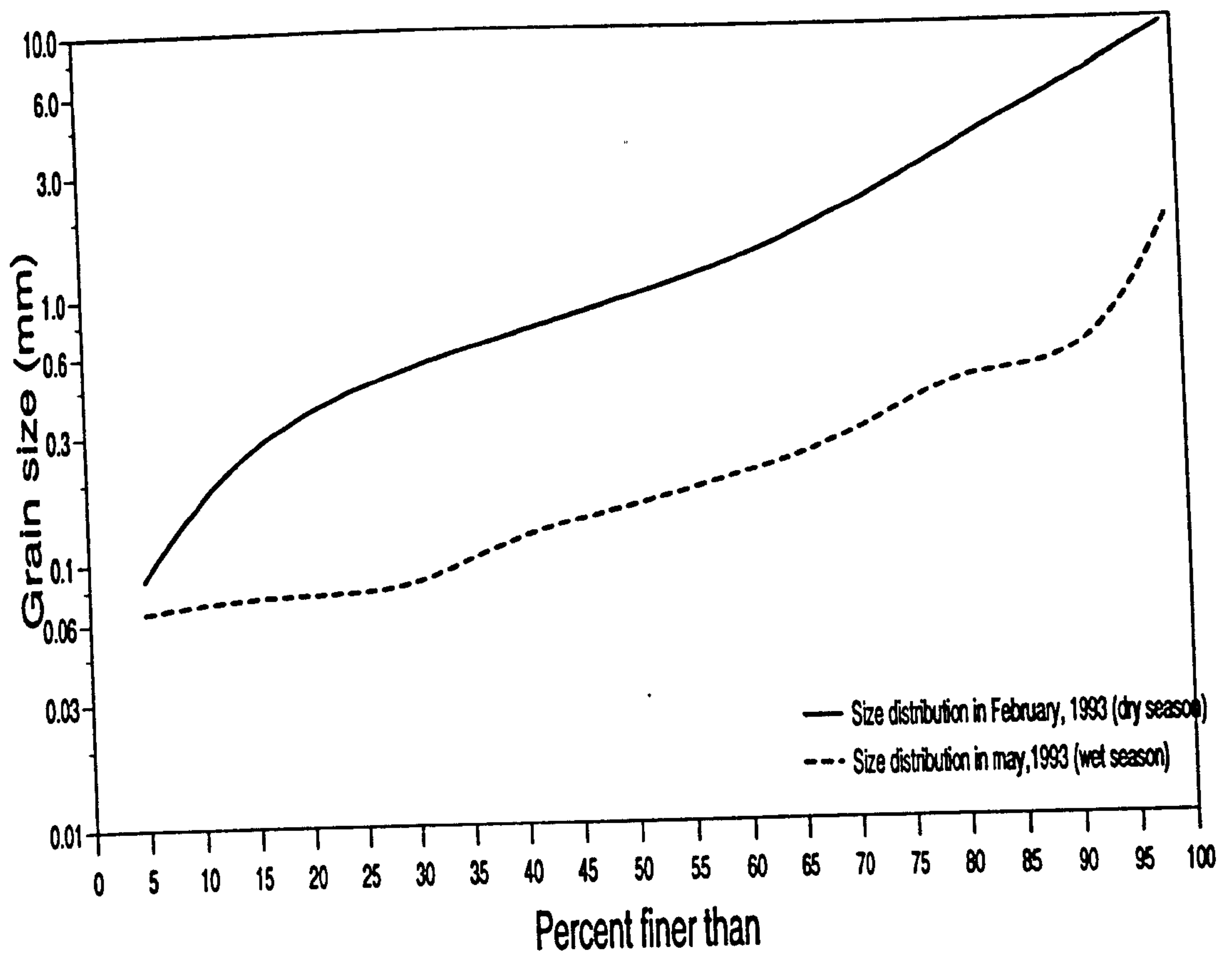


**Fig. 3.4 Particle size distribution of sediment materials obtained from the River Kibos at Nyamasaria. The samples were collected in February 1993 (dry season) and May 1993 (wet season).**

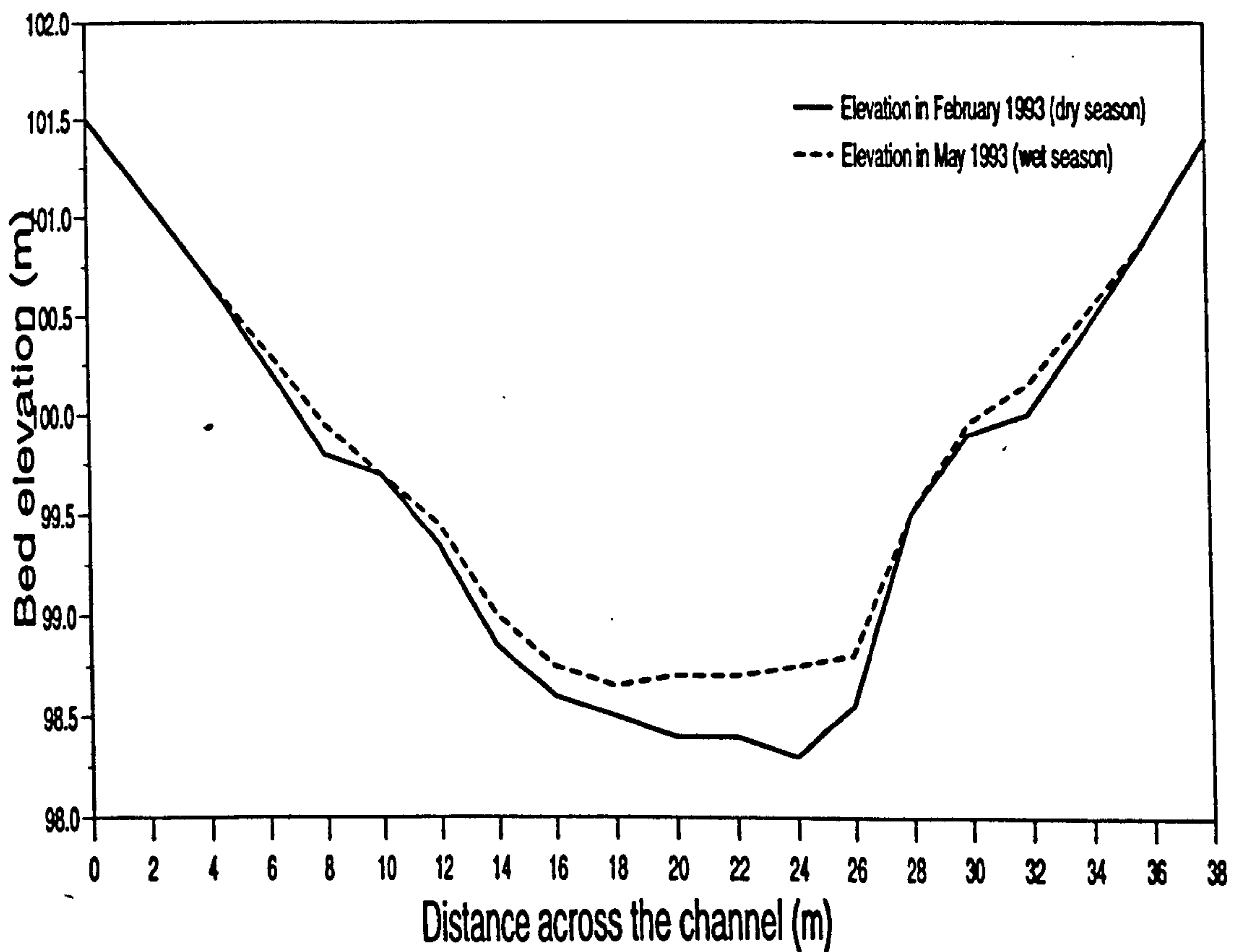


**Fig. 3.5 Cross-sectional bed elevation profiles of the River Kibos at Nyamasaria. Measurements were made in February 1993 (dry season) and May 1993 (wet season)**





**Fig 3.6a** Downstream section reach viewed from Nyamasaria bridge, showing dredged river-bed material deposited on the banks.



**Fig 3.6b** Upstream section reach viewed from Nyamasaria bridge, showing the rich riparian vegetation cover.



Whereas the  $D_{50}$  value of the particle size distribution during the dry season was about 1.0 mm, the texture changed considerably from being of good building gravel-sand aggregates to that of fine-sand with the  $D_{50}$  value reduced to about 0.15 mm during the rainy season (Figure 3.4). The bed elevation is also observed to have filled up during the rainy season (Figure 3.5). The change in the quality of the bed material may be attributed to the increased sediment yield concentration that is brought in from agricultural fields upstream, which are normally prepared towards the end of the dry season to await planting as soon as the rains start.

The change in the bed elevation was because the river was surveyed after some high flows, which may have brought in the sediments in high concentration that eventually settled in the mined depression as the high flows receded. In the background of Figure 3.6a are soil deposits on the banks of the river, showing the unwanted finer (silt-sand) materials that are dredged from the river bed after the high flows before sand harvesting can be resumed.

The aim of the sediment particle analysis was meant to illustrate that the sediment material in such sand mines is delivered from upstream sources. Data on the sediments of the area were not available, and it was not feasible to set up continuous and long-term programs to monitor the variability of the river's sedimentation processes. However, the experiment of particle size analysis was undertaken and considered to be sufficient in demonstrating that the condition of the river's bottom layer does vary with seasons. No subsequent computations and quantitative analyses were expected to be based on the results.

The term "sand harvesting or mining" has been deliberately used here in order to try and distinguish the practice from "sand quarrying", which involves digging into the river bed and banks to obtain sand aggregates from the parent geological formation of the section reach. In the case of sand harvesting/mining, only exotic sand aggregates

are meant to be tapped after they have been transported and delivered from upstream sources, irrespective of whether the parent geological material of the section has suitable mechanical properties or not.

The tendency for the grain size distribution of the bed material to increase with depth is demonstrated by Figures 3.4 and 3.5, in which Figure 3.4 is showing that the sediment particle sizes are finer in wet season, and Figure 3.5 is showing that the bed elevation is higher in the same season. This observation is noteworthy because it is part of the hypothesis for this study. It has been argued that seepage resistance, which is a function of the thickness and texture of the sediment material at the bottom of rivers, does vary with time in erodible channels - to the detriment of the fixed bed elevation assumption that is inherent in the current stream-aquifer interaction models.

### **3.3.2 Assessment of the variation of bed elevations based on the theory of rating curve analysis**

Besides the fieldwork surveys and interviews, the principle of rating curve analysis was also applied to assess the long-term effects of the mining practices on the landscape and water elevations of the section reaches. This was achieved from close observation of stage-discharge relationships, which are usually developed from graphical analysis of discharge measurements plotted on either rectangular co-ordinate or logarithmic paper to define the rating curves. Normally, a rating curve that plots as a straight line on logarithmic paper has an equation of the form:

$$Q = C (h - \alpha)^\beta \quad (3.1)$$

where  $Q$  is the discharge ( $\text{m}^3/\text{s}$ ),  $(h - \alpha)$  is the head (m) at the control section,  $h$  is the gauge height of the water surface,  $\alpha$  the gauge height of zero flow for a section control of regular shape or "effective zero flow" for a natural control of irregular shape,  $C$  is the discharge when the head  $(h - \alpha)$  equals one metre and  $\beta$  is the slope of the rating curve.

In sandy stream channels, stage-discharge relations are continuously changing with time because of scour and fill and because of changes in the configuration of the channel bed. These changes cause the shape and position of the stage-discharge relationship to vary from time to time, and a plot of stage against discharge often obscures the underlying hydraulic relationships. When combined with the influence by people, these changes impede the stream from obeying any definite relationship. However, in the present study these variations are applied to investigate the channel geometric properties of the sections, and used to conjecture about the effects of sand mining and the effectiveness of the different preservation measures.

The use of rectangular co-ordinate paper for rating curve analysis has been applied for this purpose as it is more advantageous in the study of the pattern of shifts in the lower part of the rating curve (WMO, 1980). A change in the low-flow rating curve often results from a change in the elevation of effective zero  $\alpha$ . Figure 3.7 demonstrates the change of elevation of  $\alpha$  for the Kibos road bridge section, which is easily visualised because the shift in these curves is separated by a vertical distance equal to the change in the value of  $\alpha$ .

It is also understood that falling river levels for the same discharge flow can occur as a result of varying Manning's  $n$ . But inspection of velocities of the section flows indicated that there was no definite trend to suggest changes in the average velocities of the section. Change in the Manning's  $n$  for the section was therefore insignificant.

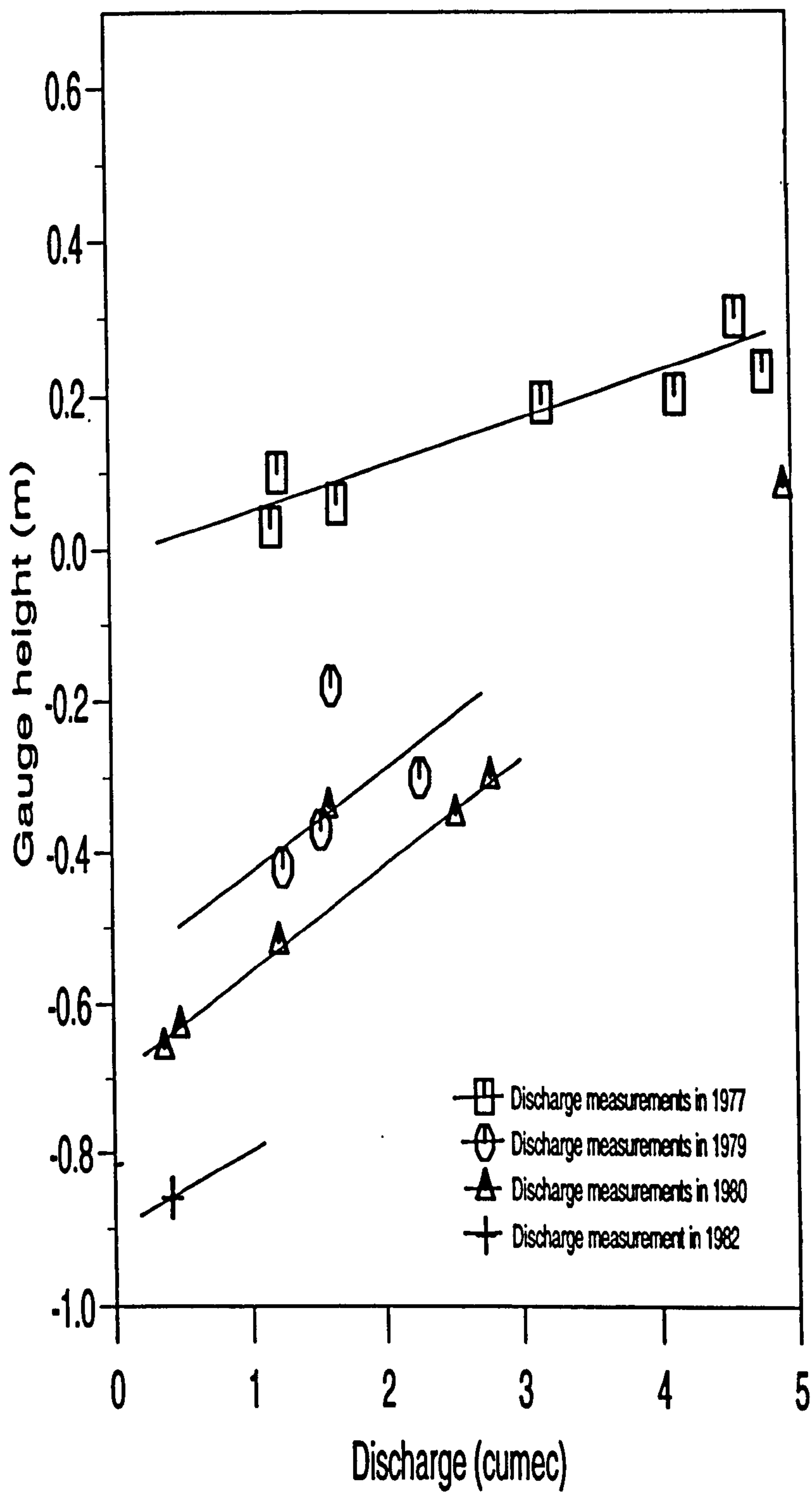


**Fig. 3.7 The rating curves at the gauging station 1HA16 (Kibos bridge), showing the falling trend of the "effective zero " flow level.**



It was also observed during fieldwork that the average width of the section had been maintained more or less the same by side-bank walls that support two bridges, the railway and road bridges, separated by a distance of about 30 m. The section was also stabilised by side bank gabbion linings. Field interviews revealed that, despite the bank linings, there had been evident degradation to the extent that the gauging staff installation was washed away some time back in 1982. Since then, no other staff has been installed at the station. Around the same time, the road bridge was destabilised so badly that by the year 1983 it had to be rebuilt again. Beyond the side bank lining protection works, the channel banks are unstable, with severe land-slide problems, as shown in Figures 3.8a and 3.8b.

A similar rating curve analysis based on data for the Nyamasaria road bridge section, which was over a weir grade control, presented a straight line on logarithmic plotting paper. Variation of the shape and position of the rating curve was negligible. It has also been found that even when the base line of a grade control section is permanent, as was the case for the control section at Nyamasaria, vegetation overgrowth and erosion/landslide of the banks within the reach commanding the control section, and back-water effects due to downstream disturbances can cause the rating curve of a given section to vary from time to time. Regarding the stability of the rating curve at Nyamasaria, therefore, it is reasonable to assume that the section reach was stabilised. Again field surveys and interviews confirmed a relatively stable reach with established bank vegetation, as observed in Figure 3.6b.

The Kibos bridge is somewhere in the middle of a reach that stretches from the Kisumu water intake station at the upstream end and the Nyamasaria road bridge at the downstream end. Based on personal observation, it was apparent that the reaches around the two ends were relatively stable, unlike the reach around the Kibos bridge. Over such a short distance of about 12 km, in the same zone of climatic and hydrogeological conditions, it is unlikely that the stretch around Kibos bridge was





**Fig 3.8a** Downstream section reach viewed from Kibos bridge, showing degraded riparian land.



**Fig 3.8b** Upstream section reach viewed from Kibos bridge, showing land slide problems on the river banks.



suffering from natural stresses. And knowing that gauging stations are normally planned and installed at relatively stable sections, it can be presumed that the falling trend of the river bed at Kibos is caused by localised human disturbances, for which sand mining was attributed the initiating cause. The improvised technique based on the rating curve data was applied to assess the variation of bed elevation around the gauging station because detailed and continuous records, such as level/contour survey, aerial photographs and satellite imageries were not available to derive long-term relationships of aggradation and degradation, or other climatically-induced changes.

Based on these field observations, it was perceived that stabilisation of in-stream sand mining sections using grade control structures was more consistent with the desire to preserve landscapes within the vicinity of the sand mines, and projection of conservation by similar control measures could be reminiscent of the river systems without the sand mining disturbances. From Figure 3.7, it is demonstrated by the falling "effective zero" flow levels that the bed elevation around Kibos bridge sand mine fell by about 0.8m during the five year period of the data analysed, despite the side bank lining preservations. This was unlike the observation at the Nyamasaria sand mine area, for which the geometrical features were demonstrated to be stabilised by the grade control weir. In the absence of better monitoring facilities, therefore, this improvised technique of rating curve analysis can be based upon to make conclusions that sand mining practices in alluvial streams can cause instability of river-banks and erosion of river-beds. In the long run the general landscape and riverine water elevations will be lowered, unless appropriate intervention such as grade control structures, are incorporated in the practice.

Lowering river levels induces groundwater depletion in that it reduces the bank storage capacity and accelerates the rate of drainage of the surrounding groundwater reserves. For instance, currently, the bore-holes at station numbers 2010 and 3550



near Kibos shopping centre dry up during dry season. In the past they have been operational throughout the year, with only seasonal fluctuation of the order of 2-4 m. In addition, the tracks and human traffic for sand collection have trampled down the bank vegetation, reduced its diversity and resilience, and compacted the flood plain to such degraded arid-looking conditions (Figure 3.3b). The impacts on the local farming community has also been negative, noting the destruction of their evergreen woodland and grazing strip along the flood plain, and deterioration of the water quality in the river. The access for their livestock to the river has also been hampered by the increased depth and slope, which the animals have to negotiate before accessing the water in the river (Figures 3.9a and 3.9b). In fact, one local farmer had reported loss of his expectant cow which slipped while trying to negotiate into the river, breaking both of its front legs. Around this place, Kibos centre, livestock grazing and drinking locations are still communal, and the commotion that takes place when various herds meet in the confining river channel is not a pleasant sight to watch, (Figure 3.9a)

By the year 1983, besides the observation in the bore holes around Kibos, Italconsult had also noted the depletionary trend of the groundwater potential in the Nyando Basin. During fieldwork, in a period of less than 3 months, the riverbed at Nyamasaria filled by about 0.5 m (Figure 3.5). The sediment material on the river banks (Figure 3.3a) illustrates the amount of dredging that occurs after the long rains in order for the miners to access the sand resource. The Rivers Nyando and Kibos are the means in which most of the water is conveyed from the areas of high rainfall, and are the main source of water for recharging the underlying unconfined aquifer on the Kano plains. It is important, therefore, that sets of more complete data, about streamflow and sediment discharge, are acquired to enable detailed quantitative analysis in order to address methods of conservation against the depletionary trend of the groundwater reserves.





**Fig 3.9a** Cows being guided into River Kibos for water.



**Fig 3.9b** Degraded riverine land near Kibos bridge, showing goats negotiating into the river.



River bed conditions have been established to be among the most influential parameters for stream-aquifer water interchange (Cunningham and Sinclair, 1979). Therefore, information about the sand mining activities, and how they are affecting the streambed condition, are needed for the investigation of the groundwater problem. It is also noted that the flood plain still experiences inundation and water-logging conditions during the rainy season, (section 3.4; and The Daily Nation, 27/4/94). This means that the water yield from upstream during rain season is high enough to fill the storage capacity of the underlying aquifer. For the average annual water table(during dry season) to be falling, it can be assumed, therefore, that it is the drainage rates of the groundwater that are increasing, rather than a reduction in the amount of recharge. This presumption of accelerated drainage still points at the need for investigation of the changes being induced on the riverbed (river stage) conditions.

The sand miners, in defence, put the blame of land degradation on the local farmers, whom they accuse of over-grazing, over-cultivation and deforestation of the riparian vegetation for building-posts and fuel-wood. The accusations and counter-accusations between the two groups are so full of tension that their co-operation for interviews and experimentation for this study was lost due to suspicion and lack of trust as to whom the research findings were meant to benefit or disadvantage. The mistake, as it was learnt later, was to be seen talking/working with the other rival groups. However, although a great deal of information on Kibos could not be obtained, the experience there became a lesson on how to interact with the local communities in order to obtain more tips and assistance about the hydrology on the other sister river, the Nyando. In the meantime, utilisation of the resources on the Kibos remains a matter of rushed competition among the rival groups.

Another lesson learned from the experience on the Kibos is that even with such obvious examples of land degradation in the field, but without adequate knowledge

and tools to demonstrate the possible causes and parties responsible, it is difficult to communicate to the local people about the damage they may be inflicting on their own resources. In particular those who depend on the river for their livelihood are continuing to utilise the river resources unabated. This stubborn attitude is frustrating the field instructors for soil and water conservation such that their preaching for sustainable utilisation of the river is now in limbo. But in all conscience, the river system should be rehabilitated to promote bank storage and restore the riparian vegetation. If possible, rather than complete prohibition from using the river, appropriate interventions should be sought with the aim of sustaining its utility values. This requires tools like mathematical models for easier and faster prediction, and assessment of the likely effects of the river development alterations to flood wave attenuation, bed-load transport, bank storage and groundwater recharging potential.

Although this analysis has, to some extent, managed to show some of the hydrological effects due to river sand mining, and how grade control structures can be corrective, such assessment results are better off when provided well in advance, because once the degradation has started, it may require many years to repair it, besides the high costs involved. A generalised theoretical approach of predictive evaluation of in-stream sand mining impacts, and mitigation interventions will be analysed with the help of the MASAI in chapter 6.

### **3.4 A Review of Flood Mitigation Alternatives on the Nyando**

#### **3.4.1 Introduction**

In nearly all of the rivers in the lake basin, floods occur in the low-lands during rainy seasons, with the Rivers Nyando and Nzoia posing the greatest danger because they



drain large low lying plains which are also heavily populated. Problems associated with the floods include: disruption of human settlements, crop and livestock damage, disease outbreaks and destruction of infrastructure. With the River Nyando's wider upstream catchment, which has higher rainfall intensity, higher density of tributary systems and steep slopes, it means that the river has all the impetuses for the flooding problems posed on the plains downstream. The low river bed gradient on the plains is also another limitation, in terms of the power for the river to clear and transport most of its bed load arriving from the highlands, which with time is incapacitating the river channel in relation to the incoming discharges. The flooding and water logging problems on the Nyando have thus become annual events and it is only the degree of damage that varies from one year to another.

The first worst recorded floods on the Nyando occurred in 1961, and ever since, serious flooding problems have been experienced on several occasions causing public outcry from all over the country. In response, the government has commissioned a number of consulting firms to carry out feasibility studies and establish the possibility of developing the river systems so that the local community may harness the benefits from the river resources, rather than be plagued by the same. Some of the main consulting study reports are by Sir Alexander Gibbs and Partners (1963), TAMS Engineers and Architects (1980), WLPD consultants (1983), and Italconsult (1983), among others. Besides the studies, other continuous water resources development programmes are being run by government agencies like the Lake Basin Development Authority (LBDA), National Irrigation Board (NIB), Ministry of Agriculture and Ministry of Water Development departments.

In all of the studies, the river's flooding phenomenon has been singled out as the main cause of distress in the region, while at the same time it stands out as the main asset that, if properly managed, could be the main stimulant of development activities in the region. In fact, it was as a result of the first study by Sir Alexander Gibbs and

Partners that led to the establishment of the two irrigation schemes viz., Ahero Pilot scheme (840 ha.) and West Kano pilot scheme (870 ha.). Other major proposals that have been identified on the river system include hydropower generation from the flows cascading down the escarpments, and land reclamation of the marshlands and swamps. As such, a number of development alternatives to tame the Nyando have been proposed. This section reviews the main proposals, which include: embankments and flood warning systems; regularisation by drainage and training; and storage reservoirs. Finally, the difficulties and conflicts involved in flood control projects are highlighted, borrowing on the experience of the 1993 summer floods on the Mississippi.

### **3.4.2 Embankment and flood warning systems**

Over-topping of river banks on the Nyando occur at fairly low discharges, especially in the last 8 - 12 km from the lake shore. From Figures 3.10a and 3.10b it can be seen how the flood discharge capacity is limited for this area, and how certain homes are prone to flooding - like the one in the background of Figure 3.10a. The photographs were taken at the beginning of the rainy season, with the streamflow measurement in Figure 3.10a giving a discharge flow rate of only 22.17 m<sup>3</sup>/s, yet the river stage was only 0.92 m below the flood level (land surface elevation). The flooding frequency in the area can also be perceived by considering the annual maximum floods in Table 3.1, while recalling that at the low flow rate of only 22.17 m<sup>3</sup>/s, the river was only 0.92 m below the flood level. In view of these, embankment dikes have been proposed to guide the river safely into the lake. The first phase will involve works to provide protection against a 25 year return period flood, of discharge 476 m<sup>3</sup>/s and depth of 2.5 m. The embankment will stretch over a distance of 24 km, from about 560 m upstream of the river gauging station RGS 1GD3, down to some 6 km downstream of the Ahero road bridge-





**Fig 3.10a** Discharge measurement on the River Nyando, on the upstream of the Ahero bridge.



**Fig 3.10b** Downstream section reach of the Nyando viewed from the Ahero bridge, showing the proximity of the flood plain to flooding.



virtually where the marshes start. Phase two will involve the same stretch, but to cater for a 50 year return period flood, of a discharge of 551 m<sup>3</sup>/s, and to raise the Ahero bridge so that it can pass the same flood. The current bridge was designed for a flood discharge of 300 m<sup>3</sup>/s.

**Table 3.1 Annual maximum discharges at the gauging station 1GD3 on River Nyando**

Year	Annual maximum recorded discharge (m <sup>3</sup> /s)
1969	65.5
1970	179.2
1971	113.6
1972	204.5
1973	154.0
1974	283.5
1975	179.2
1976	65.5
1977	353.4
1978	194.5
1979	323.0
1980	170.5
1981	137.5
1982	199.5
1983	106.5
1984	36.5
1985	254.0

Even with the embankments in position, absolute prevention of flooding cannot be guaranteed. Early warning systems will have to be established to enable the people



downstream to be notified in good time of a prevailing flood. River gauging infrastructure within the reach need improvement. Since the discharges cascading from the escarpments arrive with such high momentum and velocities, means of fast communication are essential for safe operations. Telephone and radio contacts are required while a vehicle would be an additional advantage. Automatic recorders, possibly with computer linkage facilities for data recording and analysis could be ideal, but the present automatic recorder at the RGS 1GD3 has so far been unsatisfactory. Frequent blockage by the high sediment concentration in the river, invasion of the recording mechanism by bee insects and inaccessibility by the technical staff during the rainy season has often rendered the high precision and expensive recorder inoperational during the critical times when it is needed most. A test unit could be set at a place like Ahero bridge , to where the technical staff can have access at any time throughout the year, for continuous monitoring, servicing, and comparison of its data with the data from staff gauges, before considering establishment of a full network. From experience with the field gauge recording men, it can be said that their records are not good enough for time-dependent operations. This is because on several occasions when surprise visits were paid, they were found to be mixing their work with other social activities, and often recorded the water levels without a watch for noting the time.

However, the RGS 1GD3 has previously provided relatively good and regular data for the general purposes of engineering hydrology. For instance, the Irrigation section of the MOWD have used data from the station to estimate the design peak discharges with return periods of 10, 25, 50, and 100 years around Ahero as 375, 476, 551, and 624 m<sup>3</sup>/s, respectively. The values were obtained from yearly maximum water levels recorded at the station for the period 1969 - 1985, using a rating curve established by the MOWD and Gumbel's extremal value distribution. The data are tabulated in Table 3.1, from which the plot in Figure 3.11 was obtained.

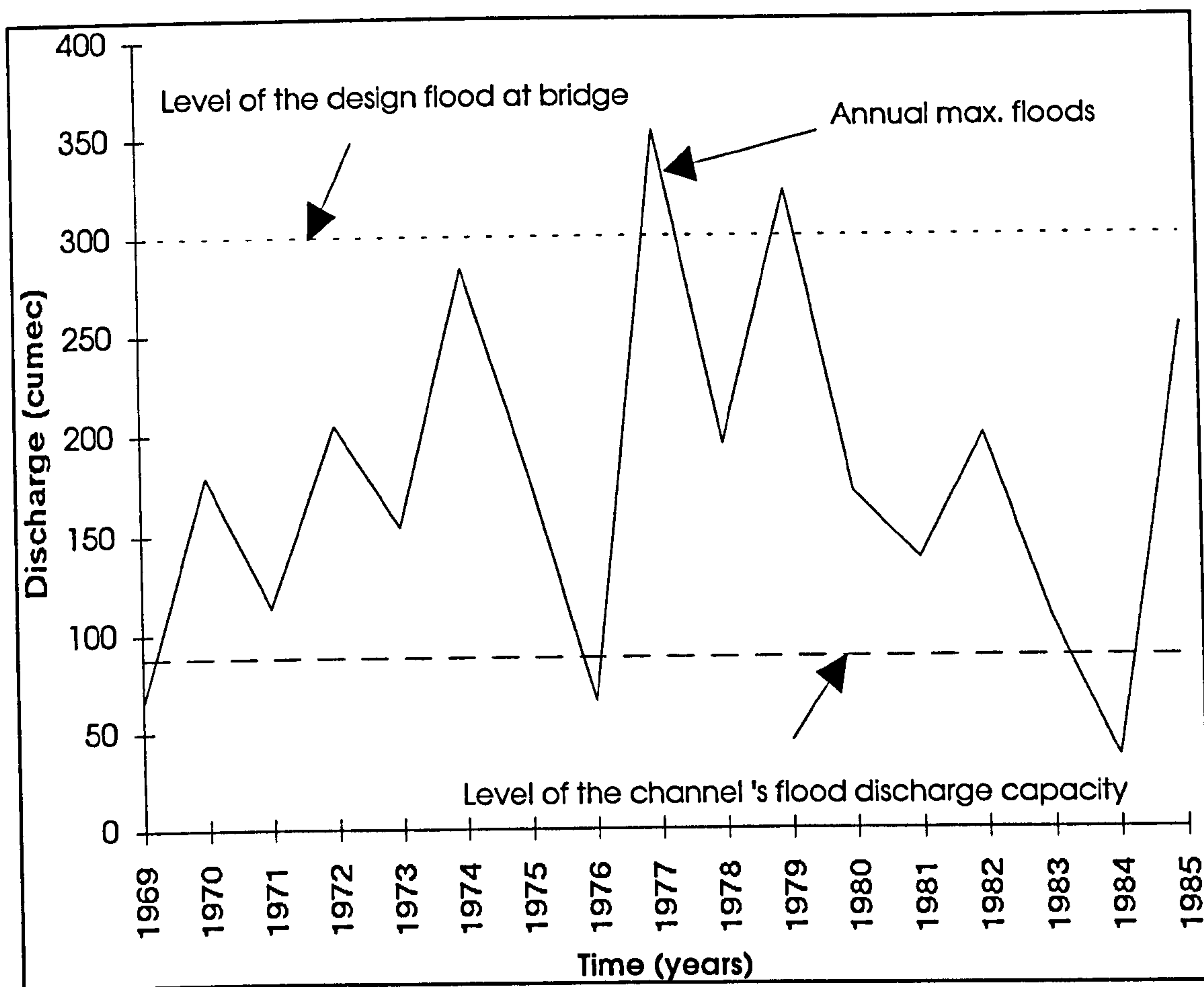


**Fig. 3.11 Annual maximum flood discharges at the gauging station 1GD3 near Ahero on the River Nyando**

The flood discharge capacity in the same river channel, around Ahero, was computed as described below.

*Computation of the flood discharge capacity for the Nyando River channel at Ahero:*

Although flood flows are spatially varied and unsteady, from a practical viewpoint, the slope-area method can be used when a peak flow discharge is required and the data available are not sufficient to justify the use of more sophisticated techniques. For instance, slope-area techniques have been used to estimate unsteady events such



as flash floods in arid regions where both streamflow and precipitation records are essentially non-existent (French, 1986).

From the cross-sectional and longitudinal profiles surveyed during the fieldwork, the geometrical properties of the channel at two adjacent sections around Ahero were as follows:

upstream cross-sectional area	$A_u = 72 \text{ m}^2$
upstream wetted perimeter	$P_u = 26 \text{ m}$
upstream Manning's coefficient.	$n_u = 0.040$
and so, upstream hydraulic radius	$R_u = 72/26 = 2.77 \text{ m}$
and upstream conveyance	$K_u = \frac{72(2.77)^{2/3}}{0.040} = 3550 \text{ m}^3/\text{s}$
downstream cross-section	$A_d = 76 \text{ m}^2$
downstream wetted perimeter	$P_d = 34 \text{ m}$
downstream Manning's coefficient.	$n_d = 0.043$
and so, downstream hydraulic radius	$R_d = 76/34 = 2.24 \text{ m}$
and downstream conveyance	$K_d = \frac{76(2.24)^{2/3}}{0.043} = 3026 \text{ m}^3/\text{s}$

Therefore, the geometric mean conveyance for the reach,  $K = \sqrt{K_u K_d} = 3278 \text{ m}^3/\text{s}$ , and the percentage change in conveyance through the reach is,  $100 \frac{(K_u - K_d)}{K_d} = 17 \%$

which is less than 30%, the limit for acceptance of the slope-area method in the estimation of flood discharges (French, 1986).

The distance between the two sections was 4982 m, and the slope of the water surface under steady state was 0.0007, meaning the fall in water surface elevation between the two sections was 3.487 m.

So, estimation of the energy slope at steady-state is;

$$S_f = 3.487/4982 = 0.0007$$

or head loss at steady-state is;

$$F_d = 3.487 \text{ m.}$$

Thus, the discharge at steady-state is;

$$Q = K (S_f)^{1/2} = 3278 (0.0007)^{1/2} = 87 \text{ m}^3/\text{s}$$

Because the reach was expanding, ( $A_d > A_u$ ), a factor of  $k = 0.5$  may be assumed. Substitution of the head loss  $F_d$ , and the mean velocity of flow for  $Q$  into the friction head loss equation gives:

$$h_f = F_d + k \left( \frac{V_u^2}{2g} - \frac{V_d^2}{2g} \right) = 3.493 \text{ m}$$

so that the next friction slope estimation  $S_f = 3.493/4982 = 0.0007$ ;

from which the next discharge estimate is  $Q = K(S)^{1/2} = 87 \text{ m}^3/\text{s}$ .

Therefore, the flood discharge capacity of the channel reach at Ahero is about 87 m<sup>3</sup>/s. Inclusion of this channel discharge capacity in Figure 3.11 illustrates the average flooding frequency at Ahero, which occurs in every year that has its annual maximum flood discharge above the 87 m<sup>3</sup>/s discharge level. The frequency of disruption to traffic using the Ahero road bridge can also be observed from the same figure, which occurs whenever the flow discharge is above 300 m<sup>3</sup>/s, the design flood discharge of the bridge. From the figure, it is apparent that the flood discharge capacity of the channel of the Nyando River at Ahero is limited. Therefore, the embankments are necessary for protecting the area. This development, and other impending alterations on the river would benefit from mathematical modelling, which have emerged as necessary tools for predictive evaluation of hydrological responses to such changes.



### 3.4.3 Drainage and training

Opening up of the river mouth and construction of a number of drainage and training channels have been proposed to allow for an easy outflow of water from within the river basin to the lake. The Nyando flood plain may be considered as a natural drainage alignment divided into two general parts with different drainage characteristics. The upper part, extending from the foot of the escarpment (1GD4) up to Ahero, is well drained and its streamflow has enough momentum to clear and transport most of the input sediment yield through the reach (Figure 3.2).

From around Ahero towards downstream, most of its stream-power is expended and the resulting low velocity flows start depositing their bedload materials, which with time are creating scattered aggregate accumulations and swamps along the course of the river. Around this transition line (the area along a straight line joining Ahero and Kibos), there is the central Kano swamp, from which other streams like Ambey and Miriu emanate. That is, the lower part of the plains covers a vast fairly flat area, bounded on the North by the central Kano swamp, to the West by Kibos river, to the East by the Nyando swamp and to the South by the lake.

In a hydrogeologic system like the Nyando, where the river is hydraulically connected to its flood plain aquifer, a flood wave traversing through the system is bound to be attenuated or accentuated, depending on the position of the groundwater level in relation to the river stage. Figure 3.12 is a plot of the variation of the river stage at Ahero against the adjacent water table recorded in the bore hole at the Ahero Catholic Mission.

Figure 3.13 shows the hydrographs obtained from the daily discharges at the gauging station 1GD3 (upstream) and at Ahero road bridge (downstream). It is observed that

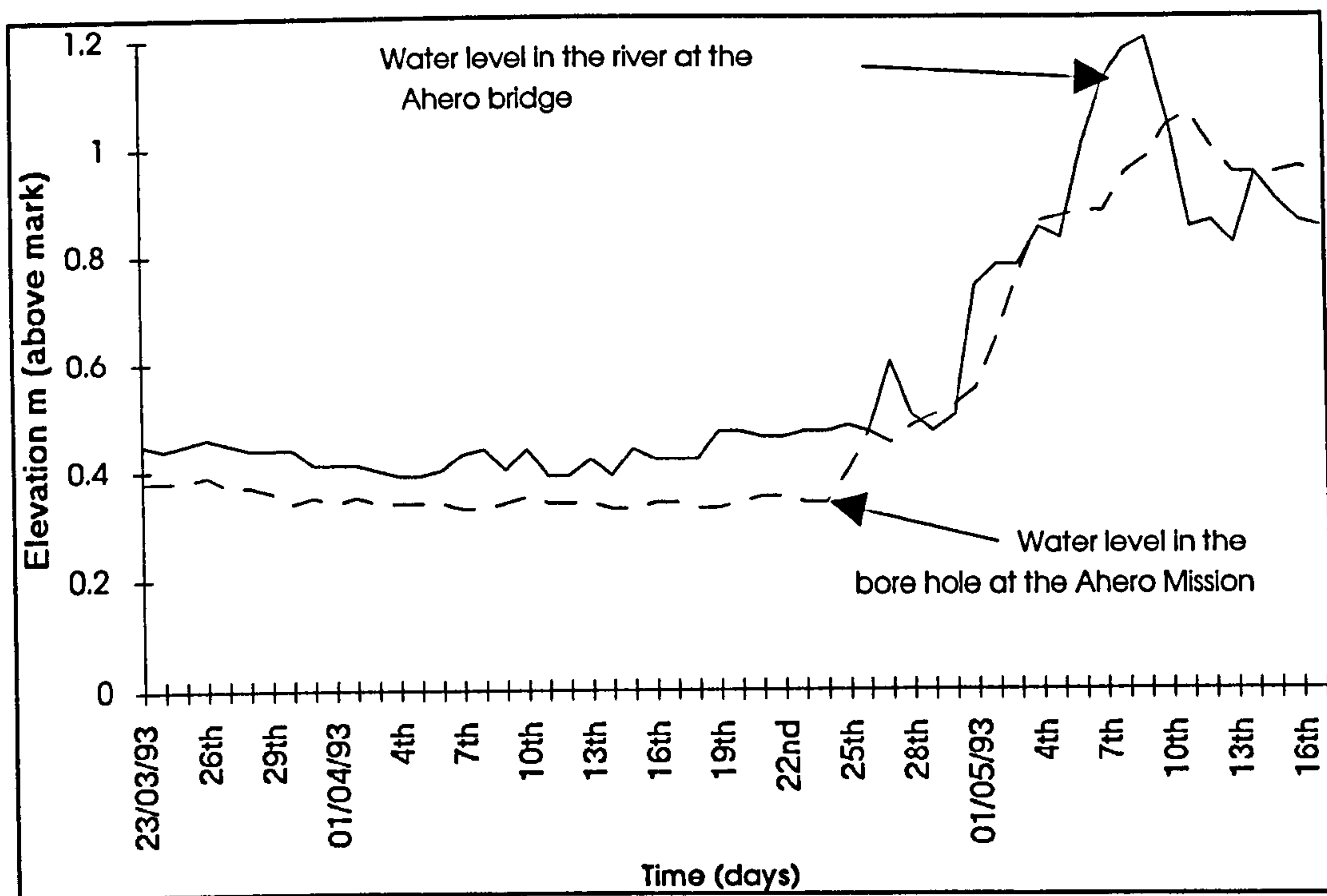


**Fig. 3.12 Variation of the water levels in the bore hole at the Ahero Catholic Mission and in the River Nyando at Ahero bridge**

the influence of the river on the bank storage, which is approximately equal to the difference between the upstream and downstream hydrographs, can range from negative to positive values. The assumption during calibration that a reach is purely effluent or influent, as is normally assumed in river routing models, can therefore be a source of error if such models were applied for flood routing estimation on the Nyando. It can also be seen that the effect of the effluent/influent phenomenon on floods passing through the Nyando is time-dependent, so its proper representation in hydrological computations is important.

The River Nyando does not flow directly into the lake, but through a vast swampy area. Therefore, most of the effects of the lake levels are expected to be expended by the marshes, and have little influence on the river levels upstream. However, there are no field data from which distinctive relationships can be derived for: linking the lake levels and river levels; establishing rainfall-runoff models; evidencing increased



over-bank sedimentology and flooding; relating fish production to flooding; assessing the importance of fish production; and evaluating the ecological values of the marshes. Field programs to measure and monitor the variables and parameters involved were not feasible, and were beyond the scope of this study.

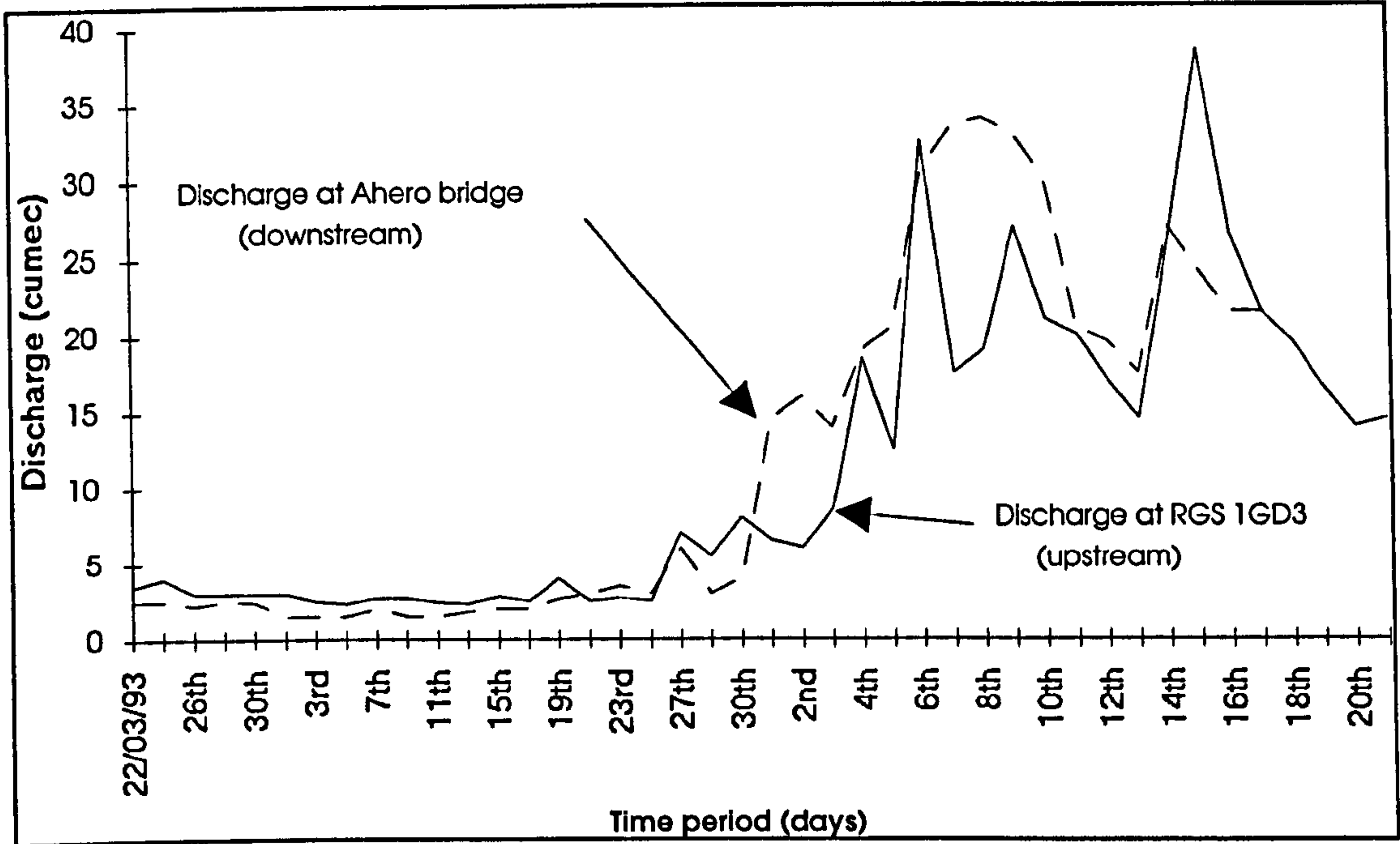


**Fig 3.13 Daily discharge hydrographs at the gauging station 1GD3 (upstream station) and at Ahero bridge (downstream station) on the River Nyando.**

Nonetheless, the proposed improvement works involve regularisation of the present river cross-sections in terms of design discharges, and increase of the longitudinal gradient by river training works to straighten the river courses at some bends and meanders. Observing that the Nyando river does not currently flow directly into the lake but merges with the water of the swamp at its confluence with the other rivers Nyaidho, Awach and Asawo, it is expected that its training works in general, and opening up of the delta swamp in particular, will affect much wider aspects of the overall hydrology of the Kano plains. The cut-offs will increase the general gradient of the river, which will eventually increase the streamflow velocity, lower the river stage, and reduce the bank storage. Channelling to open up the mouth of the Nyando means that the river will be more directly connected to the lake, and its flow will be

exposed more to the effects of the lake level variations. Application of appropriate mathematical models, incorporating the intended manipulations and boundary conditions (e.g. changed downstream boundary condition in the case of regularisation of the delta marshes) will provide, beforehand, useful results for evaluating the overall hydrological implications on the flood plain.

#### **3.4.4 Storage reservoirs**

About 23 locations on Nyando and one on Kibos have been identified as suitable sites for water storage reservoirs to ease the flooding threat downstream. However, according to Italconsult (1981), the maximum reduction of flood flows on the plains would be obtained with the construction of the two dams furthest downstream on the Nyando and Ainobngetuny tributaries, sites 8 and 5 respectively (Figure 3.2). The study has investigated the extent to which the two reservoirs could reduce the flooding menace on the flood plain, using the flood discharges measured at RGS 1GD2 to be representative of the situation at dam site 8, and flood discharges at RGS 1GB5 as representative for the situation at dam site 5, while the floods at RGS 1GD4 were taken to be representative for the area to be protected. For a given flood, ratios were obtained between discharges at 1GD2 and 1GB5 on one side and that measured at 1GD4 on the other side, taking into account the time difference between the peaks (Delie, 1985). The same procedure was applied to compare stations 1GD5 and 1GB8 with 1GD4. The variation of the ratios of the floods are shown in Figure 3.14, and the results of the computations are illustrated by the following examples:

For  $Q = 100 \text{ m}^3/\text{s}$  at 1GD4;     $Q = 70 \text{ m}^3/\text{s}$  at 1GD5 (on Nyando tributary)  
 $Q = 30 \text{ m}^3/\text{s}$  at 1GB8 (on Ainobngetuny)



Of this discharge  $10 \text{ m}^3/\text{s}$  (10 %) could be contained by a dam constructed at dam site 5 (on Ainobngetuny tributary) and  $54 \text{ m}^3/\text{s}$  (54 %) could be contained by a dam constructed at dam site 8 (on Nyando tributary). This is in the case of the reservoirs having maximum capacities to accommodate the flood volumes. Hence the remaining flood arriving at 1GD4 would be  $36 \text{ m}^3/\text{s}$  (36 %) of the original volume.

For  $Q = 350 \text{ m}^3/\text{s}$  at 1GD4;  $Q = 175 \text{ m}^3/\text{s}$  at 1GD5 (on Nyando tributary)

$Q = 175 \text{ m}^3/\text{s}$  at 1GB8 (on Ainobngetuny)

Of this flood discharge only  $19 \text{ m}^3/\text{s}$  (5 %) could be contained by a dam constructed at dam site 5 and  $145 \text{ m}^3/\text{s}$  (41 %) could be contained by a dam at site 8. Hence the remaining flood at 1GD4 would be  $186 \text{ m}^3/\text{s}$  (54 %) of the original volume.

For values of floods exceeding  $350 \text{ m}^3/\text{s}$  at 1GD4, the percentage contribution of the Nyando main channel is reduced further and so is the percentage of the discharge which could be contained by a reservoir at dam site 5 (Figure 3.14). This can be explained by the fact that the part of the Ainobngetuny basin, with highest rainfall, lowest permeability and steepest slopes lies just adjacent to the confluence of both rivers. During low flow periods the Nyando sub-basin, which is much larger in size, contributes a corresponding larger proportion of the total discharge at 1GD4. But during storm floods, runoff contribution from the Ainobngetuny sub-basin rises much faster to match or even surpass the contribution from the Nyando channel. The construction of a dam at site 5, therefore, will have less effect on flood discharges in the area to be protected. Dam at site 8 proves to be more suitable for flood protection as well as for irrigation and hydropower purposes, but both surface geological investigations as well as the information provided by the existing geologic maps show the valley bottom to be covered with a very thick alluvial deposit, which could cause serious difficulties for the construction of the dam. Detailed data and investigations are

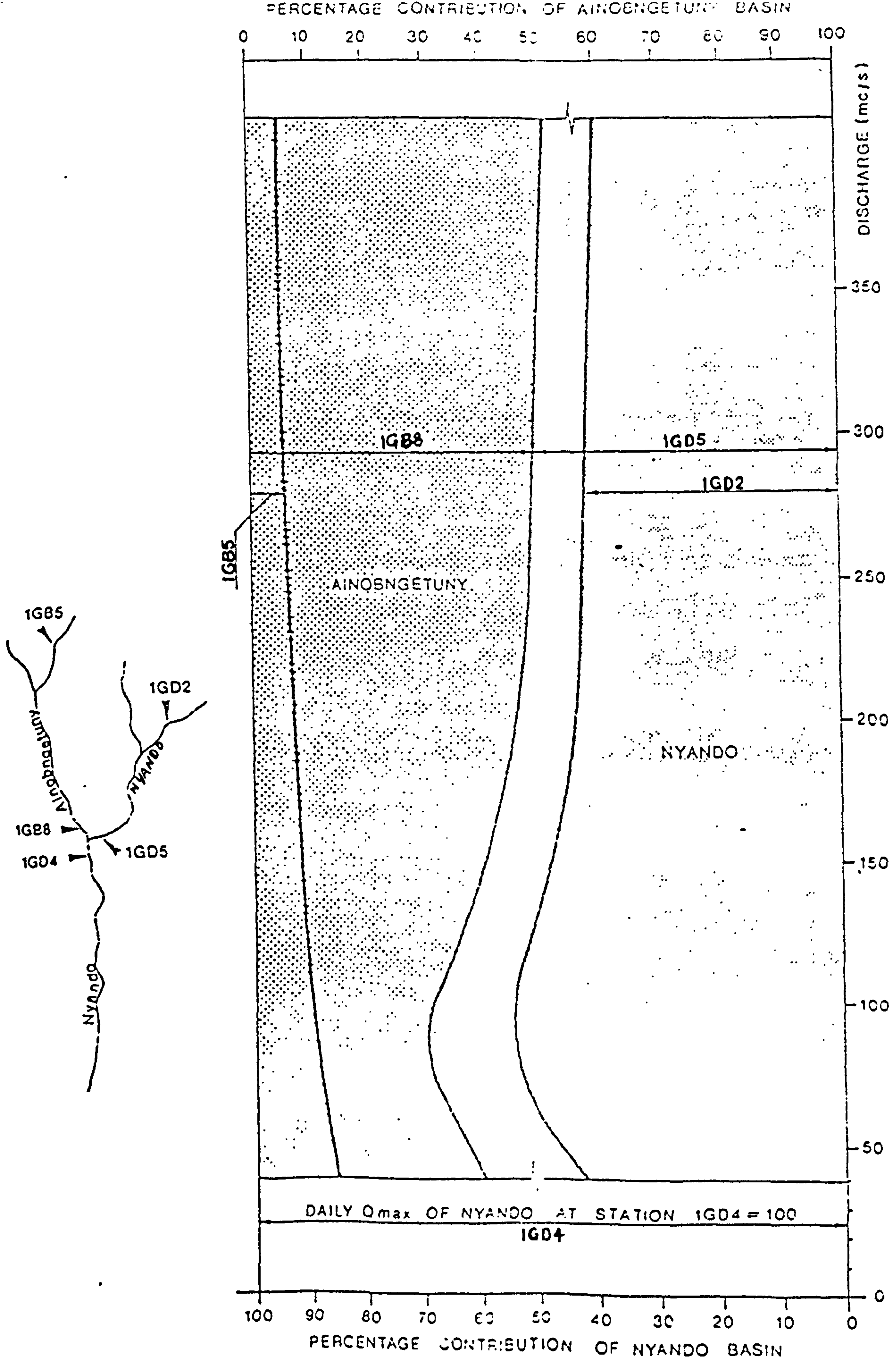


**Fig. 3.14** Variation of flood discharge contributions from the Nyando and Ainobngetuny Basins (Source: Delie, 1985)



still needed to assess the feasibility of the dam to store water, or recharge the alluvial deposits in the river valley.

However, if the dam was constructed as envisaged, it is reasonable to assume that for the relevant  $Q_{25}$  and eventually  $Q_{50}$ , (476 m<sup>3</sup>/s and 551 m<sup>3</sup>/s, respectively), the flood discharges in the area to be protected would be reduced by about 35 - 40 %, in the case of maximum flood protection at the dam site. But even under these measures, recalling that the computed flood discharge capacity of the channel at Ahero is only 87 m<sup>3</sup>/s, it can be seen that flood control by the reservoir alone cannot suffice. On this basis, bank embankments will still be required to augment the protection by the storage reservoir. When the flood defence system has both the embankments and the reservoir, a reduction in the height of the embankments of about 0.4 - 0.5 m can be saved for the system to meet the same requirement as when it was without the dam. The cost saved on the embankment in this way is far less significant when compared with the cost of putting up the dam. It is therefore not worthwhile building the dam for flood control purposes alone.

Nevertheless, should it be viable to construct the dam for other purposes such as irrigation and hydro-power generation, account could be taken to reserve a certain amount of storage capacity for flood waters, which would increase the safety of the embankment system. Under this new set-up, the need of a mathematical model is necessary for the prediction and evaluation of the effects of the new system conditions (e.g. reservoir hydrograph releases, irrigation distribution systems and sediment yield interception by the dams) to the flood plain hydrology and the river channel degradation/ aggradation below the dam.

But in overall, flooding has been acknowledged as a natural flood-plain enrichment phenomenon, when sediment materials and minerals are deposited from receding flows. The surrounding unconfined aquifers also depend on the flood flows for their

replenishment. With regard to these, complete prevention of flooding on the plains (if it was possible) would be conflicting with the desire to maintain the balance of nature in the region. On the other hand, complete evacuation of farmers and prohibition of economic activities within the flood plains to allow for flooding to take place would be conflicting with the wishes to enhance productivity in the area. The optimal solution, therefore, appears to lie somewhere in between, where flooding can still be permitted to some degree, but mitigated by a scheme operating on a real-time basis so that the plains can still be utilised for agriculture, grazing, and harvesting, etc., depending on safety predictions by flood warning mathematical models.

### **3.4.5 Difficulties and conflicts in flood control projects**

The difficulties in river engineering for flood control projects can be envisaged by considering the experiences on the Mississippi. Following the summer rains of 1993, the Mississippi, one of the most heavily engineered river in the world, burst its banks in devastating floods. In fact, the disaster has emerged as a proof for environmentalists to claim that river engineering does not work, and that it actually increases the flood levels. The amount of mistrust can be visualised from the following quote: "Engineers regard nature as their enemy and so they are at war with the rivers, and so they want to try to control them, in their arrogance. They want to play God. But they cannot succeed," (Blackwelder in BBC Horizon, 1994)

Before it was tamed, the Mississippi shifted its channel constantly. A Board of Engineers was created by the General Survey Act in 1824 with the most urgent need being to render navigation. To clear a navigable route, the Mississippi had to be deepened to at least 3 m throughout its entire length. In 1879, the Congress established the Mississippi River Commission, which included the Army Corps of



Engineers, with the responsibility of flood control in the Mississippi, besides navigation (Rasmussen, 1994). To maintain the 3 m depth, the engineers built dikes and levees to narrow the river and protect the plains from the floods. To speed up the water in the river, lower the flood levels and shorten the shipping route, the engineers straightened the river by cut-offs to bypass some meanders. By 1942, for example, the Mississippi was 240 km shorter than its original length. To cope with exceptional floods, the Corps had to build dams such that by around 1980, more than 200 flood control reservoirs were built. Besides the structural works, the Corps also realised the environmental impacts of the developments to the river. They set up programs to implement environmental matters. For example, in 1934, the Fish and Wildlife Co-ordination Act was passed, directing federal agencies on how to make use of impounded waters. In 1987 the Environmental Management Program (EMP) was established. Among other things, the EMP was to realise long-term data collection, evaluate and provide solution for short-term problems and construct and evaluate habitat projects.

But the Mississippi is such a dynamic system that keeps adjusting against the engineering and conservation works. By 1993, for instance, it was taking around \$180 million a year just to maintain the control structures and rectify the problems the river kept "throwing" up. However, by controlling the river, it was acknowledged that the engineers set the stage for an economic wonder. Cities, industries, farms etc., were established, which could never have been realised without the river engineering interventions (BBC Horizon, 1994).

Then in summer 1993, it rained heavily. The reservoirs filled up, the levees broke, farmlands were inundated, crops and livestock were lost and towns were flooded. That is, after more than 100 years of battling to control the Mississippi, nature triumphed over the river engineering works. And all too quickly the cry went up that engineering just does not work.

One clear point indicated by this example of the Mississippi is that once river engineering works have been started, one has got to be ready to keep building and repairing. The example has also shown that besides the capital costs of setting the river works, the maintenance costs to sustain the engineering and environmental systems are also substantial. Most major development projects in Kenya are based on loans or grants, which do not necessarily account for the subsequent maintenance costs. Even the engineers who install the projects, in most cases, are expatriates who may not stay to maintain the systems after the installation. Therefore, the report about the experiences on the Mississippi is very valuable, especially for those considering the funding and expertise of the river engineering projects that have been proposed.

In Kenya, since commissioning of the consultant studies (e.g. Sir Alexander Gibbs and Partners (1963); TAMS Engineers and Architects (1980); etc.) on the Nyando, the government has realised the continuing degradation and desertification of land due to bad land use and river engineering activities. It has stepped up its campaign to seek solutions for management of its natural resources, in particular optimal allocation of water resources between the environment and other development needs. In other words, the natural environment is now recognised as a legitimate demand sector in the allocation of water resources. The formation of the Permanent Presidential Commission on Soil and Water Conservation and Afforestation in 1981, to spearhead the campaign on conservation of basic resources nation-wide is a confirmation of the government's commitment to the ideals. In the case of the Nyando, where there is competition between various sectors for its limited resources during dry seasons, and flooding hazards during wet seasons, it is necessary that environmental values are estimated reliably so that environmental claims and land reclamation can be made equitably.



In particular, the aquatic and related ecosystems on the Nyando flood plains are endangered alternately by the growing demand for its water, sand and vegetation during dry periods and water logging and pollution during rainy seasons. But the economic development and flood control programmes being attempted may not sustain the river's ecosystems unless the particular degradation causes are identified and addressed in the initial planning stages. One of the biggest requirement for water in a river system is for the maintenance of riparian conditions. The requirement includes non-consumptive flows, such as seasonal flooding to "sow" mineral sediments on the flood plains, promote the seepage of minerals in solute form into the root zone, leach out the unwanted excess salts, promote germination and provide a regime to maintain diversity, and provide consumptive use requirement for transpiration.

Considering the dynamics of biotic aspects of ecotones, the driving force is the hydrological system described by the mean annual discharges and the superimposed fluctuations of floods or low flows in the river, and the water table distribution in the neighbouring aquifers. Riparian ecotones buffer the water quality and contribute to a smoothed discharge (Pinay and Decamps, 1988), but on the other hand their dynamics are strongly dependent on the hydrologic fluctuations of the river. In addition to the geological information given that the Kano plain was formed by the fluctuations of the rivers of the area during the formation of the Kavirondo Rift Valley, it should also be emphasised here that even today, the physical conditions (hydrology and fluvial morphology) are still the dominant determining factors for the biological units of the river systems. According to Brookes (1994), stream and flood plain communities are controlled by both physical and biological systems, and the interaction of the aquatic system with the terrestrial system is essential for the biological diversity. This is also the case for the variation of physical parameters at different scales in position and time. So, the spatial and temporal fluctuations of these parameters (river bed levels, sediment yield, water table, river courses, flood

level and frequencies, etc.) in the present state of the Nyando system, and how they are being/going to be changed, have to be addressed and included in the development studies if sustainable developments in the area are to be realised.

However, before adopting any given river engineering system, it is desirable to make a priori assessments of the impacts of the project to the riparian hydrology and ecosystems. Mathematical and conceptual models can be helpful in this respect. For example, a simple ecological valuation method has been suggested (Appendix 4), which can be applied to correlate the effects of the riparian ecosystems to the average annual river (or water table) levels. The MASAI, on the other hand, has been calibrated and applied for predictive evaluation of the hydrological and fluvial impacts that would result, following the river training alterations that have been proposed for a section reach on the Nyando River near the NIB village at Ahero. The results are discussed in chapter 5.



## **4. ANALYSIS AND MODELLING OF ALLUVIAL STREAM-AQUIFER INTERACTION.**

### **4.1 Introduction**

In the previous two chapters it has been outlined how people were involved in the development of water resources systems, especially rivers and flood plain aquifers. With respect to that, a number of contributions have been made for simulating river-aquifer interactions and related time-dependent flow problems by solving the unsteady flow equations numerically. But the solutions have been obtained based on the simplification that the effects due to sedimentation processes are negligible. For example, Rovey (1975), Cunningham and Sinclair (1979) and Younger (1990), modelled linked stream-aquifer systems, considering a sediment layer at the bottom of the river, but restricted their modelling to regime boundary channels, as discussed in chapter two.

Alluvial rivers are normally in a continuous state of evolution. Geologically, they are the agents whereby the weathered rock of the uplands are eroded and transported, and their development is mainly influenced by both water and sediment flowing through them. The water flow, with or without sediments, concentrates in the channels and runs downstream scouring or accruing more soil material, thereby reshaping the channel profiles. To properly plan, design and operate a water resources project,

therefore, it is necessary to anticipate the river flow in all its conditions, and to predict the effects of the sediment being transported by the river, and the sediment composing the bed and banks of the river. With this in mind, there are many more related questions posed to the developer desiring to make use of the river. For instance, in water resources management related to the subject under study here, one of the questions that is likely to spring into mind is - how does the movement, detention and/or mining of sediment aggregates affect the condition of both streamflow and groundwater, noting that movement of the sediments is primarily driven by the shear forces exerted by the streamflow, and detention or erosion of the bed material have a direct influence on the conveyance factors of water flow, both over and through the bed. This is to say that alluvial channel profile configurations are so interrelated with their corresponding water and sediment discharges that any change in any one of them is likely to affect the other variables.

In this chapter, therefore, a solution for Modelling Alluvial Stream-Aquifer Interaction, MASAI, is developed, which considers the time-dependent sediment processes as well. That is, in addition to the equations of channel water routing and groundwater flow, as explained in chapter two, sediment routing functions have also been included to form a set of equations from which a solution procedure with expanded capability for analysing groundwater transfer to/from alluvial rivers, including scouring/filling channels, is finally developed.

However, the present study does complement the other contributions to some degree in that it centres on hydrological responses to changes in the rivers' conditions. In the simulations reported by others (e.g. Cunningham and Sinclair, 1979 - as described in chapter 2), the condition of the streambed remained invariable, and thus variation of the limiting media to interchange flow did not occur. Normally, it is possible that, at certain times, like during low flow when the so-called filter skin is formed at the bottom of the river, the sediment layer may be the limiting factor to water movement



between the two bodies, whereas at other times, like when the river is in spate and most of the sediment clogging materials have been washed away, the riverbed's seepage resistance may fall to equal that of the aquifer in the neighbourhood, making the aquifer itself to be the media limiting the water transfer to/from the river. In systems made by people, like check-dam grade controls, rates of sedimentation processes and longitudinal profile changes may be even more apparent. Obvious physical problems associated with these kinds of projects include changes in the general landscape and water-table profiles of the area, which may necessitate analyses of fluvial and the corresponding hydrological responses to the new system set-up.

It is also noted that analyses of the mathematical properties, like stability, efficiency, etc., of the existing numerical methods dealing with river and aquifer systems, are available in the literature, (e.g. Price, 1974 and Storm, 1991 - as described in chapter 2). That is why, here, emphasis has been shifted to that of assessing some of the assumptions prevalent in the procedures describing the mechanism of stream-aquifer interaction. But it has to be re-emphasised that problems involving simplifying assumptions in hydrologic phenomena cannot be avoided completely. Hydrogeologic variability ensures that models cannot precisely correspond to real-world processes. Nevertheless, the hydrologist attempting to describe or model a hydrologic system must be conscious of the limitations of his assumptions. The extent to which invalid assumptions reduce the accuracy of interpretation or prediction will depend on the degree of divergence from the real-world problems. Fortunately, the degree of sensitivity to the different assumptions differ for different hydrologic problems, minimising the total number of assumptions that ought to be dealt with in any one particular problem. Here, instead of the assumptions neglecting the aspects of sediment transport and storage on the interface boundary of stream-aquifer interacting systems, this study is focused on the effects of variation of sedimentation to the interchange between the two units.

Based on the solutions and appraisals of the foregoing literature review (chapter 2), therefore, the Saint Venant equations which govern water flow in open channels have been applied for the streamflow routing. These equations are subsequently linked with the channel sediment continuity equation and the Boussinesq equation for groundwater flow, in such a manner as to allow coupling of the numerical solutions. However, as a prelude to analyses of linkage and solution procedure, numerical development of the Saint Venant, sediment continuity and Boussinesq equations are analysed first. Although such development background is available in the current literature, a brief analysis of their numerical development is necessary to identify the type and quantity of mathematical and physical assumptions inherent in the equations of flows. Such information lends perspective to subsequent analyses of the model's predictive capability.

## 4.2 Streamflow Routing

River water routing provides computations of transient stages and discharges at selected points along a channel from a given stage/discharge hydrograph at the upstream boundary of the channel reach. The differential equations describing sediment laden streamflow routing are based on the water continuity, water momentum and sediment continuity equations - Eqs. 4.1, 4.2, and 4.3 respectively:

$$\frac{\partial Q}{\partial x} + \frac{\partial A}{\partial t} - q = 0 \quad (4.1)$$

$$\frac{\partial Q}{\partial t} + \frac{\partial}{\partial x} \left( \frac{Q^2}{A} \right) + gA \frac{\partial H}{\partial x} - gAS_0 + gAS_f - qu_i = 0 \quad (4.2)$$



$$\frac{\partial Q_s}{\partial x} + (1-\lambda) \frac{\partial A_b}{\partial t} - q_s = 0 \quad (4.3)$$

with the equation notations as given previously in section 2.2.

The water routing equations are derived based on the following assumptions, (Strelkoff, 1970; French, 1986; Chang, 1988a):

- (i) The channel is sufficiently straight and uniform in the reach so that the flow characteristics may be physically represented by a 1-D model,
- (ii) The velocity is uniformly distributed over the cross-sections,
- (iii) Hydrostatic pressure prevails at every point in the channel,
- (iv) The water surface slope is small,
- (v) The density of the sediment laden water is constant over the cross-section,
- (vi) The unsteady flow resistance coefficient is assumed to be the same for steady flow in alluvial channels and is approximated from resistance equations applicable to alluvial channels or from field surveys.

Since sediment movement and changes in channel geometry are slow in comparison with flow velocities and changes in stream discharges and depths, it can be assumed that in a short time interval  $\Delta t$ , changes in the value of  $(\partial A_b / \partial t)$  are generally much smaller than that of  $(\partial A / \partial t)$ . The solution obtained by solving the three equations simultaneously can therefore be obtained by first solving Eqs. 4.1 and 4.2, and later correcting the solution of Eqs. 4.1 and 4.2 using Eq. 4.3.

It has already been stated in chapter 2 that available mathematical models for solving gradually varied unsteady flow problems can generally be grouped into two categories i.e.: (1) hydraulic models which solve the St. Venant equations, and (2) hydrologic models which solve various approximations of the St. Venant equations.

Earlier hydrologic models tended to provide only a lumped behaviour of a certain system, such as Puls's storage routing and the Muskingam routing (Wilson, 1990), which gives only the "external description" of the phenomenon. They are useful when a forecast of discharge or of flow volume has to be made in one section as a function of upstream inflows, provided that backwater effects do not modify the rating curve of the section. If the rating curve is continuously modified by downstream level conditions, one has to use the full dynamic description. This is even more true if one needs an internal description of the reach.

The time needed to solve the full dynamic description (St. Venant equations) of large systems is considerable. This is the reason why many hydrologists have been trying to simplify the equations in most practical applications. Todini (1991), for example, has developed an intermediate model, the Parabolic and Backwater (PAB), which combines both the simplicity of the so-called hydrologic models to the accuracy of a hydraulic model. But because even the St. Venant equations themselves are based on some assumptions, and their solutions also assume certain simplifications, the threshold of hydraulic models from hydrologic models is not that obvious. In fact, according to Abbott (1991), hydrologic models have developed as subsequent generation from earlier generations of hydraulic modelling. The degree of simplification, and number of assumptions adopted depend on the problem being addressed.

Because the primary objective of this study was not a streamflow routing problem, but to investigate the effects of groundwater interaction with the streamflow, the full dynamic description of streamflow routing is retained. But this does not preclude use of other simplified streamflow routing methods in such studies.

Analytical solutions for the St. Venant equations are not available. The procedure of solving them is obtained by using numerical methods and digital computers.



A large number of papers have been presented on numerical methods for flood routing, but it should be expected that experience with each of the methods will show which is the best suited to particular applications. For instance in addition to reports about the applications of some schemes to real field practices (Quinn, 1972 ), four methods considered to be most significant: - (1) Leap-Frog Explicit method, (2) Lax-Wendroff two-step Explicit method, (3) Four-Point Implicit method and (4) Fixed Mesh Characteristic method, - were tested by Price (1974). He found the Four-Point Implicit method by Amein and Fang (1970) to be more efficient for flood routing problems, with the optimal accuracy obtained when the finite difference time step is chosen approximately equal to the space step divided by the kinematic wave speed.

Amein and Chu (1975) also noted that discharge  $Q$ , rather than velocity  $V$ , was the preferred dependent variable in the governing equations because  $Q$  is, in general, a much smoother function of  $x$  and  $t$ . For example, between two adjacent sections the area and average velocity may vary significantly while the value of  $Q$ , which is the product of the area and average velocity would change smoothly.

Chang (1988a) has also reported that because the implicit finite-difference scheme is applicable to any fixed grid, and it has possible unconditional stability, it has been adopted in virtually all major modelling systems. Therefore, the implicit four-point method has been adopted because of the above reasons.

The numeric solution of Eqs. 4.1 and 4.2 is executed in two basic steps, first by replacing the differential equations by algebraic finite difference equations, and next by obtaining the solution of the difference equations. The scheme, which is developed from the concept of linear interpolation, is thus derived as follows.

Consider the line AB in the direction of the  $x$ -axis (Figure 4.1), then if:

$$AP = \omega.AB \tag{4.4}$$

the value of a function  $\phi$  at P can be expressed in terms of  $\phi(A)$  and  $\phi(B)$ , i.e.:

$$\phi(P) = \omega \phi(B) + (1 - \omega) \phi(A) \tag{4.5}$$

where  $\omega$  is the implicit space weighting factor, and  $\phi$  defines any of the hydraulic variables Q, H,  $S_f$ , etc.

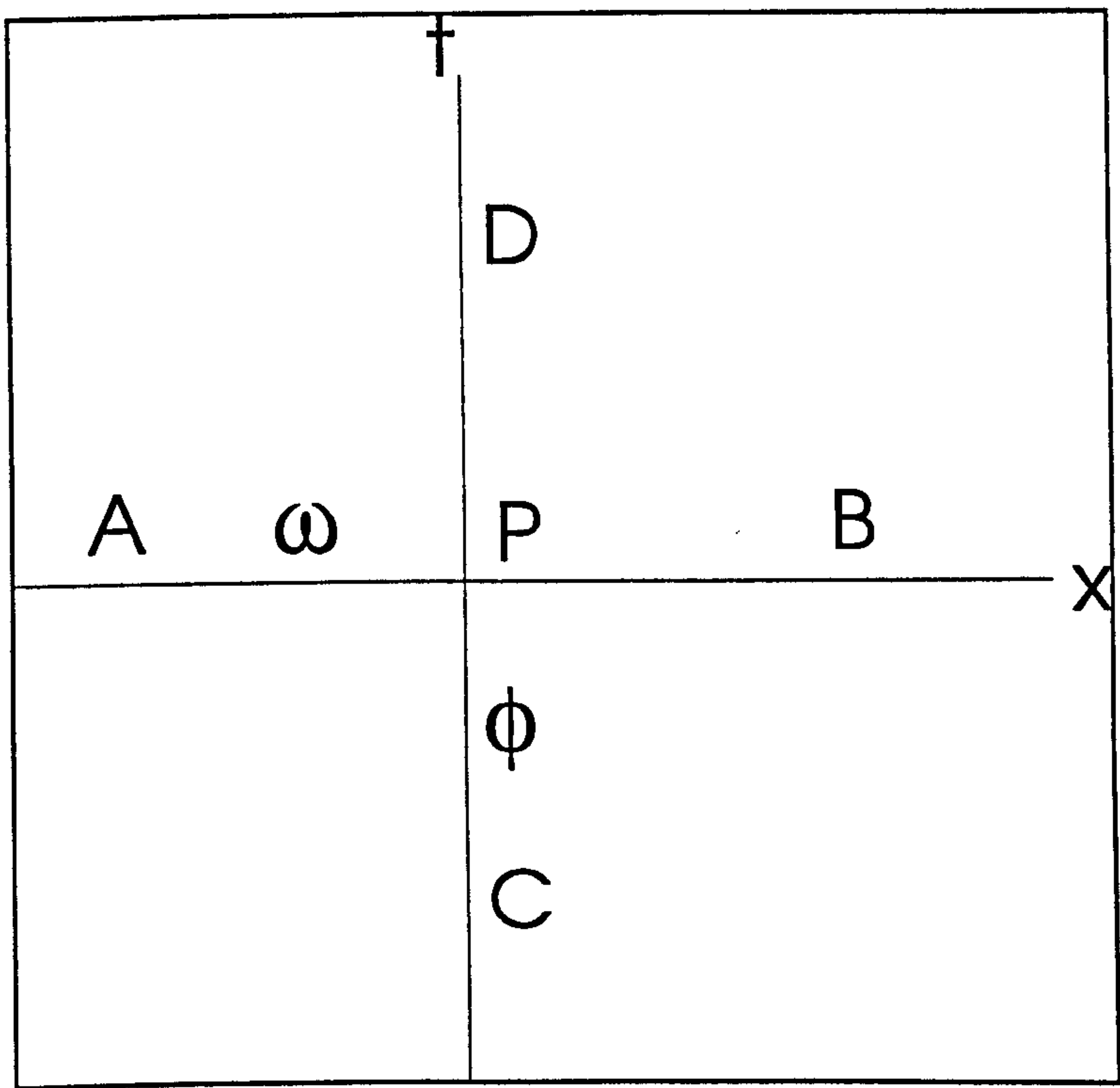


**Fig. 4.1** A sketch for the definition of the weighting factors.

This argument can be extended to a function of two independent variables so that if P also lies on the line CD in the direction of the t-axis:

$$\text{and } CP = \phi.CD: \tag{4.6a}$$

then similarly,



$$\phi(P) = \phi \phi (D) + (1 - \phi) \phi(C) \quad (4.6b)$$

$\phi$  being the time weighting factor.

When several points are considered, the implicit method of Eqs. 4.1 and 4.2 is applied over the discrete points of a rectangular grid on the (x, t) plane. The grid points are determined by the intersection of straight lines drawn parallel to the x-axis and t-axis. The lines parallel to the t-axis represent locations along the channel while those drawn parallel to the x-axis represent times. The network forms a line mesh with spacing  $\Delta x$  in the x-axis and  $\Delta t$  in the t-axis. The points of intersection are identified by two indices, a subscript "i" to designate the x-position of the point, and a superscript "j" to designate the t-value, (Figure 4.2).

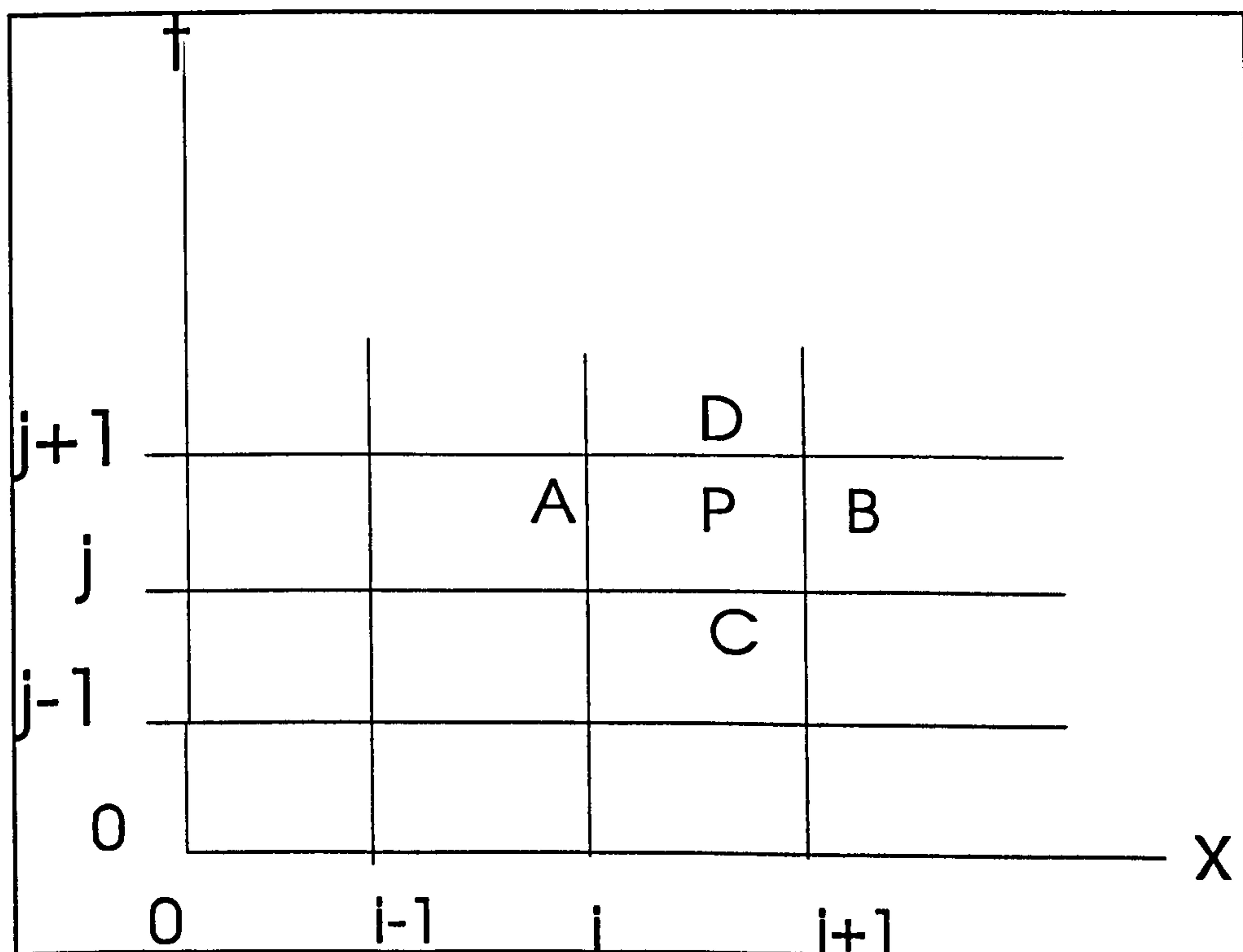


**Fig. 4.2 Line mesh on the (x, t) plane for describing the implicit method.**

As initial values, it may be assumed that at the beginning time  $t = t^0$  ( i.e.,  $j = 0$ ), the

discharge and stage values at all locations in the channel are known. And for the boundary conditions, like the upstream boundary  $x = x_0$  (i.e.  $i = 0$ ) or downstream boundary  $x = x_n$  (i.e.  $i = n$ ), it may be assumed that the discharge or stage values at all times through the required period (hydrograph) are available. The formulation then assumes that all the variables are known at time step  $t^j$ , and that it is desired to find the values of the variable in future at the time  $t^{j+1} = t + \Delta t$ . The unsteady flow equations, Eqs. 4.1 and 4.2 are applied in finite difference form to a point P centred within the four-point grid. This is in contrast to the explicit method where the equations are applied to a point on the row  $t^j$  at which all the variables are known.

Applying Eqs. 4.4 and 4.5, the average values of the function  $\phi$  at the four points A, B, C and D can be expressed in terms of the four corner values around point P as:

$$\phi(A) = \phi\phi_i^{j+1} + (1-\phi)\phi_i^j \quad (4.7a)$$

$$\phi(B) = \phi\phi_{i+1}^{j+1} + (1-\phi)\phi \quad (4.7b)$$

$$\phi(C) = \omega\phi_{i+1}^j + (1-\omega)\phi_i^j \quad (4.7c)$$

$$\phi(D) = \omega\phi_{i+1}^{j+1} + (1-\omega)\phi_i^{j+1} \quad (4.7d)$$

To obtain the value of  $\phi$  at P, either Eq. 4.5 or 4.6 is applied along the line joining AB or CD respectively. Using line CD:

$$\phi(P) = \phi\phi(D) + (1-\phi)\phi(C) \quad (4.8a)$$

and using Eqs. 4.7c and 4.7d

$$\phi(P) = \phi(\omega\phi_{i+1}^{j+1} + (1-\omega)\phi_i^{j+1}) + (1-\phi)(\omega\phi_{i+1}^j + (1-\omega)\phi_i^j) \quad (4.8b)$$



To obtain the partial derivative of  $\varphi$  at P in t,

$$\frac{\partial \varphi}{\partial t}(P) = \frac{\varphi(D) - \varphi(C)}{\Delta t} \quad (4.9a)$$

or

$$\frac{\partial \varphi}{\partial t} = \frac{\omega}{\Delta t}(\varphi_{i+1}^{j+1} - \varphi_{i+1}^j) + \frac{(1-\omega)}{\Delta t}(\varphi_i^{j+1} - \varphi_i^j) \quad (4.9b)$$

where  $\omega$  is the implicit space weighting factor. Generally, points in space are given equal weight, so that  $\omega = 1/2$ . The average value of  $\varphi$  at P, and its partial derivative in t can therefore be expressed from Eqs. 4.8b and 4.9b, respectively, as:

$$\varphi(P) = \frac{1}{2}[(1-\phi)(\varphi_i^j + \varphi_{i+1}^j) + \phi(\varphi_i^{j+1} + \varphi_{i+1}^{j+1})] \quad (4.10)$$

and

$$\frac{\partial \varphi}{\partial t}(P) = \frac{1}{2 \Delta t}[(\varphi_{i+1}^{j+1} - \varphi_{i+1}^j) + (\varphi_i^{j+1} - \varphi_i^j)] \quad (4.11)$$

The partial derivative of  $\varphi$  at P in x is:

$$\frac{\partial \varphi}{\partial x}(P) = \frac{\varphi(B) - \varphi(A)}{\Delta x} \quad (4.12a)$$

or

$$\frac{\partial \varphi}{\partial t}(P) = \frac{\phi}{\Delta x}(\varphi_{i+1}^{j+1} - \varphi_i^{j+1}) + \frac{(1-\phi)}{\Delta x}(\varphi_{i+1}^j - \varphi_i^j) \quad (4.12b)$$

In practice the time weighting factor  $\phi$ , has been found to have effects on the stability of the numerical scheme used. Its value ranges from 0 to 1, but when  $\phi = 0$  the

scheme is of the explicit method. For  $\phi = 0.5$ , it produces the implicit centred difference technique, sometimes referred to as the box scheme. The box scheme has been found to be accurate and stable for slowly varying flows, but produces numerical oscillations under certain transient conditions. However, it has been found that these oscillations do not arise for  $0.5 < \phi \leq 1.0$ , (Quinn, 1972; and Amein and Chu, 1975). Applying the fully implicit scheme, that is, using  $\phi = 1$ , equation 4.12b is reduced to:

$$\frac{\partial \phi}{\partial x}(P) = \frac{1}{\Delta x}(\phi_{i+1}^{j+1} - \phi_i^{j+1}) \quad (4.13)$$

When Eqs. 4.10, 4.11 and 4.13 are substituted into Eqs. 4.1 and 4.2, the following two finite difference equations are yielded:

$$\frac{1}{\Delta x}(Q_{i+1}^{j+1} - Q_i^{j+1}) + \frac{1}{\Delta t}(A_{i+1/2}^{j+1} - A_{i+1/2}^j) - q_{i+1/2}^{j+1} = 0 \quad (4.14)$$

$$\frac{1}{\Delta t}(Q_{i+1/2}^{j+1} - Q_{i+1/2}^j) + \frac{1}{\Delta x}[(Q^2 / A)_{i+1}^{j+1} - (Q^2 / A)_i^{j+1}] + \quad (4.15a)$$

$$gA_{i+1/2}^{j+1} \frac{1}{\Delta x}(H_{i+1}^{j+1} - H_i^{j+1}) - g(AS_0)_{i+1/2}^{j+1} + g(AS_f)_{i+1}^{j+1} - (qu_l)_{i+1/2}^{j+1} = 0$$

where,

$$q_{i+1/2}^{j+1} = \frac{1}{2}(q_i^{j+1} + q_{i+1}^{j+1}) \quad (4.15b)$$

$$S_{f,i+1}^{j+1} = \frac{1}{x_{i+1} - x_i} \int_{x_i}^{x_{i+1}} S_f(x, t) dx = [(S_{f,i+1}^{j+1} \cdot S_{f,i}^{j+1})]^{1/2} \quad (4.15c)$$

$$\phi_{i+1/2}^{j+1} = \frac{1}{2}(\phi_i^{j+1} + \phi_{i+1}^{j+1}) \quad (4.15d)$$



The term  $q_{i+1/2}$  is the lateral inflow per unit length, uniformly distributed between  $x_i$  and  $x_{i+1}$ , and  $u_1$  is the velocity component of  $q$  in the  $x$ -direction, assumed to be negligible in this case.

By noting that bed slope  $S_o$ , and the flow cross-sectional area  $A$ , are direct functions of bed elevations  $Z$ , and flow depth  $H$ , for respective prescribed channel geometry, and by assuming water surface slope  $S_{fi+1/2}$ , depends on the variation of depth  $H$ , and discharge  $Q$ , the finite difference form of water continuity and momentum conservation can be rewritten as:

$$F_i = \frac{\Delta t}{\Delta x} (Q_{i+1}^{j+1} - Q_i^{j+1}) + \frac{1}{2} [(A_i^{j+1} + A_{i+1}^{j+1}) - (A_i^j + A_{i+1}^j)] - \quad (4.16)$$

$$\frac{\Delta t}{2} (q_i^{j+1} + q_{i+1}^{j+1}) = 0$$

and

$$G_i = \frac{1}{2} [(Q_i^{j+1} + Q_{i+1}^{j+1}) - (Q_i^j + Q_{i+1}^j)] + \frac{\Delta t}{\Delta x} [(Q^2 / A)_{i+1}^{j+1} - (Q^2 / A)_i^{j+1}] +$$

$$\frac{g \Delta t}{2 \Delta x} (A_i^{j+1} + A_{i+1}^{j+1}) (H_{i+1}^{j+1} - H_i^{j+1}) - \frac{g \Delta t}{2 \Delta x} (A_i^{j+1} + A_{i+1}^{j+1}) (Z_i^{j+1} - Z_{i+1}^{j+1}) +$$

$$\frac{g \Delta t}{2} (A_{i+1}^{j+1} + A_i^{j+1}) (S_{fi+1}^{j+1} \cdot S_{fi}^{j+1})^{1/2} = 0 \quad (4.17a)$$

where

$$\frac{1}{\Delta x} (Z_i^{j+1} - Z_{i+1}^{j+1}) = S_{oi+1/2}^{j+1} \quad (4.17b)$$

is the bed slope, and the subscript  $i$  is the space counter starting from upstream,  $F$  denoting the continuity function and  $G$  denoting the momentum function.

The friction slope, which is a quadratic function of  $Q$  and  $K$  is expressed as:

$$S_f = \frac{Q \cdot Q}{K^2} \quad (4.18)$$

where  $K$  is the channel conveyance, commonly expressed as:

$$K = \frac{AR^{2/3}}{n} \quad (4.19)$$

in which  $n$  is the Manning's roughness coefficient given as a function of  $Q$  and  $H$ . A suitable expression for  $S_f^{j+1}$  is, (Strelkoff, 1970 ):

$$S_f(Q, H) = S_{f,i}^j + \left(\frac{\partial S_f}{\partial Q}\right)_i' (Q_i^{j+1} - Q_i^j) + \left(\frac{\partial S_f}{\partial H}\right)_i' (H_i^{j+1} - H_i^j) \quad (4.20)$$

From Eqs 4.18 and 4.19,

$$\frac{\partial S_f}{\partial Q} = 2S_f \left( \frac{1}{Q} + \frac{1}{n} \frac{\partial n}{\partial Q} \right) \quad (4.21)$$

and

$$\frac{\partial S_f}{\partial H} = -2S_f \left[ \frac{1}{A} \left( \frac{5}{3} T - \frac{2}{3} R \frac{dP}{dH} \right) - \frac{1}{n} \frac{\partial n}{\partial H} \right] \quad (4.22)$$

where  $T = (\partial A / \partial H)$  is the water surface width at depth  $H$ , and  $P$  is the wetted perimeter.

Eqs. 4.16 and 4.17 now constitute a system of two non-linear algebraic equations with four unknowns. By themselves, they are not sufficient to evaluate the unknowns at the points  $(i, j+1)$  and  $(i+1, j+1)$ . However, two unknowns are common to any two contiguous rectangular grids. For  $n$  points on the row  $(j+1)$ , there are  $(n-1)$



rectangular grids with  $(n-1)$  interior points P. The combination of all the rectangular grids provide  $2(n-1)$  equations for the evaluation of  $2n$  unknowns. The required two additional equations for the evaluation of the unknowns are obtained from the upstream and downstream boundary conditions.

At the upstream, the discharge may be given as a function of time in the form of a hydrograph, that is:

$$G_0 = Q_i^{j+1} - Q(t^{j+1}) = 0 \quad (4.23a)$$

with  $Q(t^{j+1})$  as the discharge at the upstream entrance at time  $t^{j+1}$ . This gives a supplementary equation. If the stage of the upstream section is known as a function of time, then:

$$G_0 = H_i^{j+1} - H(t^{j+1}) = 0 \quad (4.23b)$$

becomes available as an alternate supplementary equation provided by the upstream boundary.

If at the downstream boundary the stage-discharge relationship is known from the properties of the control section, then:

$$F_n = H_n^{j+1} - H(Q_n^{j+1}) = 0 \quad (4.24)$$

gives the second supplementary equation.

Therefore, Eqs. 4.16 through 4.24 simulate the water continuity and momentum equations of gradually varied unsteady flow by means of a system of finite difference equations. The equations constitute  $2n$  non-linear algebraic equations with  $2n$

unknowns. Newton's iterative method is applied for evaluation of their solution at time  $t^{j+1}$ . The details of Newton's method are explained in Appendix 1.

Numerical techniques similar to the one discussed here are favoured for many applications because they can be readily used with unequal distance steps and their stability-convergence properties can be controlled. Schemes of the implicit finite difference are thus used in many standard unsteady flow models, like the National Weather Service (USA) and the USGS model, (French, 1986).

After computing the flow conditions at each node at the time step  $t^{j+1}$ , their values are applied for the computation of the corresponding sediment transport capacities. The sediment transport capacities are then applied to estimate the amount of the entrainment and/or deposition of the sediment material at the nodes, at the time step  $t^{j+1}$ . The estimation is based on the finite difference approximation of the sediment continuity equation, Eq. 4.3, and the sediment boundary conditions.

## **4.3 Riverbed Sedimentation**

### **4.3.1 Introduction**

To account for sediment routing through the channel reach, the values of the hydraulic variable,  $Q$ ,  $H$ , and  $V$ , obtained from the previous water routing scheme are adopted. Although the phenomena of erosion and deposition in channels are of a three dimensional (3-D) nature, it is assumed here that the net erosion or deposition of sediment between two neighbouring sections is uniformly distributed in the channel in accordance with the potential shear stress distribution. In these circumstances, a 1-D dynamic model is considered adequate to produce a tractable solution of the 3-D nature (Chen, 1973). It is also assumed that the river reach under



consideration is in its middle to low-land ranges so that the channel slope is small and the sediment materials are predominantly of non cohesive sands. The storage change in the sediment continuity function is thus accounted for by change of the sediment bed layer, with suspended load flowing through as wash load.

The sediment routing equation, Eq. 4.3 has two unknown variables,  $Q_s$  and  $A_b$ , assuming  $q_s$  is known in advance. Another relationship is therefore required to make the variables determinate. This is provided by an appropriate sediment transport relationship, which is applied together with the flow conditions provided by the water routing scheme in order to compute the sediment discharge  $Q_s$ . The Ackers-White function has been selected in this study because of its recommendations for sandy riverbeds, and because of its relatively better estimation of the bedload during the fieldwork on the Nyando River in Kenya. The Ackers-White function is given in Appendix 3 at the end of this text.

#### **4.3.2 Residual transport capacity**

In natural alluvial channels, there is usually a wide gradation of sediment sizes, and different sizes are transported at different rates. The sediment transport formulae are used to determine the potential carrying capacity of a specific flow, but these formulae are not directly applicable to establish the capacities of the individual size fractions. An account must be made as to what extent the streams potential capacity is filled up by material of all fractions that are already in motion.

Gessler (1971) was one of the first people to recognise the importance of armouring in alluvial channels. He presented armouring as a problem of the probability of movement of particles, with armouring changing the probability of grains to stay in place on the bed. He stated that after a stable armour layer is developed, the

sediment transport ceased. The problem with Gessler's approach is that his probability for a grain to remain in place is defined in terms of his experimental set-up. He introduced clear water into a flume with a gravel bed. Erosion took place as finer materials were removed until an armouring coat formed and sediment transport ceased. In the general case, there is sediment input from upstream, and for steady flow an equilibrium should develop. This was the basis for an alternative approach by Parker and Klingeman (1982) to the problem of armouring.

Parker and Klingeman (1982) claim that armouring of streambeds does not necessarily cause the cessation of sediment movement, but rather causes a change in its structure. They predicted pavement size by use of a relative probability of movement, rather than Gessler's probability of staying in place. Their experiments recirculated sediments until unequilibrium pavement developed. The sediment supply was then stopped, and an equilibrium armour developed. The final armour, equivalent to Gessler condition, was somewhat coarser than should be expected, (Vanoni, 1986)

Rahuel et al (1989) introduced an empirical equation for computing equilibrium unit-width solid transport for uniform material of diameter  $d_k$ , based on a hiding factor, which reflected the influence of sediment particles of the whole mixture to the transport of the class of particle diameter  $d_k$ . Although Rahuel et al (1989) based their estimation of the hiding factor on a formulae by Karim and Kennedy (1982), they noted that in particular applications, the generic coefficient had to be reformulated to account for local conditions.

Computation of the range in size fractions can also be based on the procedure introduced by Borah et. al. (1982), to track the carrying capacities of the size fractions. This is done through a variable they formulated, called "residual transport capacity". The residual transport capacity is defined as the stream's ability to carry



any additional load of a particular size fraction in the presence of all the size fractions already present in the flow.

Unlike the other methods described above, whose equations and coefficients are derived from experiments under particular conditions, Borah et al (1982) formulation is based on physical relationships, without dependent coefficients. Simulation results by the FLUVIAL model, which uses the residual transport capacity procedure has also been applied in the field and produced satisfactory results (Chang, 1988a). It has been selected here because of its physical meaning, as explained below.

According to Borah et. al. (1982), a flow may have the potential to transport a given size fraction of sediment as estimated by using one of the sediment transport formulae, but its residual capacity depends on the sediment material of all the size fractions already present in the flow. Consider, for instance, a flow carrying a load  $c_1$ , of uniform size,  $d_1$ , and let  $T_1$  be the corresponding potential capacity of the flow for that size. Then,

$$T_{r1} = T_1 - c_1 = T_1 - T_1(c_1 / T_1) \quad (4.25a)$$

is the residual transport capacity of the flow for that size material.

The last term in Eq. 4.25a represents that portion of  $T_1$  already consumed by the material in transport. Similarly, if the latter were of a different size,  $d_2$ , the residual capacity for the  $d_1$  size material, in the presence of the load  $c_2$ , would be:

$$T_{r1} = T_1 - T_1(c_2 / T_2) \quad (4.25b)$$

where  $c_2/T_2$  may be envisaged as that fraction of  $T_1$  already consumed by the load  $c_2$ . If both sizes are simultaneously present in the flow, then:

$$T_{ri} = T_i - T_i(c_1 / T_1) - T_i(c_2 / T_2) = T_i[1 - \sum_{i=1}^2 (c_i / T_i)] \quad (4.25c)$$

This expression can be generalised to any size fraction,  $d_i$ , and for an arbitrary number,  $n$ , of the load fractions  $c_1, c_2, \dots, c_n$  as follows:

$$T_{ri} = T_i[1 - \sum_{j=1}^n (c_j / T_j)], \quad i = 1, 2, 3 \dots n \quad (4.25d)$$

The quantity,  $\sum (c_j / T_j)$ , represents the fraction of the potential capacity,  $T_i$ , taken up by all the size fractions in transport. Therefore, the quantity within the square bracket,  $\Omega$  is the remaining fraction of  $T_i$  for transporting additional material of size  $d_i$ . At any instant  $\Omega$  is the same for all size fractions.  $T_i$  depends uniquely on the local flow and the properties of the  $d_i$  fraction, while  $T_{ri}$  depends on all these parameters, as well as on the size composition of the sediment load.

The sediment transport capacity is affected by the spatial variation in sediment discharge. This non uniformity in sediment transport is associated with changes in channel boundary conditions, which reflect sediment depletion (and storage). Diffusion also affects sediment transport. The diffusion process affects essentially the suspended load during entrainment (and deposition) because certain sediments require considerable time or distance in settling or attaining their transport capacity. Therefore, suspended load may not adjust immediately to the flow conditions. The scale of sediment transport "capacity-exceeded", therefore, depends on the discontinuity of both the channel boundary conditions, and also of the sediment discharge concentration. Although the sediment transport capacity shows the competence of the streamflow to transport certain grain sizes, in addition, the availability of the grains in the channel is what determines the actual amount of sediment that will be transported. For example, in rigid channels (e.g. concrete



channels), clear first flowing water will have high sediment transport capacity, but will not transport any material until such particles are provided on the channel bed or in the flow.

Therefore, when  $\Omega > 0$ , any size fraction available for entrainment at the bed surface, and for which  $T_i \neq 0$ , will be removed by the flow and added to the same sediment size class already in transport. Thus,  $\Omega > 0$  identifies an eroding bed condition. Similarly, when  $\Omega < 0$ , the stream carries a load in excess of its potential capacity and will deposit the excess sediment on the bed. Therefore,  $\Omega < 0$  characterises an aggrading bed condition. When  $\Omega = 0$ , there is no net load change and the transport process remains in a pseudo-equilibrium condition. By continuously tracking the value of  $\Omega$ , the dependence of the individual residual capacities on the composition of the sediment load, and the exchange of sediment load with the bed, may be readily simulated.

#### **4.3.3 The sediment mixing layer**

Since only part of the bed material is susceptible to movement, it is useful to adopt the notion of a mixing layer within which all particles are subject to entrainment through contact with the near-bed water flow (Rahuel et. al., 1989). Below this layer the bed is assumed to remain undisturbed. Although the role of this mixing layer is more clearly appreciated for scour than deposition, nevertheless, it must be recognised that both erosion and deposition may occur simultaneously, net deposition representing a situation in which there is a greater flux of particles settling to the bed than that of the particles being entrained into flow. Of course the entrainment component of this dynamic balance depends strongly on the availability of particles in the mixing layer, as represented by the grain-size distribution of the layer.

Usually, river beds are only partially armoured, and the degree of armouring often

varies with seasonal changes in the rate of flow and sediment transport. To fully evaluate the streambed's long-term stability, it is necessary to relate the degree of armouring to characteristics of the flow and sediment in the channel. But none of the methods mentioned in the previous section related the time scale of the armouring process and the flow and sediment characteristics.

Rahuel et al (1989) computed the exchange of particles between the mixing layer and the underlying material without considering the time scale. Borah et al (1982) also used a mixing layer concept. However, to control the erosion/deposition process, they introduced an additional active layer concept and a rather complex ordering procedure for the removal of the various grain size fractions. The other functions by Gessler (1971), and Parker and Klingeman (1982) do not relate sediment sorting to the time and characteristics of flow.

Lee and Odgaard (1986) related the degree of armouring to characteristics of the flow and sediments in the channel, in order to provide a numerical procedure of correlating the temporal change of the composition of the bed-surface layer with changes in the rate of sediment transport near the channel bed. The rate at which sediment is entrained into the fluid is dependent on the time step chosen for the numerical computation, and it must be calibrated with measured data. Their model presentation is simpler and it contains a minimum number of floating variables. Because of these reasons, the method has been adopted, and extended to include grain-size selection from the sediment-laden flow during deposition in aggrading rivers. The procedure is explained below.

If for instance  $\Omega > 0$ , then the stream has a potential transport capacity,  $T_B = \sum T_{fi}$ , to entrain sediment size fractions. In the event of this stream flowing over an erodible reach of length  $L$ , it will pick up sediment at the rate which may be described for each grain-size class fraction by the equation first introduced by Bayazit (1975) as:



$$T_B = f_{si} \Delta t = L \Delta Q_{si} \quad (4.26)$$

in which  $T_B$  = total potential bed material transport capacity of the flow per unit width,  $f_{si}$  = fraction of grains in class interval  $i$ ,  $\Delta t$  = time interval,  $\Delta Q_{si}$  = weight of the grains in class interval  $i$  that are removed from the bed surface mixing layer during the time interval  $\Delta t$ , per unit area of the mixing layer. Hence, the additional sediment discharge rate per unit width  $q_s = T_B \cdot \Sigma f_{si}$ . The time interval  $\Delta t$  is assumed to be small enough that  $T_B$  and  $f_{si}$  can be taken to be constant within this period of time.

The thickness,  $T_s$ , and particle size distribution of the mixing layer may vary throughout the simulation period, but the layer is assumed to be homogeneous within itself at any given time. The thickness may be described as a function of the dunes and ripples moving through the channel, or as a function of the flow depth (e.g. Lee and Odgaard 1986):

$$T_s = 1/2 \cdot H_s (1 - C_s) \quad (4.27)$$

where  $C_s$  = coefficient with values between 0 and 1,  $H_s$  = dune height as given by Yalin's (1964) relation:

$$H_s = (H/6) (1 - \tau_{cr} / \tau) \quad (4.28)$$

where  $H$  = flow depth,  $\tau$  = bed-shear stress, and  $\tau_{cr}$  = critical bed shear stress.

The total weight of bed material that leaves the mixing layer (per unit area) during the time interval  $\Delta t$  is obtained by summing up the contributions from all class intervals:

$$\Delta Q_s = \Sigma(\Delta Q_{si}) = 1/L \cdot (T_B \cdot \Delta t) \cdot \Sigma f_{si} = (T_B \cdot \Delta t) / L \quad (4.29)$$

It is assumed that the material eroded from the mixing layer ( $\Delta Q_s$ ) is replaced by bed material of the same weight from the layer below the mixing layer. At the end of the time interval  $\Delta t$ , the weight of the grains in class interval  $i$  in the mixing layer is then (per unit area):

$$m_i' \cdot Q_{Fs} = m_i \cdot Q_{Fs} - f_{si} \cdot \Delta Q_s + p_{si} \cdot \Delta Q_s \quad (4.30a)$$

in which

$$Q_{Fs} = \rho_s g \cdot T_s \quad (4.30b)$$

is the weight per unit width of the mixing layer bed materials, and  $\rho_s$  = density of sediments,  $g$  = acceleration due to gravity,  $m_i$  = fraction of grains in class interval  $i$  in the mixing layer at the beginning of the time interval  $\Delta t$ ,  $m_i'$  = fraction of grains in class interval  $i$  in the mixing layer at the end of the time interval  $\Delta t$ , and  $p_{si}$  = fraction of grains in class interval  $i$  in the parent bed material. Hence, at the end of time interval  $\Delta t$ :

$$m_i' = m_i + (\Delta Q_s / Q_{Fs}) (p_{si} - f_{si}) \quad (4.30c)$$

As the numerical process proceeds, the amount per unit width of sediment leaving the mixing layer ( $\Delta Q_s$ ) decreases and, gradually, coarsening of the material in the mixing layer occurs. Eventually, the rate of sediment entrainment becomes negligible, at which point the armour layer is fully developed, and the sediment discharge in the flow remains steady for the particular reach.

If on the other hand  $\Omega < 0$ , then the stream has the potential to deposit sediment for size fractions present in the flow. The negative notation of  $\Delta Q_s$  symbolises that it is



the weight of the grains being dropped onto the river bed's mixing layer, rather than being entrained from the layer. It is also assumed here that for the material added to the mixing layer ( $\Delta Q_s$ ) the same weight of material is removed from the mixing layer. At the end of the time interval  $\Delta t$  the weight of the grains in class  $i$  in the mixing layer is (per unit area):

$$m_i' \cdot Q_{Fs} = m_i \cdot Q_{Fs} + f_{si} \cdot \Delta Q_s - m_{si} \cdot \Delta Q_s \quad (4.31a)$$

And the fraction of grains in class interval  $i$  in the mixing layer at the end of time interval  $\Delta t$  is:

$$m_i' = m_i - (\Delta Q_s / Q_{Fs}) (m_{si} - f_{si}) \quad (4.31b)$$

As the numerical process proceeds, the amount per unit time of sediment leaving the water flow ( $\Delta Q_s$ ) decreases, and a gradual dilution of the concentration of the sediment-laden flow occurs. Eventually, the rate of sediment deposition will cease after the excess load has been dropped, leaving a steady sediment concentration at the particular section.

#### 4.3.4 Sediment routing

The sediment transport, residual transport capacities and mixing layer functions, as presented above, and sediment inflow into the reach as upstream boundary condition, provide the execution steps followed to estimate the sediment discharge  $Q_s$  along the reach in the time interval  $\Delta t$ . Given  $Q_s$ , the corresponding cross-sectional area change  $\Delta A_b$  in Eq. 4.3 becomes determinate, i.e.:

$$\Delta A_b = -\frac{\Delta t}{1-\lambda} \left( \frac{\partial (Q.C)}{\partial x} - q_s \right) \quad (4.32)$$

assuming the sediment concentration  $C = Q_s/Q$ , and  $q_s$  as a predefined function.

Eq. 4.32 is a quasi linear hyperbolic equation governing the propagation of the sediment concentration. Its solution can be computed by applying the finite difference method. Referring to Figure 4.3, point A is in the upstream section of the channel reach, C is in the downstream section and B and M are somewhere in two adjacent interior sections. Applying the concepts of the implicit 4-point scheme, as explained in section 4.2, the partial derivatives of the function  $\phi$  at M is:

$$\frac{\partial \phi}{\partial x}(M) = \frac{1}{\Delta x} (\phi_{i+1}^{j+1} - \phi_i^{j+1}) \quad (4.33)$$

and

$$\frac{\partial \phi}{\partial t}(M) = \frac{1}{2\Delta t} (\phi_{i+1/2}^{j+1} - \phi_{i+1/2}^j) \quad (4.34)$$

$\phi$  representing  $Q$ ,  $C$  etc.

The net volumetric change of sediment per unit length of the channel bed for the various sections can then be computed in the following way.

1. For the interior points:

With reference to Figure 4.3, application of Eq. 4.33 to Eq. 4.32 at point B gives :



$$\frac{1}{2\Delta x}[(QC)_i^j - (QC)_{i-1}^j + (QC)_i^{j+1} - (QC)_{i-1}^{j+1}] = \quad (4.35)$$

$$\frac{1}{2}(q_{si-1/2}^j + q_{si-1/2}^{j+1}) - \frac{1-\lambda}{\Delta t} \Delta A_{bi-1/2}$$

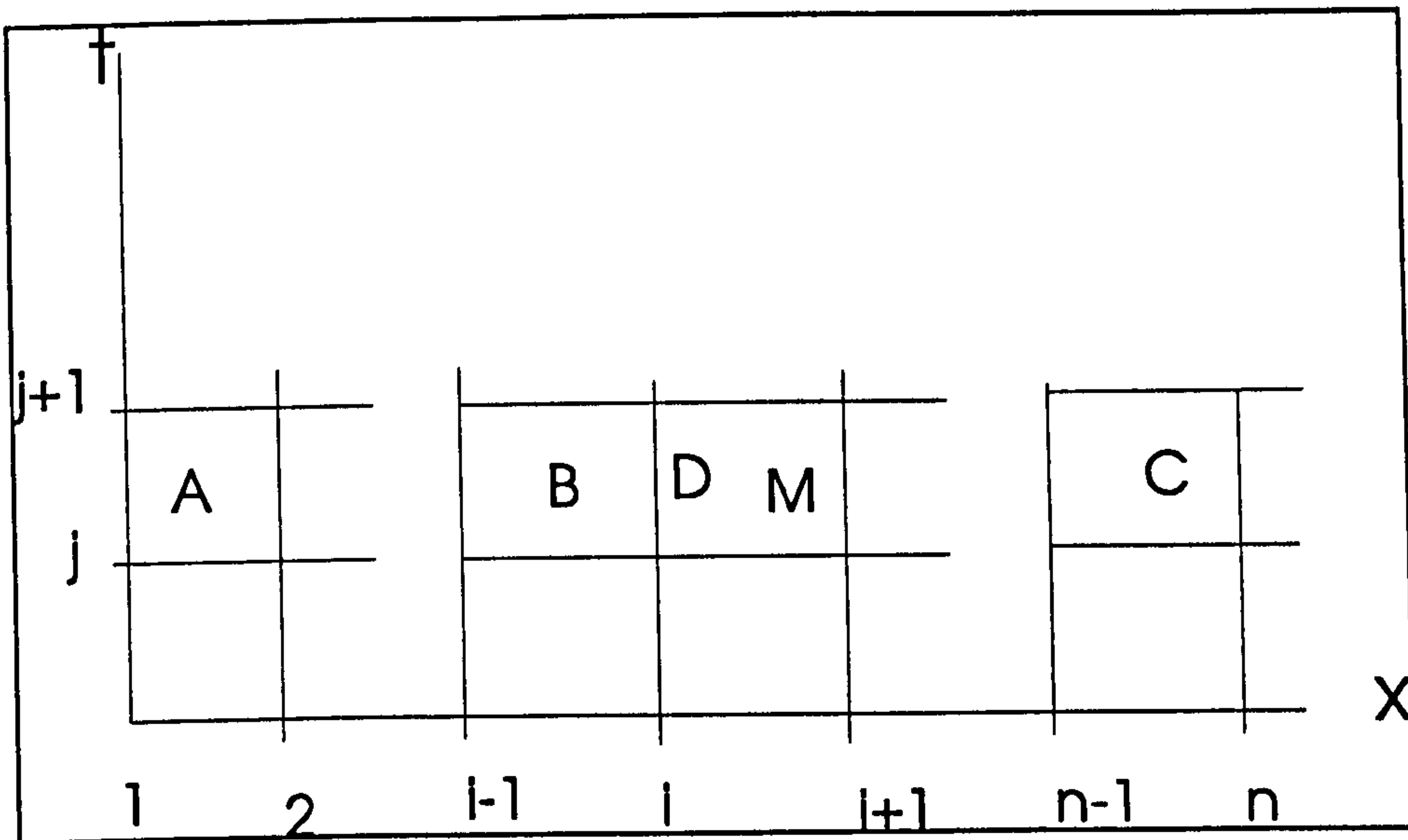


**Fig. 4.3 Network for describing the sediment routing implicit method.**

where  $\Delta A_{bi-1/2}$  = the net eroded/deposited volume of sediment per unit length of the channel bed between sections (i-1) and i.

$q_{si-1/2}$  = the lateral sediment inflow per unit length between sections (i-1) and i.

$C_i^{j+1}$  = the average sediment concentration estimated from field survey and/or theory, for the computed flow conditions at sections i and time step j+1

Rearranging Eq. 4.35 with the term  $\Delta A_{bi-1/2}$  as the subject:

$$\Delta A_{bi-1/2} = \frac{\Delta t}{2(1-\lambda)} (q_{si-1/2}^j + q_{si-1/2}^{j+1}) + \frac{\theta}{2(1-\lambda)} [(QC)_i^j - (QC)_{i-1}^j + (QC)_i^{j+1} - (QC)_{i-1}^{j+1}] \quad (4.36)$$

Similarly, when Eq. 4.35 is applied to point M in Figure 4.3:

$$\Delta A_{bi+1/2} = \frac{\Delta t}{2(1-\lambda)} (q_{si+1/2}^j + q_{si+1/2}^{j+1}) - \frac{\theta}{2(1-\lambda)} [(QC)_{i+1}^j - (QC)_i^j + (QC)_{i+1}^{j+1} - (QC)_i^{j+1}] \quad (4.37)$$

$\Delta A_{bi}$  can now be estimated from:

$$\Delta A_{bi} = 1/2 (\Delta A_{bi-1/2} + \Delta A_{bi+1/2}) \quad (4.38)$$

Substituting Eqs. 4.36 and 4.37 into Eq. 4.38 gives:

$$\Delta A_{bi} = \frac{\Delta t}{4(1-\lambda)} (q_{si-1/2}^j + q_{si-1/2}^{j+1} + q_{si+1/2}^j + q_{si+1/2}^{j+1}) - \frac{\theta}{4(1-\lambda)} [(QC)_{i+1}^j - (QC)_{i-1}^j + (QC)_{i+1}^{j+1} - (QC)_{i-1}^{j+1}] \quad (4.39)$$

2. At the upstream boundary:

Let  $Q_{so}^j$  denote the inflow sediment discharge from the upstream end of the reach at time  $t_j$ . This value can be estimated from the sediment discharge hydrograph at the upstream boundary. If it is not available, then  $Q_{so}^j$  can be assumed to be equal to  $Q_{s1}^j$ . Eq. 4.36 is applied to point A in Figure 4.3, assuming  $\Delta A_{b1} \approx \Delta A_{b1+1/2}$ .



$$\Delta A_{b_1} = \frac{1}{2(1-\lambda)} [\Delta t (q_{s1+1/2}^j + q_{s1+1/2}^{j+1}) - \theta [(QC)_2^j - (QC)_0^j + (QC)_2^{j+1} - (QC)_0^{j+1}]$$
(4.40)

3. At the downstream boundary:

Assuming  $i = n$  in Eq. 4.36 and  $\Delta A_{bn} \approx \Delta A_{bn-1/2}$ , then:

$$\Delta A_{b_n} = \frac{1}{2(1-\lambda)} [\Delta t (q_{sn-1/2}^j + q_{sn-1/2}^{j+1} - \theta [(QC)_n^j - (QC)_{n-1}^j + (QC)_n^{j+1} - (QC)_{n-1}^{j+1}]$$
(4.41)

The cross-sectional area changes,  $\Delta A_b$ , obtained in this sediment routing scheme are the corrections for the time increment  $\Delta t$  that need to be applied for the channel configuration changes. With  $\Delta A_b$  being the total correction, it is possible for both the bed and banks to have deposition or erosion, and it is also possible to have deposition along the banks but erosion in the bed, and vice versa.

However, this study considers the case where lateral bank erosion is assumed to be negligible, i.e.  $\Delta A_b = B \cdot \Delta Z$ , where  $B$  is the channel width and  $\Delta Z$  is the bed elevation (profile) change. After the changes in the bed elevations have been determined, the other flow conditions in the reach are adjusted according to the following relationships:

- a.  $Z_i^{j+1} = Z_i^j + \Delta Z_i$
- b.  $(H_i^{j+1})^2 = (H_i^{j+1})^1 - Z_i^{j+1}$
- c.  $C_j^{j+1} = (Q_{s_i} / Q_i)$
- d.  $(A_i^{j+1})^2 = (A_i^{j+1})^1 - \Delta A_i$  (4.42 a-g)
- e.  $V_i^{j+1} = Q_i^{j+1} / A_i^{j+1}$

$$f. \quad R_i^{j+1} = A_i^{j+1} / P_i^{j+1}$$

$$g. \quad S_{fi}^{j+1} = [(n_i^{j+1})^2 \cdot v_i^{j+1} \cdot |v_i^{j+1}|] / (R_i^{j+1})^{4/3}$$

where  $Q_i^{j+1}$ ,  $(H_i^{j+1})^1$ ,  $(A_i^{j+1})^1$ ,  $P_i^{j+1}$  and  $n_i^{j+1}$  are the values evaluated by solving Eqs. 4.1 and 4.2 at time step  $t^{j+1}$  according to the water routing scheme presented in the previous section.

After adjusting the channel flow and bed elevation conditions, the new conditions are then related to the groundwater conditions so as to evaluate the interaction potential between the river and aquifer at each section along the channel reach. But first, the state of the groundwater potential at the time step  $t^{j+1}$  has got to be determined.

#### 4.4 Groundwater Flow on Flood Plains

The lateral flow,  $q$ , appearing in the channel water routing equations, Eqs. 4.1 and 4.2, may include tributary, overland and/or groundwater seepage contribution into the channel. In the absence of seepage flow, the three equations describing water and sediment routing in channel, together with the corresponding boundary and initial conditions, are by themselves sufficient to evaluate transient streamflows. But in situations where the river's wetted perimeter permits the passage of water, an additional formulation may be required to define the variable seepage flow, and subsequently link the river and groundwater systems.

In practice, most alluvial rivers only partially penetrate their underlying aquifers, and so alluvial rivers and aquifers can be highly connected (Rushton and Redshaw, 1979; Dillon and Liggett, 1983; Younger, 1987 and Storm, 1991). The distribution of the river flow conditions are described by the channel water and sediment routing schemes described above. On the flood plains, the 2-D equation is assumed in order



to idealise and describe the general transient groundwater distribution. That is:

$$mK_2 \left[ \frac{\partial^2 \psi}{\partial x^2} + \frac{\partial^2 \psi}{\partial y^2} \right] = S \frac{\partial \psi}{\partial t} - R \quad (4.43)$$

so that in the aquifer directly below the river:

$$S = S_c \text{ and } R = q(x, t, H, Z_b) + q_L \quad (4.44a)$$

and elsewhere in the neighbourhood where the aquifer is unconfined:

$$S = S_y \text{ and } R = I(x, y, t) \quad (4.44b)$$

in which  $\psi$  = groundwater hydraulic head,  $m$  = saturated thickness of aquifer,  $K_2$  = effective hydraulic conductivity of the aquifer,  $S_c$  = aquifer storage coefficient,  $S_y$  = aquifer specific yield,  $I$  = vertical recharge to the aquifer,  $q$  = seepage water transfer/recharge from the river (per unit length),  $q_L$  = lateral surface water contribution from tributaries, overland runoff, abstractions, etc.,  $H$  = depth of river flow,  $x$  = longitudinal distance along the river,  $y$  = distance in the lateral direction,  $t$  = time, and  $Z_b$  = thickness of sediment material at the bottom of the river..

Again, such equations describing most practical groundwater problems can hardly be solved analytically. Their solutions are often obtained by numerical means. For consistency, the finite difference technique, as explained for channel flow routing previously, has been adopted.

Using figure 4.3, a central difference approximation to  $\partial^2 \psi / \partial x^2$  at  $(x_o, t_o)$  is obtained by approximating the first derivative at  $(x_o + (\Delta x/2), t_o)$  and at  $(x_o - (\Delta x/2), t_o)$  and then obtaining the second derivative by taking a difference between the first

derivatives at those points, i.e.:

$$\frac{\partial^2 \psi}{\partial x^2} = \frac{\frac{\psi_{i+1}^j - \psi_i^j}{\Delta x} - \frac{\psi_i^j - \psi_{i-1}^j}{\Delta x}}{\Delta x} \quad (4.45a)$$

which simplifies to:

$$\frac{\partial^2 \psi}{\partial x^2} = \frac{\psi_{i-1}^j - 2\psi_i^j + \psi_{i+1}^j}{(\Delta x)^2} \quad (4.45b)$$

j being the time step counter whereas i is the space step counter in the longitudinal direction. Similarly:

$$\frac{\partial^2 \psi}{\partial y^2} = \frac{\psi_{k-1}^j - 2\psi_k^j + \psi_{k+1}^j}{(\Delta y)^2} \quad (4.46)$$

and

$$\frac{\partial \psi}{\partial t} = \frac{\psi_{i,k}^{j+1} - \psi_{i,k}^j}{\Delta t} \quad (4.47)$$

k being the space step counter in the lateral direction. These approximations may be improved by evaluating the space derivatives somewhere between time  $t^j$  and  $t^{j+1}$ , so that if time step  $t^{j+1}$  is weighted by a factor  $\alpha$  and time step  $t^j$  is weighted by  $(1 - \alpha)$  then

$$\frac{\partial^2 \psi}{\partial x^2} = \alpha \frac{\psi_{i+1,k}^{j+1} - 2\psi_{i,k}^{j+1} + \psi_{i-1,k}^{j+1}}{(\Delta x)^2} + (1 - \alpha) \frac{\psi_{i+1,k}^j - 2\psi_{i,k}^j + \psi_{i-1,k}^j}{(\Delta x)^2} \quad (4.48a)$$



A similar expression can be written for  $\partial^2 \psi / \partial y^2$ . Adopting  $\alpha = 1$  for a fully implicit scheme, for the same reasons as given in section 4.2, and substituting the approximations into Eq. 4.43 yields the finite difference form of the transient ground water equation as :

$$\psi_{i,k}^{j+1} = \psi_{i,k}^j + R \frac{\Delta t}{S} + \xi(\psi_{i-1,k}^{j+1} - 2\psi_{i,k}^{j+1} + \psi_{i+1,k}^{j+1} + \beta(\psi_{i,k-1}^{j+1} - 2\psi_{i,k}^{j+1} + \psi_{i,k+1}^{j+1})) \quad (4.48b)$$

where  $\xi = (T \cdot \Delta t) / [S (\Delta y)^2]$  and  $\beta = (T \cdot \Delta t) / [S (\Delta y)^2]$

That is, the new groundwater potential at mesh point (i, k) is expressed in terms of the initial value at the node and the new values at the four nodes surrounding that node. Eq. 4.48b represents a system of linear equations for  $\psi_{i,k}$  at time level  $t^{j+1}$ . This system can be solved directly using matrix or iteration methods. The iterative successive over relaxation (SOR) method has been used in this case.

## 4.5 Linkage of Alluvial Stream-Aquifer Systems

Water transfer to/from a groundwater recharging river is characterised, among other things, by the difference between the groundwater potential and the elevation of the water in the river, the surface area of the river, the river's flood wave duration, and seepage resistance of the river bottom layer. A typical relationship between groundwater potential in an aquifer and flow from the aquifer into a river is illustrated in Figure 4.4 by the full line. The seepage resistance is a function of the geology of the area and the nature of the sediment layer formed on the river bed.

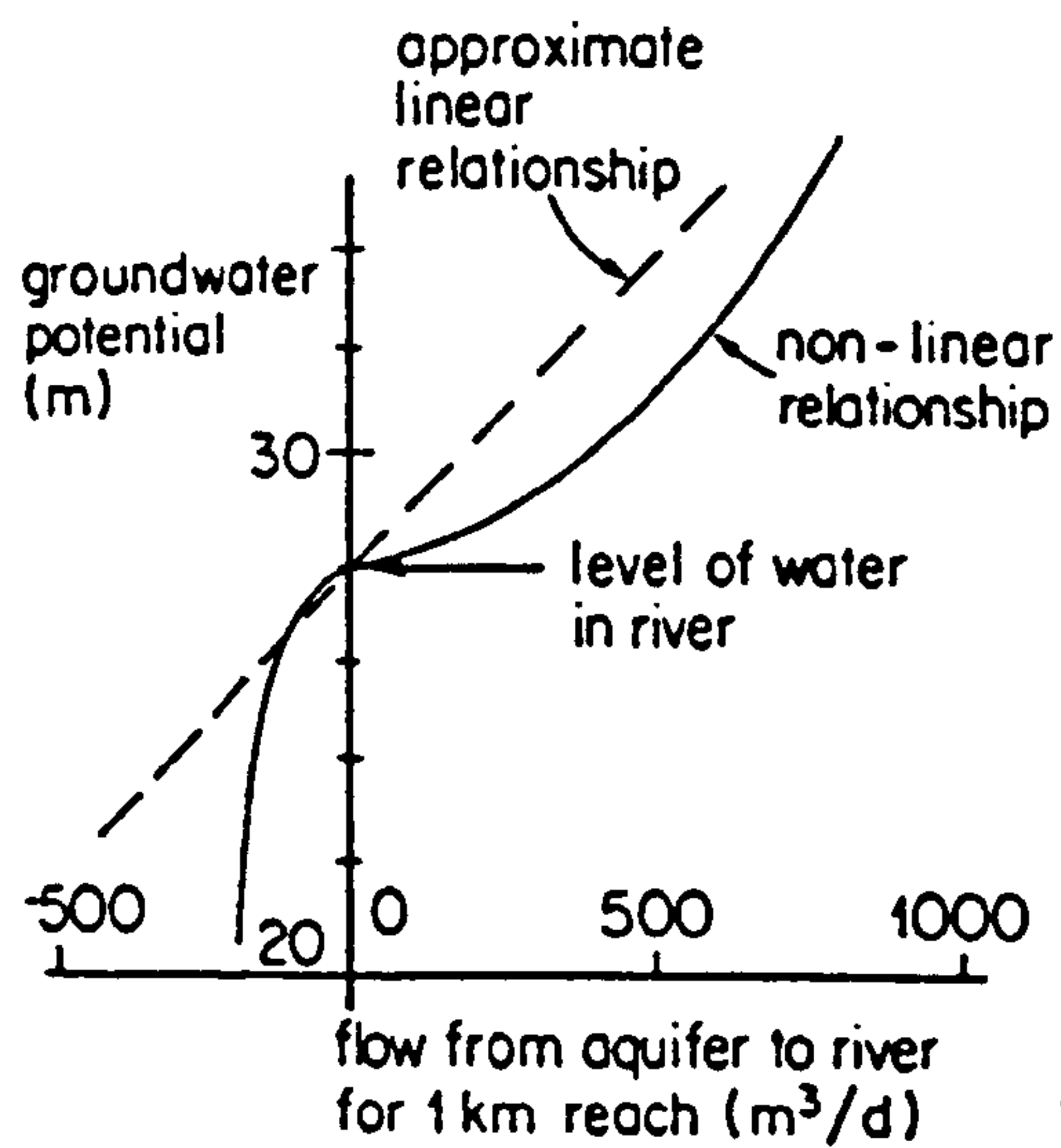


**Fig. 4.4.** A typical relationship between flow from aquifers to rivers, and groundwater potential, (*Source: Rushton and Redshaw, 1979*)

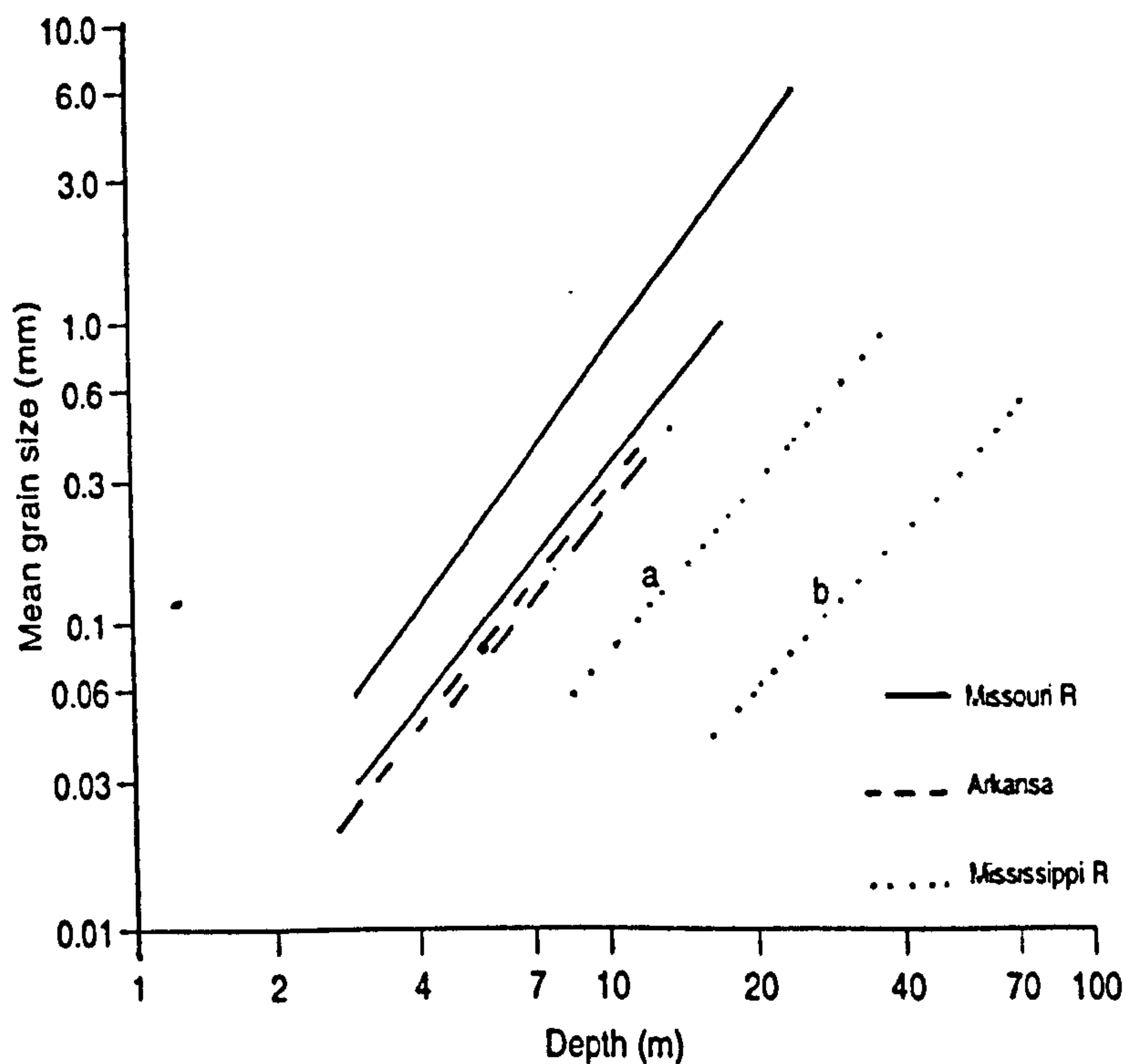


**Fig. 4.5** Grain size versus depth for alluvial sediments of the Missouri, Arkansas and Mississippi River valleys, ( a = for 1956; b = for 1966). Data for the Mississippi is in terms of the effective grain size,  $d_{10}$ , and the others are for  $d_{50}$ . (*Source: Sharp, 1977*)



It is notable from Figure 4.4 that the actual flow from the river into the aquifer, after the groundwater potential has fallen below the river level, is usually considerably less than the flow in the reverse direction for a similar head difference. This is largely due to the presence of a less permeable exotic sediment layer on the river bed delivered by the river from upstream sources.

In the event of scouring, the average hydraulic conductivity may have to be re-adjusted for different scour levels since observations from some major rivers have shown vertical grain-size distribution beneath the zone of deposition consistently changes downwards. The following examples illustrate this observation.

Figure 4.5 shows typical patterns of grain size distribution for alluvial sediments of the Missouri, Mississippi and Arkansas Rivers (Sharp, 1977). Experimental determination of the average hydraulic conductivity of the alluvium showed the same exponential pattern, of the hydraulic conductivity increasing with the grain size. The results of the permeameter test relating the average hydraulic conductivity to the sediment particle sizes are plotted in Figure 4.6. Sharp (1977) used the  $D_{50}$  variable presumably because he wanted to distinguish the difference between the coarseness of the sediment materials of the different rivers, and to show how the texture of the sediments affected the hydraulic conductivity of the materials. By correlating the grain size with the depth for the same materials, he obtained the exponential relationship between the hydraulic conductivity and the depth of the alluvium as:

$$K_2 = C_a Z_{b2}^n \quad (4.49)$$

where  $C_a$  is an empirical constant. From Eq. 4.49, demonstrated graphically in Figure 4.7, the representative transmissivity can be calculated by integrating  $K_2$  over the saturated thickness of the alluvium.

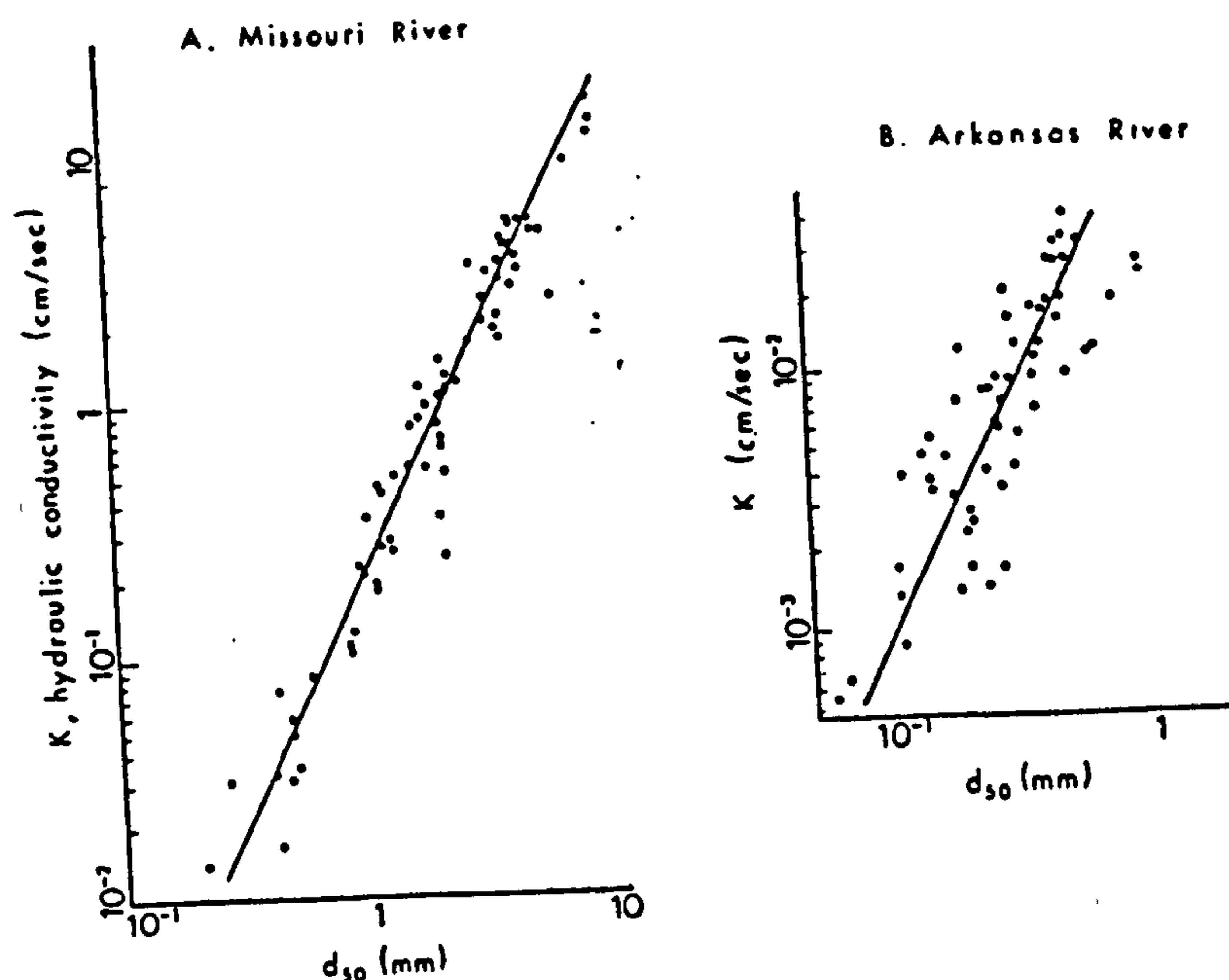


**Fig. 4.6. Hydraulic conductivity versus mean grain size of alluvial sediments for (A) the Missouri River and (B) the Arkansas River , (Source: Sharp 1977)**

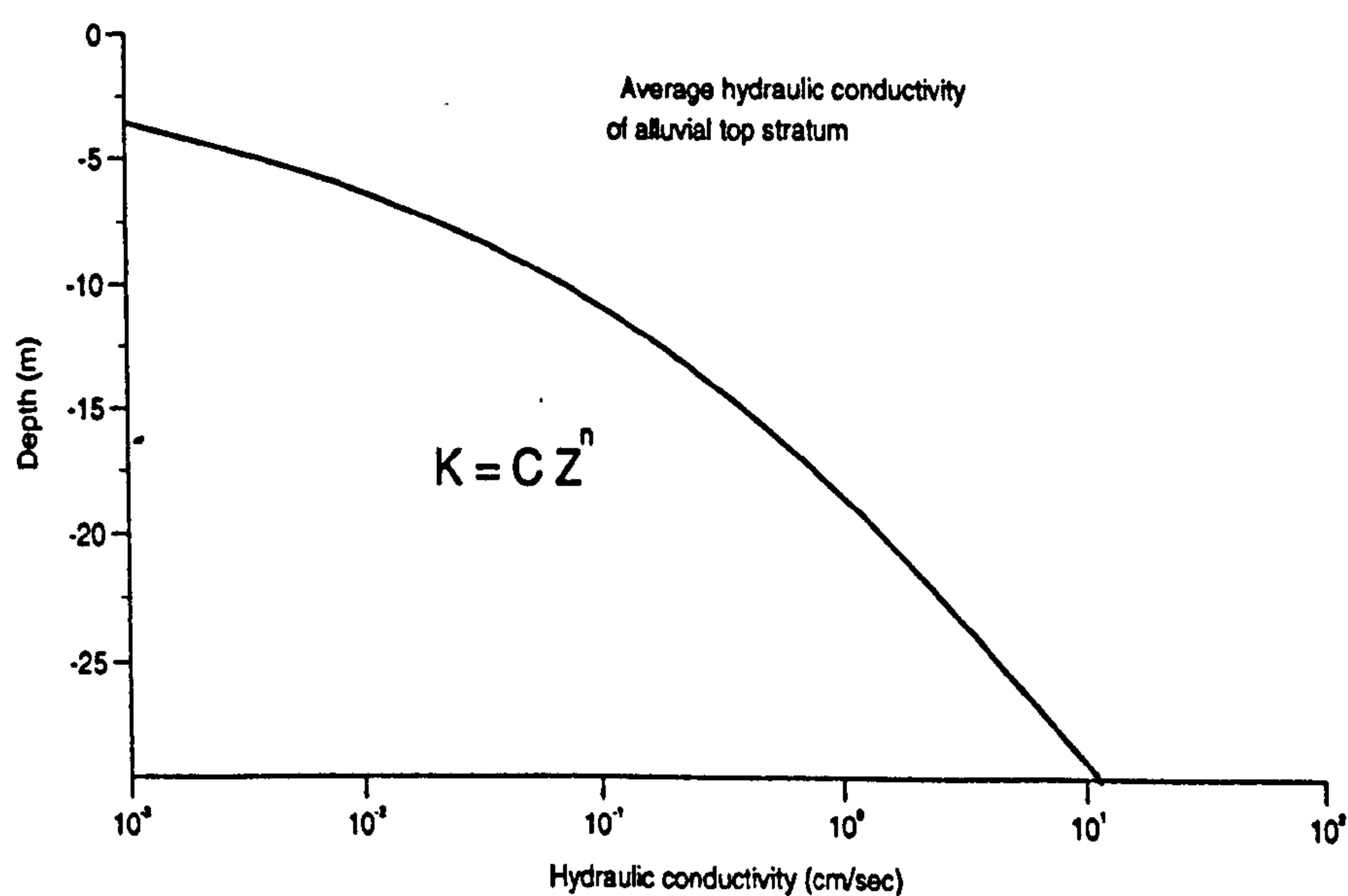


**Fig. 4.7. A general pattern of the hydraulic conductivity increase with depth, for the Rivers Missouri and Arkansas sediment data, (Source: Sharp, 1977)**



The curve, as plotted in Figure 4.7, ends at a depth of about 3 m presumably because Sharp (1977) measured the depth with reference to the land surface as the datum (zero) level, and the average river bed was 3 m below the land surface. The average hydraulic conductivity of the top stratum (banks) is indicated on the diagram. The results of the sediments from the Kibos (chapter 3) showed similar results of finer sediments forming a layer over coarser sediments.

However, the theoretical evaluation of the hydraulic conductivity of the sediment layer at the bottom of the river is complex, given that it tends to vary even for the same material when subjected to different seepage flows. For instance, when the seepage is entering the river, the resultant force is upwards such that the sediment particles are pushed apart in a manner analogous to the quick-sand effect. This leads to loose packing, high permeability, and increased erodibility of the sediments. When there is seepage from the river into the ground, its resultant force is downwards, in addition to the hydrostatic and gravitational forces, leading to an effect of compaction. The net result is to lower the permeability (Younger et al, 1993). Because of lack of adequate theory, its evaluation is often left as a matter of field or laboratory calibration. A methodology for its field experimentation and computation will be presented in the next chapter in the section describing field calibration.

The other assumptions often adopted, but perceived here as possible causes of discrepancies in the analysis of field problems related to alluvial channel developments, are those of: (1) fully penetrating streams and (2) confined or unconfined aquifer conditions under the river. Take, for example, a shallow unconfined aquifer having an eroding stream running across it. Then, with time, it is possible that the river can erode the bed material until the bed elevation has fallen to the non-erodible impermeable bed-rock, thereby becoming a fully penetrating stream.

On the other hand, for a fully penetrating river, it is possible that due to some upstream changes the input sediment concentration can be increased to start causing aggradation downstream. Depending on the geography and geology of the system, this processes can continue until eventually shallow unconfined aquifers are formed below the river.

Similarly, for a partially penetrating river with a layer of an impermeable but erodible material at the bottom of the river, it is possible that with time this material can be eroded so that the aquifer becomes unconfined. The reverse can take place if sediment laden streamflow delivered impermeable material on the bottom of a river which was initially permeable. In other words, alluvial stream-aquifer systems subject to changes may be both confined and unconfined, and these conditions may vary both spatially and temporarily. In interacting alluvial stream-aquifer systems, therefore, it is necessary that the simulation formulation represents the propagation of both the liquid and solid phase adjustments.

The groundwater equation for seepage through  $n$  layers of porous media is obtained from Darcy's expression relating the total hydraulic head driving a flow  $q$  (Bear & Verruijt, 1987), i.e.:

$$\sum_{i=1}^n (\Delta H)_i = q \sum_{i=1}^n \frac{Z_{bi}}{K_i} \quad (4.50)$$

where  $q$  = groundwater seepage rate,  $K_i$  = hydraulic conductivity of individual medium,  $Z_{bi}$  = thickness of individual sediment medium,  $(\Delta H)_i$  = head difference across each sediment medium and  $n$  = total number of the sediment media.

Current stream-aquifer interaction models do not consider the water transfer/recharge as a function of the sedimentation variability, a feature which if ignored would



impede the capability of the model to analyse hydrological phenomena on evolving streams. Here, having considered the sedimentation processes, it is regarded that the physical aspects of the main features in the alluvial stream-aquifer systems have been represented and their interaction can now be related in a mathematical form. From the mathematical formulation, a more general technique can be developed with the capability to analyse field hydrological problems, even those of evolving channels.

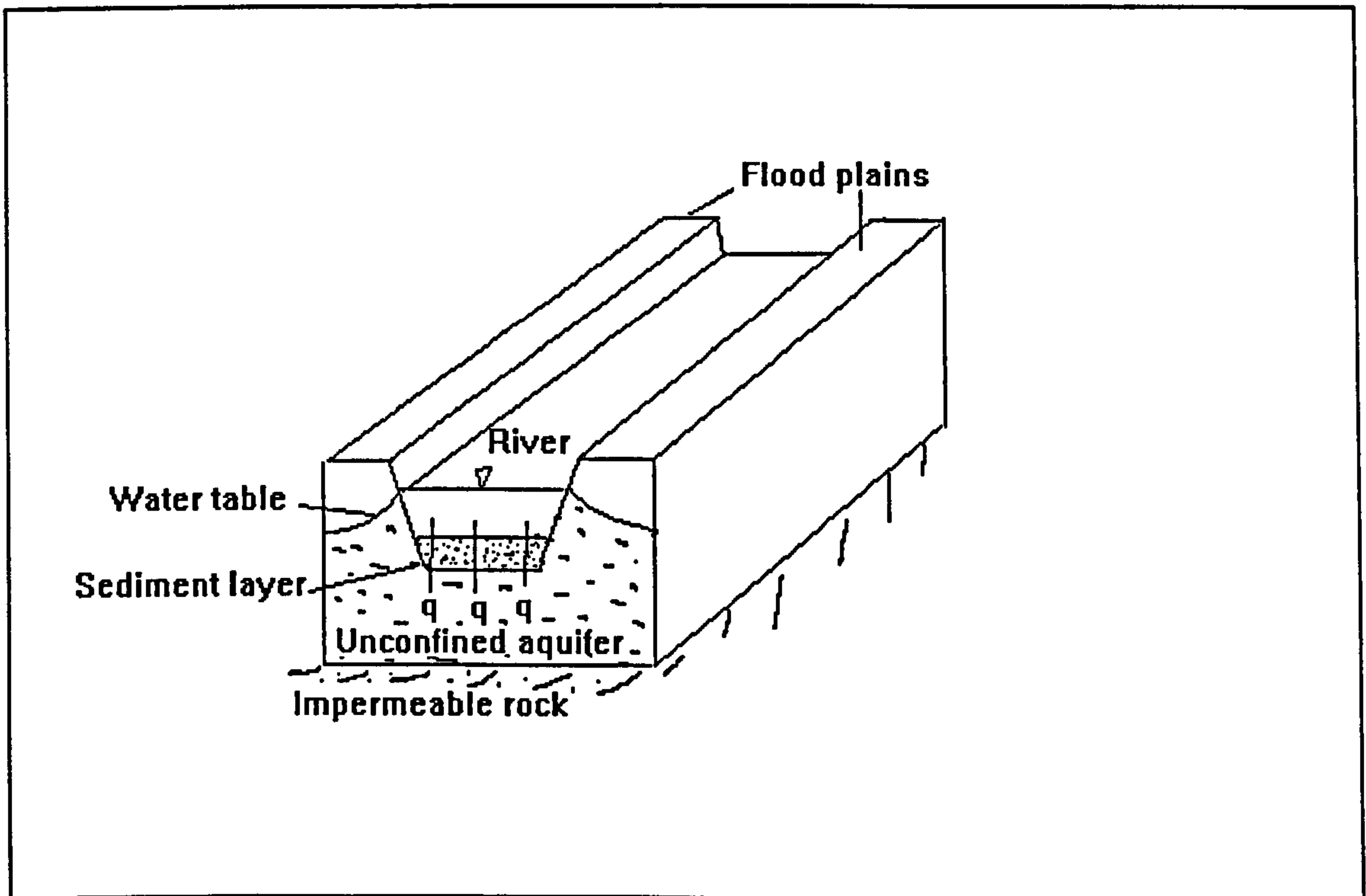


**Fig. 4.8 A schematic sketch of a groundwater recharging river**

Considering a groundwater recharging stream as depicted in Figure 4.8, and assuming that seepage from/into the river is predominantly vertical through the channel bed, then Eq. 4.50 can be rearranged to give the seepage rate as :

$$q = \frac{\sum_{i=1}^n (\Delta H)_i}{\sum_{i=1}^n \frac{Z_{b_i}}{K_i}} \quad (4.51)$$

This assumption of predominant vertical flow is reasonable, considering Sharp's (1977) report that most of the groundwater flow between the river and bank storage is through the river bed and not the banks, because : (1) the river bed has greater surface area, (2) the river bed is closer to the zone of greater hydraulic conductivity and (3) maximum pressure head acts on the bed. Furthermore, the banks, in general, have low hydraulic conductivity because they have different sediment size fractions, with a higher clay percentage than in the bed (Schumm, 1969), which tend to infiltrate into the banks, thereby decreasing the permeability and the contribution of the stream-aquifer interchange through the banks.

Eq. 4.51 demonstrates that the lateral flow is as well a function of the sedimentation changes,  $q = f(\Delta H_i, Z_{bi}, K_i)$ . For clarification, two porous media comprising a sediment deposit layer over an alluvial aquifer layer are assumed (Figure 4.7). Then:

$$q = \frac{k_1 k_2}{k_1 + k_2} \sum_{i=1}^2 (\Delta H)_i \quad (4.52)$$

where  $\sum (\Delta H)$  is the total potential head across the two media,  $k_1$  and  $k_2$  are coefficients given as  $k_1 = K_1 / Z_{b1}$ ,  $k_2 = K_2 / Z_{b2}$ , with the hydraulic conductivity as  $K_1$  and  $K_2$  and the thicknesses as  $Z_{b1}$  and  $Z_{b2}$  for the sediment layer and aquifer, respectively. If the specific sediment seepage resistance is defined as  $\zeta = 1/K_1$  so that  $k_1 = 1/\zeta \cdot Z_{b1}$  then:

$$q = \frac{k_2}{1 + \zeta Z_{b1} k_2} \sum_{i=1}^2 (\Delta H)_i \quad (4.53)$$

Assuming that the pressure head in the aquifer at the reference point remains the same as  $\psi_a$ , then the potential difference is given by,  $\sum (\Delta H)_i = H + Z_{b1} + Z_{b2} - \psi_a$ ,

and so:



$$q = \frac{k_2}{1 + \zeta Z_{b1} k_2} (H + Z_{b1} + Z_{b2} - \psi_a) \quad (4.54)$$

Since the solution to this equation is dependent on contemporary values of streamflow, streambed and groundwater processes, it can be used to account for transient groundwater transfers and to link open channel and groundwater hydrology. The equation summarises the modifications introduced in the theory of alluvial stream-aquifer interaction, in order to suppress the assumption of boundary rigidity for alluvial channels that are hydraulically connected to aquifers. It is noticed that in this mechanism the bed elevation changes due to sedimentation,  $Z_{b1}$ , are represented independently from the aquifer elevations  $Z_{b2}$ , so that in the event of aggradation, the different hydraulic properties for the exotic sediment accumulations can still be accounted for exclusively, by assigning  $Z_{b1}$  and  $K_1$  with the appropriate field values. Even when the sediment deposit is washed away such that  $\Delta Z_{b1} = 0$ , the equation is still applicable, only that in this state the sedimentation variation will be affecting the aquifer material itself.

The contemporary variables in the stream-aquifer linking function, Eq. 4.54 are, therefore, corrected at time  $t^{j+1}$  through the processes whereby: the streamflow routing processes provide  $H$ ; the sediment routing processes provide  $Z_{b1}$ ; and the groundwater processes provide  $\psi$ . The parameters  $k_2$ ,  $Z_{b2}$  and  $\zeta$  are provided by predefined functions or field data. The lateral groundwater flow rate,  $q$ , at time  $t^{j+1}$  can then be evaluated before the computations are moved onto the next time step  $t^{j+2}$ . In the presence of other lateral discharges as tributary, overland, abstraction, etc., obtained from field data, all of them are summed up and added to the lateral groundwater flow before moving to the next time step. The computation procedure is as follows :

The initial variable values,  $H^0$ ,  $\psi^0$  and  $Z_{b1}^0$  at time  $t^0$  are used to compute a steady seepage flow  $q^0$ , which is applied in the routing solution to evaluate the new water conditions after a short time period  $\Delta t$ . At this time,  $t^1$ , the new computed values,  $H^1$ ,  $\psi^1$  and  $Z_{b1}^1$  are used to compute a new water transfer,  $q^1$ , for routing in the next time step. The procedure is then repeated until the total time period in consideration is covered, as illustrated by the flowchart in Figure 4.9

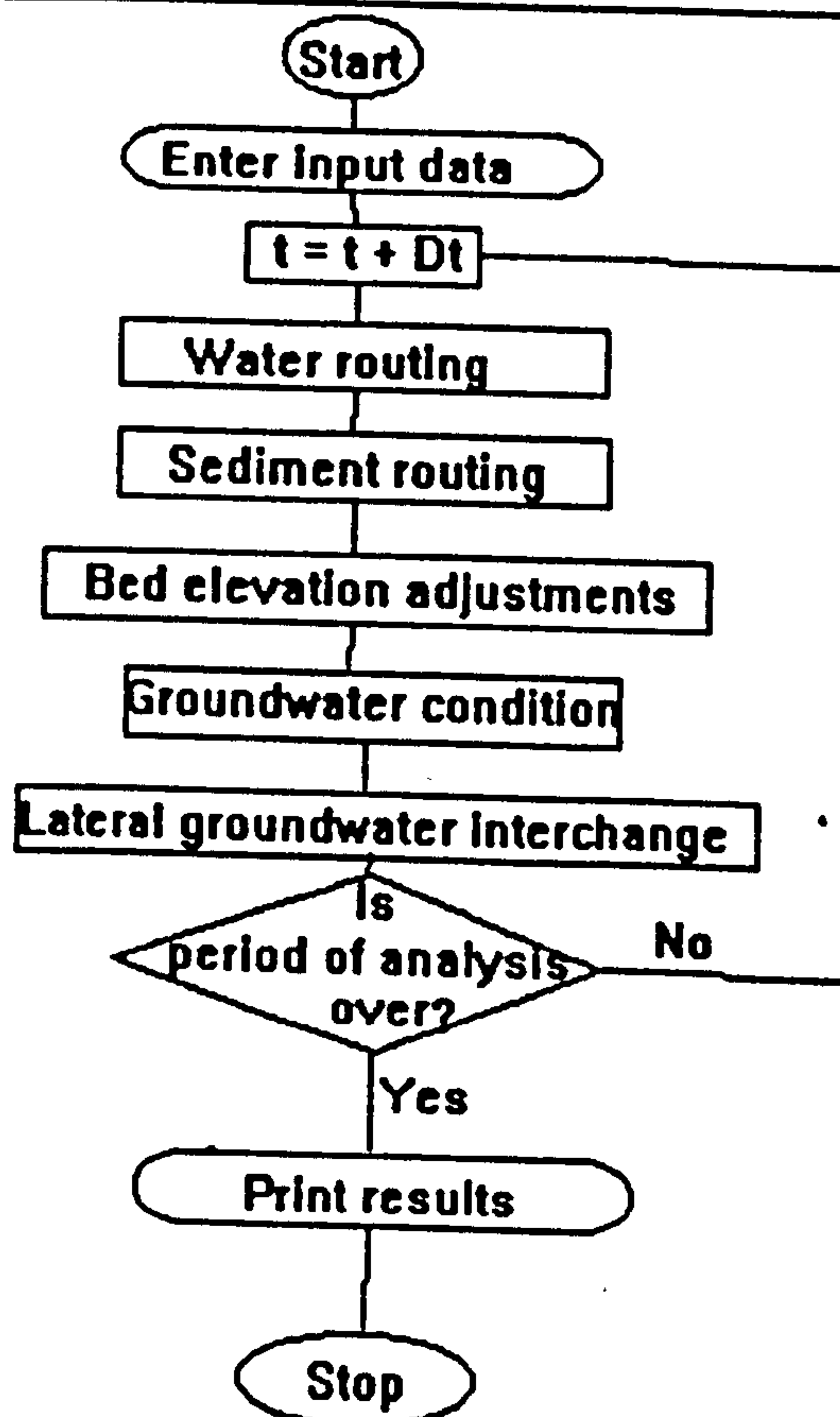


**Fig. 4.9** Flow chart showing the major steps of computation of the Model for Alluvial Stream-Aquifer Interaction (MASAI)



The additional advantage of the MASAI concept, in comparison with the current water and sediment routing models (e.g. HEC-6, 1977; and FLUVIAL-12 by Chang, 1988a), is its ability to account for the transient groundwater contribution to streamflow. In comparison with the current stream-aquifer interaction models (e.g. Cunningham and Sinclair, 1979), the advantage is its ability to account for transient channel bed adjustments. However, the model has its own limitation in that it assumes that the channel width does not vary with time, and that the streamflow is hydraulically connected to the underlying aquifer throughout the study period. This modified solution procedure has more physical sense in erodible channels that carry highly variable flood events. In such systems, linkage of open channels to groundwater by purely empirical relationships, as are often used in estimating the baseflow contribution to streamflow, does not interpret the operative physical processes. Use of such "black box" or lumped modelling element eliminates many of the problems involved in making assumptions, but gives little insight into the hydrological and fluvial processes involved in scouring/filling channel systems. The solution procedure developed here has shed more light on the processes.

The merits and limitations of distributed models have already been outlined in section 4.2, (and in Beven and O'Connell, 1982; O'Connell, 1991; Storm, 1991, etc.). Therefore, if the data for describing patchy boundary and initial conditions, and computer facilities are not limiting, the distributed deterministic modelling approach developed herein will provide better results that describe the operative physical processes in erodible channels. Verification and calibration of the model are analysed in the next chapter in a way to verify the computer program developed, before the modelling approach is applied to give more insights into alluvial stream-aquifer interaction.

A computer program in FORTRAN 77, exemplifying the modelling approach, on a channel reach on the Nyando River is included on a floppy disk (Appendix 5).

## **5. MODEL VERIFICATION, CALIBRATION AND APPLICATIONS**

### **5.1 Introduction**

The primary objective of this study has been to model a mechanism linking the three primary hydrologic phenomena involved in alluvial stream-aquifer systems, that is; water and sediment routing in channels and groundwater flow in the underlying unconfined aquifers. The aim of this chapter is to verify that the computer programs of the finite difference equations of the three hydrological phenomena - streamflow routing, sediment routing in channels and groundwater flow - and the scheme linking them to form the MASAI (as developed in chapter 4), are working. Development of the schemes of the primary hydrologic phenomena are well established in the literature (see for example, Amein and Fang, 1970; Chen, 1973; Cunningham, 1977; Wang and Anderson 1982; Lu, 1984; French, 1986 and Chang, 1988a).

During this stage, field data for alluvial channel and aquifer conditions, before and after some changes, are necessary. But unfortunately, hydrogeological data sets with such complete information are rarely obtained in the field, especially because of the wide range in both spatial and temporal scales of the processes involved. For instance, whereas streamflow changes may take only minutes or a few hours to be



observed, channel degradation and groundwater depletion changes may take days or even months before they can be noticed. To supplement the process of verification and demonstrate the ability of the computer programs to simulate the dynamic behaviour of water flow in alluvial channels and plain aquifers, therefore, a summary of data sets from existing literature has been employed. This is acceptable since for physically-based modelling it is possible to transfer information from studies made elsewhere (Beven and O'Connell, 1982).

Although quantification of predictive uncertainty is essential for testing of the overall performance of a model, however, by far the most straightforward and meaningful method of evaluating predictive uncertainty is that of direct graphical comparison of model prediction with corresponding values of observed (or tested) data. The method has been widely accepted and used (e.g. Rahuel et al, 1989; Chang, 1990; Todini, 1991). The advantage of the method is that it does not require the reader to necessarily have had some statistical knowledge in order to understand the comparison/difference between the model simulations and the actual values. Therefore, in this section, verification has been based on graphical comparison of the results simulated by the MASAI, with the results obtained from published (or tested) models. The verification is aimed to show that the model is able to simulate results that are comparable to those of verified models. At this preliminary stage, detailed statistical tests of the comparisons were not worthwhile because errors of the other models were not stated. Detailed test of the predictive uncertainty of the model will be presented in the next section, based on data obtained from the Nyando River.

## **5.2 Verification of the Model**

The following three applications have been selected to form progressive verification of the MASAI: (1) Water routing in a trapezoidal irrigation canal; (2) Water and

sediment routing in hypothetical channels; (3) Stream-aquifer interaction due to a flood wave traversing through an alluvial plain.

### **5.2.1 Water routing in a trapezoidal irrigation canal.**

To demonstrate the ability of the water routing program to simulate the dynamic behaviour of water flow in channels, a numerical experiment was carried out using the following geometrical data:

length of channel = 4500 m.

bottom width = 2.7 m.

channel slope = 0.0002

Manning's roughness coefficient = 0.016

slope of the banks = 1.5 (i.e. 3v:2h)

the section was trapezoidal,

This data refers to an existing irrigation canal run by La Societe du Canal de Provence, where a number of experiments were carried out (Todini, 1991) to derive flood routing procedures for the real-time operation of sluices.

For this test, the simulation was carried out by adding to the initial discharge of  $Q = 3.65 \text{ m}^3/\text{s}$ , a sudden increase of  $\Delta Q = 2.95 \text{ m}^3/\text{s}$ . The initial water level conditions in the example were set to the uniform flow conditions of 1.14 m over the entire channel reach, while the downstream condition was taken to be 100 km downstream and kept at a critical depth throughout the experiment.

The results obtained by applying the water routing code are shown in Figures 5.1a and 5.1b, in comparison with other results of the Parabolic and Backwater (PAB)



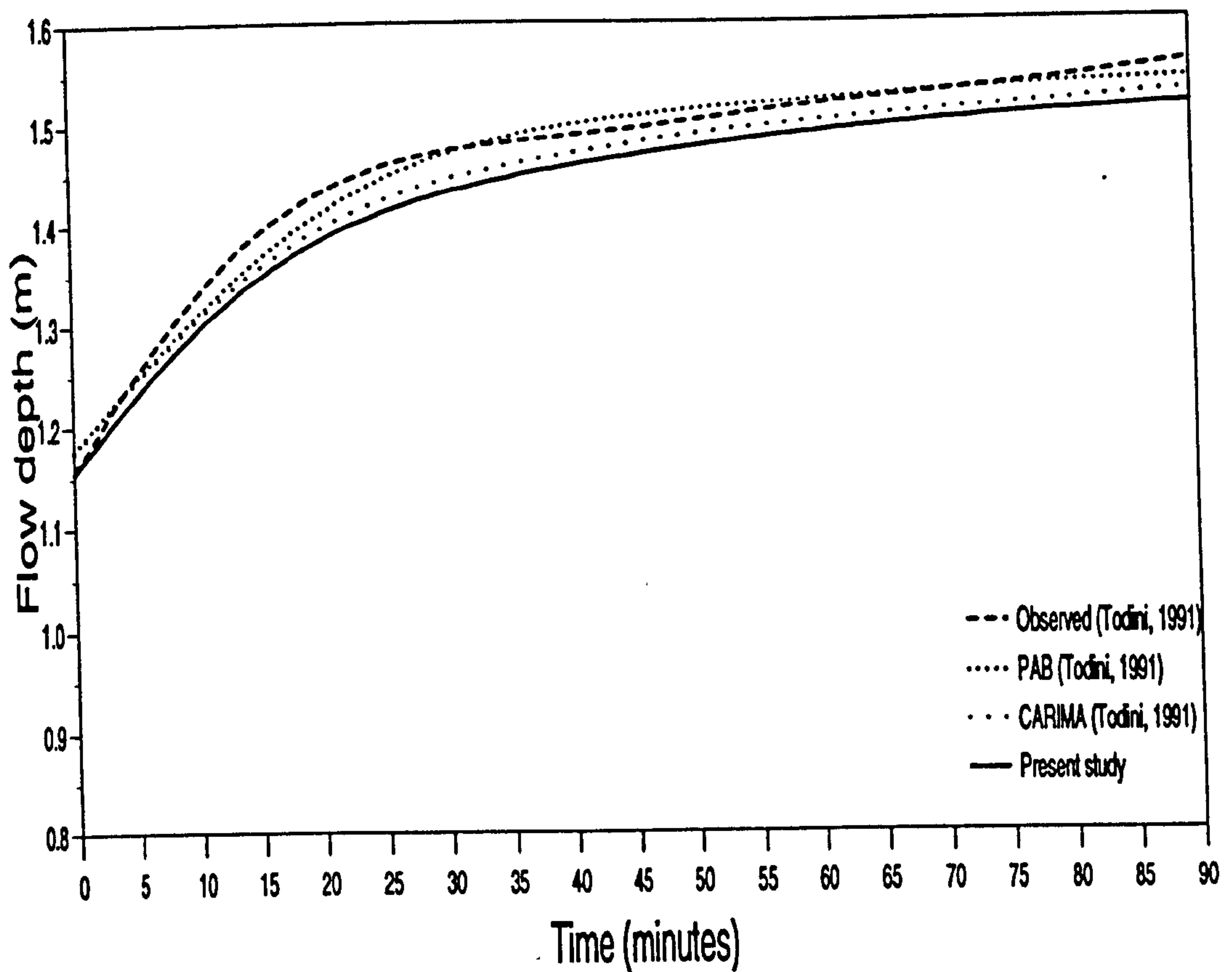


**Fig. 5.1a Comparison results of water routing in a canal at a distance 475 m from the upstream section**

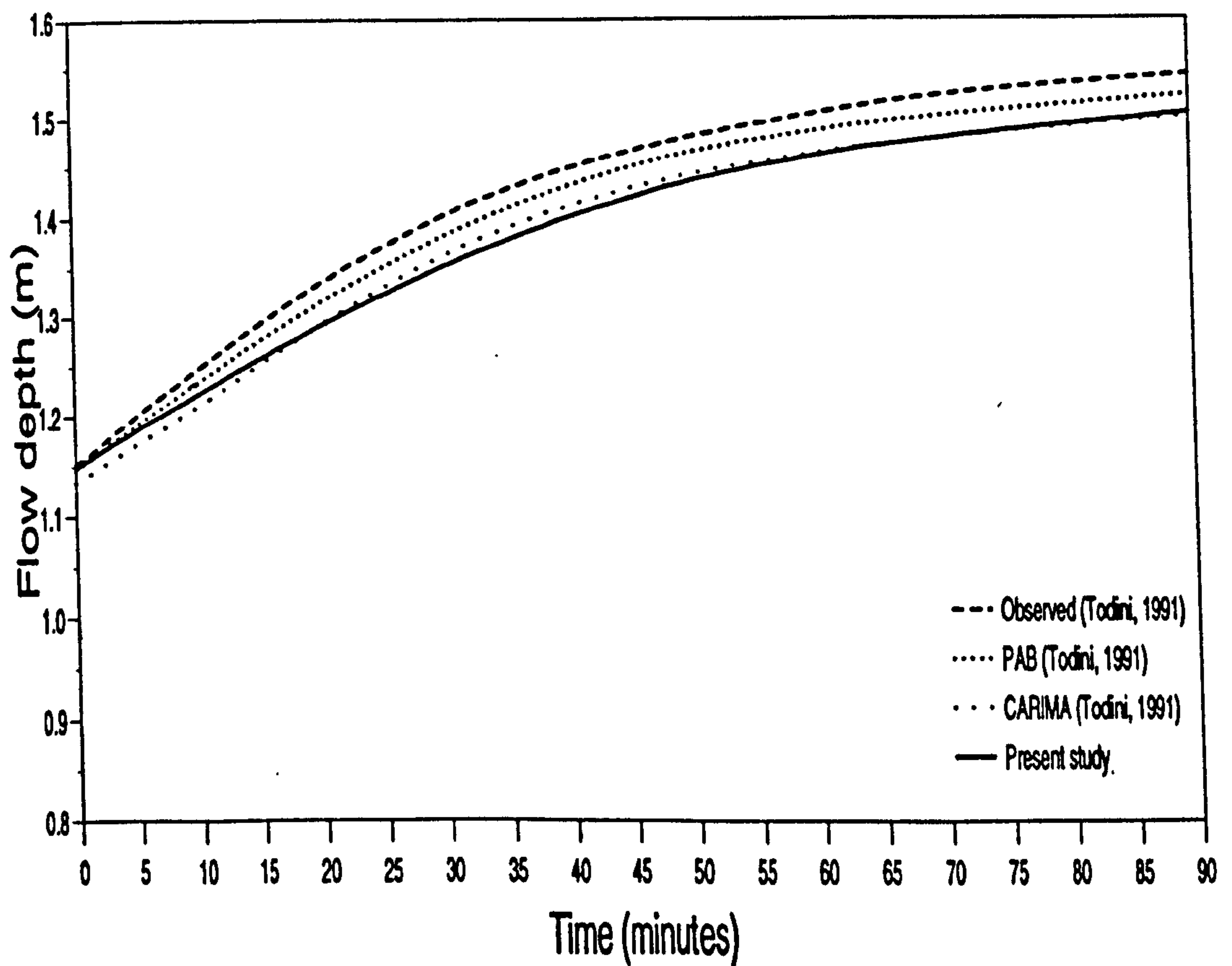


**Fig. 5.1b Comparison results of water routing in a canal at a distance 1575 m from the upstream section**

approach, Carima of Sogreah, and the experimental observations (Todini, 1991). The simulation results, based on comparison of graphical plots, are observed to compare well, although the channel parameters used were not calibrated, according to Todini (1991). For instance lack of account for seepage losses/gains, a realistic phenomenon in the field when considering irrigation efficiency, could be responsible for the deviation of the computed results from the observed values. Therefore, comparison of the simulated and published results (Figures 5.1a and 5.1b), verifies the computer program for water routing. Comparison of the results with those of CARIMA, which is also based on the implicit finite difference scheme, are in closer agreement from a practical viewpoint, having a maximum deviation of about 1 cm only.

### **5.2.2 Water and sediment routing in hypothetical channels.**

In the preceding example, only water routing in a supposedly stable channel was verified. In this simulation, verification is for the sediment routing program, and its linkage to the water routing sub-program. To illustrate this, Chang and Richards (1971) model has been reproduced and solved by the water and sediment routing code of the MASAI. The channel system used has the following characteristics:

#### **1. Channel properties:**

- (i) length of the channel,  $L = 14$  km,
- (ii) the mean sediment concentration,  $C_s = K V^m H^n$

where  $K = k / (g \omega)$

$k$  = the coefficient of sediment transport capacity,

$g$  = gravitational acceleration,

$\omega$  = the mean fall velocity of the sediment,

$V$  = the mean velocity of flow, and

$H$  = the depth of flow.



In this example, Chang and Richards assumed that:

$$k = 7.55 \times 10^{-5}$$

$$m = 3$$

$$n = -1$$

$$\omega = 0.002 \text{ m/s}$$

(iii) the bed slope,  $S_o = 0.0003$ ,

(iv) the Manning's roughness coefficient,  $n = 0.01$ ,

(v) the sediment volume ratio,  $(1-\lambda) = 0.528$ ,  $\lambda$  being the porosity.

2. Initial boundary conditions:

The initial flow depth were calculated from the backwater curve computation (Chow, 1959) with  $Q_o = 6.2 \text{ m}^3/\text{s}/\text{m}$  (normal flow depth at 14 km upstream of the dam  $H_1 = 2.15 \text{ m}$ ) and  $H_n = 4.0 \text{ m}$  ( at the upstream side of the dam).

Letting  $\Delta x = 2.0 \text{ km}$ , the initial depth of flow are as given in Table 5.1:

**Table 5.1 Characteristics of the initial conditions for the channel in Chang and Richards (1971) model.**

Section	Distance from upstream (km)	Depth (m)	Bed elev. above datum (m)
1	0	2.150	104.2
2	2	2.158	103.6
3	4	2.184	103.0
4	6	2.293	102.4
5	8	2.549	101.8
6	10	2.957	101.2
7	12	3.456	100.6
8	14	4.000	100.0

### 3. Upstream boundary conditions:

The inflow discharge hydrograph was defined by a constant discharge:

$$Q = 6.2 \text{ m}^3/\text{s}/\text{m}$$

### 4. Downstream boundary condition:

$$H_n = 4.0 - \Delta Z_n$$

where  $H_n$  and  $\Delta Z_n$  are the flow depth and the bed elevation change at the upstream side of the dam, respectively.

The simulated results are presented in Figure 5.2. It is shown that the results produced by the water and sediment routing codes programmed here are, for practical purposes, similar to those computed by Chen (1973) and Chang and Richards (1971). The slight difference could be because of the different finite difference schemes employed by the researchers. Unlike the fully implicit scheme used here, Chen used the linear-centre-implicit method and Chang and Richards and Hsu and Chu used the method of characteristics. Different methods have different advantages and disadvantages, besides accuracy (Amein and Fang, 1970; French, 1986; Todini, 1991).

To demonstrate bed degradation, another simple example from Chen's (1973) application results has been used to describe another hypothetical unit-width channel. The channel has a reduction in bed particle sizes and bed-slope along the channel in the downstream direction due to the effects of sediment sorting. When the inflow discharge and the bed material load are kept constant, the channel is in equilibrium, that is, no erosion or deposition occurs in the channel reach. In order to present the same picture of the system as described by Chen (1973), the same English units have been retained, but with the corresponding values in SI units, as given in brackets. The basic data for the routing are:



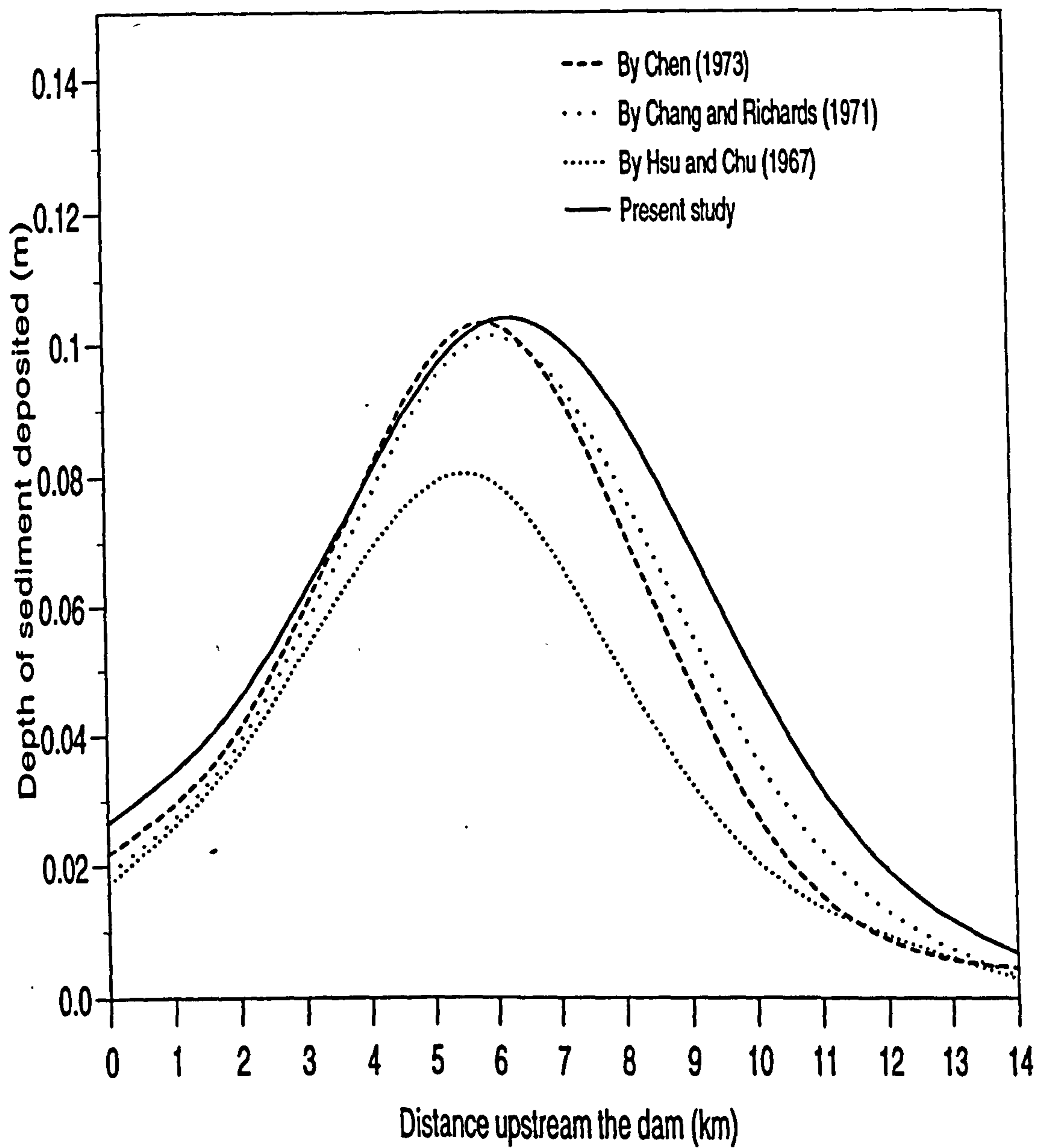


**Fig. 5.2 Bed elevation profiles upstream of a dam, after 30 minutes of sediment laden flow through the reservoir**

1. Channel characteristics in the reach:

- (i)  $L = 30.0$  miles (48.27 km),
- (ii)  $S_{0i} = 0.00075 e^{-0.00162 x_i}$ ,
- (iii)  $n = 0.031$ ,

where  $L$  = length of the reach;  $S_{0i}$  = bed slope at section  $i$ ;  $x_i$  = distance in miles from the upstream boundary section 1 to section  $i$ ;  $n$  = Manning's roughness coefficient.

2. The sediment transport function in Chang and Richards (1971) model was used to simulate the sediment concentration, i.e.

$$C_s = KV^m H^n,$$

with the notations as described in the last example.

3. Upstream boundary conditions:

A discharge hydrograph was assumed at the upstream end of the reach such that:

$$0 < t \leq 200 \text{ min.}, Q = 25 + 35 \sin(t\pi/200) \text{ cfs/ft (2.32 + 3.25 sin}(t\pi/200 \text{ m}^3/\text{s/m})$$

$$\text{and } t > 200 \text{ min.}, Q = 25 \text{ cfs/ft (2.32 m}^3/\text{s/m)}$$

4. Initial flow conditions:

- (i) water flow,  $Q_i = 25.0$  cfs/ft (2.32 m<sup>3</sup>/s/m),
- (ii) sediment concentration,  $C_{si} = 250$  ppm,
- (iii) The initial depths are the normal depths in the channel reach. The other values at every section are given in Table 5.2.

5. Downstream boundary conditions:

A rating curve at the downstream end of the reach was used to establish the boundary condition of the form:

$$H_n = 0.115Q_n + 3.07$$



where  $H_n$  = depth at the downstream section  $n$ ;  $Q_n$  = corresponding discharge at the downstream section  $n$ .

**Table 5.2 Characteristics describing the initial conditions for the channel applied by Chen (1973). The SI values are given in brackets (i.e distance in km and depth and bed elevation in m)**

Section	Distance from upstream (miles)	Depth H (ft)	Bed elevation above datum(ft)
1	0 (0)	5.859 (1.786)	173.590 (52.910)
2	3.0 (4.83)	5.868 (1.789)	161.739 (49.298)
3	6.0 (9.65)	5.876 (1.791)	149.945 (45.703)
4	9.0 (14.48)	5.885 (1.794)	138.209 (42.126)
5	12.0 (19.31)	5.894 (1.796)	126.528 (38.566)
6	15.0 (24.14)	5.902 (1.799)	114.905 (35.023)
7	18.0 (28.96)	5.911 (1.802)	103.339 (31.498)
8	21.0 (33.79)	5.919 (1.804)	91.828 (27.989)
9	24.0 (38.62)	5.928 (1.807)	80.363 (24.495)
10	27.0 (43.44)	5.937 (1.810)	68.975 (21.024)
11	30.0 (48.27)	5.945 (1.812)	57.630 (17.566)

Again, the water and sediment routing computer program was applied to evaluate the variation in the channel bed elevations. The computed water surface elevations are shown in Figure 5.3a, in comparison with the results obtained by Chen (1973). The results show the same pattern, but with slight differences in the estimated values because of the difference in the finite difference schemes used, as explained in the previous step.

By assuming zero sediment inflow at the upstream section, the channel bed was eroded, and the eroded material was deposited downstream of the scoured portion as shown in Figure 5.3b. A combination of this simulation and the one demonstrated previously in Figure 5.2 illustrates that the simulations can be used to describe changes in channel characteristics near check-dams. Therefore, based on the simulation test results, as illustrated in Figures 5.2, 5.3a and 5.3b, the water and sediment routing algorithm is accepted as being applicable for the purposes of this study.

If the sediment yield input and bed load material in the channel can be accurately calibrated, this program can also be used to describe armouring effects and elevation changes caused by various types of hydraulic structures. For example to demonstrate the changes in the characteristics of the channel and bed material caused by degradation downstream of a grade control structures/weir, the Ackers-White (1973) function was used to calculate the bedload transport while the technique by Lee and Odgaard (1986) was applied to compute the loading of the individual particle sizes.

The channel used to simulate the changes is described by the following data:

1. Initial flow conditions:

(i) water flow,  $Q_0 = 500 \text{ m}^3/\text{s}$  and

(ii) flow depth,  $H_0 = 5.06 \text{ m}$

where  $H_0$  is the normal depth for the flow conditions.

2. Channel characteristics in the reach:

Length of the channel reach,  $L = 30 \text{ km}$

Bed slope,  $S_0 = 0.00075$

Channel bed width,  $b = 30 \text{ m}$

Channel side slopes,  $(H:V = 3:2)$



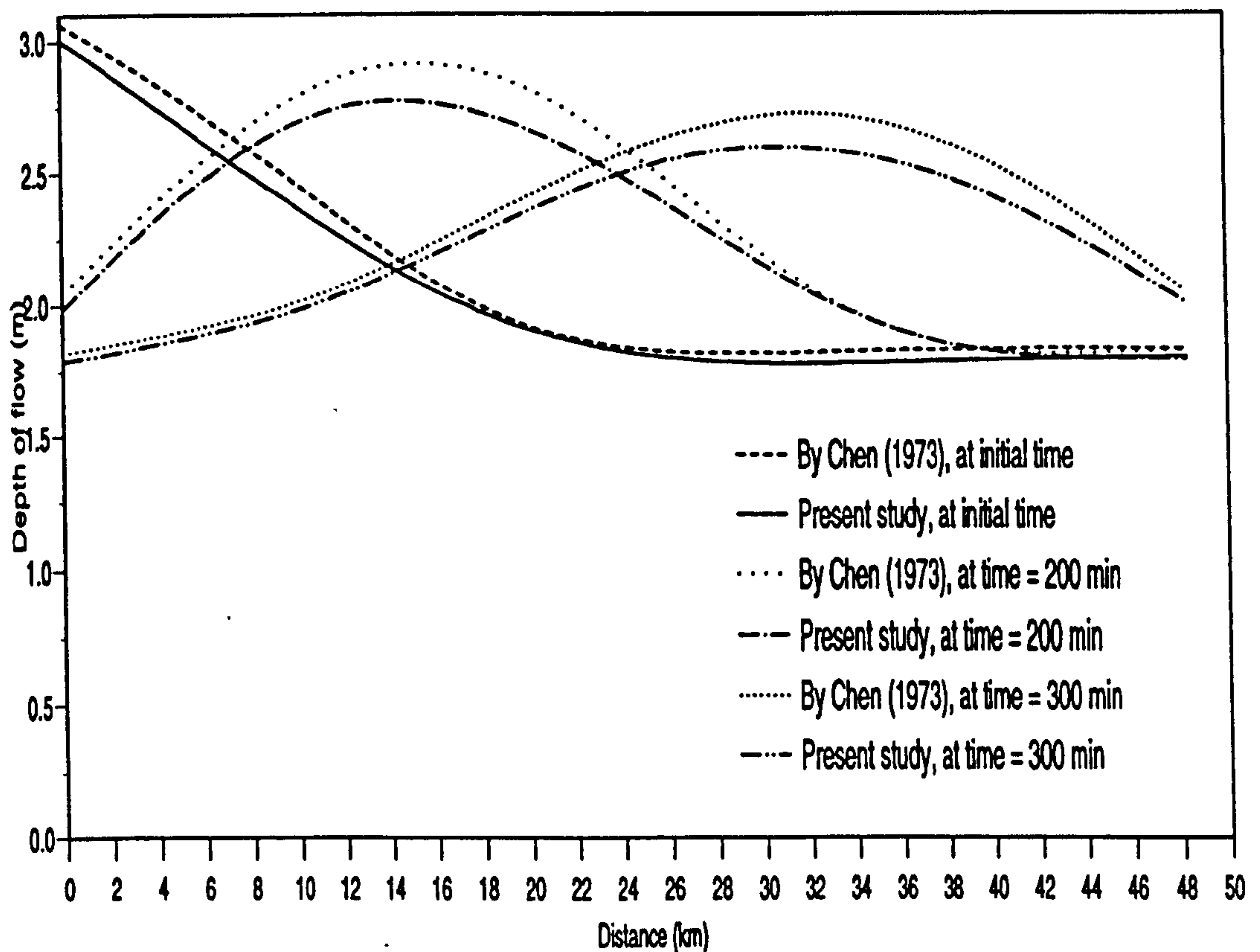


**Fig. 5.3a** Variation of water flow depth with time and distance, in a unit width channel

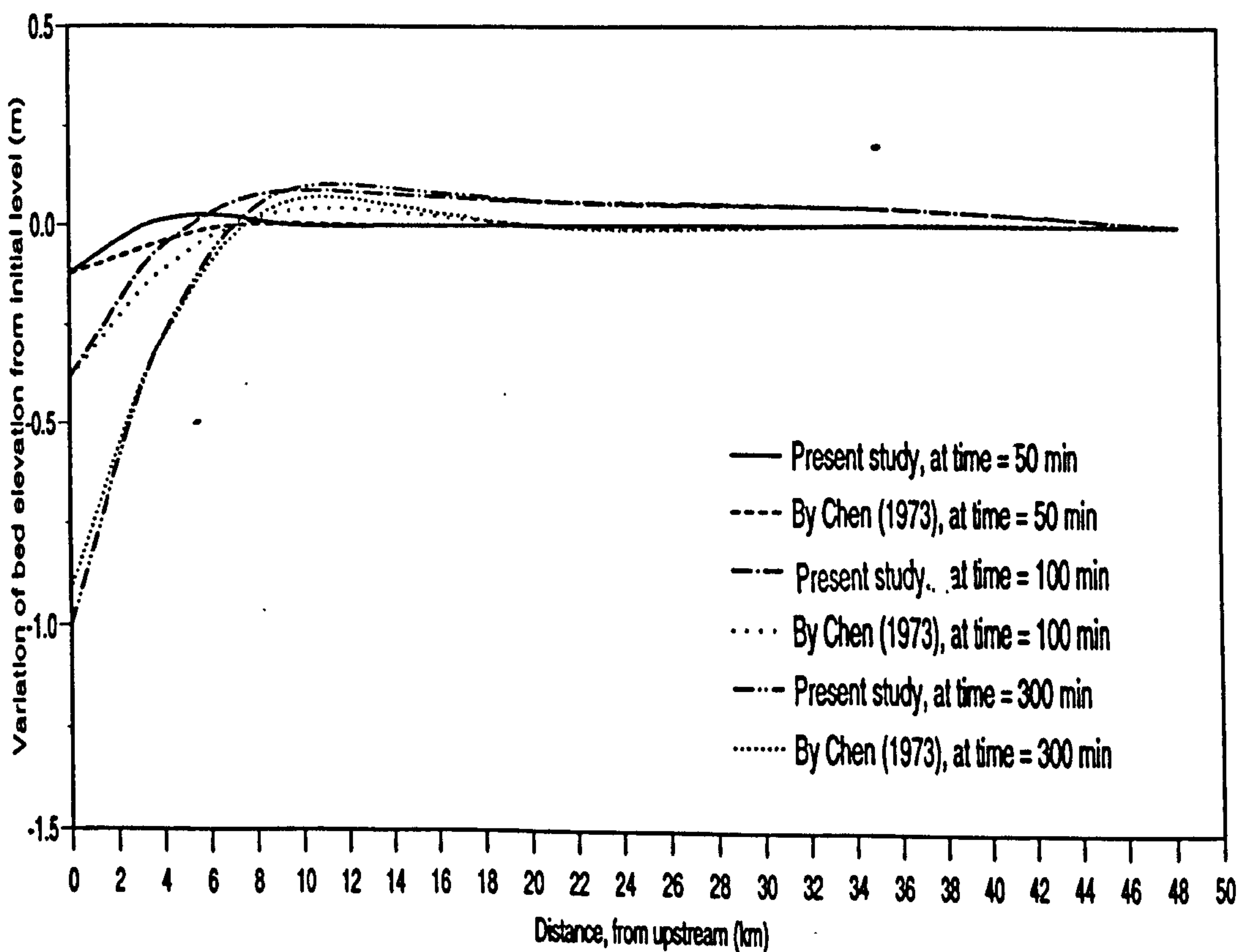


**Fig. 5.3b** Degradation of the bed of a channel when upstream sediment input is zero

Bed material porosity,  $\lambda = 0.67$

Specific gravity of the material = 2.65

The sediment layer of the bed has the particle size distribution based on the results of a sample obtained from fieldwork, as given in Table 5.3.

**Table 5.3 Sediment particle size distribution for the example of bed armouring**

Geometric mean diameter (mm)	Fraction by weight (%)
0.2	30
0.8	30
2.0	25
6.0	10
10.0	5

**3. Upstream boundary condition:**

- (i) Assume a constant inflow discharge of  $Q = 500 \text{ m}^3/\text{s}$ , and
- (ii) no sediment discharge,  $Q_{SO} = 0.0$

**4. Downstream boundary condition:**

This was fixed by a rating curve computed by the Alam and Kennedy (1969) method for the given flow conditions.

This time, however, it is also recognised that the friction factors of flow in erodible channels are usually larger than those of comparable flows in rigid boundary channels by a factor of two or more. In erodible channels, the friction factors are strongly dependent on the geometry of the bed features, which is a function of flow depth and velocity, and also of the properties of the fluid and bed material. Alluvial



river beds deform into ripples, dunes, etc. when the bed load is moved by water flow. The total resistance, in general, can be considered to be the sum of the grain resistance and the form resistance due to the bed undulations. In this example, therefore, the friction factor was computed by the Alam and Kennedy (1969) method as a function of grain-size Froude number, from which the downstream rating curve (Figure 5.4a) and the Manning's  $n$  (Figure 5.4b) were estimated for the simulation computations. This method was chosen for consistency, considering that it was developed based on sandy channel beds, as is the case here.

The degradation and aggradation that would result in a reach downstream of a dam under the given flow conditions is illustrated in Figure 5.4c. The variation of the bed particle size distribution at the upstream section of the reach is shown in Figure 5.4d. The figure demonstrates the development of an armouring coat from the accumulation of coarser grains. These numerical experiments are presented to demonstrate the ability of mathematical models for water and sediment routing to estimate the effect of alternative flow regulation measures on the long term stability of channel beds. However, despite a large amount of research (e.g. Alam and Kennedy, 1969; Lovera and Kennedy, 1969; Ackers and White, 1973; Yang, 1976; Yang, 1978; Lu, 1984; etc.), the resistance laws proposed by the various researchers for mobile sand beds are by no means as well understood as the laws for rigid bed channels (Garde and Ranga Raju, 1985). Vanoni (1986) assessed models of water and sediment transport in alluvial channels and concluded that movable-bed models did not yield satisfactory results. He recommended that the processes involved should be calibrated with field data, preferably from the site to be modelled. Chang (1988a) presented an evaluation of sediment functions and concluded that nearly all formulas contained coefficients that were established based on particular field data and such data should not be used to evaluate the accuracy of the formula.

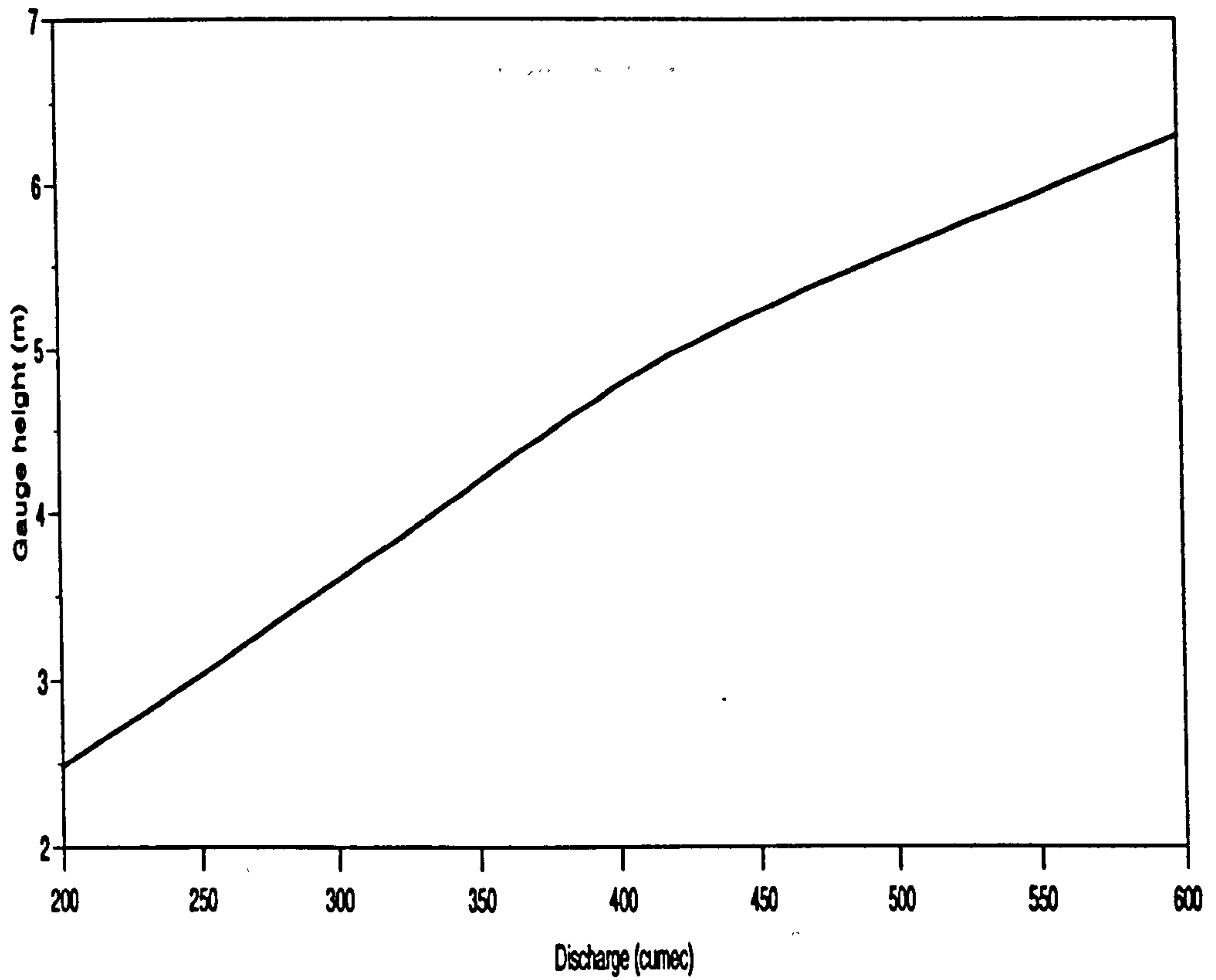


**Fig. 5.4a** Computed downstream rating curve using the Alam and Kennedy (1969) method

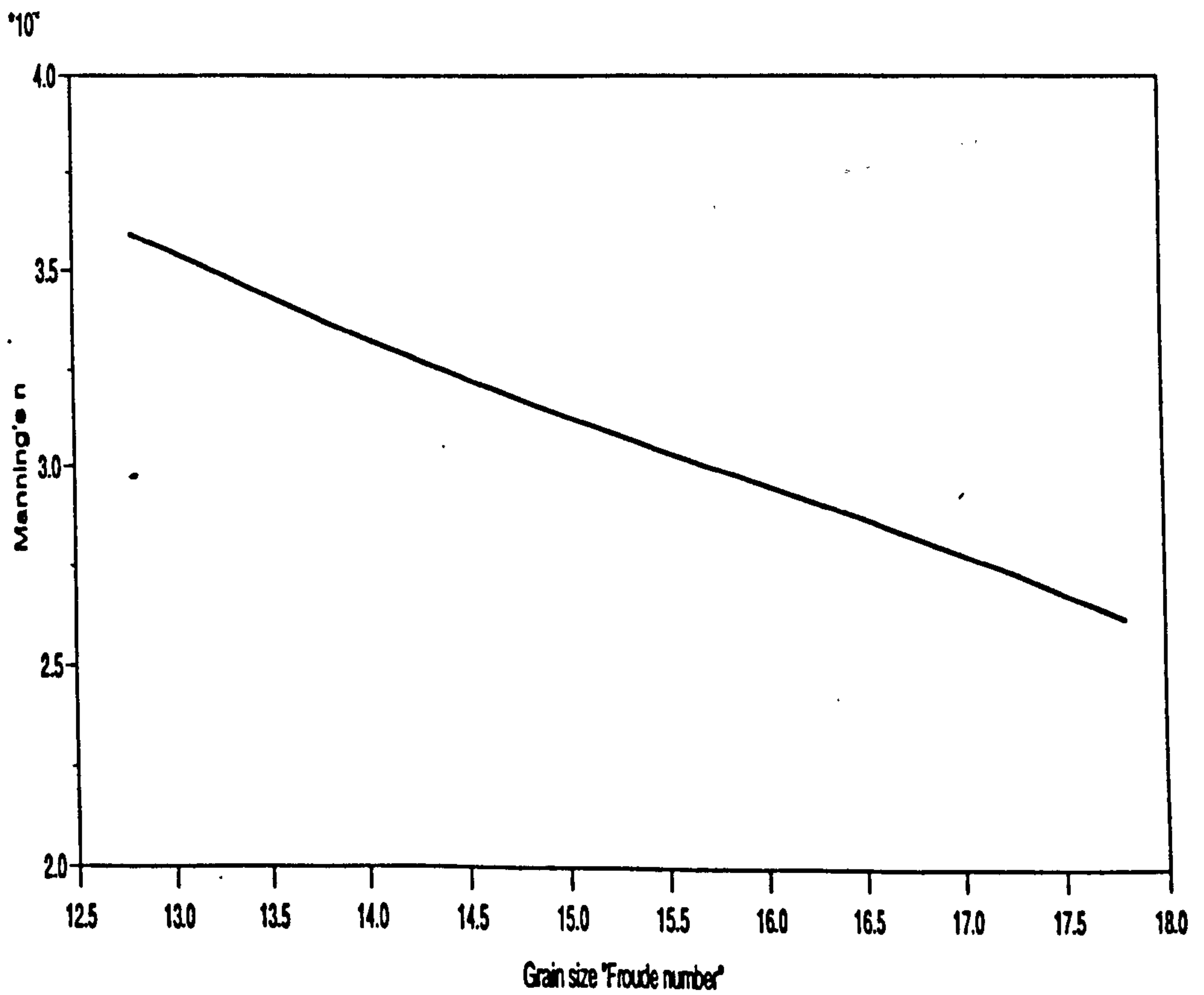


**Fig. 5.4b** Computed Manning's n using the Alam and Kennedy (1969) method



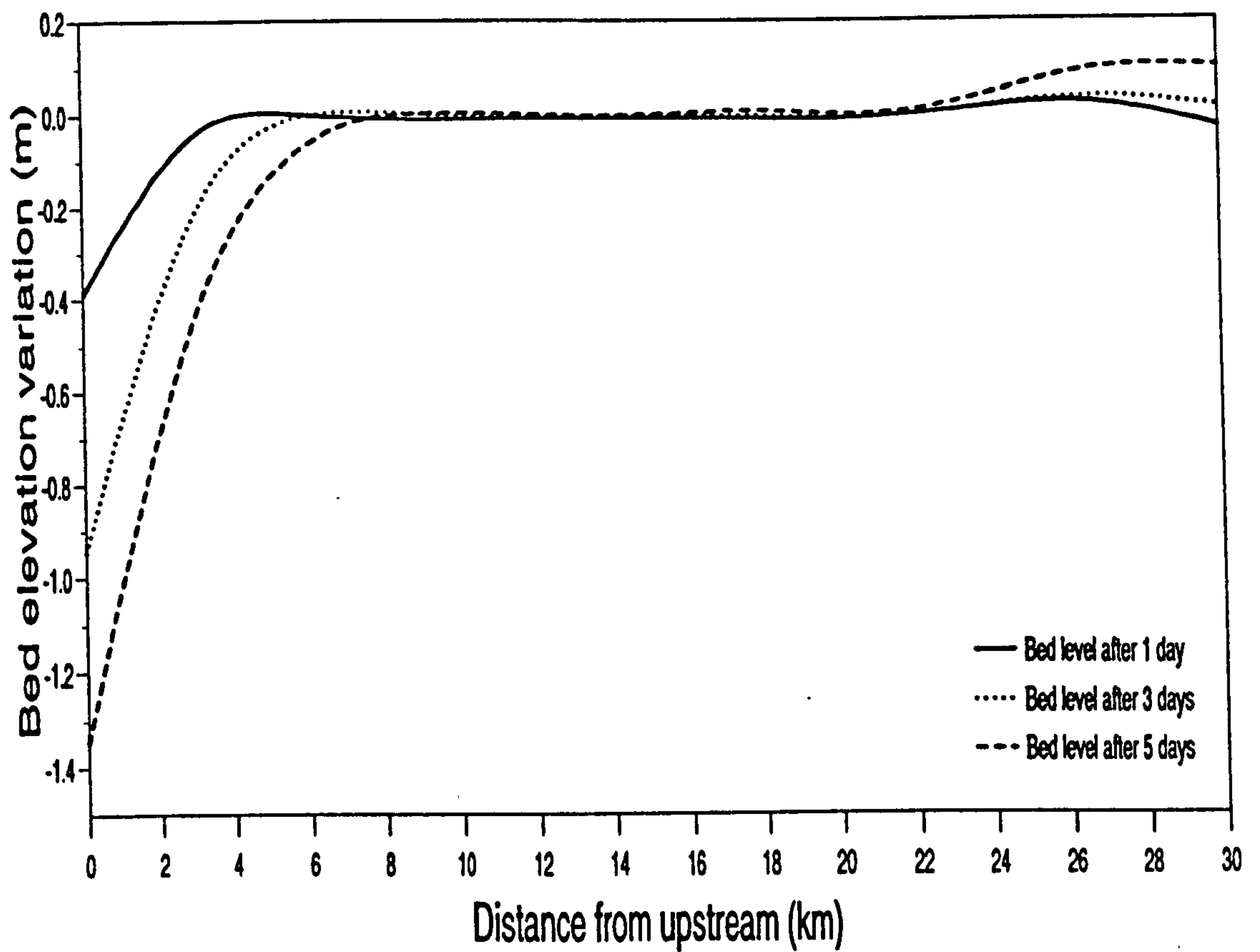


**Fig. 5.4c Simulated results of river bed degradation below a structure, using the Ackers-White (1973) bed material load and the Lee and Odgaard (1986) size loading functions**

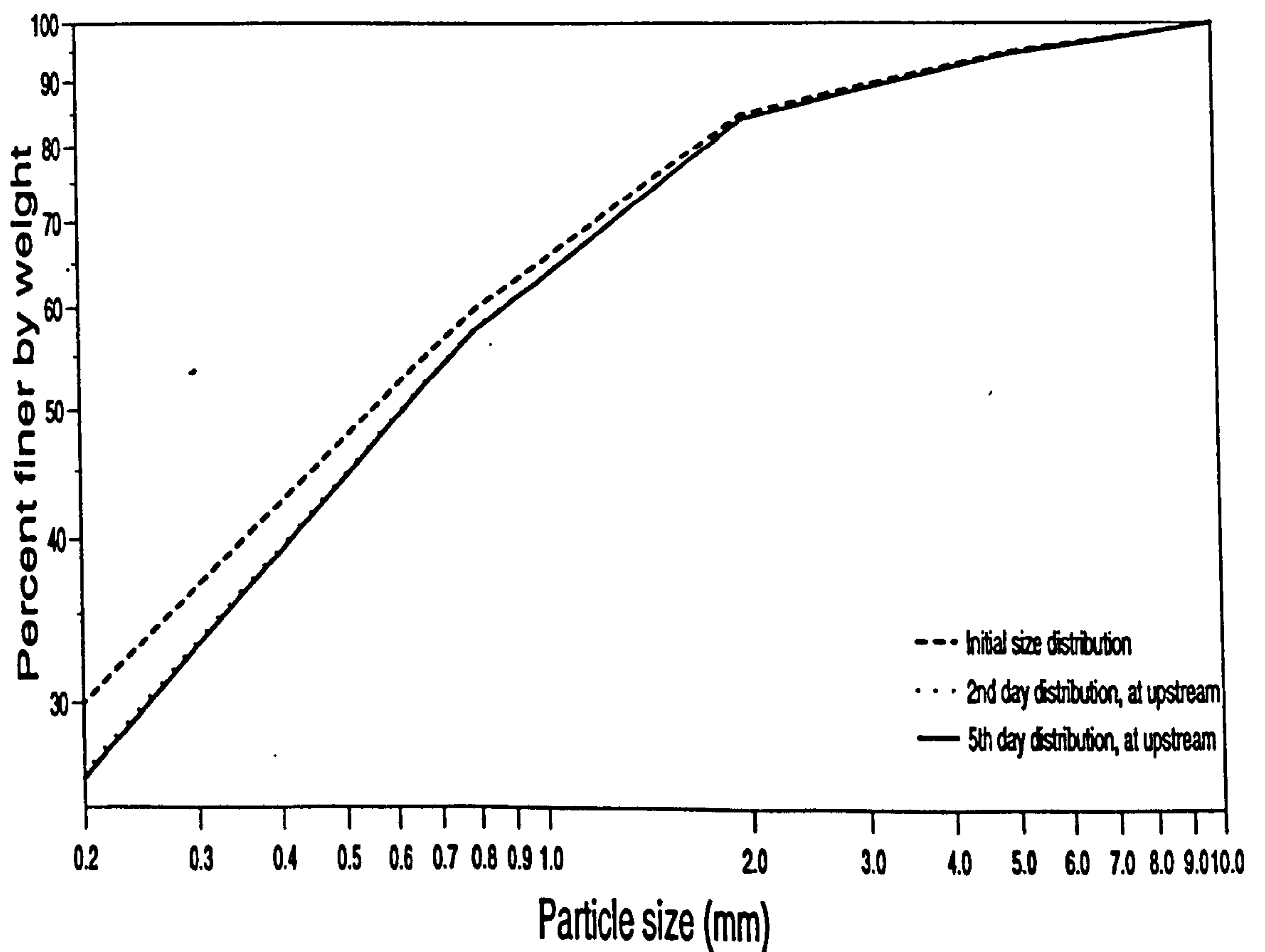


**Fig. 5.4d Change in bed material size distribution caused by the degradation**

Bathurst and Wicks (1991) asserted that further studies are needed to improve the understanding of sediment dynamics in overland and channel flows, the behaviour of cohesive sediment and of sediment mixtures with non uniform size distribution, storage dynamics, bed sediment infiltration and contaminant adsorption. Therefore, whenever sediment routing models are applied for natural channels, it is recommended that the Manning's roughness coefficient is estimated from field data as a calibrated parameter.

By showing the temporal variation of the Manning's roughness,  $n$  (Figure 5.4b), and the longitudinal bed elevation profiles (Figure 5.4c), the results demonstrate how the sedimentation processes can influence the stream-aquifer exchange for alluvial channels. This can be visualised by recalling that Manning's  $n$  affects the speed of flood waves, and hence the opportunity time for water exchange between the aquifer and the floods. The value of Manning's  $n$  varies because of the armouring effect of the river bed. Depending on the magnitude of the flood, its sediment concentration, duration, and the sediment particle size distribution in the mixing zone on the river bed, the finer particles are washed out of the mixing zone until the coarser area on the bed becomes immobile (Lee and Odgaard, 1986; Rahuel et al 1989). The coarser armour coat so formed increases the Manning's  $n$  because  $n$  is a function of the particle size of the bed (Alam and Kennedy, 1969; Chang, 1988a). Whereas the physical parameters of the stream bed and the aquifer material may determine the seepage rate, the total amount of water that will be exchanged is a product of the rate and the opportunity time available for the seepage flow to take place, and this opportunity time is what is affected by the Manning's  $n$ . Variation of the bed elevation profiles also affect the speed of passage of the flood wave, seepage resistance across the wetted perimeter and the hydraulic gradient between the stream-aquifer systems.



### 5.2.3 Flood wave modifications due to stream-aquifer interaction

The aim of this example is to test the groundwater flow sub-program and its linkage to the streamflow routing program. The test is based on the hydrological system defined by Pinder and Sauer (1971), who modelled the system for the purpose of investigating the modification of a flood wave due to bank storage effects. In this application, an input discharge hydrograph was routed through a channel reach; in one example the channel was assumed to be impervious and, in the other, leakage through the wetted perimeter of the channel to a plain aquifer was permitted. The difference between the resulting stream discharge hydrographs for the two simulations at the same point in space and time indicates the effect of water leakage, and thus the interaction of the flood wave with the aquifer. To retain the picture of the system as described by Pinder and Sauer (1971), the same English units have been maintained, but with the corresponding values in SI units, given in brackets.

The flood plain aquifer in this problem extended 140000 ft (42672 m) along the length of the channel and was 1400 ft (427 m) across the valley. It was surrounded by impermeable materials on all sides. The initial saturated thickness ranged from 220 ft (67 m) at the upstream boundary to 90 ft (27 m) at the downstream boundary. The streamflow was along the axis of the valley through a straight channel with a constant cross-section and slope of 0.001. The hydraulic conductivity of the aquifer (assumed homogeneous and isotropic) was 0.01 ft/s (0.003 m/s) and that of the stream bed along the wetted perimeter was four times that of the aquifer and was therefore not a limiting factor in the amount of water entering the aquifer. The channel was 100 ft (30 m) wide and the initial depth of flow was 20 ft (6 m). The river was sub-divided into smaller reach elements, in this example into a total of ten river elements, and the interchange flow values were the net seepage rates either into or out of the river over each of the elements. This hypothetical hydrological system was studied in terms of its response to the passage of a flood wave superimposed on the baseflow of an initial

steady flow, which had the following characteristics: peak flow was 28000 cfs (792 m<sup>3</sup>/s), taking 2 hours to reach the peak, and the hydrograph base time was 12 hours. The steady flow discharge of the stream prior to the introduction of the flood wave was 18000 cfs (509 m<sup>3</sup>/s). The computed results are presented in Figures 5.5a and 5.5b, in comparison with those obtained by Pinder and Sauer (1971). Because some parameters for the example were not stated in Pinder and Sauer's experiment, like the specific yield of the aquifer, it was assumed in this simulation as 0.15. This assumption, together with the difference in the finite difference schemes may be accountable for the differences in the results.

Otherwise both simulations have the same pattern, showing that the effect of stream-aquifer interaction (bank storage) is cumulative in the downstream direction and may have a considerable impact in regulating flood discharges in the lower reaches of streams. The modification of the flood hydrograph in Figure 5.5a at the station 50000 ft (15240 m) downstream of the upstream station was much less than the modification at the station 140000 ft (42672 m) downstream of the upstream station, Figure 5.5b. From the results, it is observed that at the section 50000 ft (15240 m) downstream, the change in the peak discharge of the flood wave, (the discharge above the initial steady discharge), was reduced to about 550 cfs (15.57 cumec), whereas at the section 140000 ft (42672 m) downstream, the flood wave was reduced to about 250 cfs (7.08 cumec). It is also apparent from the figures that bank storage attenuates flood waves, that is, it decreases the peak discharge and extends the hydrograph base time. From these results, it can be concluded, generally, that provided the appropriate parameters can be determined for field problems, the hydrologic behaviour of a regime stream-aquifer system can be simulated. It can also be concluded that the length of the river reach has effects on the modification of the flood wave and the bank storage. By comparing the simulation test results with the results obtained by Pinder and Sauer,



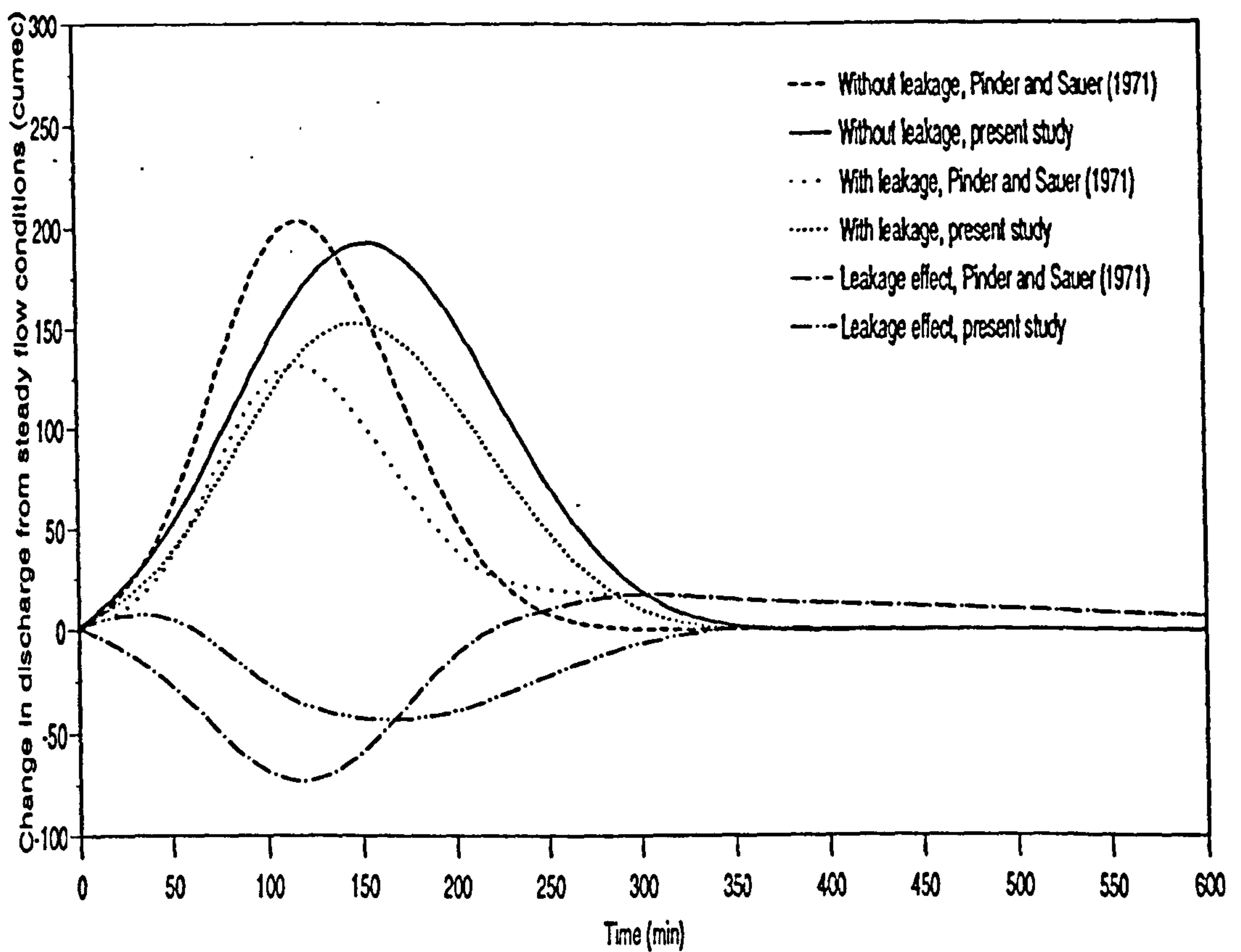


**Fig. 5.5a Flood wave attenuation at a distance 15240 m from the upstream boundary, for a stream with and without leakage into the aquifer**

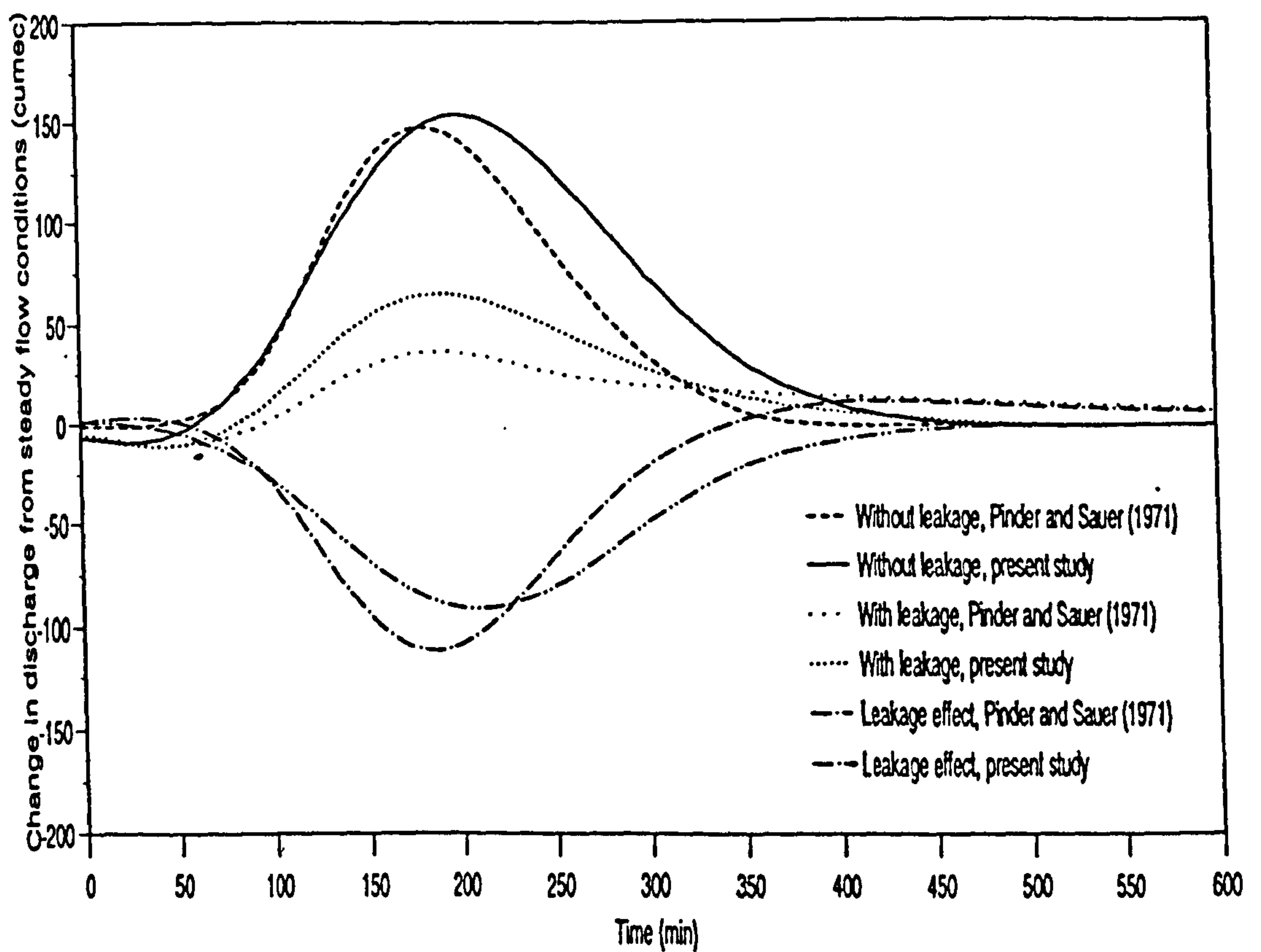


**Fig. 5.5b Flood wave attenuation at a distance 42672 m from the upstream boundary, for a stream with and without leakage into the aquifer**

it is demonstrated that the stream-aquifer interaction program is working and acceptable for the purposes of this study. Derivation of the program for the MASAI was accomplished by linking the tested sediment routing sub-program to the tested stream-aquifer interaction sub-program, based on the linkage mechanism described by Eq. 4.54, as described in chapter 4.

Pinder and Sauer (1971) did not apply their model to real-world data, but used it to investigate the theoretical effects of bank storage phenomena on flood waves. However, Pogge and Chiang (1977) applied the Pinder and Sauer (1971) model to real-world data from sites in West-Central Kansas. They concluded that the model performed adequately in simulating the responses of the stream-aquifer interaction. Therefore, given that the MASAI has also produced similar results with those obtained by Pinder and Sauer (1971), it can be concluded that it has been verified and is applicable to field conditions, given the necessary data. Pogge and Chiang (1977) also noted the critical importance of selecting a suitable value for the roughness coefficient ( $n$ ) in the equation employed for streamflow routing. For example, they found that the bank storage occurring in the study area will be reduced by about 50% if the value of  $n$  is decreased from 0.055 to 0.035, probably because of the shorter duration period of the flood wave when  $n$  is equal to 0.035.

## **5.3 Model Calibration and Test of Predictive Uncertainty**

### **5.3.1 Calibration**

The calibration was based on the fieldwork carried out on the Nyando River in Kenya, for which the general hydrogeology of the river system was explained in chapter 3. Only the calibration procedures are outlined in this section.



Considering the amount and complexity of the data required, the techniques employed in the field ranged from simple observations and interviews, assessment of historical records, to actual field measurements and computations. The actual measurements were made to estimate most of the river parameters, but because it can be argued that geological properties do not change much within an engineering period, historical records provided the source of most of the groundwater data.

The fieldwork for the calibration methodology is explained in a step-by-step procedure as follows:

1. The site was on a single well defined channel reach of the River Nyando, extending from the gauging station 1GD3 upstream, to the Ahero road bridge downstream, covering a total distance of 18.432 km. The sectional profiles were based on a chainage level survey done during the fieldwork. The survey was run from the RGS 1GD3 along the river banks, establishing bench-marks from which the river's bed elevations, water surface levels and cross sectional profiles were to be surveyed from at subsequent stages. Although the river was winding over a few sections, its well defined cross-sectional area was observed to contain and maintain relatively uniform flow that could be represented by a one-dimensional model. The flows were assumed to be steady since measurements were timed when there were no significant stage variations throughout these particular experimentation periods. The survey data for the various stations are recorded in Table 5.4.
2. The mean cross-sectional area and top width at each section were obtained from hydrographic surveys done during the same period. Investigation of the cross-sectional profiles plotted on transparencies revealed a general trapezoidal shape with about the same side slope for all stations, but with varying bottom widths. The composite section technique was therefore applied to average the geometric side slope

**Table 5.4 Characteristics of the Nyando River channel near Ahero**

Station	Distance from upstream	Bed elevation	Channel bottom
number	station (m)	(m)	width (m)
1GD3	0	1160.3	26.5
(2)	3250	1157.5	19.0
(3)	7050	1155.2	16.5
(4)	13450	1149.3	15.5

of all the individual sections to give an average representative value. The value, obtained as 1.5 horizontal units to one vertical unit was fitted in the general trapezoidal equation for estimating the various cross-sectional areas and top widths as functions of flow depths.

3. The mean rating curve for the upstream section (1GD3) was obtained from the Ministry of Water Development of Kenya, having the following relationship:

$$\begin{aligned} h &= 5.774 Q^{3.428} & \text{for } h \leq 0.96 \text{ m.} \\ h &= 5.586 Q^{2.616} & \text{for } h > 0.96 \text{ m.} \end{aligned} \tag{5.1}$$

where  $H$  is the river stage (m) and  $Q$  is the corresponding discharge ( $\text{m}^3/\text{s}$ ). A discharge measurement experiment was carried out in the field in order to validate the stage-discharge relationship of the station.

The downstream station and rating curve were established and calibrated during the fieldwork study period. The relationship was determined empirically by means of discharge measurement in the field. The discharge flow rates at the station (Ahero bridge) were measured periodically by a Tamaya UC2 current meter, while noting the



concurrent river stages. By wading (or boat procedures, depending on the river level) the current meter was used to measure the average flow velocities at selected points across the river section (Table 5.5). The velocities at the selected points across the river were measured at 0.6 of the depth of flow from the surface, which was the recommended level of measurement in the area. From the measured velocity and the corresponding area of the sub-section, the area-velocity method is applied to compute the average streamflow discharge through the whole river cross-section. Table 5.5 is a summary of the results obtained from one of the experiments.

Stage-discharge relationships are usually developed from a graphical analysis of the measurements plotted on either rectangular co-ordinate or logarithmic plotting papers. A rectangular co-ordinate paper has been used because it has certain advantages, particularly in the study of the pattern of shifts in the lower part of the rating (World Meteorological Organisation, 1980). This situation is envisioned because the streambed in the area is mainly composed of loose sand material. A change in the low-flow rating at many sites result from a change in the elevation of effective zero, which means a constant shift in gauge height. A shift of this kind is more easily visualised on rectangular co-ordinate paper because on such paper the shift curve is parallel to the original rating curve, the two curves being separated by a vertical distance equal to the change in the value of  $\alpha$ .

Based on a number of measurements, like those summarised in Table 5.5, the values of the river stage were obtained and plotted against the corresponding discharges, to describe the downstream stage-discharge relationship shown in Figure 5.6. Two relationships were derived as:

$$\begin{aligned} h &= 0.0275 Q - 0.60 & \text{for } h \leq 1.3 \text{ m} \\ h &= 0.0360 Q - 0.37 & \text{for } h > 1.3 \text{ m} \leq 1.62 \text{ m.} \end{aligned} \quad (5.2)$$

**Table 5.5 A form of current meter gauging records (used during fieldwork on the Nyando River)**

REPUBLIC OF KENYA

W.D. 480a

HYDROLOGY SECTION

**CURRENT METER GAUGING (MID-SECTION METHOD)**

NAME OF OBSERVER N. O. ORINA & Co Date 28 / 4 / 1993

RIVER NYANDO DRAINAGE AREA 1 STATION (See Notes) 16D NISC

METHOD (Strike out where not applicable): Wading, boat, cableway, bridge (down or up-stream face) Wading

METER: Make Tamaya W.D.D. No. UC2 Prop. No. — Weight — kg.

TIME OF STARTING 1335hrs Time of Finishing 1355hrs Initial Point WEKB

GAUGE HEIGHT: at Start 0.70m at Finish 0.71m MEAN 0.71m.

**NOTES.—**(1) If discharge is not taken on line of standard section, state actual site below.

(2) If discharge taken at a site other than a regular gauging station, describe position of discharge site, give Lat. and Long. and number of cadastral sheet or other full description.

Approx. 100 metres u/s of Ahera Road/Bridge

MEANS AND TOTALS																	
AREA		16.332		sq. ml. MEAN VEL.		0.30		m./sec. G.H.		0.71m		DISCHARGE		4.825		cume.	
Dist. from Initial point	Depth	Width	Area	Discharge	VELOCITY		Time Secs.	Revs.	Depth of Observation from Surface	REMARKS							
					Mean in vertical	At point											
28.2	0	1.60	—	—	—	—	—	—	—	WERB							
27.0	.65	1.10	.715	.014	.02	.02	10	—	.6								
26.0	.80	1.00	.800	.120	.15	.15	10	—	.6								
25.0	1.00	1.00	1.000	.360	.36	.36	10	—	.6	Bed load + silt sample test							
24.0	.99	1.00	.990	.485	.49	.49	10	—	.6								
23.0	.94	1.00	.940	.450	.50	.50	10	—	.6								
22.0	.90	1.00	.900	.432	.48	.48	10	—	.6								
21.0	.95	1.00	.950	.399	.42	.42	10	—	.6								
20.0	.90	1.00	.900	.368	.42	.42	10	—	.6								
19.0	.93	1.00	.930	.372	.40	.40	10	—	.6	Bed load + silt sample test							
18.0	.98	1.00	.980	.363	.37	.37	10	—	.6								
17.0	.85	1.00	.850	.349	.41	.41	10	—	.6								
16.0	.90	1.00	.900	.360	.40	.40	10	—	.6								
15.0	.90	1.00	.900	.297	.33	.33	10	—	.6								
14.0	.90	1.00	.900	.216	.24	.24	10	—	.6								
13.0	.88	1.00	.880	.167	.19	.19	10	—	.6	Bed load + silt.							
12.0	.88	1.00	.880	.062	.07	.07	10	—	.6								
11.0	.82	1.00	.820	.008	.01	.01	10	—	.6								
10.0	.65	1.00	.650	.003	.005	.005	10	—	.6	1/2 of above							
9.0	.47	.95	.447	.000	.001	.001	10	—	.6	1/4 of above							
8.10	—	.45	—	—	—	—	—	—	—								
TOTAL			16.332	4.825													

Sheet No. 1 of 1 Sheet Comp. by Jim Check by B. Shwartz

**GPK(L)**



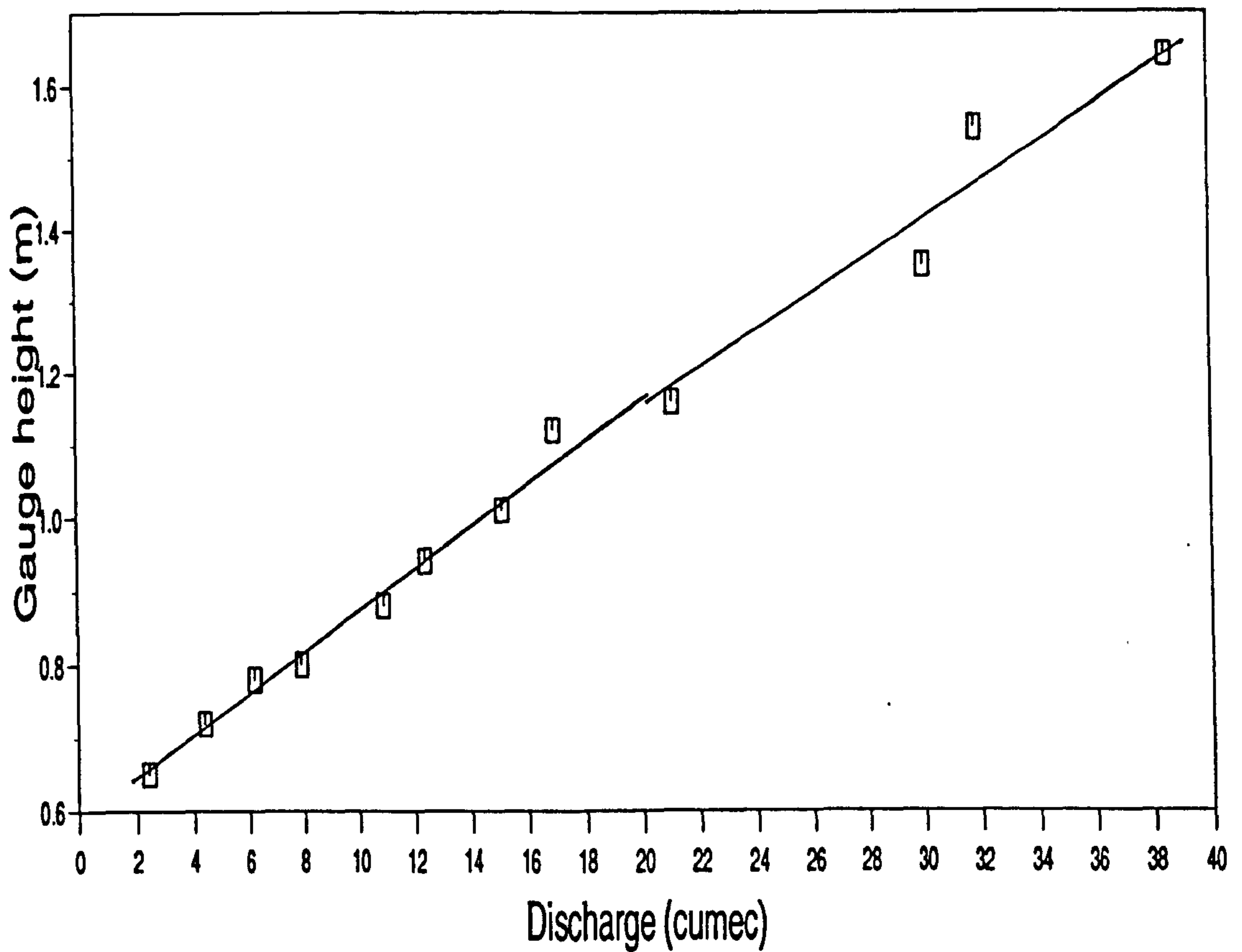


**Fig. 5.6 The stage-discharge relationship at the Ahero Road bridge on the Nyando River**

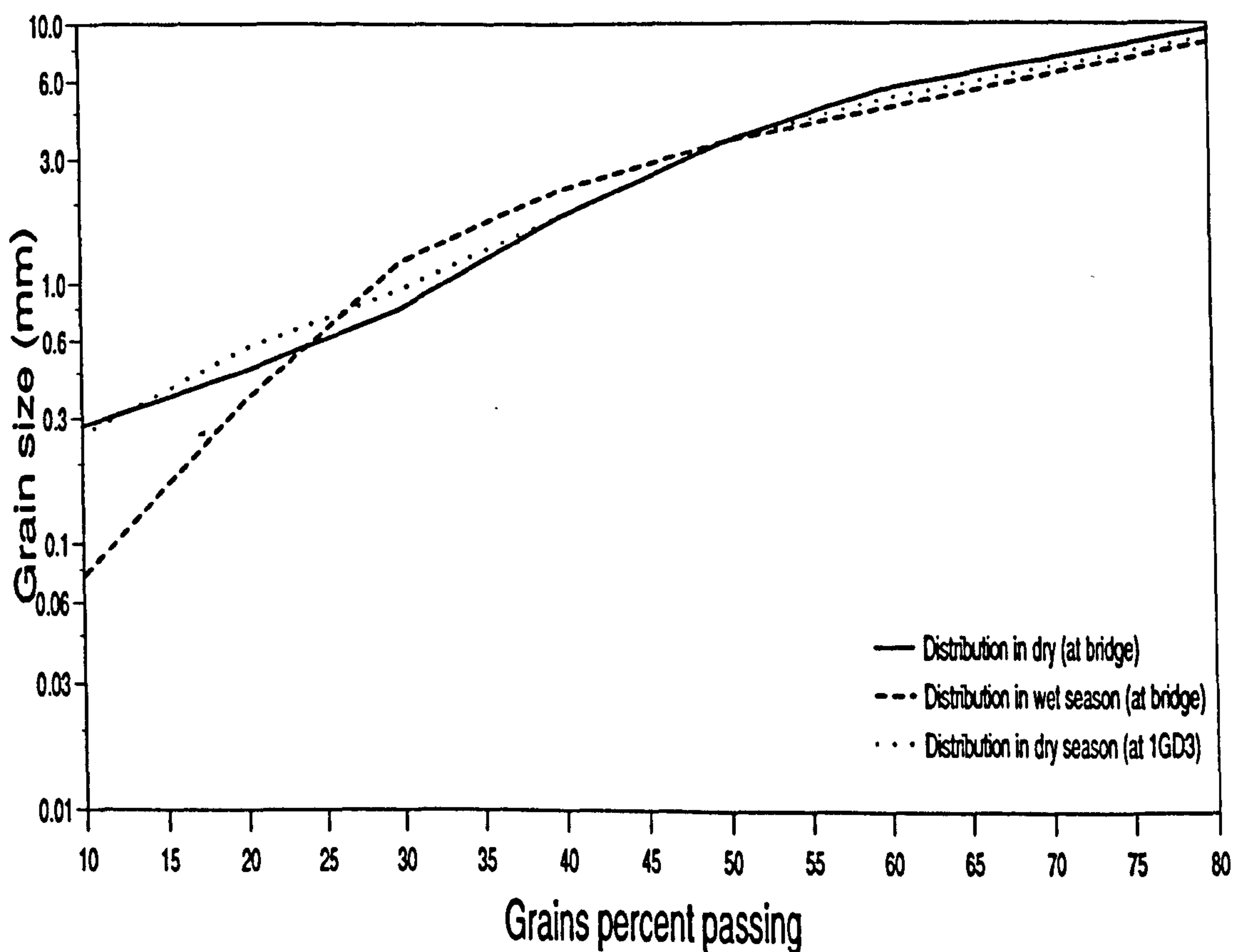


**Fig. 5.7 Sediment particle size distribution at the gauging station 1GD3 and Ahero bridge, on the River Nyando. Measurements were taken in February 1993 (dry season) and May 1993 (wet season)**

The relationship does not appear to be good because the range of the discharge measurements from which the rating curves were derived was small,  $2.8 \text{ m}^3/\text{s} \leq Q \leq 39.7 \text{ m}^3/\text{s}$ , and the number of measurements, 12, were also few. However, the objective of the stage-discharge relationship was mainly to establish the downstream boundary condition of the study reach. Therefore, the number of discharge measurements made and the range of the discharge flows are limiting for any detailed analysis to establish a gauging station. A channel control, as is the case here, consists of the physical features of the channel which determine the stage of the river at a given point for a given rate of flow. These features include the size, slope, roughness, alignment, constrictions and expansions, and shape of the channel. The reach of a channel that acts as the control may lengthen as the discharge increases, introducing new features that affect the stage-discharge relation. The river channel at this location, which floods almost annually, has a flood discharge capacity of about  $87 \text{ m}^3/\text{s}$ , as computed in section 3.2.3. All of the flow measurements were less than half the capacity of the channel section. Therefore, considering the amount and quality of the data obtained, detailed analysis or extrapolation, of the rating curves were not worthwhile. The relationships were helpful, however, for estimating the downstream boundary condition for this particular study.

4. The average energy gradient was estimated from the average water surface slopes. Under relatively steady conditions the river stages at the nodal points along the river reach were recorded. The slope between each pair of the adjacent stations was estimated by computing the ratio of their elevation difference to the longitudinal distance between them. The field values are tabulated in Table 5.6.

5. Manning's roughness coefficients,  $n$ , at each station were computed by the Manning's equation:



$$n = \frac{R^{2/3} S^{1/2}}{V}$$

(5.3)

where R is the mean hydraulic radius, S is the water surface slope and V is the average velocity of flow. The field values of n, obtained under the same steady conditions as for the water surface slope are also included in Table 5.6. Considering the channel bed and bank material throughout the reach, and the small river stage variation experienced, the values of the Manning's n were assumed to remain the same so long as the river did not burst its banks. For comparison purposes, the Italconsult team used average values of the Manning's n of 0.033 for the river channel and 0.05 on the flood plain.

Table 5.6 Observed hydraulic properties of River Nyando near Ahero

Station	Bottom width	River stage	Velocity	Water surface	Manning's
	(m)	(m)	m/s	slope (%)	n
1GD3	26.5	1160.585	0.34	0.062	0.032
2	19.0	1158.538	--	0.063	0.034
3	16.5	1156.220	--	0.084	0.036
4	15.5	1149.660	--	0.081	0.040
Bridge	30.5	1146.720	0.23	0.060	0.043

6. A quantitative relationship between the bed load and discharge flow could not be derived because of the limited data. However, fieldwork measurements were used as a guide in the selection of an appropriate bedload equation under the given field conditions. Prior theoretical examination of the recommended bedload functions (Chang, 1988a) had led to the selection of the equations by Yang (1973), and Ackers and White (1973) as those among the most suitable for sandy streams. The equations

were used to compute bedload discharges and their results compared with the observed field data of the corresponding flow conditions. The final bedload equation was therefore selected by fitting the computation results to the observed data.

The portable Helen-Smith sediment sampler was used to measure the bedload. With its mouth (of area 15 x 15 cm<sup>2</sup>) facing upstream, the sampler was held firmly on the bed for two minutes and its bag-catch obtained for further laboratory tests. Since a set of three bag-catches was normally obtained by holding the sampler for 2 minutes at three positions along a cross section, the average bedload transport rate in kg/s was computed as:

$$Q_s = [(\text{sum of sample catch at the section}) / (3 \times 2 \times 60)] \times [(B \times 0.15) / (0.15 \times 0.15)]$$

where B is the width of the river at the river section.

Samples of bed material were also collected for further laboratory tests. A summary of the laboratory tests, conducted at Egerton and JKCAT university laboratories are given below:

*(i) Particle size analysis of the bed material - by the Mechanical method:*

From the main sediment samples brought from the field, smaller samples (in line with the apparatus in the laboratory) were prepared for further experimentation. One of the smaller samples, after oven-drying, weighed 631.7 g. The sample was submerged in one litre of sodium hexa-metaphosphate dispersion solution and allowed to stand for one hour. The material was then washed through sieve number 200 (0.075 mm) using tap water. The remaining sediment that did not pass through the sieve was oven-dried again, weighed and sieved using a mechanical shaker. The Results from one of these experiments are given in Table 5.7.

The 0.1 % lost during experimentation is acceptable since it is less than the tolerance value of 2 %. The results are presented in Figure 5.7, showing the particle size

distribution of the bedload at 1GD3. The experiment was done on samples obtained during both rainy and dry seasons on both Rivers Nyando and Kibos. Results for the sample collected during the rainy season are also plotted on the same figure. On average the texture for both samples were of gravel-sand type, but with increased fine sand in the sample collected during the rainy season.

**Table 5.7 Sediment particle size analysis of a sample from the Nyando River near Ahero**

Sieve No	Sieve size (mm)	Wt. retained (g)	% Retained	% Pass
3/8"	9.51	120.6	19.1	80.9
4	4.75	168.4	26.7	54.2
10	2.00	88.8	14.1	40.1
20	0.85	63.4	10.1	30.0
30	0.60	33.0	5.2	24.8
40	0.425	41.0	6.5	18.3
60	0.250	69.4	11.0	7.3
100	0.149	29.5	4.7	2.6
200	0.075	1.0	0.2	2.4
	PAN	0.4+15.2	2.5	-0.1

*(ii) Specific gravity test:*

In another laboratory test, measurements were made to obtain results for the specific gravity of the samples. Typical results from one of the experiments are as follows:

mass of jar full of water	=	805.2 g
mass of jar with dry soil	=	346.1 g



$$\text{mass of jar with soil filled with water} = 859.5 \text{ g}$$

$$\text{mass of empty jar} = 258.4 \text{ g}$$

Therefore

$$\text{mass of dry soil} = 346.1 - 258.4 = 87.7 \text{ g.}$$

$$\text{mass of soil and water} = 859.5 - 258.4 = 601.1 \text{ g}$$

$$\text{mass of water present with soil} = 601.1 - 87.7 = 513.4 \text{ g}$$

$$\text{mass of water when jar was full} = 805.2 - 258.4 = 546.8 \text{ g}$$

$$\text{so mass of water of same volume as soil} = 546.8 - 513.4 = 33.4$$

and the specific gravity of the sediments is

$$S_g = \frac{\text{mass of the sediment}}{\text{mass of same volume of water}}$$

$$= 87.7 / 33.4 = 2.62$$

### (iii) Porosity test

A known volume of dry sediment was added to a known volume of water to obtain results for computing the porosity of the sediments. The results were as follows :

$$\text{water volume level before adding soil} = 100.0 \text{ cm}^3$$

$$\text{volume level after adding 50 cm}^3 \text{ of soil} = 134.7 \text{ cm}^3$$

$$\text{so volume of the voids} = (100 + 50) - 134.7 = 15.3 \text{ cm}^3$$

$$\text{and the porosity of the sediments} = \frac{\text{volume of voids}}{\text{volume of solids}}$$

$$15.3 / 50.0 = 0.306$$

### (iv) Permeability test:

A constant head permeameter was used to estimate the hydraulic conductivity of the bedload layers. In this set-up a sample of the sediments was filled in a cylindrical device that maintained a steady flow of water through the sediments and enabled measurements of flow rate and head loss across the sample column to be made. The

test was according to usual laboratory permeability test. It was not possible to simulate and investigate the degree of compaction in the field. Particular results from one of the experiments are given below:

diameter of permeameter cylinder	=	0.075 m
length of soil column	=	0.50 m
constant head across the soil column	=	0.50 m
volume of water collected	=	0.036 m <sup>3</sup> .
period of collection	=	30 min.
cross sectional area of the sample	=	4.4 x 10 <sup>-4</sup> m <sup>2</sup>
water flow rate = 0.036 / (30 x 60)	=	2 x 10 <sup>-5</sup> m <sup>3</sup> /s

and the hydraulic conductivity  $K_2$ , =  $(0.5 \times 2 \times 10^{-5}) / (0.5 \times 4.4 \times 10^{-3})$   
= 0.0045 m/s.

The sediment sampled during rainy season on the River Kibos had significantly different features. For example, its hydraulic conductivity was  $3.3 \times 10^{-5}$  m/s compared with 0.0045 m/s for the dry season.

*(v) Selection of the bedload function:*

The bedload, as measured in the field, was compared with the computed values obtained by the Ackers-White (1973) and Yang (1973) functions, according to the plots in Figure 5.8. With reference to the figure the Ackers-White function is seen to be a fairer predictor except for very low flows. This could be attributed to the disturbance caused by the sampler, which were notable as a result of the sampler's weight tending to hold back and stabilise the local bedload. The error due to the disturbances is assumed to diminish in significance at higher flows. So the Ackers-White function was selected for the given conditions.

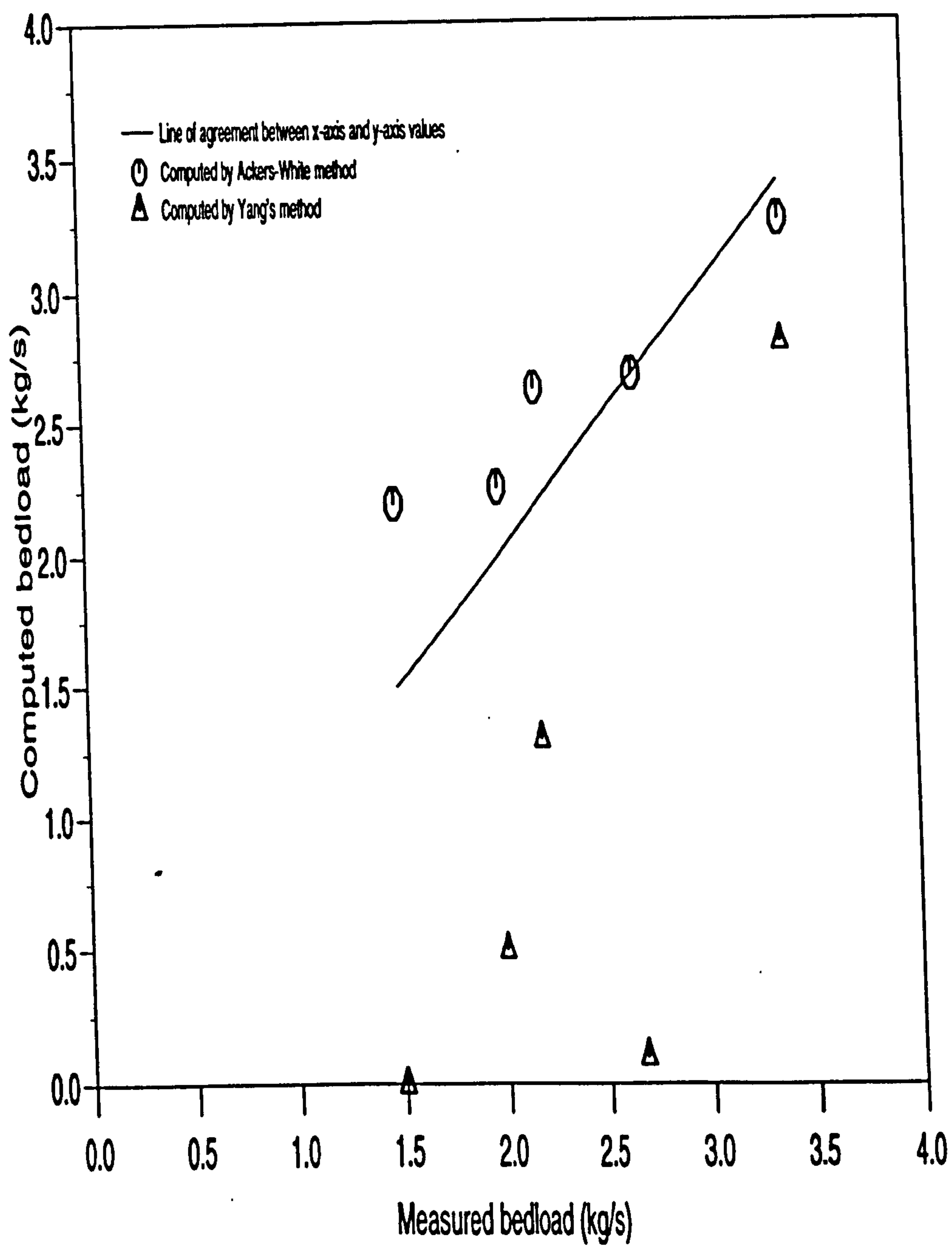


**Fig. 5.8 Comparison of computed and measured bed material load**



7. Observation wells for pump tests and other geological investigations were not available, and their establishment was not feasible. So with the assumption that the geological parameters do not change much with time, study reports by Italconsult (1983) were relied upon to provide estimates of the aquifer's hydraulic conductivity and specific yield. Two working bore holes, one run by the Ahero Catholic Mission and another by Onjiko Secondary School were used to monitor the water table fluctuations in the area during a transition period from dry to rainy season. Because the bore holes continued to operate during the study period, a lighting electronic dipper was used to take daily levels between 5.00 - 6.00 am., ( before resumption of the daily pumping ), with the assumption that the groundwater attained its rest level over the night. Figure 3.12 was presented in chapter three to show the fluctuations of the water table in the Ahero Catholic Mission borehole, about 60 m from the river, in comparison with the river stage at Ahero bridge. Water levels in the Onjiko borehole, 1.2 km away from the river showed no response to the changing season and streamflows. Considering that the measurements had taken place for more than a month since the rains started, the lack of significant change in the Onjiko bore hole signifies the low infiltration rates of the Kano plain soils around Ahero. Occasional observations of water levels in a hand-dug well at Ahero Girls school, about 117 m away from the river showed very small variations in the water levels. From these and other investigations along the river banks, it was estimated that the influence of a flood wave on the groundwater level in the reach was negligible for distances over 150 m, which became the boundary limit of the aquifer grid network on either side of the river. The principle of no flow across the boundary was used as the boundary condition on either side of the flood plain aquifer. The average aquifer hydraulic conductivity and specific yield, estimated from the Italconsult (1983) reports were 0.0001 m/s and 0.1, respectively.

8. The channel bed layer's hydraulic conductivity had no records and was difficult to measure in the field. So besides field results, laboratory experiments, as

explained in procedure 6-(iv), were also employed to estimate its value. In the field, sets of readings were made when the water conditions were considered to be relatively steady. The lateral flow was estimated by computing the difference in volume flow rate between the inflow at the upstream boundary and the outflow at the downstream end over a known period of time, assuming that change in the channel storage was negligible. The river bed elevation was assumed to lie along the harder sandstone-like material below the river. Any other loose material on top was assumed to be bedload in transit, so that the elevation difference between the levels of the sandstone and the top of the loose material gave the thickness of the bed sediment layer. The differences between the river stages and the groundwater levels in the shallow well at Ahero Girls School gave one set of the hydraulic head differences between the river and the water table. Another shallow well excavated by the river-side, 11 m away from the river, gave another set of the hydraulic head differences between the river and the aquifer.

From the relationship developed for water interchange between streamflow and groundwater, (Eq. 4.54), a plot of the results,  $q$  versus  $\Sigma\Delta H$  on a graph paper should yield approximately a straight line with the slope equal to  $k_2/(1 + \zeta Z_{b1} \cdot k_2)$ . Knowing the hydraulic resistance of the aquifer  $k_2$  and the thickness of the streambed layer  $Z_{b1}$ , then the specific resistance  $\zeta$ , hence the hydraulic conductivity  $K_1=1/\zeta$  of the sediment layer can be computed from the gradient of the graph.

However, these particular readings from both wells did not give reliable results. It was found that readings from the well at Ahero girls' school did not have any relationship with those of the river, probably because of the irrigation canals passing near the well. The excavated bore hole 11 m away had very inconsistent results, also probably because of the disturbances caused by continuous usage of the well during the time of the experiment. The field measurements, therefore, failed to show any meaningful relationship. As such, the laboratory permeability test results were

employed to estimate the sediment layer's resistance. Given that the bed layer has much coarser material than the aquifer materials, its hydraulic conductivity was expected to be higher than that of the aquifer. It will not, therefore, be the limiting factor in the water interchange between the river and aquifer. Otherwise the field calibration procedure described here should be preferred because the laboratory technique does not account for the "uplift" and "compaction" effects, which may cause the conductivity of the streambed of the same material to vary with the direction of the seepage flows.

9. Five infiltration tests were made along the flood plain using a double rings infiltrometer. The two concentric rings were driven into the soil to a depth of about 10 cm and water was added inside to maintain a depth of about 5 cm in the inner tube. Results from one of the experiments are illustrated in Table 5.8, and results from all of the experiments gave an average basic infiltration rate of about 8 mm/hr. However, this was another experiment done to validate values derived from the Italconsult (1983) study reports, which agreed with the recorded low infiltration capacities of the region. Infiltration results were necessary, not only for estimating groundwater recharge from precipitation, but also from flood flows, given the high flooding frequency of the river.

10. An upstream inflow hydrograph (Figure 5.9) served as the upstream boundary condition whereas the downstream stage-discharge relationship (Figure 5.6) served as the downstream boundary condition.

Values given for the model parameters in the above procedure consisted, at best, of only rough approximations estimated in most cases by relatively crude field measurement techniques. For some parameters, such as Manning's  $n$ , published information is available (Chow, 1959) which allows limits to be set regarding the uncertainty of the parameter estimate. This is not the case for the other parameters



such as streambed conductivity, for which only the judgement of the researcher is responsible for determining if the value used in the model is reasonable.

**Table 5.8 Infiltration test results for the Nyando flood plain near Ahero**

Elapsed time since start (min)	period (min)	Water added (litres)	Water added (mm)	Instantaneous infiltration (mm/hr)
0.5	0.5	-	-	-
1.0	0.5	36.0	0.9	108
1.5	0.5	-	-	-
2.0	0.5	32.0	0.8	96
3.0	1	6.1	6.1	84
4.0	1	6.0	1.4	84
6.0	2	10.0	2.4	72
8.0	2	9.2	2.2	66
10.0	2	9.0	2.2	66
15.0	5	18.0	4.3	52
25.0	10	34.0	8.1	49
40.0	15	25.0	6.0	24
60.0	20	18.0	4.3	13
85.0	25	17.0	4.0	10
120.0	35	25.0	6.1	8

Because of the nature of parameter uncertainty, calibration of the model for the study area was not simply a matter of inputting the measured parameter values into the model. Calibration involved matching of a simulated discharge hydrograph to an observed discharge hydrograph. The problem of matching the model output to

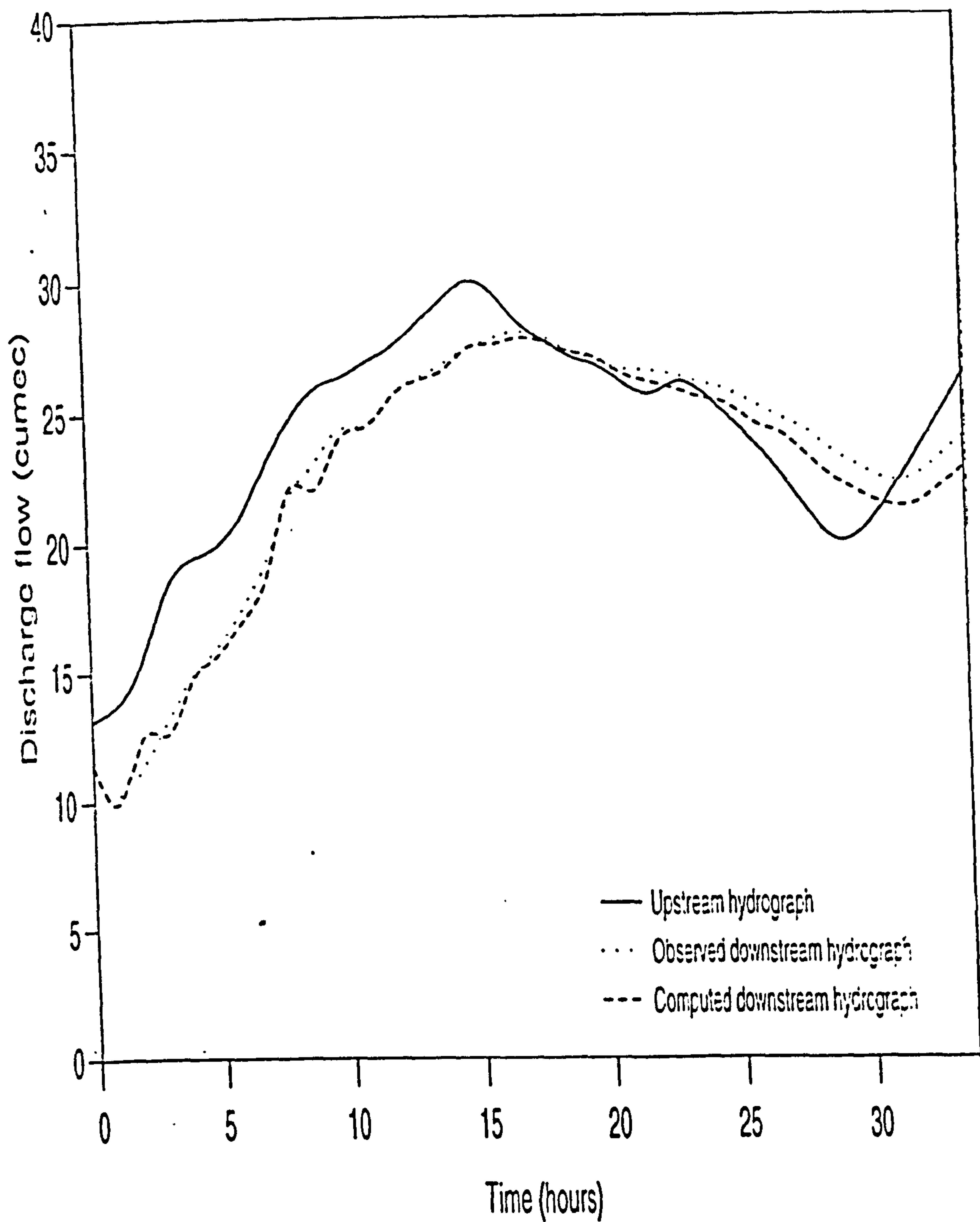


**Fig. 5.9 Simulated and observed discharge hydrographs on the River Nyando, at the Ahero road bridge (downstream station)**

an observed streamflow hydrograph was accomplished through an optimisation procedure based on the function (O'Connell, 1991):

$$F^2 = \sum_{i=1}^n (Q_i - \hat{Q}_i)^2 \quad (5.4)$$

where  $Q_i$  is observed downstream discharge,  $\hat{Q}_i$  is computed downstream discharge and  $n$  is the total number of observations. The optimisation function was minimised through successive adjustment of the model parameters. The adjustment consisted of repeated trial and error runs using alternative combinations of parameter values (taking care to ensure that no value exceeded reasonable limits). In particular, one parameter was adjusted in turn while holding the other parameters constant, at values obtained at the end of the last optimisation run, and comparing the model's downstream discharge output against the corresponding system output. The model was considered calibrated when no significant decrease in the value of the optimisation function could be achieved by further variation in parameter values. The model input consisted of an upstream hourly hydrograph and the output consisted of the streamflow hydrograph at the downstream station (Figure 5.9). Observation wells in the surrounding plain aquifer were not available to measure the output of the bank storage. However, the downstream output was assumed to suffice because under such short-term measures it is reasonable to assume that the leakage effect into/out of the aquifer is given by the difference between the upstream input and downstream output flows, assuming there are no other lateral flows as tributary or overland flows within the reach. From the trial runs, the final parameter values accepted for the simulations were: 0.002 m/s for aquifer hydraulic conductivity; 0.15 for aquifer specific yield; and 0.004 m/s for the hydraulic conductivity of the streambed. The rest were as estimated in the field, as presented in the calibration procedure steps 1 - 10, above. A comparison of the results by the model with the observed downstream hydrograph are given in Figure 5.9.



5.3.2 Test of predictive uncertainty

Comparison of the statistical properties is undertaken (Table 5.9) to provide a general overview of the model's performance.

Table 5.9 Computation of the statistical properties of observed and predicted discharges, (time is in hours and the discharges are in m<sup>3</sup>/s)

Time t	Input	Obsvd. O	Comptd. O'	Q <sup>2</sup>	Q <sup>3</sup>	(Q-Q'') <sup>2</sup>	Q' <sup>2</sup>	Q' <sup>3</sup>	(Q'-Q''') <sup>2</sup>	(Q-Q') A	A <sup>2</sup>
0	13.2	10.2	11.5	104	1061	154.7	132	1521	124.1	-1.32	1.74
2	15.0	11.4	12.9	130	1482	126.3	166	2147	94.9	-1.53	2.35
4	19.3	15.0	14.9	225	3375	58.4	222	3308	59.9	0.06	0.01
6	20.8	17.6	17.1	310	5452	25.4	292	5000	30.7	0.48	0.23
8	24.6	22.2	22.5	493	10941	0.2	502	11239	0.0	-0.28	0.08
10	26.2	24.8	24.3	615	15253	4.7	590	14349	2.8	0.54	0.29
12	27.4	25.8	25.7	666	17174	10.0	660	16975	9.4	0.12	0.01
14	29.2	26.8	26.6	718	19249	17.3	708	18821	15.7	0.20	0.04
16	29.5	27.8	27.5	773	21485	26.6	756	20797	23.6	0.25	0.06
18	27.8	27.8	27.6	773	21485	26.6	762	21025	24.6	0.20	0.04
20	26.9	27.0	27.0	729	19683	19.0	729	19683	19.0	-0.03	0.00
22	25.4	26.6	26.1	708	18821	15.7	681	17779	12.0	0.50	0.25
24	25.6	26.0	25.4	676	17576	11.3	645	16387	7.6	0.55	0.30
26	23.6	25.2	24.3	635	16003	6.6	590	14349	2.7	0.85	0.72
28	21.0	24.2	23.1	586	14172	2.4	534	12326	0.2	1.11	1.22
30	20.4	22.8	21.7	520	11852	0.0	471	10218	0.9	1.11	1.23
32	23.2	22.4	21.3	502	11299	0.1	454	9664	1.8	1.07	1.15
34	26.5	24.0	22.8	576	13824	1.8	520	11852	0.00	1.16	1.35
TOTALS				9739	240187	507	9414	227440	428		11.1

where O'' and O''' are the averages of the observed (O) and predicted (O') discharges, respectively.

Analysis of this type is meaningful only in relation to the particular field problem tested and thus a generalised statement as to model predictive uncertainty in all possible situation is precluded. In this study, predictive uncertainty has been tested based on comparison of observed and simulated downstream river discharge at Ahero bridge on the Nyando. An initial step to show the predictive uncertainty consisted of a comparison of basic statistical properties computed from a set of observed and simulated downstream discharges. The statistical properties of the observed and simulated results are thus computed and presented in Table 5.10. The results indicate good agreement between predicted and observed mean values. Standard deviation values are also seen to be in close agreement, while skew values diverge slightly.

**Table 5.10 Statistical properties comparing the observed and predicted hydrographs**

	Mean (m <sup>3</sup> /s)	Standard Deviation (m <sup>3</sup> /s)	Coefficient of Skew
Observed data	22.6	29.8	0.011
Predicted data	22.4	25.2	0.002

As stated previously, however, the most straightforward method for evaluating predictive uncertainty is that of direct comparison of graphical plots of model predictions with corresponding values of observed field data. Plots of this type readily facilitate the construction of confidence bands which in turn allow probabilistic inferences to be made regarding the reliability of model predictions. If confidence bands are chosen for the 95% level, as is customarily the case for this type of analysis, then the probabilistic inference would be that the true value of an output variable corresponding to any predicted point on the straight line in the middle of the band has a 95% probability of lying between the confidence limits at that point.

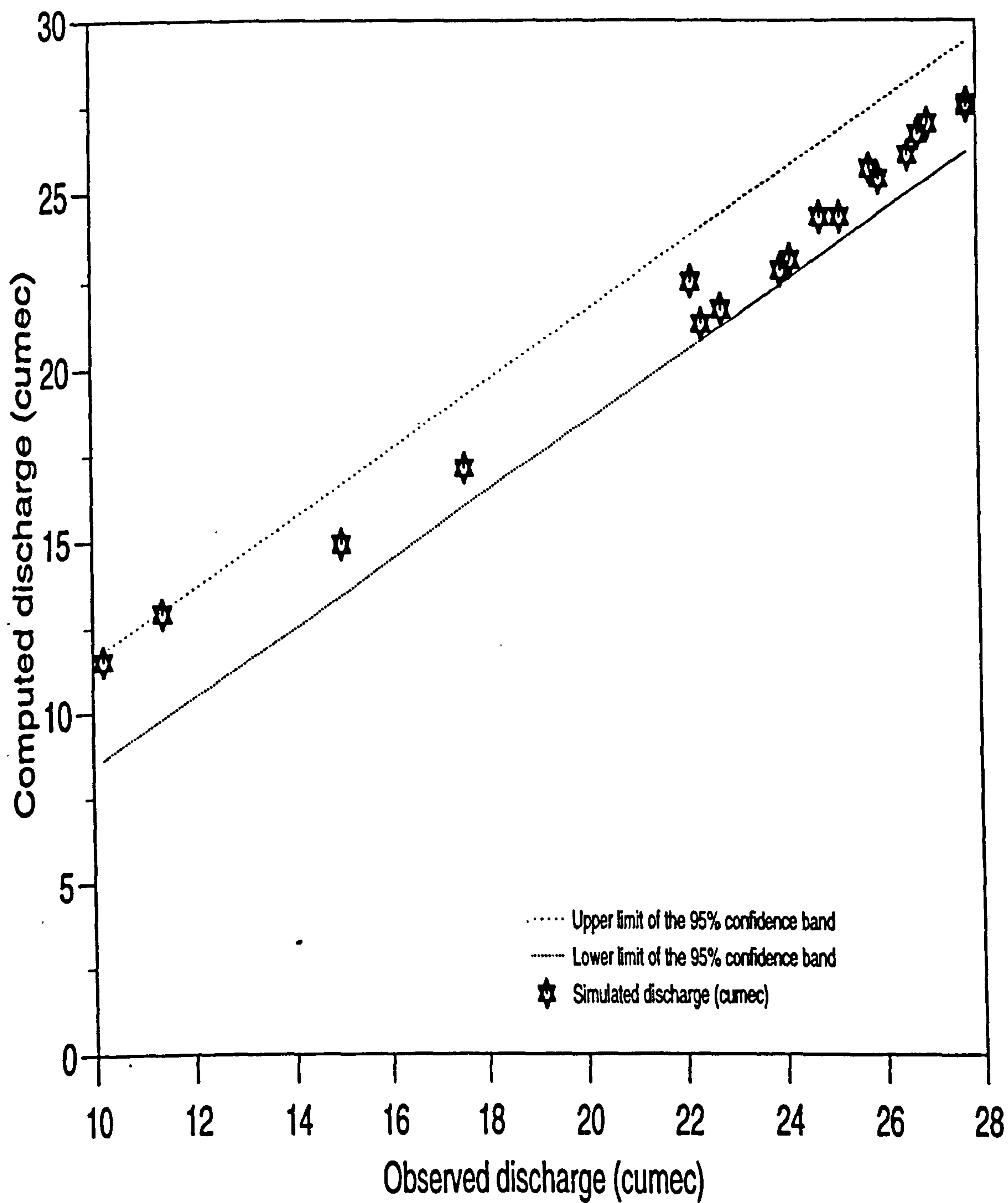


**Fig. 5.10 Observed and simulated streamflow discharges at the Ahero Road bridge**



Results of this graphical analysis for the River Nyando concerning the uncertainty associated with the model's predictions of river discharges at the Ahero bridge are shown in Figure 5.10. The plotted points are the results of modelling, and the observed flood event (in April, 1993) over the 18.432 km reach of the Nyando. This comparison results are significant in that they serve to quantify the degree of accuracy with which streamflows can be numerically simulated in the channel reach. In general, a good degree of predictive accuracy was observed for the river flow simulations. The unbiased point scatter and the narrow 95% confidence band seen in Figure 5.10 indicates that the predictive uncertainty has been minimised for the flow conditions.

#### **5.4 Application of the MASAI for Predictive Analysis of the Hydrological Responses due to the Proposed Cut-off works on the River Nyando Near the Ahero NIB Village**

Field calibration and predictive uncertainty results are useful in giving the analyst a rough idea of what he/she is likely to obtain by applying the model to simulate another event. The results in the previous section established that the calibration was satisfactory, and the predictive uncertainty of the model were minimal. The MASAI is therefore validated to simulate the hydrological behaviour of the Nyando at Ahero, following the proposed river-training alterations on a reach near the Ahero NIB village, which lies within the calibrated reach.

The river-training alterations involve cut-offs of new channels to by-pass some meander and bends of the present course of the river. Complete details of the cut-off channels were not available. However, the plan layout of the re-routed river was available, from which the changes in the longitudinal distances along the river could be calculated. The section stations along the river, as surveyed during fieldwork, are

not among the sections that will be cut off or by-passed. Therefore, the same stations along the river reach are used to describe the channel boundary, (as was the case before training), except for the distance spacing between the stations which will be shortened by the training cut-offs. Reduced distances between stations along the river will in turn increase the average bed slope of the corresponding reach. The main difference between the channel in its present state, and after training are given in Table 5.11.

Changes in the geological properties, including the channel materials and Manning's  $n$  were assumed to be negligible. In other words, all other parameters and boundary conditions were assumed to remain the same, since they are not mentioned in this particular project. The hydrologic behaviour being addressed, therefore, is the system responses due to the alteration of the route of the river alone.

The impacts of the training developments are visualised better by comparing the discharge output through the river system before and after the training alterations. As stated above, the design discharge of the new course of the river was not stated. Therefore, the same upstream hydrograph, as obtained during calibration, was applied to simulate the effects of the changes to the streamflow. The first numerical experiment routed the flood wave through the river system before training. The second simulation was based on the river system after the training alterations (Figure 5.11).

Before training, the flow depth of the peak discharge at the NIB village, (section 8 in Table 5.11), was 1.36 m. After training, the depth of the peak discharge at the NIB village, was reduced to 1.14. The explanation that can be given to these changes is that after training, the corresponding channel slope is increased, which in turn increases the velocity of flow in the reach. For a given streamflow discharge, the cross-sectional area of flow is smaller for fast moving flows, which in turn reduces

the flow depth in a given cross-section. Based on these predictions, it is observed that after the training alterations, the flood level will be lowered by about 22 cm. With regard to the NIB village, therefore, the project is deemed to achieve its purpose - mitigating the menace of floods in the village.

**Table 5.11 Distances between sections of a reach on the Nyando, before and after cut-off works near the Ahero NIB village**

Section	Distance measured from upstream station (1GD3)	
	Before training (m)	After training (m)
1GD3	1843	1843
2	1843	1843
3	1843	1843
4	1843	1843
5	1843	1843
6	1843	1656
7	1843	1219
8(NIB)	1843	1843
9	1843	1843
10	1843	1425
Ahero Bridge	1843	1843

But, the hydrological changes being imposed on the river may not be limited to within this particular reach around the NIB village. Furthermore, for a long time now the main concern on the Nyando has been to mitigate the flooding problems all along the flood plain. In fact, the flooding problems have been reported to be most crucial in the reach from around the Ahero bridge downwards to the lake. To assess the impact of the training alterations at the Ahero bridge section, which is the gateway to



the most flood prone area, the flow levels at the section before and after training are simulated and analysed.

Before training, the depth of flow of peak discharge at Ahero bridge (section 11 in Table 5.11) was 1.33 m, and after training it was predicted to increase to about 1.43 m. This means that the hazards of floods will be aggravated. The reason that can be attributed to this change is that after training, the upstream flows (around the trained area) are accelerated, whereas the velocity of flow downstream is not. As a result, the rate of water input at the bridge section is increased, unlike the water output from the area. This can lead to water accumulation around the bridge, and aggravate the flooding problem in the area towards downstream.

From the observations, it is noted that after training alterations at the NIB, the flooding problems will not only be transferred from the area, but will also be aggravated in the reaches downstream. It can also be recalled that the results by Pinder and Sauer (1971), (section 5.2.3), demonstrated that the bank storage effects are cumulative with the distance downstream, (Figures 5.5a and 5.5b). The simulation results here are quite in line with their observations, showing that shortening of the river reach through training at the Ahero NIB will reduce the bank storage effects and intensify the flooding menace towards the downstream boundary.

The other impacts due to the river training can be seen in terms of the erosive power of the new flow conditions. It has already been stated that one of the geologic weaknesses of the Kano plains is its susceptibility to develop into deep gullies under fast moving flows. Simulated results for sediment yield in the reach, before and after the training, are presented in Figure 5.12. Sediment yield, as shown, is the accumulated bulk volume of bed material load having passed a given cross section at a given time during the flood. Spatial variation of sediment yield as simulated are for 16 hours.

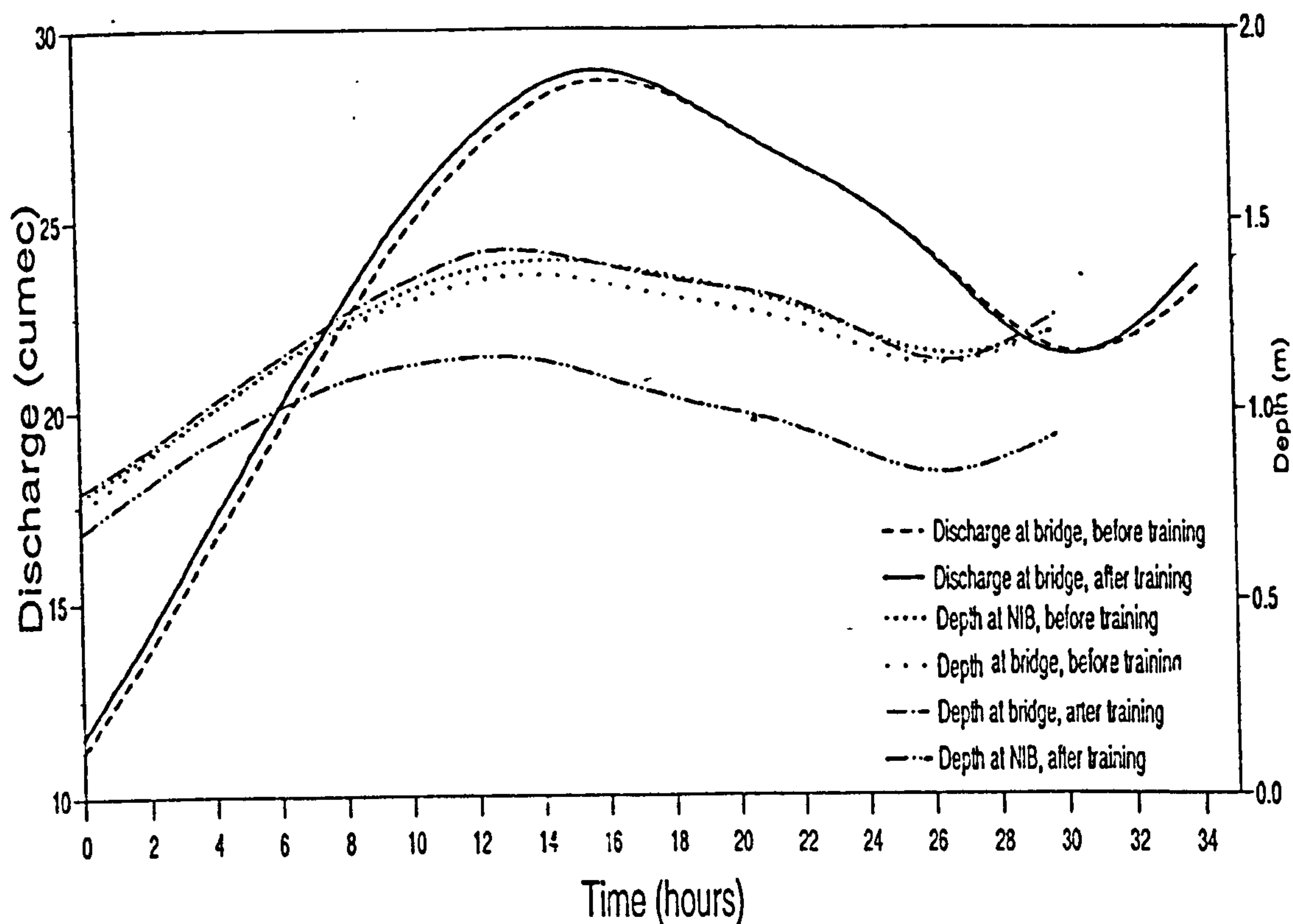


**Fig. 5.11 Predicted discharge and flow depth hydrographs, before and after training alterations on the Nyando River, near the NIB village**

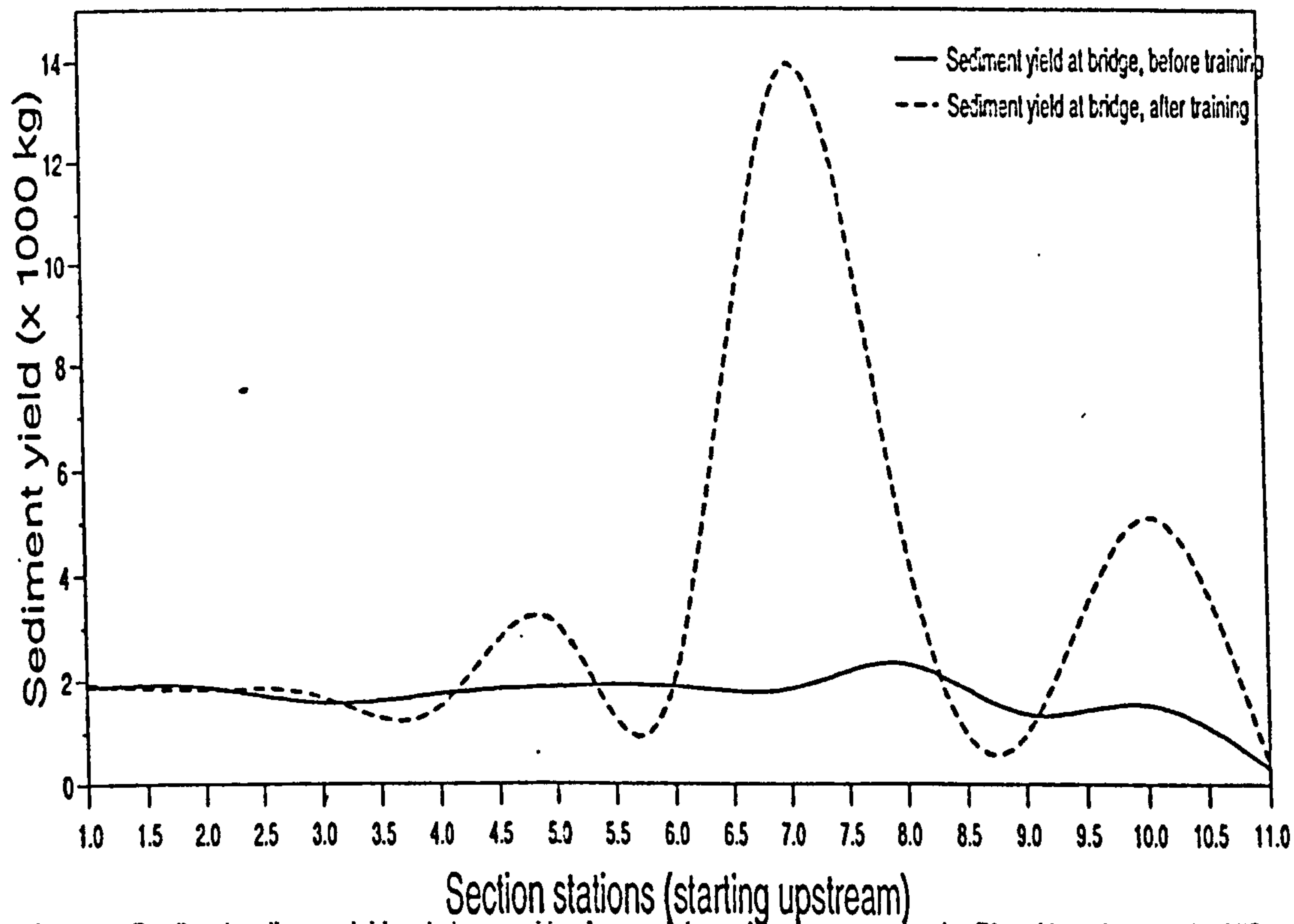


**Fig. 5.12 Predicted sediment yield distribution, before and after training alterations on the Nyando River near the NIB village**

The spatial variation of sediment yield is closely related to the potential for aggradation and degradation along the study reach. A decreasing yield in the downstream direction indicates that sediment load is partially stored in the channel. Such sediment storage is associated with aggradation of the channel bed. On the other hand, an increasing yield in the downstream direction means sediment removal from the channel bed, or degradation of the bed. A uniform sediment yield along the channel indicates sediment balance, i.e., dynamic equilibrium.

As shown in Figure 5.12 the spatial patterns of sediment yield are such that before training, the river reach is more or less in a state of dynamic equilibrium, except for a slight increase in sediment storage towards the downstream end. But after the training works, sediment yield is not uniform any more. It is observed that some reaches will be scouring at higher rates (positive gradient), while others will be filling at equally high rates (negative gradient). For example, the reach between sections 6 and 7 has sediment yield increasing towards downstream, meaning that aggradation is taking place. In the reach between sections 7 and 8.5, the sediment yield is falling towards downstream, meaning that scouring is taking place. Relating Figure 5.12 to Table 5.11 it can be observed that scour is generally taking place in the reaches where the flows have been accelerated by the training cut-offs. Aggradation on the other hand will take place in reaches where the flows are retarded.

In the long run, both of these aggradation and degradation effects have negative impacts. While degradation of the river bed may be viewed to be in line with the development objectives of mitigating floods, however, lowering the river stage beyond certain limits is also ruinous. This is because the river is used for irrigation and livestock as a water source, so that falling levels will be limiting the potential to command the irrigation fields and livestock watering points, or increase pumping costs. Besides, discontinuous sediment yield will eventually leave certain reaches



degraded with high unstable banks, while other reaches may be incapacitated by sediment deposits, causing more flooding and waterlogging problems.

From this predictive analysis, therefore, it is perceived that the river training development planned at the NIB will alleviate the danger of flooding at the NIB village, but aggravate the problem downstream of the reach. Other river engineering works, such as opening up of the river mouth will be required at the same time to accelerate output discharges from this flood-prone reach, or embankment in order to defend against the raised flow levels. It is also noted that after training, the reach will be subject to non uniform sediment yield. This can cause certain reaches to be destabilised and suffer from land slide and gully erosion, whereas other areas may suffer from choked-up and waterlogged conditions. It is advisable, therefore, that the plan of river training by cut-offs is redressed, considering the whole flood plain of the Nyando River.

## **6 CONCEPTUAL ANALYSIS OF THE EFFECTS OF SEDIMENTATION ON STREAMFLOW HYDROGRAPHS**

### **6.1 Introduction**

So far, emphasis on the application of the Model for Alluvial Stream-Aquifer Interaction (MASAI) has been directed towards showing its viability for practical problems. In the presentations, in chapter 5, both real and theoretical hydrological systems have been used to explain its capability. The aim of the examples was to illustrate cases to which the model can be calibrated and applied to solve or predict certain hydrological behaviour. In the process, the examples have also stimulated an interest to simulate more interaction of streamflow and groundwater in order to gain insight into other hydrological phenomena. The interest was realised based on the ability of the MASAI to simulate stream-aquifer interaction in erodible channels, which is an additional advantage over other models, as discussed in chapters 2 and 4.

For instance, the example in section 5.2.2 was used to show how the model can be applied to simulate sediment transport/storage upstream of a check-dam. Another example in section 5.2.3 was used to show how flood waves can be attenuated by the effects of bank storage. When the two examples are visualised together, it is realised that the concept of the MASAI can be applied as a criterion for evaluating soil and water conservation practices.

In engineering practices, before claiming success or failure, one requires reference scales on which to measure and compare the achievements. Meaningful evaluation of river engineering plans, as is the case in most other engineering works, requires qualification, if not quantification of levels or trends to which the development plans aim to attain or shift towards. In the case of riverine soil and water conservation, for example, deviation of streamflow hydrographs and sediment yield curves can be adapted as the measurement reference scales. Based on these, and the aforementioned capabilities of the MASAI, it is possible to evaluate the inter-relationships among the individual components of certain hydrologic systems, as well as to determine the influence of various parameters or interventions on the system outputs.

Sensitivity analysis from previous stream-aquifer interaction models have generally indicated that the values of parameters describing the stream-aquifer interface (e.g. streambed thickness, slope, roughness and hydraulic conductivity) have far more influence on system output than the values of aquifer transmissivity and storativity (Matlock, 1965; Pogge and Chiang, 1977; Cunningham and Sinclair, 1979), as discussed in chapter 2. This means that change in any one of the parameters of the stream-aquifer boundary is likely to affect the hydrologic behaviour of the system. It is also noted that it is this boundary condition that is most likely to be changed due to either natural or cultural conditions occurring in the upstream catchment and/or within the river reach itself. Tracking estimation of transient variation of the boundary condition is therefore important in simulations describing the hydrologic behaviour of linked alluvial stream-aquifer systems.

The interdependence of streamflow and sedimentation processes, and their close relationship with the condition of the underlying land geology provides a means by which the hydrologic processes of sediment and water yield can be applied to evaluate the impacts of land degradation and conservation. The approach here is based on this



understanding and is advanced through the following steps: (1) effects of system parameters on baseflow hydrographs; (2) influence of sedimentation on baseflow hydrographs and (3) evaluation of riverine land degradation and conservation applications. Because of limitations in data provision, conceptual hydrologic systems have been used; based on that of Pinder and Sauer (1971) for steps (1) and (2), and on the River Kibos system for step (3).

## **6.2 Effects of System Parameters on Baseflow Hydrographs**

Streamflow is that part of precipitation and/or snow melt, as well as any other flow that coalesces into a natural channel to run downstream in a continuous mass flow. A hydrograph is a graphical expression of the rate of flow past a stream gauging station over a period of time. The contributing components of a natural hydrograph for a river channel in direct connection with an unconfined aquifer are basically the baseflow and surface runoff (Wilson 1990). Surface runoff is, for convenience, assumed to contain two other components: overland flow and interflow. Overland flow is the water running over the ground surface into river channels largely due to the influence of the slope of the land surface. Interflow refers to water travelling horizontally through the upper horizons of the soil, perhaps in artificial drain systems or above an impermeable layer immediately below the surface. Baseflow, on the other hand is defined as the groundwater contribution from the aquifer bordering the river, which keeps on discharging more and more slowly with time until the water table in the aquifer is level with the river stage.

Since streamflow is a product of water flow over land and/or through the underlying soil geology in a particular watershed, then its amount and rate of flow, in a way, expresses the natural and cultural characteristics of the watershed system that produces it. The main natural factors affecting the volume and rate of streamflow,

and consequently the shapes of hydrographs are: precipitation (intensity, duration, etc.), drainage basin characteristics (size, shape, orientation, tributary density, slope etc.), soil geology (permeability, specific yield etc.) and land surface cover (forests, aridity, etc.); whereas the cultural activities include land use practices (farming, urbanisation, etc.) and river engineering works (check-dams, training etc.). Besides the cultural practices, land cover is the other factor that is being substantially modified by people and thus causing change to the output of the hydrologic systems. However, in this study attention is limited to the baseflow hydrographs because it is their generation that is mainly controlled by the stream-aquifer boundary condition - which has been the main subject of this study. The other components of the hydrograph can be observed in other references such as Stalling (1957), Crane, (1980), Chow et. al. (1988), Wilson (1990), etc.

Depending on the direction of baseflow, rivers may be classified into three categories, that is: losing, gaining and intermittent streams. A losing stream is one that recharges groundwater (baseflow is negative). For example irrigation channels and many natural rivers crossing arid areas operate as losing streams. A gaining stream, on the other hand is one that is receiving groundwater discharge (baseflow is positive). In other words it acts as a drain for bordering aquifers. Intermittent streams are those that act as both losing and gaining streams depending on the season; they tend to dry up during the dry season. The contribution from a losing stream takes place at the expense of contributing aquifers on other parts of the stream, since baseflow cannot be sustained on a wholly losing stream. Such a stream will dry up completely in rainless periods, and is called an ephemeral stream.

From this explanation, it is seen that under certain conditions streamflow can contribute to groundwater storage, and at different times or under different conditions, groundwater can contribute to streamflow discharge. In fact, groundwater contribution (baseflow) can be such an important factor in streamflow generation, like

in humid areas with drainage basins underlain by highly permeable geologic formation, that groundwater can account for as much as 70-80% of the annual discharge of streamflows (Younger, 1987). The baseflow recession curve is the plot showing the variation of baseflow with time during periods of groundwater drainage into the river. In essence it is a measure of the drainage rate of groundwater storage from the adjoining aquifer. Previous analyses of streamflow hydrographs have produced relationships of the recession curve according to Eq. 6.1, (Wilson, 1990):

$$Q_b = Q_0 \cdot e^{-\alpha t} \quad 6.1$$

where  $Q_b$  is the baseflow after a time period  $t$ ,  $Q_0$  is the baseflow at the start of the time period,  $\alpha$  is the recession constant representative of the system responses and  $e$  is the natural logarithm.

Among other things, diverse morphological factors due to variation of sedimentation parameters do affect the baseflow, resulting in considerable variations both in time and space. A quantitative, or at least qualitative knowledge of these variations is necessary for interpretation and use of streamflow data in making low-flow estimates for the purposes of effecting pollution control through regulation of streamflow, managing groundwater recharge or soil and water conservation schemes, mitigating general impacts of drought, etc.

In order to analyse the baseflow contribution, it is necessary to separate it from the surface runoff component of the system. The MASAI algorithm provides an ideal technique of hydrograph separation, unlike other methods of separation, which are a bit arbitrary and to some degree unrealistic in that they do not account for most other aquifer and channel contributions. Ideal baseflow is hereby defined as that flow to the stream from depletion of an aquifer when other effects such as water evaporation, deep percolation, recharge and abstractions are absent from the system. The technique



involves determining the initial steady state solution for the entire system, routing a hydrograph through the channel, and recording the movement of groundwater into and out of bank storage. Specifically, as already explained in section 5.2.3, the baseflow component is determined by routing a sediment laden inflow hydrograph, first assuming an impermeable channel bottom, then again with the impervious restriction removed. The baseflow or leakage hydrograph is considered to be the difference of these two hydrographs, being positive when there is resultant gain by the river, and negative for resultant loss from the river.

To illustrate the effects of some of the system parameters on the baseflow, three system parameters, hydraulic conductivity of the aquifer, specific yield of the aquifer and the hydraulic conductivity of the river bottom sediments were varied for different simulations while routing a flood wave through the system. The flood wave hydrograph applied in the simulation is plotted in Figure 6.1.

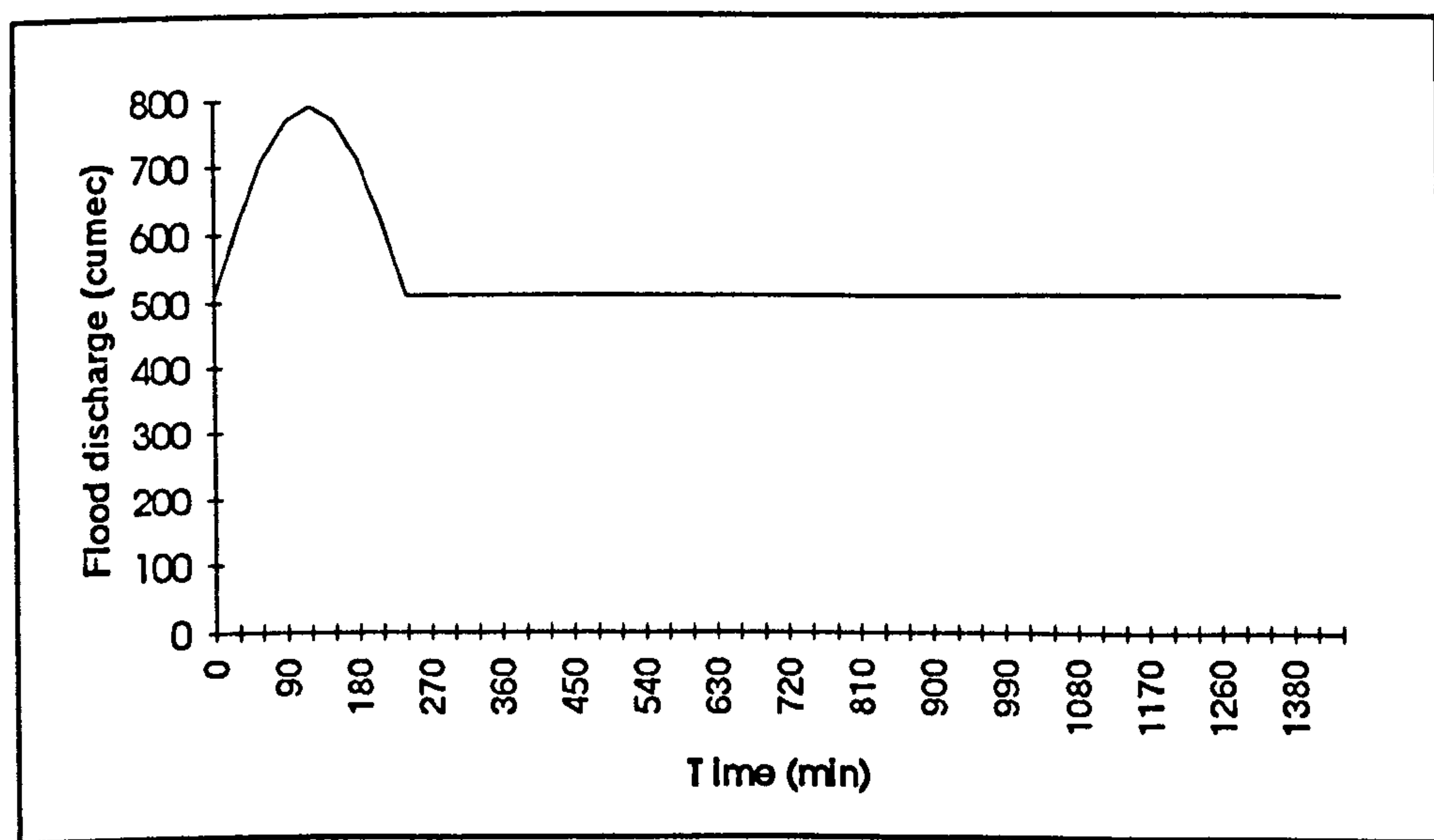


**Fig. 6.1** A plot of the flood wave hydrograph used in the modelling

Some notable observations demonstrating the effect of the three parameters on the system baseflow are presented in Figures 6.2a, 6.2b, and 6.2c respectively.

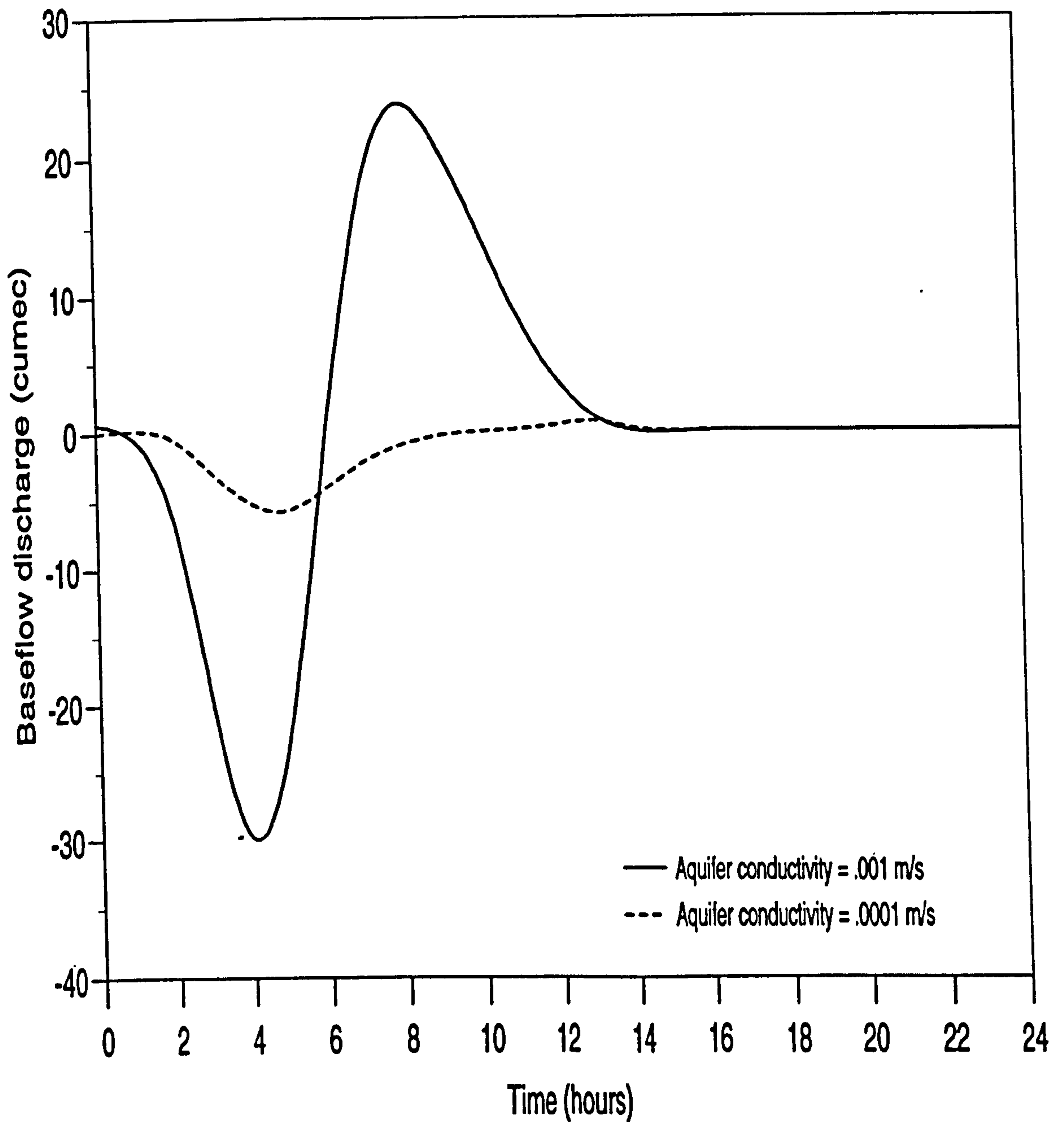


**Fig. 6.2a** Baseflow hydrographs at the downstream station for varied hydraulic conductivity of the aquifer. The specific yield of the aquifer is 0.03 and the hydraulic conductivity of the river bed is 0.0001 m/s

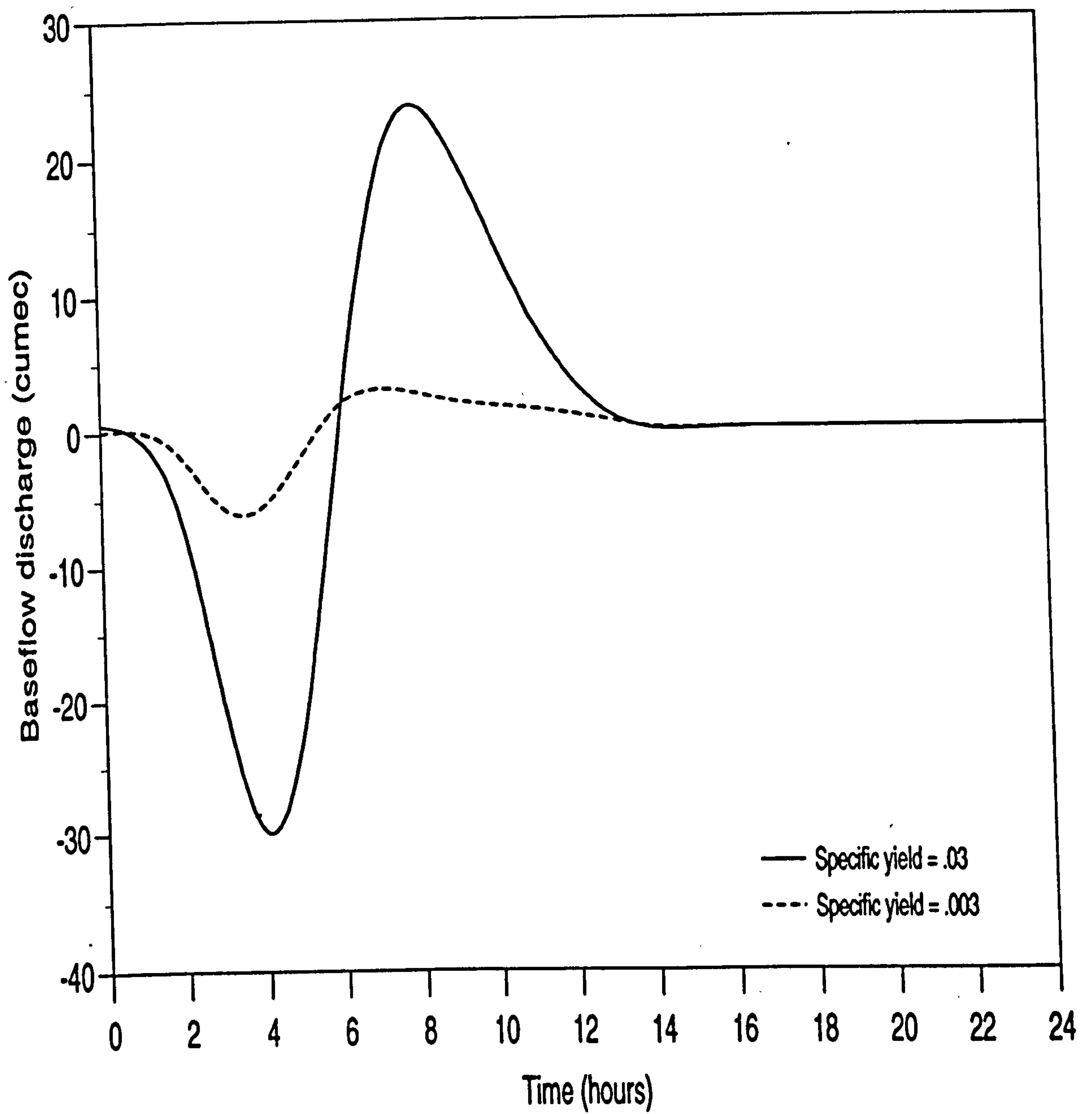


**Fig. 6.2b Baseflow hydrographs at the downstream station for varied specific yield. The hydraulic conductivity of the aquifer is 0.001 m/s and that of the river bed is 0.0001 m/s.**



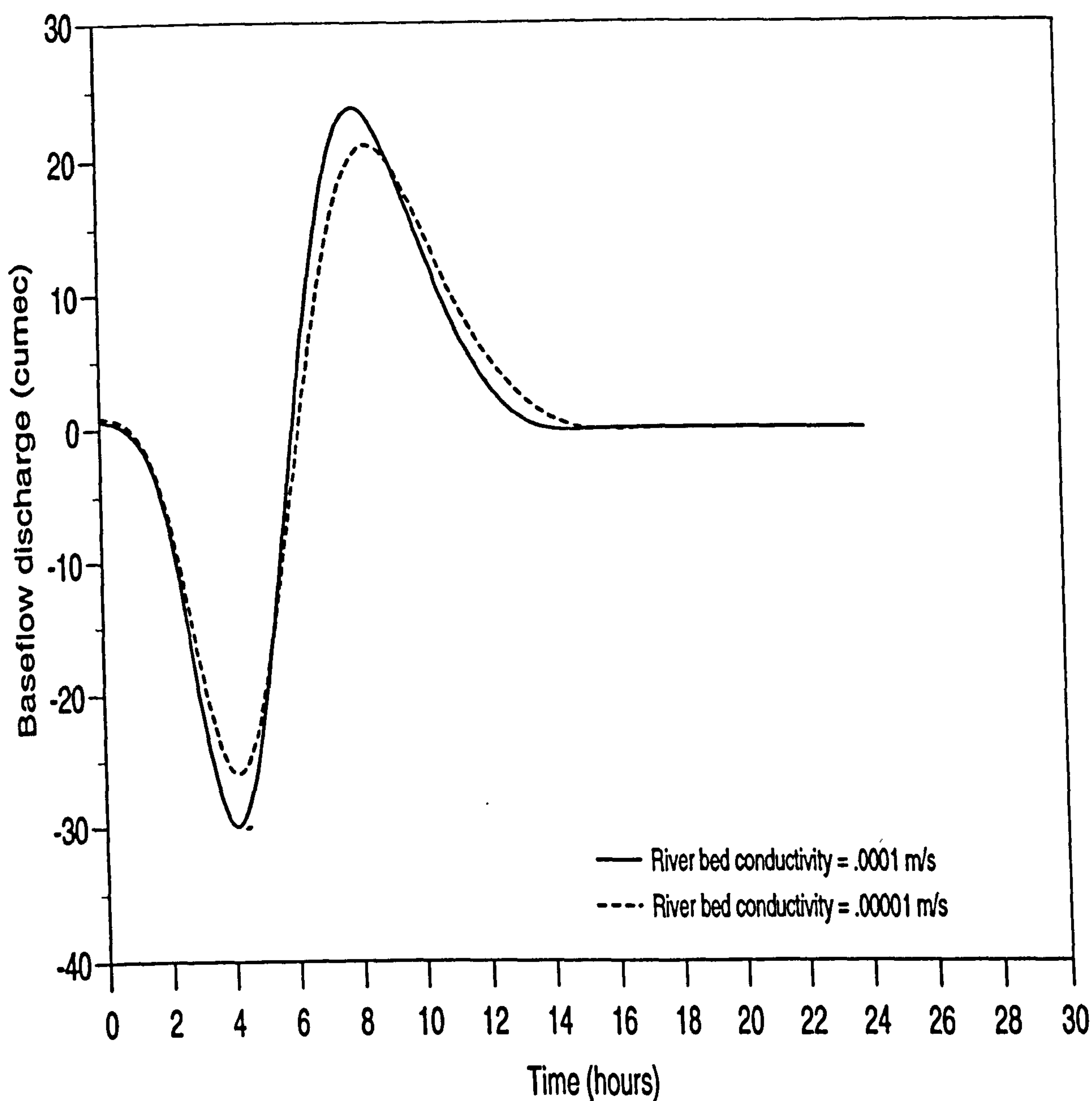


**Fig. 6.2c** Baseflow hydrographs at downstream station for varied hydraulic conductivity of the river bed. The specific yield and hydraulic conductivity of the aquifer are 0.03 and 0.001 m/s, respectively.

The simulations demonstrate, for example, that when the hydraulic conductivity of the aquifer is reduced from 0.001 m/s to 0.0001 m/s (Figure 6.2a), the minimum baseflow value is increased from about -30 m<sup>3</sup>/s to -6m<sup>3</sup>/s, and the time of occurrence of the minimum baseflow is increased by about one hour. The maximum baseflow value is reduced from about 24 m<sup>3</sup>/s to 1 m<sup>3</sup>/s, and the time of occurrence of the maximum baseflow is increased approximately by three hours. The rate of hydrograph recession is reduced markedly. Similarly, when specific yield is decreased from 0.03 to 0.003 (Figure 6.2b), the minimum baseflow value is increased from about -30 m<sup>3</sup>/s to -6 m<sup>3</sup>/s while the time of occurrence is decreased by about one hour. The maximum baseflow is decreased from about 24 m<sup>3</sup>/s to 3 m<sup>3</sup>/s and the time of occurrence of the maximum baseflow is reduced by about 2 hours. The rate of baseflow recession rate is reduced markedly. Likewise, when the hydraulic conductivity of the streambed is decreased from 0.0001 m/s to 0.00001 m/s (Figure 6.2c), the minimum baseflow value is increased from about -30 m<sup>3</sup>/s to -25 m<sup>3</sup>/s, and change in the time of occurrence of the minimum baseflow is negligible. The maximum baseflow value is reduced from about 24 m<sup>3</sup>/s to 21 m<sup>3</sup>/s, and the time of occurrence of the maximum baseflow is slight. The rate of baseflow hydrograph recession is also decreased slightly.

Although similar results have been produced showing the effects of the properties of stream-aquifer interacting systems of stable interface boundaries, (e.g. Cunningham and Sinclair, 1979), here, attention has been focused on river systems with mobile boundary interfaces that are subject to changes as a result of stress conditions within the river system. Under normal circumstances, such properties as hydraulic conductivity and specific yield of aquifers for real-world systems are unlikely to be changed except in very exceptional cases. It is the characteristics of the river channels that are most vulnerable to manipulations by people as they become more and more dependent on both land and water resources. Therefore, attention has been accorded to streambed adjustments due sedimentation processes because it is the river bed that

is most easily varied, yet it plays such a crucial role in influencing the behaviour of baseflow hydrographs.

## **6.3 Effects of Sedimentation on Baseflow Hydrographs**

### **6.3.1 Introduction**

Any phenomenon that produces a pressure gradient between streamflow and groundwater will cause the baseflow to vary. Flood waves and their periods of duration are the basic variables that are closely related to the pressure gradient variation. Their influence on baseflow have been previously demonstrated by Todd (1955). Likewise, any medium developing between streamflow and groundwater media will produce a pressure gradient and affect the seepage resistance between the two hydrologic units, hence vary the intensity of the stream-aquifer water interchange. Under such circumstances, channel sedimentation changes are the main causes responsible for the evolution or regression of the intervening boundary layer at the bottom of the river.

Among other demonstrations of the interrelationships between baseflow and the characteristics of hydrologic systems, it is the analytical study by Singh (1968) which came closest to relating baseflow to the stream-aquifer boundary variation, when he illustrated that baseflow recession curves depended on the degree to which the river channel was entrenched in the aquifer. He then demonstrated that baseflow recession curves for a stream that is fully penetrating an aquifer or is underlain by a shallow aquifer do not follow the classic exponential relationship (Eq. 6.1), unlike recession curves for a stream that is partially penetrating a deep aquifer, which produces a more or less straight line on semi-logarithm graph paper.



In this study, inclusion of the sediment routing module in the MASAI formulation has given it the additional capability to analyse the effects of sedimentation on the baseflow hydrographs.

### **6.3.2 Simulation of the effects of sediment yield on baseflow hydrograph**

Attention is directed towards those changes that are closely related to sediment yield and sedimentation processes, which are considered to be common hydrological phenomena, as well as being the main governors controlling the boundary parameters that have been reported to be influential to baseflow. Numerical experiments based on the same hydrologic system used in section 6.2 have been performed to assess the influence of varying the input sediment concentration and particle sizes.

High sediment concentration values have been used because it is in channels with such high sediment load that the problem of sedimentation is likely to occur. Some records showing rivers of such high sediment load are: 850 ppm for Tiber River (Italy); 40000 ppm for Yellow River (China); 550 ppm for Nile (Egypt); 7500 ppm for Waipapa (New Zealand); 19400 ppm for Colorado (USA); and 2900 ppm for Kosi (India). These are only the average values, which rise to higher values during peak periods (Garde and Ranga Raju, 1985).

In this experiment, an initial input sediment concentration of 5000 ppm was assumed. The results show that in the event of the concentration of sediment input increasing from 5000 ppm to 25000 ppm, (Figure 6.3a), the minimum baseflow value is decreased from about  $-30 \text{ m}^3/\text{s}$  to  $-48 \text{ m}^3/\text{s}$ . The time of occurrence of the minimum baseflow is not changed. The maximum baseflow is also decreased from  $24 \text{ m}^3/\text{s}$  to  $18 \text{ m}^3/\text{s}$ . The time of occurrence of the maximum baseflow is also negligible.

The particle size distribution of the sediment input was based on the results in Table 5.3. In the first routing, the particle size distribution was decreased by multiplying by a factor of 0.2, and in another simulation the particle sizes were increased by a factor of 5. The simulation results in Figure 6.3b demonstrate the hydrological implications in the event of altering the upstream particle size distribution. In the event of increasing the particle sizes, the minimum baseflow value is reduced slightly, from about  $-30 \text{ m}^3/\text{s}$  to  $-31 \text{ m}^3/\text{s}$ , and the maximum baseflow value is also decreased slightly, from about  $24 \text{ m}^3/\text{s}$  to  $23 \text{ m}^3/\text{s}$ . There is no change in the times of occurrence of either the maximum or minimum values. Baseflow hydrographs are also plotted on the figures, assuming conditions when the input concentration is zero.

To appreciate the usefulness of these simulations, one needs to put the problem of modelling in perspective. Cunge (1983) put it that: "Mathematical modelling may have a scientific or an engineering purpose. It is not necessary that there be a coincidence of models built with these different aims. The former help a researcher to understand the mechanisms of studied physical phenomena and, possibly, to check the hypothesis related to it. The latter should simulate observed reality in order to predict the consequences of modifications which one wishes to make or the consequences of events which have not been observed so far." Younger (1990) has also reiterated that the usefulness of applying models to study field phenomena is now widely appreciated. As he succinctly quotes: "models can provide a disciplined format for assessing the consistency within and between concepts of the governing processes and data describing the relevant coefficients. Sensitivity analysis of models can also help in defining priorities for fieldwork, since it is logical to expend most resources on the measurement of those parameters which have the most profound influence on model performance".

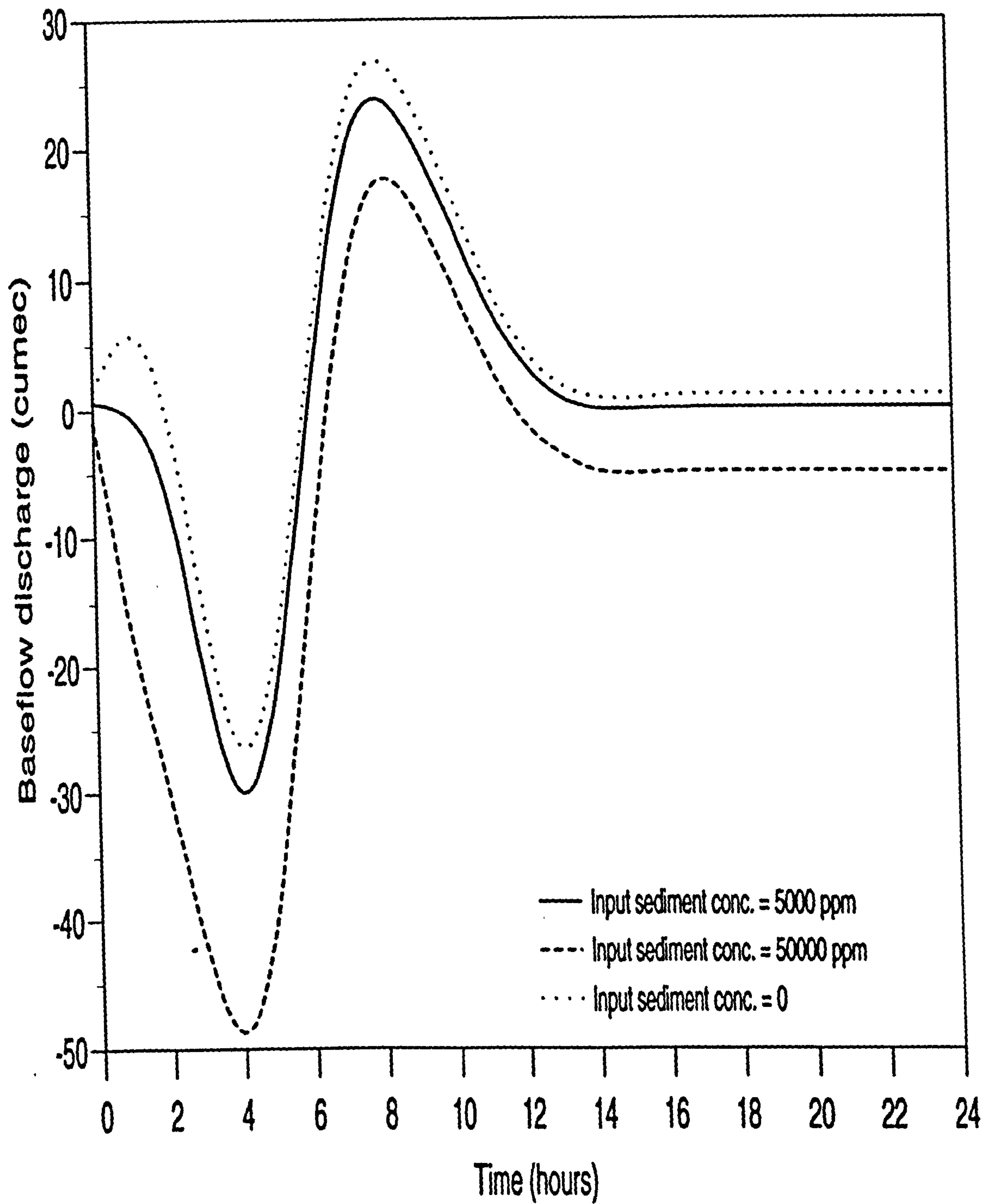


**Fig. 6.3a Baseflow hydrographs at the downstream station for varied concentration of input sediments.**



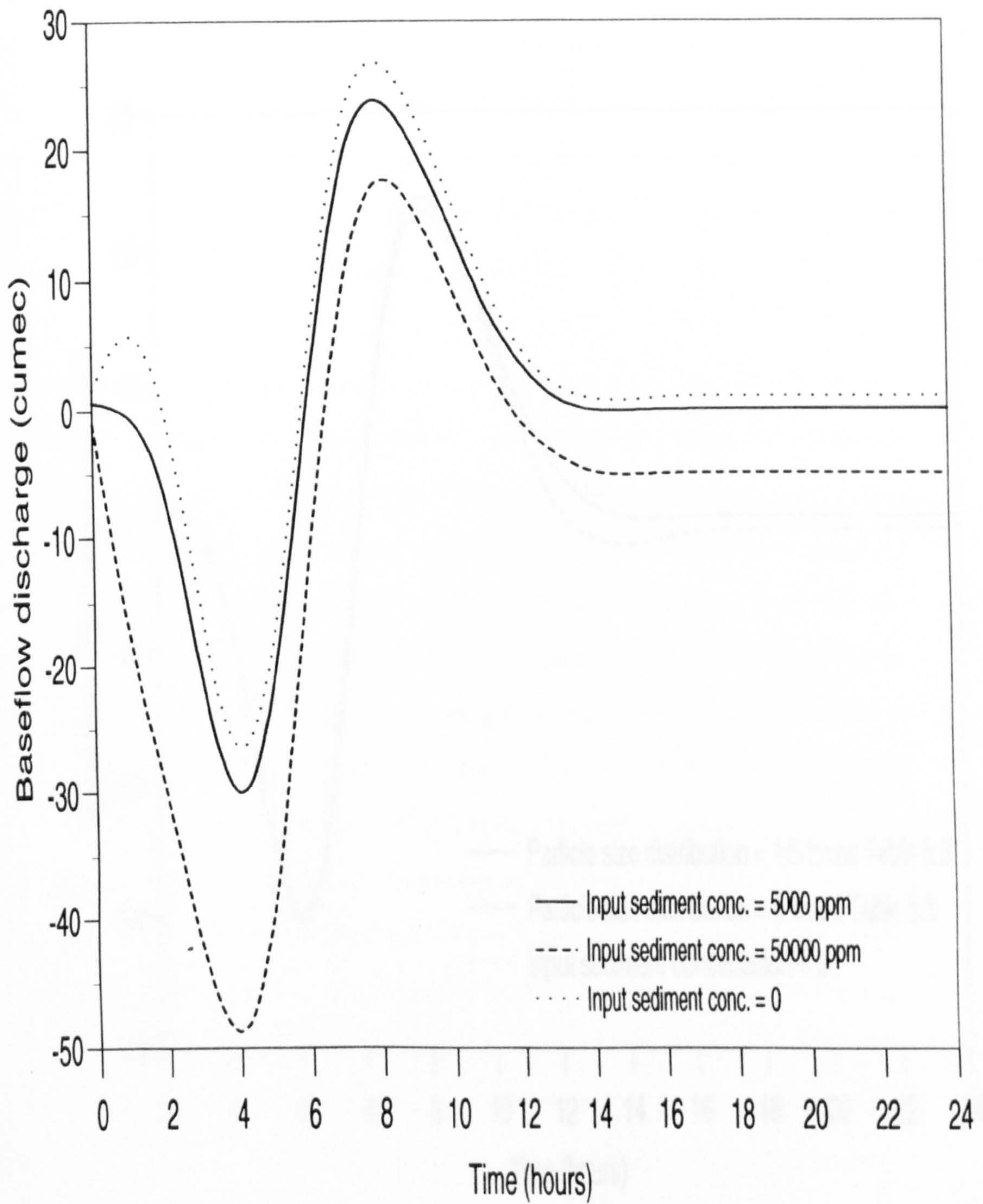


**Fig. 6.3a Baseflow hydrographs at the downstream station for varied concentration of input sediments.**

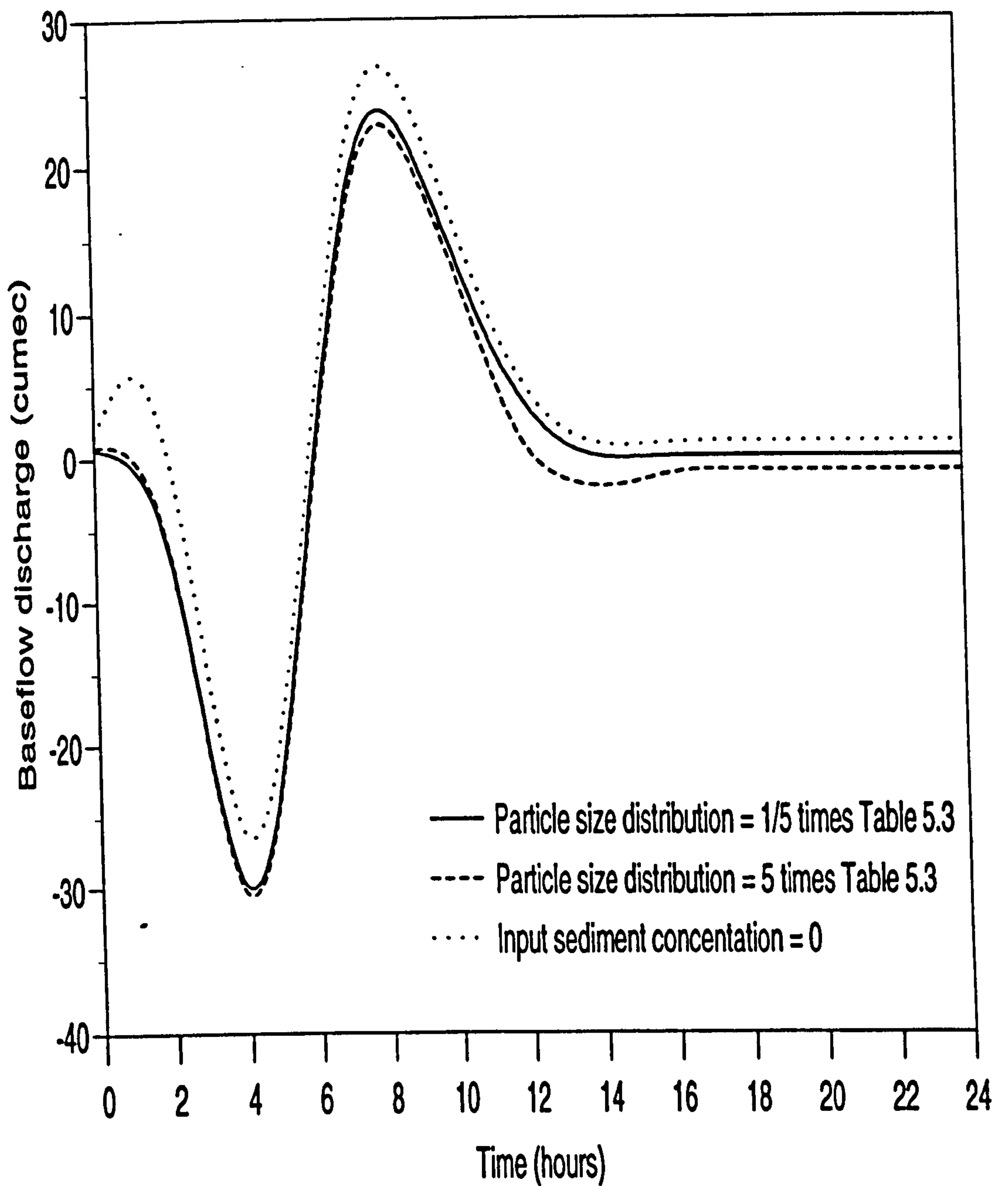


**Fig. 6.3b Baseflow hydrographs at downstream station for varied particle size distribution of input sediments**

In addition to the above expressions, one needs to understand the difference between a gaining river and a losing river, or rather, a drainage and an irrigation canal. The main difference between the two channels is the position of the water level in the channel in relation to the water table elevation in the surrounding aquifer. The water level in the channel is related directly to the bed elevation, which in turn can be altered by sediment transport/storage in the channel. Non-uniformity in sediment transport, in real-world, is caused by natural stresses such as droughts, or land-use and river engineering changes such as deforestation, dams, mining, etc.

In carrying out these numerical experiments, therefore, it was hypothesised that one of the variables of the input sediment was varied, considering the present dependence of people on river systems (e.g. Pearce, 1994). The numerical experiments (Figures 6.3a and 6.3b) exhibit that the effects of varying the concentration of upstream sediment yield is more transferable to downstream reaches than that of varying the particle size distribution. This means that it would be more sensible to expend more effort concerning possibilities that could cause change in the concentration of upstream sediment yield, than concerns that cause change in the size of upstream sediments. The demonstration is quite in line with what can be expected for practical problems in the field. This is because beyond a certain range of particle size distribution, the flow condition may not be able to transport and spread the sediment input over the channel bed in the reach downstream. And even if sediment transport took place, the large particles may take days or even years before they are delivered in downstream reaches. This means that clogging or alteration of the bed elevation, so as to affect stream-aquifer interaction, is not widespread. In the event of changing the concentration of the input sediment yield, transportation and/or deposition towards downstream is widespread, along with the corresponding stream-aquifer interaction effects. Besides the graphical results depicted above, a sensitivity index is also used to show the influence of sedimentation on baseflow.



### 6.3.3 Sensitivity analysis of baseflow to sediment yield

The purpose of conducting a sensitivity analysis on any hydrologic model is to establish relative sensitivities among respective parameters. This information is useful particularly from the standpoint of determining the accuracy to which individual parameters must be known in order to ensure successful model operation. However, the term influence is also used concurrently because the main aim here is to determine/predict the influence as a result of change of the parameter rather than just knowing the accuracy of the parameters in their status quo. While observing the changing needs by humankind, this information is useful from the viewpoint of determining the accuracy to which individual parameters/variables must be updated in order to ensure reliable model predictions. For the purposes of this study, therefore, the term sensitivity is formally defined as:

*"A measure of how variation in a particular model input parameter is transmitted through and reflected in corresponding variation of the model output"*

Therefore, the influence of a parameter is assessed by defining a sensitivity index,  $X$ , by the root mean square value of the difference between the model output of the parameter and the model output after some variation to the parameter. Mathematically  $X$  is expressed as

$$X = \left[ \sum_{i=1}^n \frac{(Q_i - \check{Q}_i)^2}{n} \right]^{1/2} \quad (11)$$

where  $Q_i$  = simulated output of the prevailing parameter value, at time step  $i$

$\check{Q}_i$  = simulated output after some variation to the parameter at the same time  
step  $i$

$n$  = number of time steps considered.

Thus, by systematically changing individual parameters while keeping the other model inputs constant, the relative influence due to change in each of the system parameters to the model output can be examined by a comparison of the  $X$  values.

In carrying out this sensitivity analysis, an initial model solution was obtained for the parameter values defined by the Pinder and Sauer (1971) model. Parameter sensitivities were then computed with respect to the model's baseflow output, by changing each parameter in question by a factor of 10 while keeping all other parameters at their original values. The results of this analysis are displayed in Table 6.1.

**Table 6.1 Results of sensitivity analysis of the model's baseflow output.**

System parameter being changed	Sensitivity value, $X$
Specific yield of aquifer, $S_y$	13.2
Hydraulic conductivity of aquifer, $K_2$	14.3
Hydraulic conductivity of the streambed, $K_1$	2.3
Concentration of input sediments, $C_s$	12.5
Particle size of input sediments, $D_{50}$	1.6

Table 6.1 shows the relative influence of changes of various system parameters to the model's baseflow output. It is observed that, under these conditions, baseflow is most sensitive to changes in  $S_y$ ,  $K_2$ , and  $C_s$ . Change of sediment particle size distribution had the least effect on the baseflow hydrographs. The influence due to change in the hydraulic conductivity of the streambed is smaller probably because of the thinness of the layer used in this experiment. However, its influence can still be imagined, noting

that the initial thickness of the bed layer was only 0.1 m, compared to that of the aquifer of at least 27 m.

The results have brought to light the sensitivity of baseflow to sedimentation effects. They have quantified the effects, showing that the influence due to variation of sediment concentration is about 8 times that due to variation of particle size distribution. Given the transient nature of sediment transport/storage in alluvial rivers (Schumm, 1969; Simons, 1979; Walling, 1983 and Pickup, 1988), the results confirm the need for more efforts in monitoring sediment yields, and reflection of their influence in streamflow modelling.

## **6.4 Evaluation of Riverine Land Degradation and Conservation Applications**

### **6.4.1 Introduction**

An application of the MASAI concept which particularly lends itself to the solution of practical problems is the evaluation of soil and water conservation on riverine plains. Considering that baseflow hydrographs (which are themselves indicators of the rate of groundwater depletion) are influenced by sedimentation transport/storage (e.g. Figure 6.3a), their characteristics can thus be applied, in conjunction with the MASAI concepts, to evaluate the impacts of certain soil and water conservation/harvesting practices.

How land use affects streamflow can be visualised by recalling that streamflow is a product of water moving over and through the land system. Generally, as the water flows over and through the land systems into channels, it exerts a tractive force on the soil surface. If this drag force is sufficiently large, soil particles are dislodged and



transported along with the water. These processes of soil and water transportation are retarded by the presence of grass, weeds, trees, discontinuous slopes and other obstacles in the water-ways.

However, when the land is brought under cultivation, deforestation is carried out, water-ways and river channels are trained, etc., the soil mass is thus exposed to the abrasive action and accelerated soil and water losses may take place on both the land surface and in the channels (Hyrni, 1986). Other factors which change the nature of soil and water equilibrium include urbanisation, quarrying operations, road construction, dam construction, etc. The quantity of fertile soil lost in this way is very large, leading to land degradation effects such as reduced productivity of the land, undesirable deposition of the eroded material, increase in the frequency of flooding in the choked channels, depletion of groundwater reserves in scoured channels, etc.

Several soil and water conservation measures have been proposed to check on the losses, depending on the type and extent of the damage. The cultural (or biological) methods of soil and water conservation include crop rotation, mulching, tree planting, land terracing, etc. On the other hand gully erosion, river channel degradation and groundwater mining have been mitigated by constructing check dam grade controls across waterways to retard the hydraulic and/or fluvial flows (Troeh et al, 1980 and Goldman et al, 1986). The grade controls also ensure maintenance of certain higher river stages, which provide corresponding higher hydraulic gradients to support seepage fluxes necessary for recharging the groundwater reserves.

Streamflow and sediment discharges in their various aspects are recognised criteria of the watershed condition, and also of the effectiveness of the watershed management. Total yearly amounts of both water and sediment discharges, seasonal regularity, and frequencies and extremes of high and low discharges provide useful indications of the net result of conservation projects. On alluvial stream-aquifer systems, therefore,

analysis of baseflow and sediment discharges, which are themselves strongly dependent on the water condition in the river and the surrounding aquifer, and on sediment transport and storage, can provide a basis for predicting the hydrologic impacts of the management practices on the system. Two field examples closely connected with water and sediment yield/storage are presented below in a way to illustrate how simulations by the MASAI can be applied for evaluating riverine land degradation and conservation practices.

#### **6.4.2 Simulation of the effects of sediment yield on baseflow recession**

Variation of either water runoff or sediment yield from upstream reaches in turn affects the concentration or size distribution of the total sediment load delivered into downstream reaches. And whenever the sediment concentration or size gradation into a given reach amounts to less than its transport capacity, the channel scours, whereas when the incoming load is greater than its transport capacity, the channel bed fills. The Danube River (chapter 2), has provided a good example illustrating the problem of varying sediment yield in river systems.

Simulation by the MASAI code is able to track down the evolution/depletion of the time-dependant river-bed conditions due to sedimentation processes, along with its influence on the baseflow hydrograph. However, in this study only the transient growth and/or regression of the bed thickness and variation of the bed slope profiles are tracked down in the simulations. The other boundary parameters (hydraulic conductivity and Manning's roughness), which have also been identified to be influential to baseflow, have not been included in the simulations, but it is possible to correlate them as functions of the depth of alluvial accumulation, or amount of discharge (Sharp, 1977 and Alam and Kennedy, 1969).

Baseflow recession curves have been generated here to show the influence of river bed sedimentation on the rate of groundwater depletion from neighbouring aquifers. The theoretical hydrologic system employed in section 6.2 is used. In this case, an inflow hydrograph was routed through the system, maintaining a flood flow of 500 m<sup>3</sup>/s for three days in order to acquire steady conditions, and then suddenly reduced the flood flow to a baseflow of 200 m<sup>3</sup>/s, where it remained throughout the experiment. By modelling the system responses under these particular conditions it was possible to isolate and study the behaviour of baseflow recession curves at any desired location. Results illustrated by the curves in Figures 6.4a and 6.4b are for the downstream boundary section of the system, and are typical of those obtained using a variety of system characteristic values, save for the levels and rates of the recession which vary with every characteristic in question. It is also interesting to notice that although different sedimentation parameters of pseudo-equilibrium channels produced different rates of baseflow recession curve, Figure 6.4a, they at least demonstrate that the simulated baseflow recession curves, which in these analyses involved channel sediment routing effects as well, in a way conform to the theoretical exponential relationship given by Eq. 6.1, (i.e., their plot on semi-logarithmic paper produces more-or-less straight lines of negative gradients). By assuming a hydraulic conductivity of zero for the river bottom means that baseflow is precluded and only channel flow and storage are considered. In this particular set-up, the effects of channel storage at the downstream station was observed to persist for about 10 hours (the time elapsed since the flood flow of 500 m<sup>3</sup>/s was reduced to the baseflow of 200 m<sup>3</sup>/s).

The first set of results, Figure 6.4a, was obtained by holding the upstream input sediment concentration at 5000 ppm, while varying the hydraulic conductivity of the river bed (which is a function of sediment particle size) between zero and 0.0001 m/s. In the second experiment (Figure 6.4b), the hydraulic conductivity of input sediments



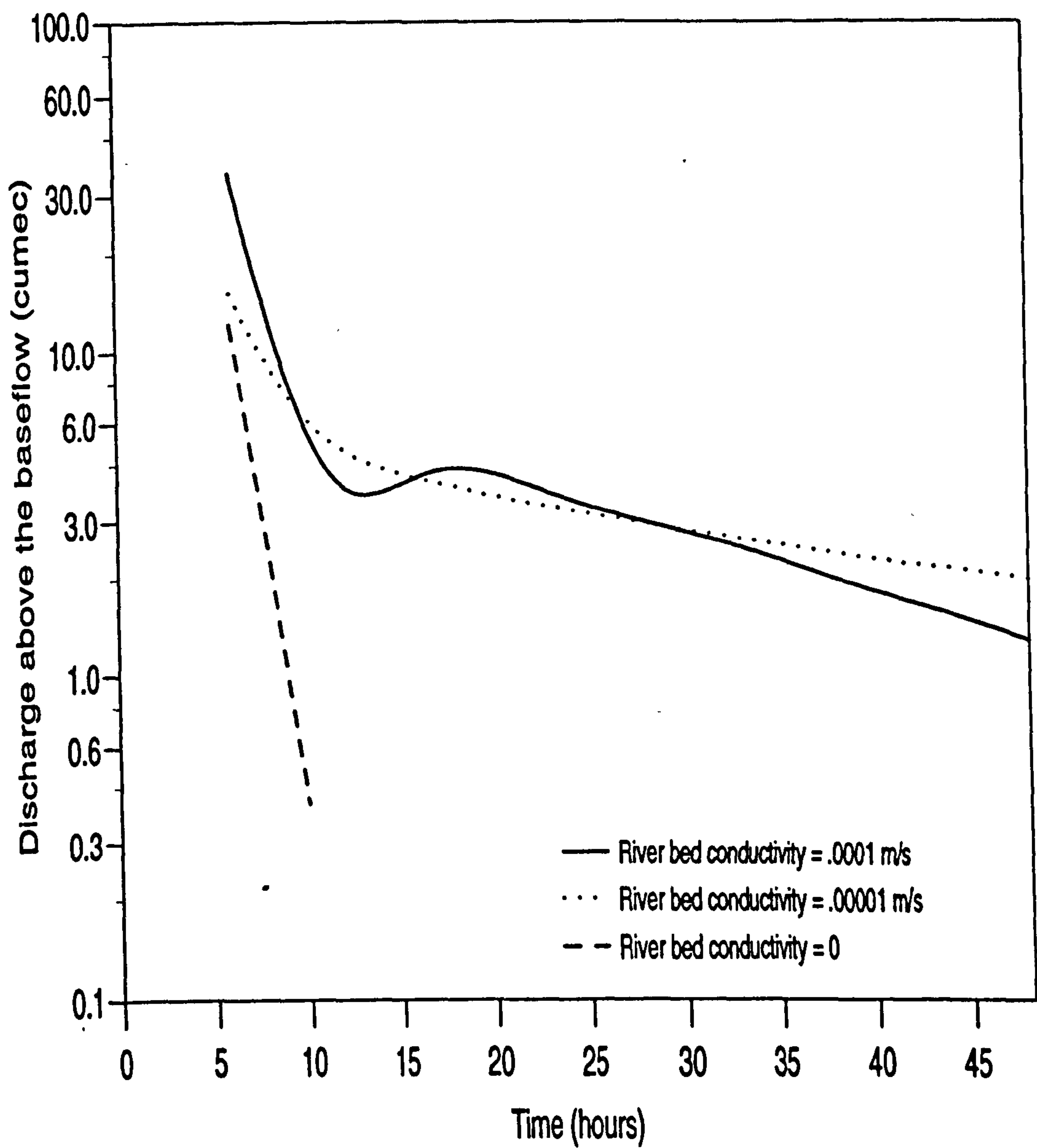


**Fig. 6.4a Baseflow recession curves resulting from variation of the hydraulic conductivity of the river bed**

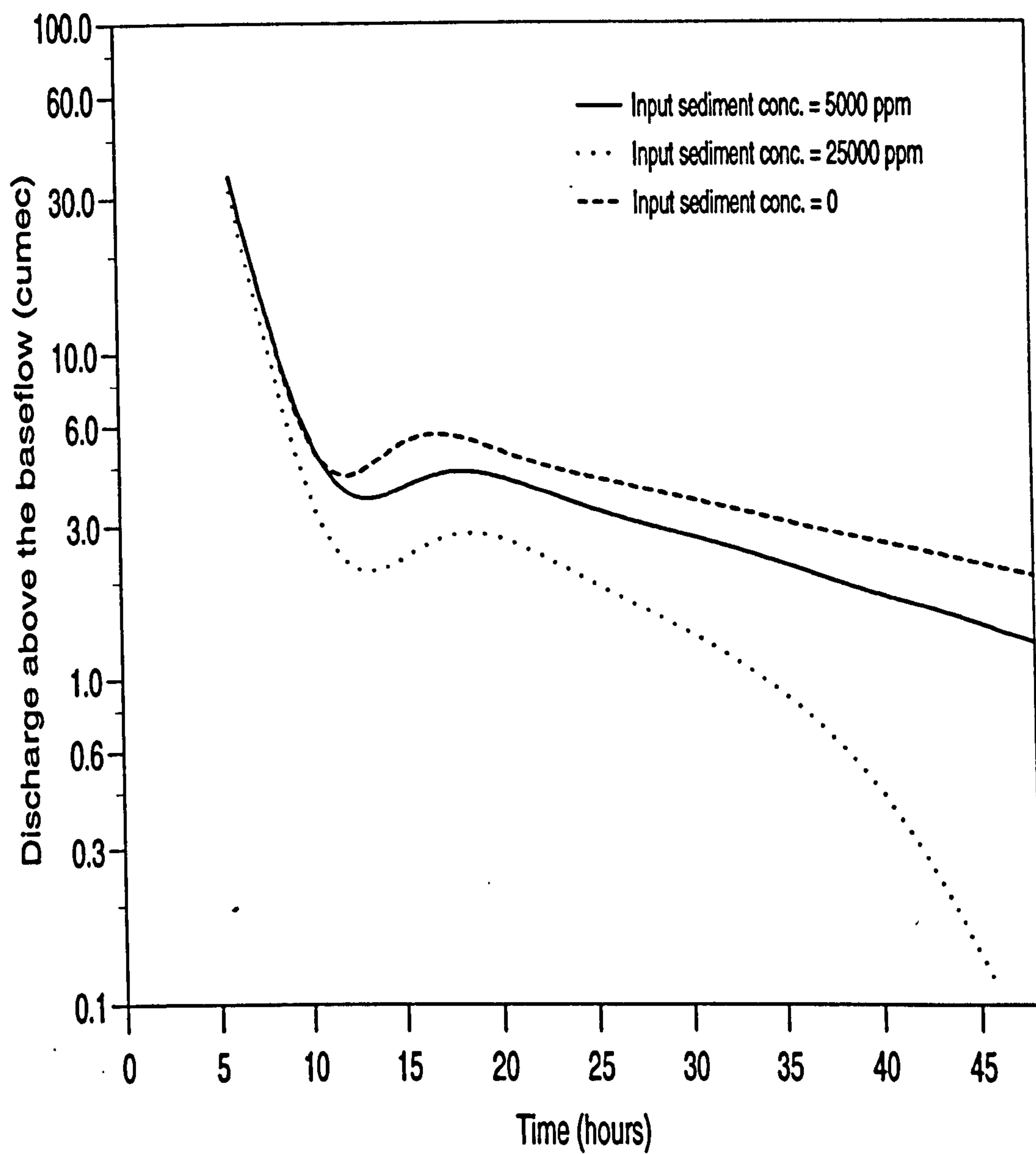


**Fig. 6.4b Baseflow recession curves resulting from variation of the input sediment load**

was held at 0.0001 m/s, while the concentration of input sediments was varied between zero and 25000 ppm.

To interpret the nature of these relationships it is necessary to recall both Eq. 4.54 describing the mechanism of the stream-aquifer water interchange, and the results of the comparative study (Figure 6.2c), where it was demonstrated that the magnitude, timing and duration of the baseflow hydrographs are affected by seepage resistance (hydraulic conductivity) of the river bed sediment layer, besides other aquifer and channel properties. In Figure 6.3a, it was also shown that the baseflow hydrograph resulting from input of lower sediment concentration had a higher peak of baseflow. This can be visualised by relating the proportionality of the thickness of the sediment deposit to the seepage resistance across the deposit. The relationship is such that the lower the concentration of the input sediment discharge, the lower the rate of deposition on the bed, hence the lower the resistance to seepage flow. This results higher rates of seepage. If the concentration is low enough for erosion to take place, and lower the river level, then the hydraulic gradient is tilted even further, to promote more water loss from the aquifer into the river.

It is this same phenomenon of seepage resistance by the interface boundary layer between the stream and the aquifer that causes the variation of baseflow recession curves in Figures 6.4a and 6.4b. In the presentations, the baseflow discharges are plotted against the time elapsed since the upstream flood flow was suddenly reduced from 500 to 200 m<sup>3</sup>/s. For instance, with the hydraulic conductivity of 0.00001 m/s (Figure 6.4a), the baseflow recession is dissipated more slowly because of the increased resistance across the interface sediment layer. Groundwater depletion (baseflow recession) is most clearly observed after the channel storage effects, i.e., after the 10th. hour. The slight rise in the recession curves after about 15 hours indicate the time when the maximum baseflow contribution from bank storage arrived at the downstream station, coming after the channel storage had ceased around the



10th hour. Therefore, the trough at around the 12th. hour shows the time when the downstream section began receiving appreciable amounts of bank storage, which rises to a maximum during the 15th. hour before beginning to diminish again. The baseflow recession curve for zero hydraulic conductivity disappears in the 10th hour because there is no bank storage contribution to sustain the river after the channel storage has passed.

Because seepage resistance increases proportionally with the thickness of the sediment layer, then as the thickness is increased by deposition, the resistance to the stream-aquifer water exchange is also increased. The simulation results in Figure 6.4b provide more insights into the interrelationship between baseflow recession curves and sediment yield, whose capacity is varied through the input sediment concentration. It is demonstrated that, with higher bed load input, less groundwater is depleted because of faster build-up of the seepage resistance by the evolving streambed layer. Increasing sediment concentration correspondingly increases the rate of evolution of the streambed layer, which induces not only the seepage resistance, but also the hydraulic gradient against baseflow into the river. That is why the baseflow contribution decreases with increasing concentration of the sediment yield into the reach. It is also worthwhile to notice the revelation by the simulation results, which demonstrate that beyond certain levels of sediment yield input, the baseflow recession curve does not conform to the idealised recession curve relationship given by Eq. 6.1.

Singh (1968), demonstrated similar findings for a river that was continuously losing water into adjacent aquifers. He did analytical studies on the effect of aquifer leakage (as a result of high groundwater withdrawal, evaporation or deep percolation leakage) conditions, whereby the traversing river may become more and more influent, resulting in baseflow recession curves that are steeply deviating from the theoretical exponential relationship described by Eq. 6.1. Here, it is as a result of river bed evolution, which correspondingly increases the hydraulic gradient towards the aquifer,

making the river to become more and more influent, and therefore presents the same feature of steeply deviating recession curve from the theoretical exponential relationship. Problems associated with this type of change of streamflow hydrology include development of waterlogged conditions, declining streamflow discharge in downstream reaches, etc.

Singh also produced results for an aquifer that was gaining more water from other sources (like high precipitation, infiltration from irrigation canals, etc.), which demonstrated that baseflow recession curves deviated from the theoretical exponential relationship by becoming flatter and the river becoming more and more effluent. With the assumed model conditions the extent of bed scour was not well pronounced, and so the flattening deviation is also not large enough to be noticed. Nevertheless, though small, the deviation is suggested. By bringing in Singh's argument, it can be explained that, in the case of river bed degradation, the river stage is lowered and the hydraulic gradient is tilted towards the river. The baseflow recession curve will thus deviate from the idealised exponential relationship, but this time becoming flatter as the river becomes more and more effluent. Problems associated with this type of change of streamflow hydrology include, excessive drainage of adjacent groundwater reserves, instability of river banks and neighbouring infrastructure, etc.

This analysis of the impact on baseflow by channel sedimentation changes, in fact, can be regarded as a complement to the contributions by Todd (1955), Singh (1968) and Cunningham and Sinclair (1979); in that while Todd (1955) demonstrated how the amplitude and period of duration of a flood wave affect baseflow recession, Singh (1968) demonstrated how channel entrenchment, aquifer recharge and leakage affect baseflow recession, and Cunningham (1979) related and demonstrated how the aquifer parameters of hydraulic conductivity and specific yield affect baseflow recession. In this study, it has been demonstrated that variation of sediment transport/storage affect baseflow hydrographs (Figure 6.3a).

Other studies which have related the condition of streambed to stream-aquifer water exchange include those of Younger (1990), Novak (1991); Pearce (1994), among others. Therefore, in this study an approach has been developed whereby knowing the impending development changes on alluvial river systems, together with the knowledge of the development-sediment yield relationship, the impacts of the developments to the baseflow (hydrologic) behaviour of the river system can be analysed.

For example, in watershed management it is believed that deforestation, over-cultivation and over-grazing are among the primary causes of soil erosion in upstream watersheds and increased sediment delivery in downstream reaches, presumably leading to aridity (Grainger, 1990). Nonetheless, from the above analysis demonstrating the influence of sediment delivery on baseflow, it can also be conjectured that rivers from highly eroding watersheds may have diminishing streamflow discharges due to in-stream aggradation which consequently induce the river to become more and more influent. If this water leaving the influent streams is lost through evaporation, deep percolation, etc., then the net amount of discharge arriving in downstream reaches will be reduced. It also seems that this is the principle upon which groundwater recharge by grade control weirs or check-dams is based. That is, the check-dams cause upstream river stage to rise and bed elevation to aggrade due to sedimentation, promoting the river in the reach to become more influent (recharging) while downstream reaches may receive diminishing streamflow discharges.

This is to say that hydrological responses due to in-stream aggradation can be positive or negative. The responses are resourceful when it is desirable to recharge groundwater in upstream reaches and/or mitigate flooding problems in downstream reaches. They are destructive when the upstream recharge is in excess, causing



waterlogging and/or depriving downstream reaches of acceptable minimum discharge amounts.

Impacts emanating from sedimentation are slow, taking several months or years to be noticed. However, that is why mathematical modelling has developed and proven its worth, by enabling such problems to be simulated and analysed so that the insights of the processes involved can be gained in a matter of minutes over a desk-top. These processes would otherwise require a lot of time and resources to be observed in the field, during which period the associated damage may already have been done.

Although it has been assumed in this modelling that sediment transport and storage in river channels can be reasonably estimated, nevertheless, this does not mean that the writer is underrating the scarcity and uncertainty of such data for simulation of real-world problems. The problem of uncertainty concerning sediment yield from upstream catchments and delivery in channels, especially in tropical regions like Africa is widespread (Walling, 1988), probably because of high variability in catchment and land use changes. The impacts of such high and variable sediment yields on river engineering systems and streamflow hydrology could be devastating, leading Petersen (1993) to remind water resources developers and researchers that African hydrology needs redress with special attention to the sedimentation problem. Considering the scarcity and uncertainty of data for calibration of models dealing with sedimentation processes, it is noted here that the variation of the streambed condition need not be estimated by such dynamic sediment routing procedures alone, but any method which can describe the variation of the bed levels in time and space can be applied.

In addition to the streambed adjustments, incorporation of a sense of practicability may be required so as to account for other side effects arising from such variations. The corresponding factors to consider include: consolidation, sediment infiltration,

quick-sand effect, sediment size distribution, human influence, etc. In fact, because it seems that uncertainty in data provision and process description for sedimentation is likely to continue, hybrid modelling involving a stochastic component may be appropriate.

#### **6.4.3 Simulation of the hydrological and fluvial impacts due to in-stream sand mining schemes**

It has already been stated that river sand and gravel for construction purposes are among the many resources obtained from alluvial river systems. Normally, the source of river sand is not necessarily of the geological formation of the area at which the quarry is located. Rather, it is in the upstream catchment areas from where the soil sediments are yielded and transported by streamflow, only to be deposited in the quarry area as a result of limitations in sediment transport capacity. Therefore, it is desirable that the excavation rates do not exceed the delivery rates, so as to avoid continuous falling elevation levels of the river bed, river stage and water table of the surrounding aquifer. But because it is difficult to balance human-made development demands with the hydrologically driven sand deliveries, and because of high costs and difficult conditions of transporting the sand, circumstances may lead to intensive use of quarries dug in alluvial rivers close to sites of road bridges nearer to the developments. This can lead to excavations of depths, spatial extension or numbers of in-stream quarry pits that exceed the balance necessary for the dynamic equilibrium of the water and sediment yield/storage of an area. In the long run, in order to restore the dynamic equilibrium, the conditions so induced by the quarries may adjust their surrounding bed and water levels with significant impacts on the environment as they affect the flood levels, sediment yield, erosion of adjacent land and infrastructure, depletion of groundwater, and so on.

A good understanding is needed to show how these impacts are related, as they normally occur concurrently in river channels with disturbances of this nature. For the purpose of river resources management, it is necessary to determine the amount of both water and sediment yields as affected by the sand mining. The yields may be obtained by integrating the rates of the baseflow discharges and sediment transport over the time period, if the rates can be evaluated. These sediment materials and groundwater discharges are affected by channel storage associated with river channel changes, and such storage changes are significant in the presence of in-stream sand quarries. While sediment is stored in the quarry pit, it will also be depleted during headward and downstream erosion. Groundwater depletion, more commonly, is accelerated because of the increased hydraulic head towards the streamflow in the quarry pits.

While in-stream quarrying appears to be a necessary practice of harvesting a natural resource from rivers, of late it is also being appreciated that there is a need for sustainable utilisation of the available resources as well. This has prompted the need for more data to depict the resource exploitation rates, which are required to form the base for accounting for optimal allocation of the resources between the environment and other development needs. Unfortunately, these data are not readily available.

In chapter three, an example showing some of the problems emanating from sand mining on the River Kibos in Kenya was described, together with the possible solution of the problems. Otherwise, disturbances resulting from such excavations do not have clear-cut solutions, because responses to the solutions may pose yet other uncertainties. In such cases it is preferable to evaluate all possible solutions before selecting the most optimal one.

In postulating about degradation by in-stream quarrying, it is the quantitative analysis of the interaction between the quarries and the underlying unconfined aquifer that has



been sought. This is so that groundwater recharge and sediment yield in the reach having the mining schemes can be evaluated. With water and sediment distribution being the major controlling factors of the riparian life, the model results can also be applied to conjecture about the responses of ecosystems to the quarrying interventions. The use of such a relatively sophisticated prediction tool is warranted by the widespread concern for any project involving a modification, however small, of the environment and by the consequent need for providing engineering evaluations that are at the same time transparent and scientifically sound.

In this analysis, a conceptual hydrologic system is modelled based on the hydrogeology of the Kibos flood plain. It consists of a flood plain aquifer which extends 10 km along the length of the channel, from upstream section 1 to downstream section 11, so that the distance between sections is 1 km and the width is 1.5 km across the plain. The hydraulic conductivity of the aquifer (assumed homogeneous and isotropic) is 0.001 m/s and the average initial saturated thickness is 75 m. The stream flows through a rectangular channel with constant cross-section and initial bed-slope of 0.0007. The hydraulic conductivity of the streambed is 0.004 m/s. The channel is 10 m wide, the initial depth of flow is 1.85 m and the Manning's  $n$  is 0.03. A quarry pit is superimposed on the system so that the hydrological responses can be studied in terms of its effects to the passage of a sediment laden flood wave. That is, in one routing the channel is assumed to have the constant bed slope of 0.0007, and in the other routing the profile of the bed is considered to have the quarry excavation. A comparison of the simulations for sediment and groundwater yields at the same point in space and time indicate the effects of the quarry system on the hydrologic regime. The flood discharge studied has the following characteristics: initial flow is 20 m<sup>3</sup>/s, peak flow is 35 m<sup>3</sup>/s, and the flood wave is sinusoidal and the time base is one week.

Prior to performing the simulations, a set of possible realistic solutions is defined first, assuming the miners have the freedom of choice to lengthen, deepen or multiply the number of quarries in a given reach. The hydrologic performance is then assessed as a function of the envisaged length, depth, or number of quarries. The general set-up of the profile of a channel reach with a superimposed quarry in the reach between distances 5 and 9 km from upstream, is depicted by the initial bed elevation profile given in Figure 6.5, in which water and bed elevation variation with time as a result of passing the sediment laden flood wave for one week is presented.

By systematically changing one of the three variables, while keeping the others constant, the relative influence due to each of the variables on the hydrologic and fluvial responses can be studied by comparing the water and sediment yields. In particular, the performance of the following scheme settings are analysed:

1. Varying the length of the quarry, as 2, 4, or 6 km long in order to evaluate the effect of length.
2. Varying the depth of the quarry as 0.5, 1.0, or 1.5 m in order to evaluate the effect of depth.
3. Varying the number of the quarry pits (as 1 or 3) in order to evaluate the effect of the number of pits in a given reach.

These dimensions have been deduced based on the observation of in-stream sand mining practices on the River Kibos (chapter 3). Because of the increasing demand for sand, there is a tendency for the mining to be spread towards upstream or downstream of the bridges at Kibos and Nyamasaria shopping centres. And because of the accelerated flows into the sand borrow pit at Kibos, there is erosion taking place at both ends of the pit, thereby continuing to increase the extent of the pit. The depths of the quarries are affected by miners who attempt to increase their rate of supply from confined reaches, like the ones nearer to the road. The MASAI was applied to evaluate the performance of the quarrying schemes, based on yields of sediment and groundwater in a period of one week.

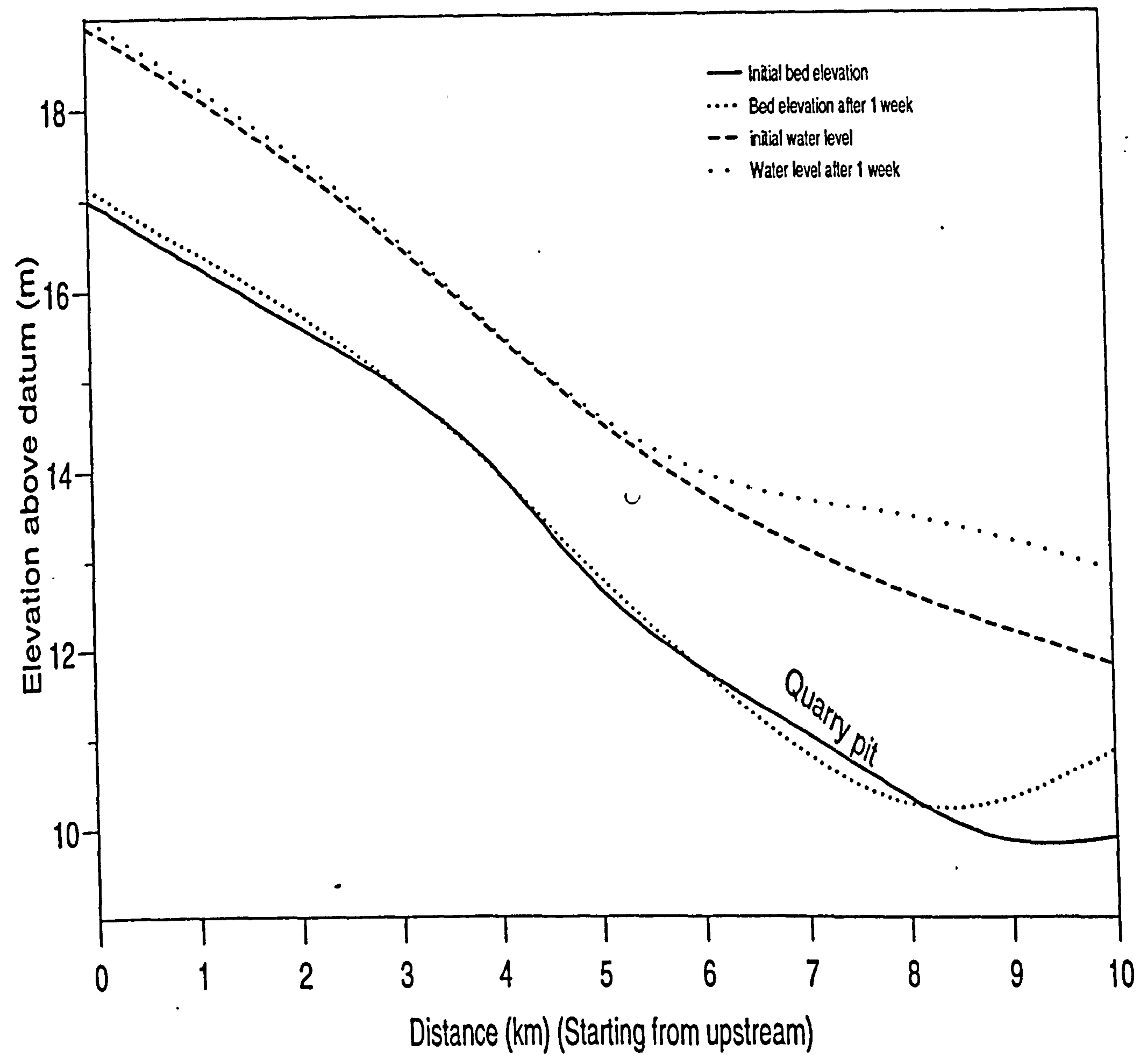


**Fig. 6.5 Predictions of bed and water surface elevations after a flood has passed through a quarry pit**



### *Effects of the Length:*

Simulated results for the sediment yield in the mining area, when the length of the quarry is varied, are given in Figure 6.6a. Sediment yield is hereby defined as the accumulated bulk mass of bed material having passed a given cross section at a given time during the passage of a flood. The spatial variation of sediment yield as simulated is for one week of the discharge passing through the reach, and is closely related to the potential for scour and fill along the study reach.

A decreasing yield in the downstream direction indicates that sediment load is partially stored in the channel. Such sediment storage is associated with fill or aggradation of the channel bed. On the other hand, an increasing trend in the downstream direction means sediment removal from the channel bed, i.e. scour or degradation of the bed. A uniform sediment yield along the channel indicates sediment balance, i.e. dynamic equilibrium.

As shown in Figure 6.6a, considering the quarry set-up in the reach between distances 7 and 9 km from upstream, the spatial distribution of sediment yield is more or less uniform up to a distance 5 km downstream. This distribution indicates that the portion of the study reach is in an approximate state of equilibrium for which the amount of sediment inflow is approximately equal to the amount of sediment outflow. Under this condition, the net scour or fill in the channel bed is negligible.

The notable increases of sediment yield just upstream of and inside the quarry pit, in the reaches between distances 5 and 6.5 km, and 7 and 8.5 km from upstream, respectively, signify net scour as the flow picks up additional material. This means that if the reaches were not rigid, then net scour will take place in the headward direction and within the quarry. At the ends of the quarry, in the reaches between distances 6 and 7 km, and 8.5 and 10 km, the sediment yield curves are decreasing

towards downstream, as the flows refill the pit. This deposition amounts to the bulk mass of sand that is delivered and is available for harvesting. If mining exceeds this rate of delivery, then the quarry floor elevation will fall, and if the mining is less than the rate of delivery, then the pit will be refilled.

The stretch over which the slope of the sediment yield curve is negative (falling towards downstream) signifies the reach where delivery is taking place, and therefore, where sand extraction may take place. The slope of the sediment curves gives the optimal rate of sand harvesting (in kg/week) at the particular section. For example, the amount that can be harvested in one week, from the upstream end of the quarry (in the reach between distances 6 and 7 is about  $(9 - 8) \times 10^3$  1000 kg, and from the downstream end of the quarry in the reach between distances 8.5 and 10 km, is about  $(17-7) \times 10^3$  or 10000 kg.

Apparently, in terms of the amount of the delivered sand, there is no clear advantage of having quarry pits of long length. From Figure 6.6a, the net amount of sand delivered is more or less the same for the three quarries of different length, with the bulk of it accumulating towards the downstream end of the quarry, and a smaller fraction at the upstream end. The only significant difference for the quarry set-ups is the location at which the sediment aggregates are delivered, although most of it is delivered towards the end of the quarry. For instance, for all set-ups, sediment material are deposited in the reach between distances 8.5 and 10 km. In addition, more material are deposited in the reach between distances 6 and 7 km of the quarry located in the reach between distances 7 and 9. For the quarry in the reach between distances 3 and 9 km, more material is deposited in the reach between distances 2 and 3 km.

It is also worthwhile noting that even within the quarries, there may be some locations that are devoid of any sand delivery. Furthermore, the distribution of the scour/fill

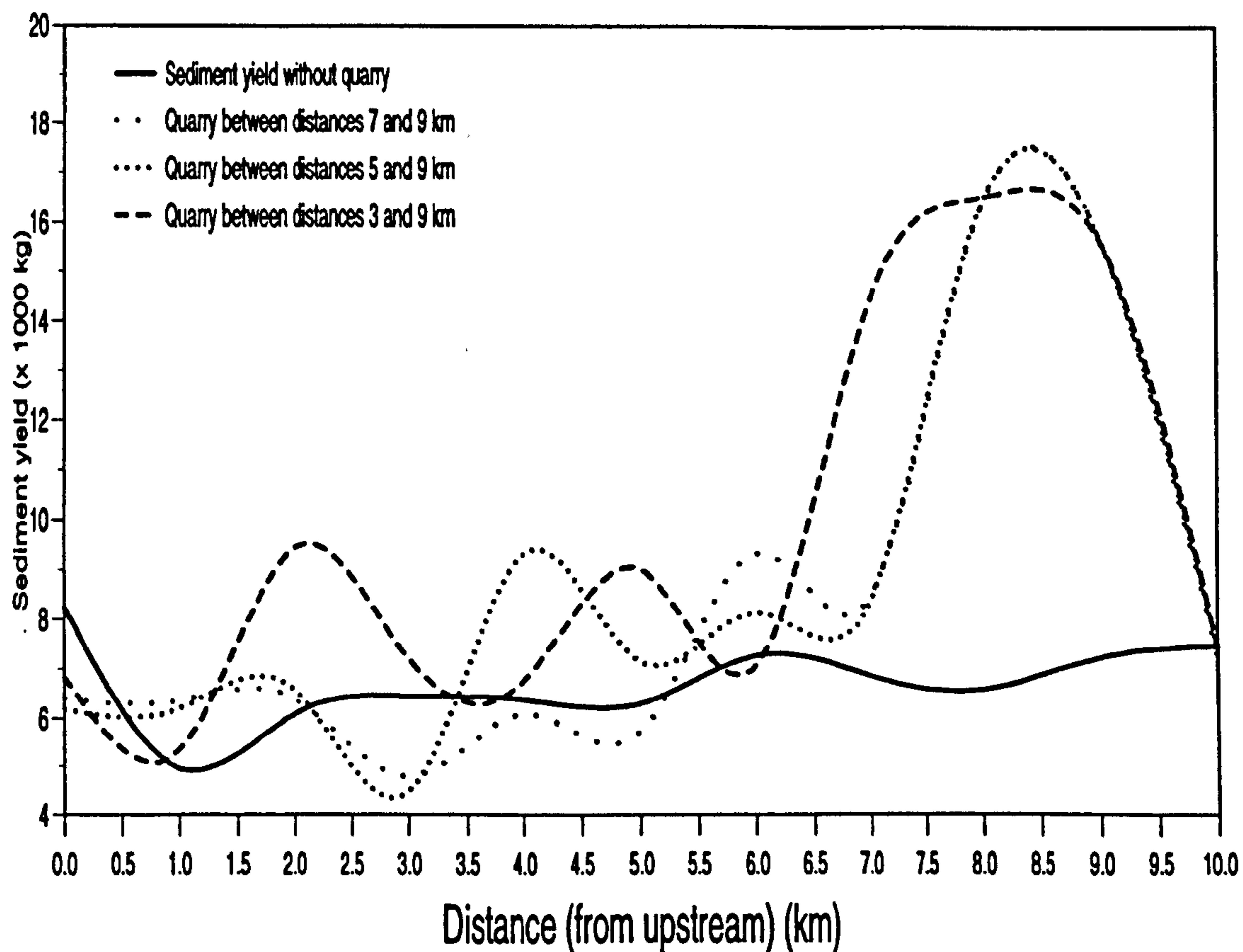


**Fig. 6.6a Cumulative sediment yield of 1 week, along a reach with quarries of varied length. The depth of the quarry is 1m**

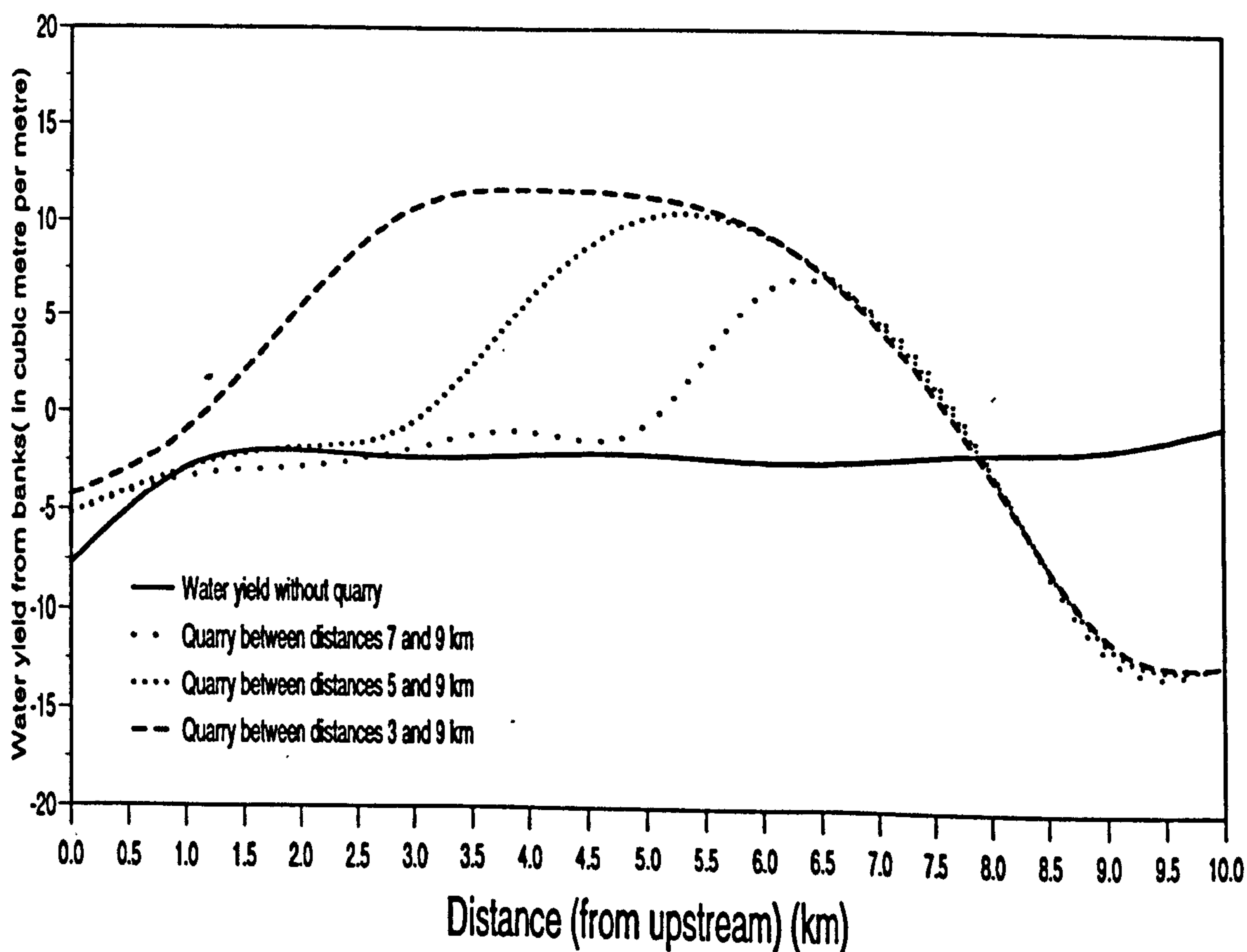


**Fig. 6.6b Water yield after 1 week of bank storage in a reach with quarries of varied length. The depth of the quarry is 1m**



implies that unless the upstream reach of the quarry is stabilised, the distribution of sand harvesting will be varied with time, because the resultant length of the quarry will be extended by scouring.

The sediment yield curve for the reach without sand quarrying is also plotted on the same figure for the purpose of comparing the disturbance to sediment transport/storage as induced by the quarry systems.

The major difference in the performance of quarries of different lengths is in the amount of groundwater mined from the surrounding groundwater reserves. Water yield is hereby defined as the cumulative volume of groundwater depleted from a given reach in the given time (Figure 6.6b). The spatial variation, as simulated, relates to one week of a flood wave through the reach. Positive water yield means net gain of water by the river, and negative yield means net loss of water by the river into the aquifer. The spatial variation of the water yield is therefore closely related to the potential for mining (positive) or recharging (negative) groundwater reserves along the study reach.

Considering the quarry set-up in the reach between distances 7 and 9 km (Figure 6.6b), the spatial distribution of water yield in the reach up to a distance 5 km downstream is more or less the same as for the case without the quarry. This means that the portion of the river is undisturbed and is losing water during the one week period. In the reach between distances 5 and 8 km, the river is disturbed so that there is resultant depletion of groundwater, more than for the river without the quarry. The depletion varies with the distance, rising to a peak of about  $7.5 \text{ m}^3/\text{m}$  (or  $7500 \text{ m}^3/\text{km}$ ) before beginning to fall again. In the reach between distances 8 and 10 km, the river is disturbed such that it is losing more water, with the recharge rising towards downstream, to a maximum of about  $12.5 \text{ m}^3/\text{m}$  or ( $12500 \text{ m}^3/\text{km}$ ) at the downstream section. Accumulation of this amount of groundwater depletion or recharge can affect

the level of the water table (and the river) significantly. The impacts of bank storage depletion on the riverine ecosystems, which are strongly dependent on the water levels, have already been discussed, (e.g. example by Pearce (1994) in chapter 2).

The spatial variation in the amount of water yield along the reach is due to spatial variation of the hydraulic gradient between the river stage and water table. In the reach up to a distance 5 km downstream, due to upstream boundary conditions, the river stage is slightly higher than the surrounding water table, whereby there is a tendency for the river to recharge the groundwater. In the reach up to 5 km downstream, there is no significant difference in the hydraulic heads between the river with or without the quarry. But in the reach between distances 5 and 8 km, the presence of the quarry creates a depression, hence a higher hydraulic gradient towards the river. This increases the drainage rate of groundwater into the river. Towards the downstream end of the quarry, due to river bed aggradation, the river stage is raised, creating a hydraulic gradient that causes the river to recharge the surrounding aquifer. The simulations also demonstrate that the amount of groundwater mined is somewhat proportional to the length of the quarry. The area between the curves of the water yield of a particular set-up and that of the set-up without the quarry gives the net amount of groundwater mined in the corresponding reach as a result of the corresponding quarry. It is observed that if groundwater reservation is a limiting factor in an area, then longer quarries may cause problems because they aggravate depletion of the surrounding groundwater reserves over longer stretches.

#### *Effects of the Depth:*

The responses are different when the depth of the quarry is varied. Although the amount of sediment delivered in the downstream end of the quarry, in the reach

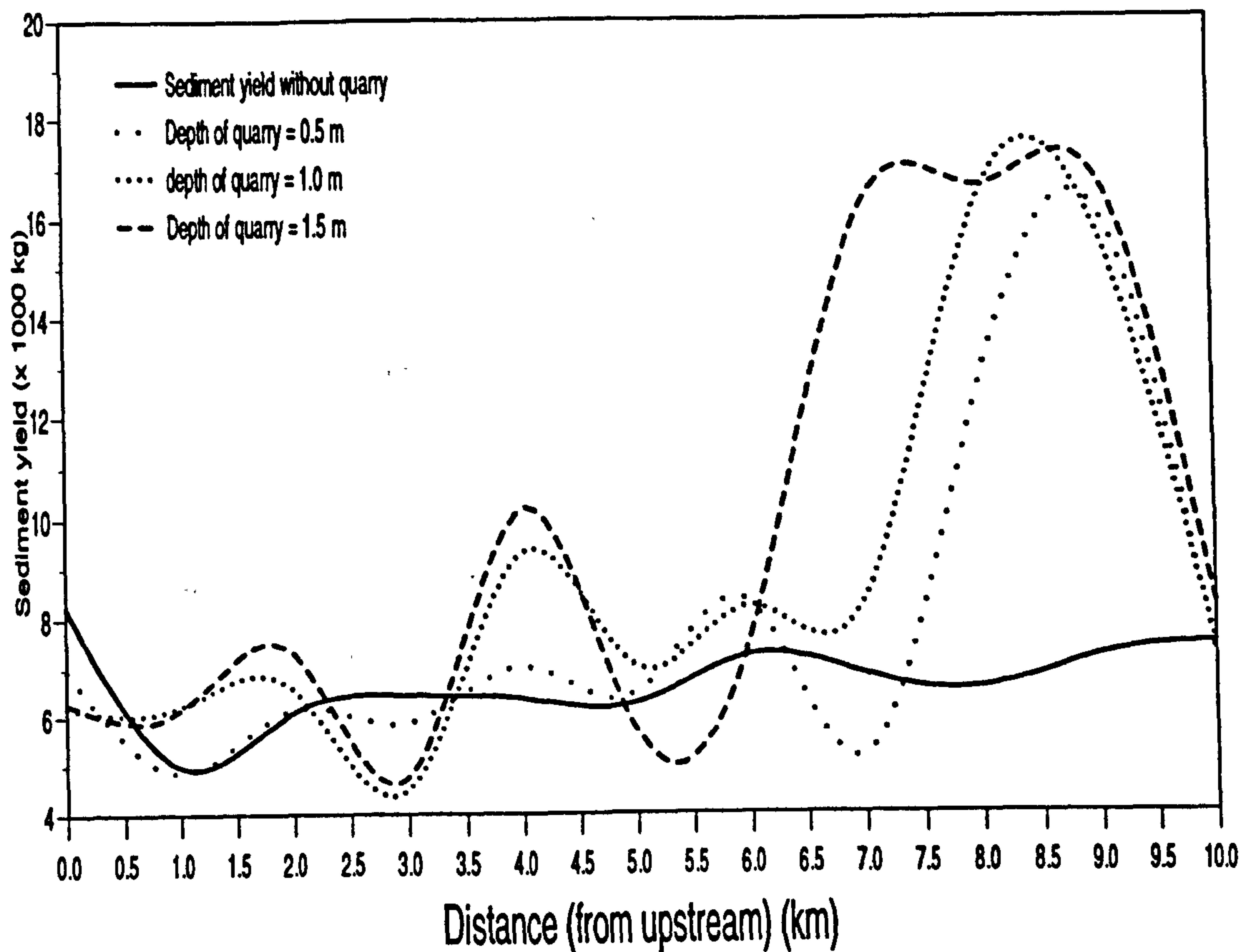


**Fig. 6.7a Cumulative sediment yield of 1 week, in a reach with quarries of varied depth. The quarries are between distances 5 and 9 km from upstream.**

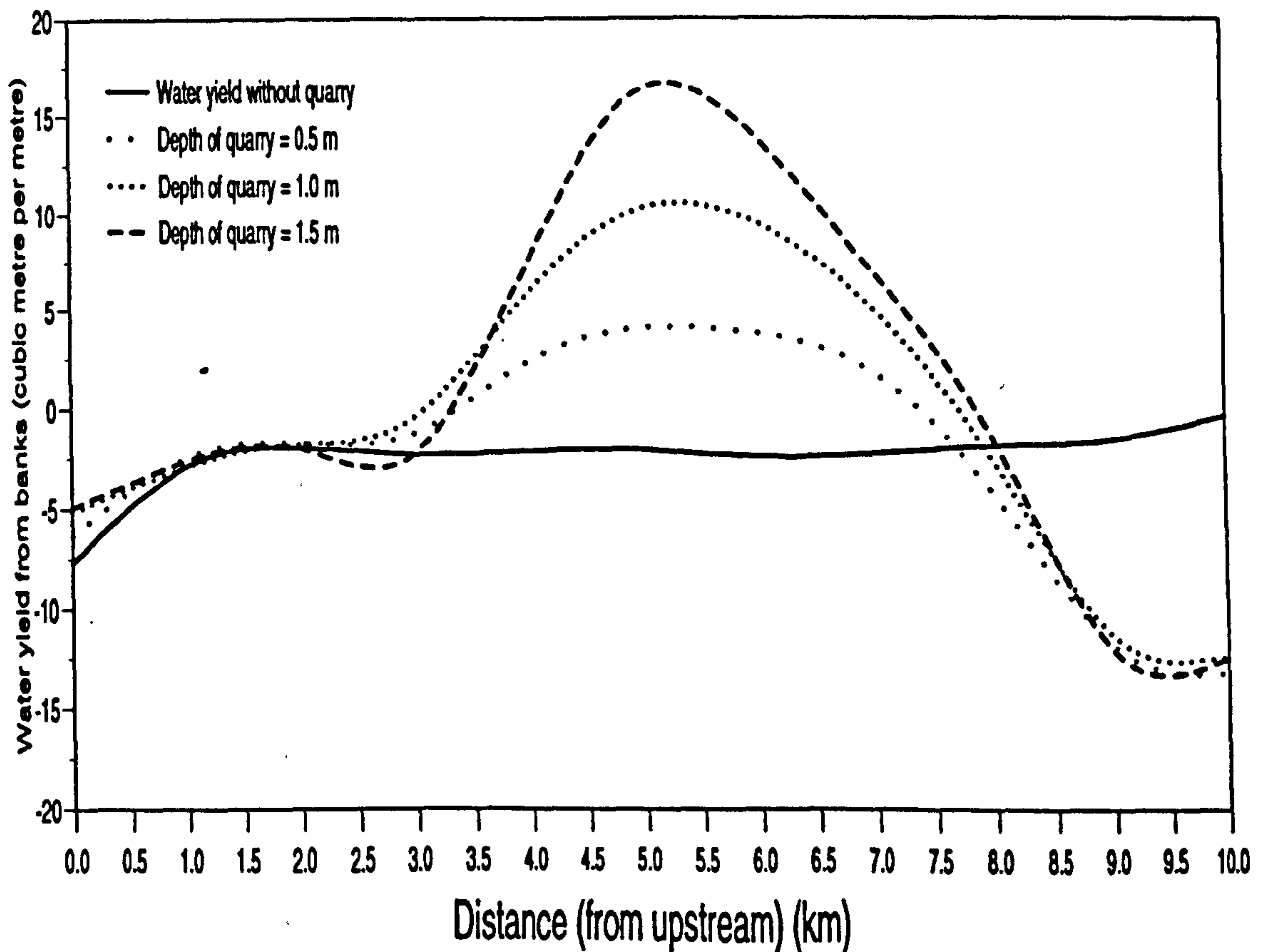


**Fig. 6.7b Water yield after 1 week of bank storage in a reach with quarries of varied depth. The quarries are between distances 5 and 9 km from upstream**



between distances 8.5-10 km, is about the same for the three set-ups, (i.e. 10000 kg), however, the amount of sediment delivered or scoured in the upstream end of the quarry is affected by the depth of the quarry. For example, Figure 6.7a shows that, for all of the quarries having different depths, the amount of sediment delivered in the reach between distances 4 and 5.5 is about 1000 kg for the quarry of depth 0.5. For the quarry of depth of 1.0 m, the amount of sediment material delivered is about 4000 kg, and for the quarry of depth of 1.5 km the delivery is about 5000 kg.

The amount of groundwater mined is again different for the various quarries of different depths. But this time the depths affects the intensity of water depletion, and not the spatial length over which water is mined. Figure 6.7b shows that in all of the three cases, groundwater mining is taking place in the reach between distances 3.5 and 8 km. But with the quarry of a depth of 0.5 m, the maximum amount of water depleted is about 5 m<sup>3</sup>/m, while with the quarry of depth of 1.0 m the maximum amount is about 10 m<sup>3</sup>/m, and with the quarry of depth of 1.5 m the maximum amount depleted is 17 m<sup>3</sup>/m.

Therefore, the simulations show that, if the location of the quarry was a limiting factor, like preferring locations nearer to a bridge, for example, then a deeper quarry may increase the rate of sand delivery, and thus enhance the potential rate of mining. But this is done at the expense of groundwater resources, besides bank stability, because deeper quarries mean more intensive depletion of the groundwater reserves in the vicinity, and severe erosion in the upstream reach of the quarry.

In general, the simulations have shown how in-stream quarrying creates the potential to erode the headward end and floor of the quarry, and depletes groundwater from underlying aquifers. They have specifically demonstrated that the length of the quarry significantly affects the spatial extent of the resulting degradation, whereas the depth

of the quarry affects the intensity of the degradation. In the long run, therefore, the mining can cause detrimental changes to the environment, especially those values related to regional water levels and landscape. These results are in line with the observations noted on the Kibos, and explains why the sand mining practices in the area are tending to degrade the river bed, destroy the riparian vegetation and deplete the surrounding groundwater potential.

#### *Effects of the Number of Quarry Pits:*

From the preceding demonstrations about the effects of length on quarries, it seems that for a given river reach, it may be beneficial to shorten and increase the number of quarries instead of having one long quarry. Having already explained the characteristics of sediment and groundwater yield curves, Figures 6.8a and 6.8b can be easily interpreted. For example, as a result of having three short quarries instead of one in the given reach (Figure 6.8a), it is noted that three distinct locations in the reaches between distances 3 and 4.5 km; 6 and 7 km; and 8.5-10 km, of sediment delivery are established, as opposed to the one having only one long quarry.

Figure 6.8b shows that a substantial amount of groundwater is conserved when three shorter quarries are used instead of one long quarry. The amount of groundwater depleted due to quarrying is given by the integral of the area between the respective water yield curve and the water yield curve for the system without the quarry. If the area is above the curve for the system without the quarry, then the quarry is causing more groundwater depletion, and if the area is below, then the quarry is causing more groundwater recharge. The amount of water conserved as a result of having three instead of one long quarry is depicted by the area between the two respective curves.

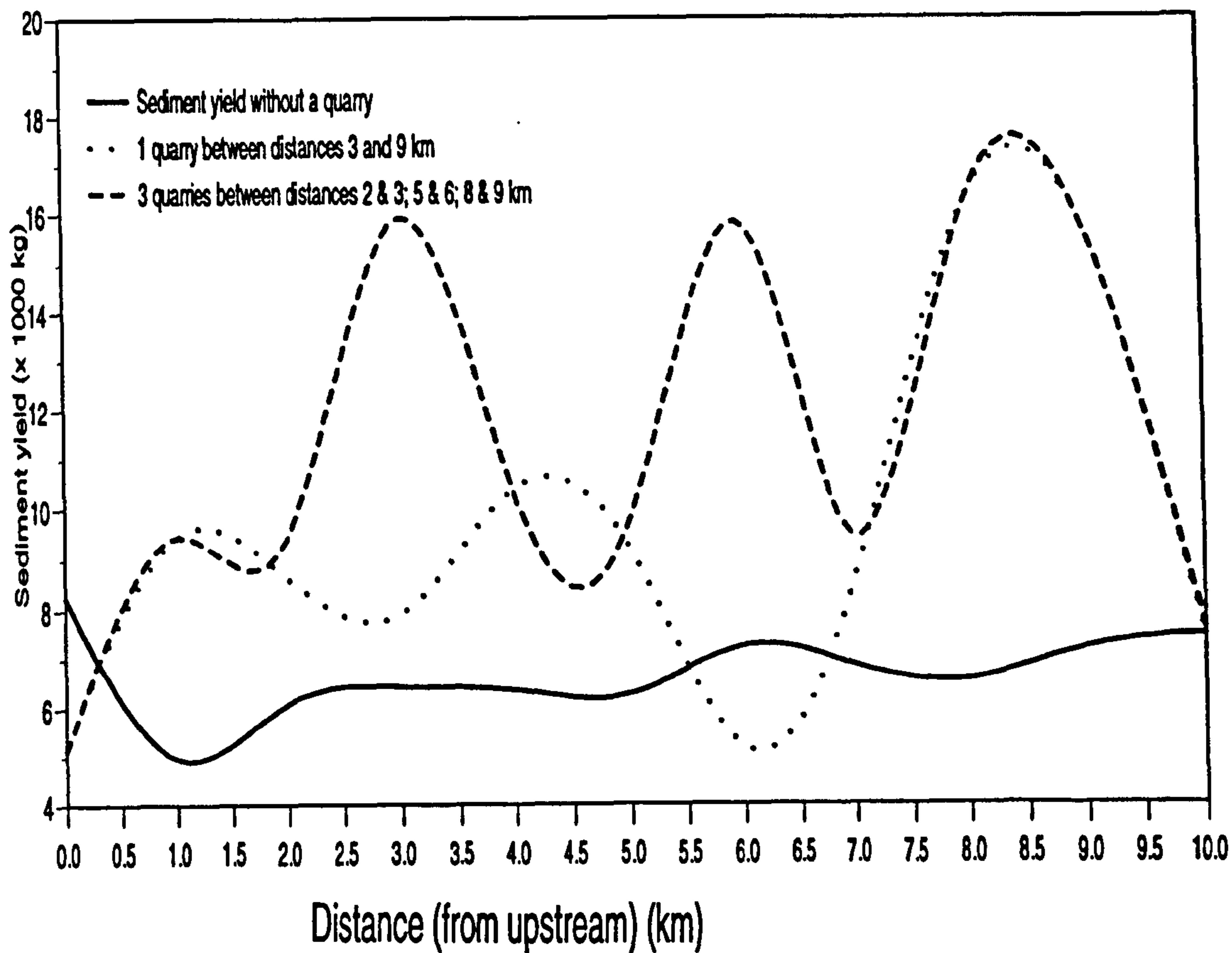


**Fig. 6.8a Cumulative sediment yield of 1 week, in a reach with varied number of quarries. The depth of the quarries is 1m**

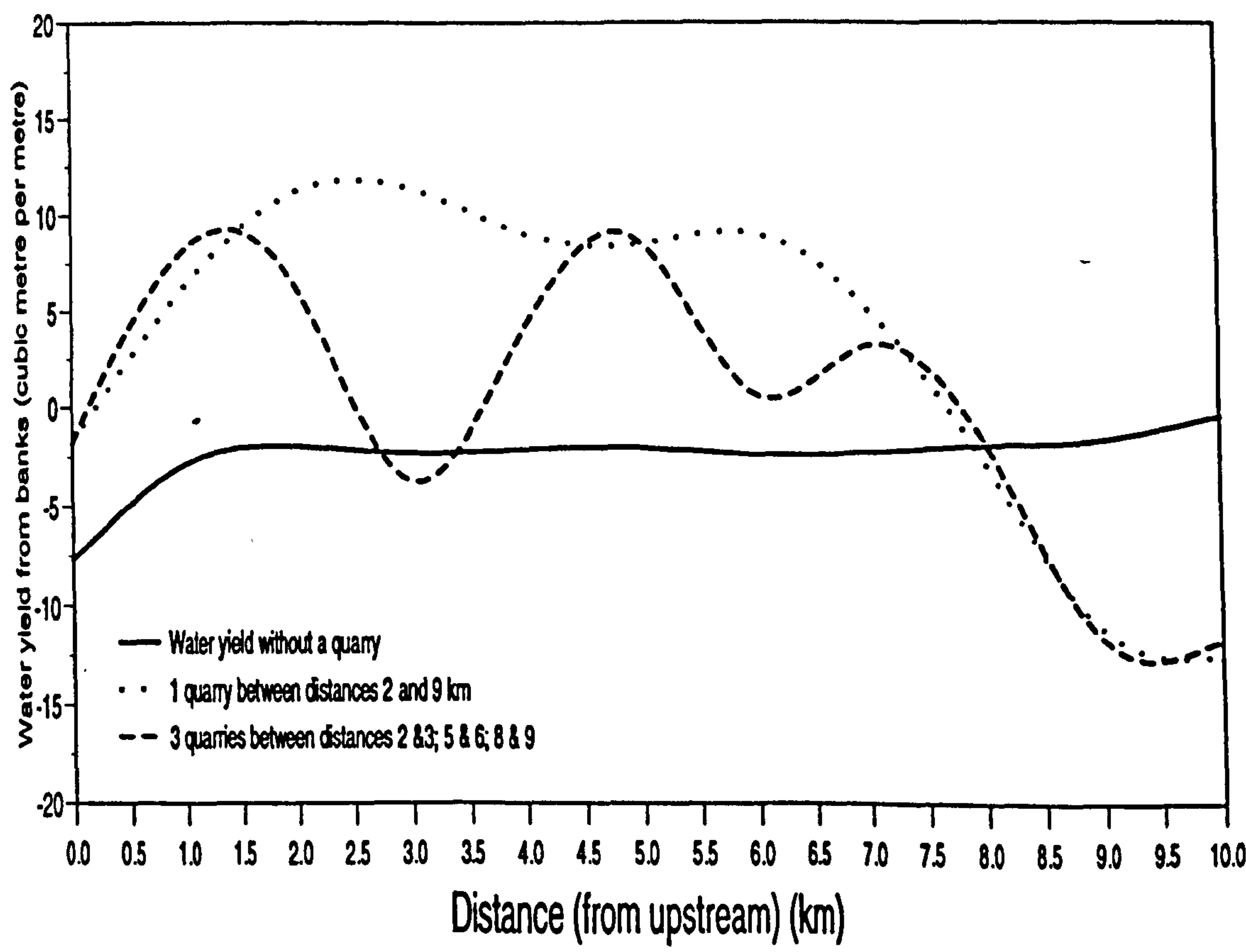


**Fig. 6.8b Water yield of 1 week from bank storage in a reach with varied number of quarries. The depth of the quarries is 1m.**



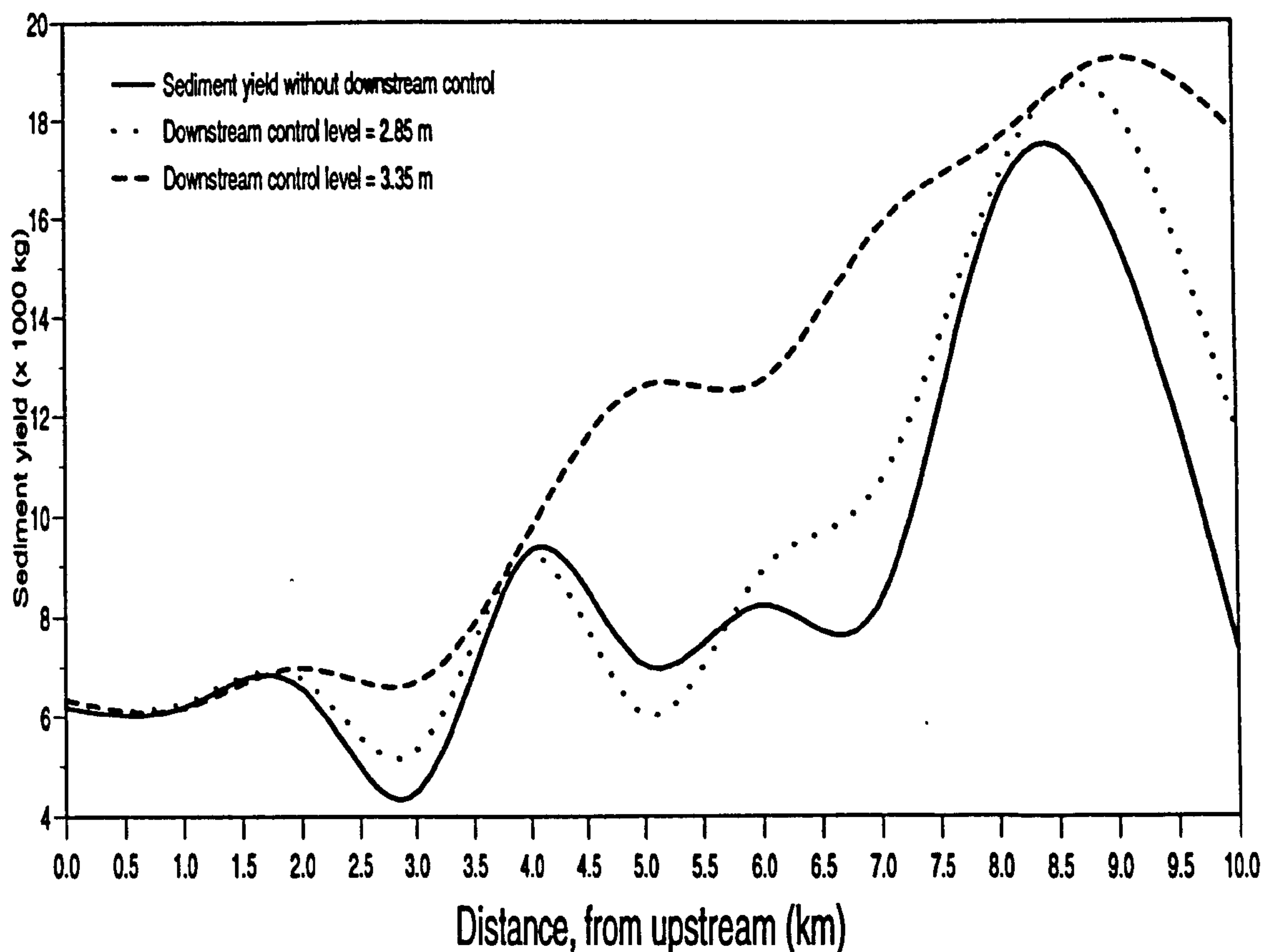
#### 6.4.4 Evaluation of the impacts of weir controls in Soil and Water Conservation practices

Grade controls weirs are normally applied along water-ways for riverine land conservation when it is desirable to promote channel stability/aggradation and groundwater recharging potential, among other things (Medina, 1976; Hofkes, 1983 and Nilson, 1983). In line with that, and for continuity, this example is concerned with the conservation of the degradation effects due to in-stream sand mining practices, as depicted by the previous examples. To demonstrate the mitigation effects of the controls, the river and quarry systems are similarly modelled as in the previous examples, but this time having the additional mitigation intervention of a weir (check-dam) at the downstream station. The quarry is located between distances 5 and 9 km. By making simulations with different mitigation combinations, while observing the trends of both sediment and groundwater yield levels, the effects of soil and water conservation/harvesting schemes can be conceptualised for mitigating the degradation effects of the quarrying system.

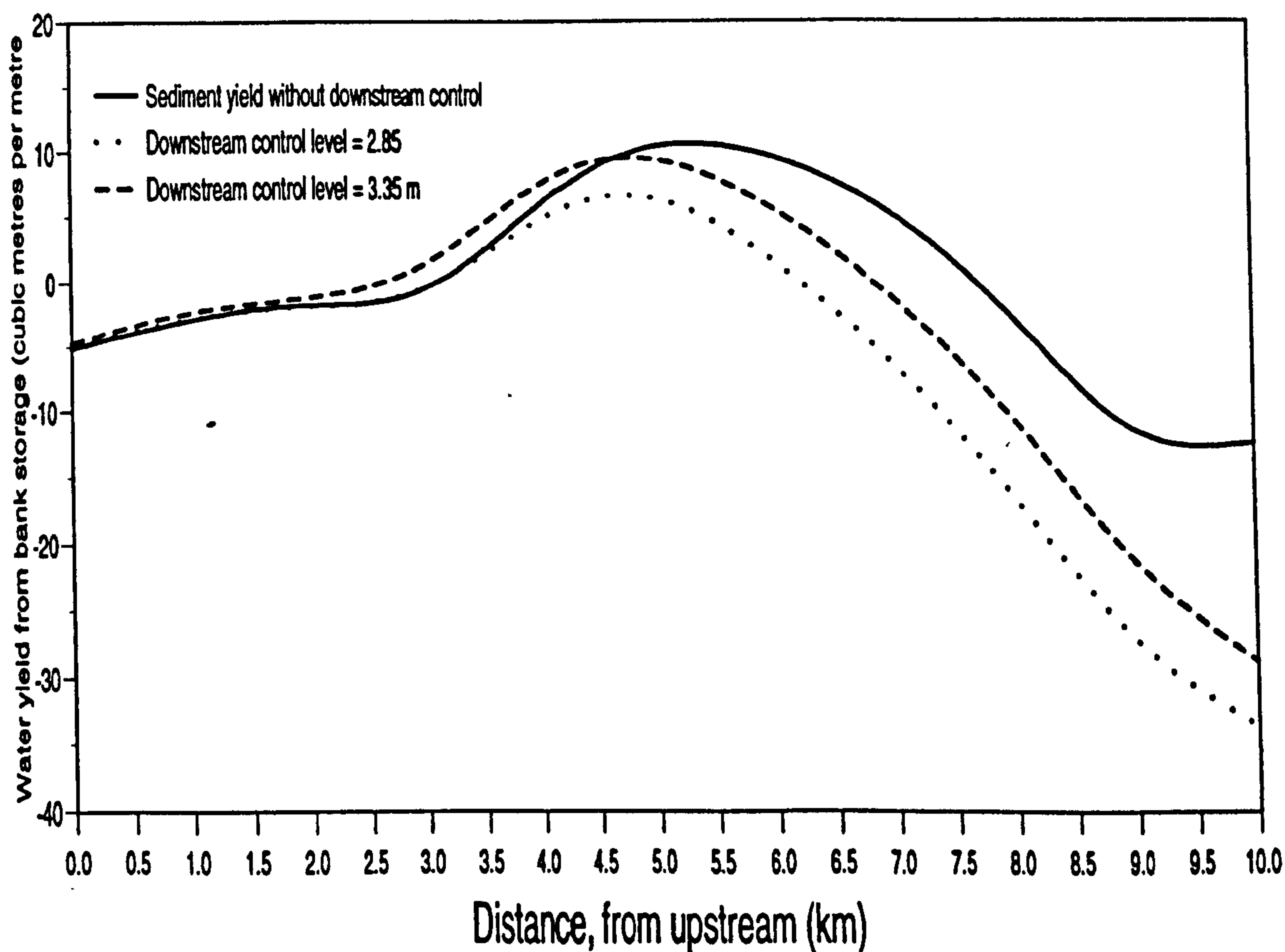
In this evaluation, the downstream boundary condition of a uniform flow relationship has been replaced with the river stage elevation maintained by the mitigating check dam. That is, a downstream weir grade control is assumed to maintain the downstream flow depth at a certain elevation above datum, and a set of simulations are carried out to route a flood through the same reach. This time, in one routing the downstream section is assumed to be without the control, while in the other routing the control is assumed to maintain the downstream depth of flow at 0.5 m above the normal depth, (which was 1.85 m). Two other similar simulations were carried out with the downstream depth of flow maintained at 1.0 m and 1.5 m above the normal depth. Again, comparison of sediment and groundwater yields in both space and time for the set of simulations indicate the mitigation effects of the grade controls.

Figure 6.9a shows the trend of shift of the sediment yield curves due to the increasing elevation of the weirs. At the upstream end of the quarry, the amount of sediment delivered decreases with increasing check-dam elevation. And at the downstream end, the amount of sediment yield flowing out of the reach increases with increasing elevation of the control, meaning that more sediment material is going out of the quarry past the weirs. For the given conditions, it means delivery efficiency is decreased with increasing elevation of the control. For example, with the control of 1.0 m above the normal depth, the sediment delivered is about 4000 kg in the upstream reach of the quarry and 6500 kg in the downstream reach of the quarry, while with the control of 1.5 m above the normal depth the sediment delivery is zero and 2000 kg in the respective reaches. For the quarry system without the downstream control, the amount of sediment deliveries in the upstream and downstream reaches of the quarry are about 2000 kg and 10000 kg, respectively.

It is also observed that in this set-up, the rate of sediment scour throughout the quarry length, with the weir of 1.5 m, is less but more or less uniform throughout the quarry reach. The distribution of the sediment yield for the quarry without the weir is not uniform. Although it would also have been expected for the delivery efficiency to increase with increasing height of the downstream control, these results have revealed otherwise. This is because with the weir, due to the back-water effects, the effects of acceleration and deceleration by the quarry are submerged so that the flow continues to accelerate as it approaches the weir. In this way, there is minimal erosion at the upstream end of the quarry, and the flow has its sediment transport potential increasing towards the weir. That is why at the end of the week (period of the analysis), the amount of sediment material past the downstream section is about 7000 kg for the quarry without the weir, 12000 kg for the control of 1.0 m, and 18000 kg for the weir of 1.5 m.



**Fig. 6.9a Sediment yield of 1 week in a reach of varied downstream control levels. The quarry of depth of 1m in the reach between distances 5 and 9 km from upstream**



**Fig. 6.9b Water yield of 1 week from bank storage in a reach of varied downstream control levels. The reach has a quarry of depth of 1m in the reach between distances 5 and 9 km from upstream**



Figure 6.9b shows the trend of shift of the groundwater yield curves due to the heights of the control systems. The extent and magnitude of the groundwater recharge was more for the quarry with the weir controls. However, the weir with the height of 1.5 m has less recharging potential because of the erosion in the channel, which lowers the water level in the river, hence the recharging potential. So with the control of 1.0 m above the normal depth, the maximum amount of water yield is about 6 m<sup>3</sup>/m, and the depletion takes place in the reach between distances 3 and 6.5 km (positive water yield). With the control of 1.5 m above the normal depth, the maximum amount of water yield is about 10 m<sup>3</sup>/m, and the depletion is in the reach between distances 3 and 7 km. The difference between the curves of water yield of the various controls and that one of the system without the control gives the extra amount of water conserved as a result of having the corresponding control.

So, by adjusting the elevation of the intervention weir, various mitigation levels against soil and water depletion can be attained. In this way, and while observing the hydrogeological properties and the geography of the region, a balance for optimal soil and water yields can be evaluated so that both the resource potential and nature can be sustained.

The above application examples have been based on theoretical analyses of numerical experimentation using simple conceptual hydrologic systems. But they have, nevertheless, managed to address real feasible problems in the field. Starting with the derivation of the baseflow hydrograph, and demonstration of its interrelationship with the sedimentation processes in alluvial river systems, the chapter has illustrated how the MASAI approach can be applied for predictive analyses of hydrological responses due to some land use and river engineering alterations. Based on the definition of baseflow recession and sediment yield curves, simple but common river engineering and cultural practices associated with in-stream sedimentation have been used to demonstrate methods of selection of schemes with minimal degradation effects.

## **7. DISCUSSION, CONCLUSIONS AND SUGGESTIONS FOR FURTHER RESEARCH.**

### **7.1 Discussion**

The first aim of this study has been to develop a mechanism for solving simultaneously the numerical translation of the Saint Venant and the sediment continuity equations for flows in open channels, and the Boussinesq equation for groundwater, and to link them through a time-dependent interface boundary layer. This was done in order to constitute a mathematical Model for Alluvial Stream-Aquifer Interaction (MASAI), for simulating water and sediment movement in natural channels, short and long term channel bed profile changes and bank storage variation. This kind of mathematical model may be calibrated and utilised for studies in planning, design and operation of groundwater recharge, in-stream sand mining, soil and water conservation, and other related transient alluvial river system processes.

The modified model framework developed herein also forms a contribution to the subject of alluvial stream-aquifer interaction processes. Inclusion of the time-dependent boundary interface in the modelling has made the solution procedure more general and capable of analysing more hydrological and fluvial phenomena in alluvial river systems.

It is also important to note that, although the channel flow solution was based on gradually varied flow conditions, the MASAI linkage solution can still take any channel routing procedure so long as it describes and feeds the variation of the flow depth,  $H$ , into the linkage expression (Eq. 4.54). Furthermore, since it seems that uncertainty in data provision and process description for sedimentation is likely to continue, hybrid models involving stochastic components for estimating the river bed elevation variation in the MASAI linkage expression may be appropriate. To hydraulicians and water resources analysts dealing with stream-aquifer interaction modelling on erodible alluvial river systems, the additional advantage with the MASAI is its ability to track the transient nature of both the lateral seepage flows and the variation of river-bed elevation profiles.

The second aim of the study has been to identify a practical case of in-stream sand mining and to demonstrate the hydrological effects of the practice. It was possible to identify such sites on the River Kibos in Kenya, for which an improvised but practical methodology was devised, based on rating curve analysis, to facilitate investigations of the hydrological and fluvial impacts of the practice on the river. The fieldwork investigations demonstrated that the channel bed elevation around Kibos bridge sand mine, whose banks were stabilised by gabbion lining, fell by about 0.8 m during the five year period of the available data, whereas the channel reach upstream of the Nyamasaria bridge, stabilised by a grade control weir, had its features preserved. Therefore, considering the results from fieldwork and numerical experiments, it is perceived that in-stream sand quarrying can cause land degradation, by lowering the riparian landscape and the corresponding water levels. In addition, the main proposals for the Nyando River flooding problems have also been reviewed so as to exemplify field cases to which the MASAI concept can be applied for predictive investigation prior to implementing the development alternatives. Such predictive assessments are now obligatory, considering the numerous uncertainties



involved in alluvial river responses to development schemes, as demonstrated by the predictive analysis of the River Nyando training plan at Ahero.

Mathematical modelling for alluvial river systems is well developed for describing the main hydraulic and fluvial processes involved in the systems. The models can be applied to evaluate the effects of different river development alternatives. They have proven their power and are widely used in the field of river engineering (e.g. HEC-6, 1977; Chen et al 1978; Lopes, 1988 and Chang 1990). However, mathematical modelling in ecology is still in its infancy, yet ecological studies are in great demand for application in river systems management, not only for ecological restoration projects, but also for environmental impact assessments. Admittedly, even the expanded MASAI algorithm cannot on its own predict the ecological/environmental impacts due to impending development changes to river systems. Notwithstanding, just as river models may rely on other models, like the catchment sediment yield and rainfall-runoff models, so is the MASAI approach meant to facilitate ecological modelling. This is possible because the MASAI is capable of making predictive analyses of river stage, sediment yield, bank storage, bed elevation variation and water table fluctuations, all of which are determinants of the riparian ecosystems.

In the past, there have been disciplinary barriers between hydraulicians, hydrologists and ecologists because of their differences in terminology, interest, resolution, academic background, etc. But because of the strong linkage of the ecological systems to the hydrological behaviour, perpetuation of these differences should now be viewed as a hindrance to progress in the analysis of most natural resources. River engineering works cause not only positive changes to the ecosystems, but may also be directly disruptive especially to the interface zones which are ecologically very sensitive and important. Close co-operation of both engineers and life scientists is therefore necessary to improve mutual understanding and provide the means to ensure sustainable and ecologically sound development. What is apparent is that

both groups of scientists appreciate the importance of water for life, which in a way is the principle upon which this study approach has been based. That is, the study assumes that if the river system's hydrological and fluvial responses to impending development alternatives can be predicted, then with ample room and transparency for the ecological viewpoint, corresponding conceptual ecological models can also be derived for describing the ecological impacts due to the changes in the river bed, river stage and water table levels. In this way, the simulations can be re-run, matching the results, exchanging ideas and making practical evaluations and adjustments - based on preferred socio-economic, ecological and engineering objectives - until an optimal balance or tolerance limit is reached.

Applications of the MASAI have been exemplified through simulations of theoretical schemes so as to gain more insights into hydrologic responses to development alterations on alluvial river systems. For example, it has been demonstrated how to evaluate the inter-relationships among individual hydrograph components of certain hydrologic systems as well as determine the effects of variation of certain system parameters and development schemes.

The model is useful particularly as a means for describing baseflow behaviour resulting from a variety of combination of aquifer and channel conditions. Current hydrograph analysis assumes that baseflow recession curves can be estimated by the decaying exponential relationship described by Eq. 6.1. Numerical experimentation results generated in this study by simulating baseflow recession curves show some degree of theoretical confirmation of this assumption, in that system hydrographs, which were obtained by linking the numerical solutions of the physical equations which approximately govern alluvial stream-aquifer systems, did in fact produce baseflow curves which conformed to the decaying exponential relationship. However, this conformity was only in the case of pseudo-equilibrium conditions. For aggrading conditions, the recession curves deviated from the theoretical relationship

by steepening, whereas for degrading channels the recession curves deviated by flattening.

This kind of analysis relating the effects of sedimentation variability to baseflow hydrographs can provide, beforehand, insights elucidating what land use changes can impart on the hydrologic behaviour of alluvial river systems. The problem of how much a given land use will change baseflow (or sediment yield) is very complex and has not been attempted. However, at least a qualitative picture of their influences, based on sediment delivery variation, and their various ramifications have been disclosed to give a rational basis for interpreting the relevant data or plans for alluvial river systems.

Generation and analysis of the baseflow recession curves, adapted as a means for estimating the rate of groundwater depletion, and sediment yield curves, adapted as a means for estimating in-stream sediment delivery, have also been presented to describe how the model could be applied for evaluation of programs requiring soil and water conservation considerations. Simple theoretical in-stream quarrying schemes were defined to which the model was applied to make numerical assessments of the schemes' performance in terms of sediment and water yields. The results showed that the length, depth and number of quarries in a given reach affect the performance, each in its own way. Application of check-dams downstream of the quarries also showed appreciable conservation of both water and soil sediments, more than in quarries without the downstream controls.

The purpose of applying a mathematical model for the somewhat cultural and small scale business practices analysed in this study is primarily to demonstrate a tool for helping to make less haphazard but rational decisions on river management and environmental matters. They are straightforward examples that are intended to increase the general awareness of mathematical simulations for projects involving not



only engineers and fellow scientists, but also other communities of the society who depend on the rivers for their livelihood, and therefore whose consent is now crucial for realising sustainable management systems

## 7.2 Conclusions

On the basis of the above discussions, the major conclusions are summarised thus:

1. An enhanced concept of mathematical modelling for alluvial stream-aquifer interaction has been developed, giving the modelling the extra capability of accounting for transient stream-aquifer water interchange for eroding and/or evolving channels.
2. The specific innovation in the enhanced concept of the MASAI is the simultaneous solution of the numerical translation of the Saint Venant and the sediment continuity equation for open channels, and the Boussinesq equation for groundwater, and their linkage through a time dependent interface boundary layer, as summarised in equation 4.54.
3. The MASAI developed herein, can be applied to estimate open channel water routing, channel aggradation and degradation, bank storage and other transient behaviours of alluvial stream-aquifer systems. Because of lack of field data, the model was tested using theoretical data from the literature. The model performed satisfactorily against results published by Todini (1991), Chang and Richards (1971) and Pinder and Sauer (1971) models. The fair agreement between the computed and the published results verifies that the model can be developed for application to real-world problems. The

calibration procedure for the MASAI has also been suggested and described in section 5.3, based on the fieldwork on the Nyando river system.

4. Because of lack of field data, numerical experiments were performed in order to give more insights into the interrelationships between in-stream sedimentation and baseflow recession. They have demonstrated that the recession curve for an aggrading river steeply deviates from the theoretical relationship described by Eq. 6.1 and the river may become more and more influent. For degrading rivers, it was illustrated that the recession curve deviates from the theoretical relationship by flattening and the river may become more and more effluent.

5. Another case exemplifying the application of the MASAI was also based on some conceptual in-stream quarrying schemes, because of the limited field data. A method of optimising the performance of quarry schemes was suggested, from which numerical simulations were performed and produced results that suggested the following conclusions:

(a) the length of the quarry significantly affects the spatial extent of groundwater depletion and the location of sediment delivery in the upstream section of the quarry, but does not affect the amount delivered in the quarry;

(b) the depth of the quarry significantly affects the amount of the groundwater mined from the surrounding vicinity, and the amount of sediment delivered in the quarry, but does not significantly affect the location of deposition;

(c) for a given channel reach, the total amount of sediment delivered can be significantly increased by setting up more short quarries instead of having one extensive quarry. The tendency to lower the water elevation in the area is also reduced by having the scheme of shorter quarries;

(d) soil and water conservation was improved with the presence of check-dam controls downstream of the quarries, but the improvement depended on the elevation of the grade control.

6. Results based on the observations and measurements on the River Kibos have demonstrated that grade control weirs can mitigate adverse degradation effects that could otherwise result from in-stream sand harvesting.

7. Application of the MASAI approach to a practical field problem, based on a plan for training a reach on the River Nyando, near the Ahero NIB village, suggests that as a result of the training development, the problem of flooding in the reach extending from the Ahero road bridge towards downstream would be intensified. It was also found that due to the improvements, significant irregularities in streambed scouring and deposition would be induced.

### **7.3 Suggestions for Further Research**

Despite the limitations due to the numerous physical and mathematical assumptions inherent in the theoretical development, as well as measurement error and inadequacy of field data, the MASAI concept has demonstrated promising results as a useful tool for hydrological investigations. However, the results provided by the numerical experimentation by no means constitute a completely comprehensive assessment of



the model's capabilities and limitations. Development of the model was achieved through adoption and synthesis of concepts of solutions contributed by streamflow-sediment routing and stream-aquifer interaction modellers, assuming their models' capabilities and limitations. Therefore, by assuming the basic concepts, and developing such an expanded model framework, certain items were likely to be encountered which fell outside the scope of the present study. Such items are henceforth suggested as topics for further research, which include:

1. Inclusion of an unsaturated module so that soil water can also be accounted for, in cases of ephemeral streams which may occasionally be hydraulically disconnected from the underlying plain aquifer. This became apparent by noting that some of the river developments actually promote aggradation, which in turn increases the chances of the streamflow becoming disconnected from the underlying aquifer during dry periods.
2. Consideration of two-dimensional mathematical schemes for streamflow and sediment routing, given that lateral erosion/morphological changes can significantly affect the stream-aquifer contact area, with corresponding influence on the magnitude of the water interchange between the two hydrologic units.
3. Assuming field data can be obtained, test the estimation of the river bottom hydraulic conductivity in situ according to the method described in step 8 of the calibration procedures in chapter 5.
4. Considering the influence of the riverine landscape and water surface elevations on riparian ecosystems, develop further the conceptual ecological assessment method suggested in appendix 4, so that it can be applied to relate river and water table levels to the ecological potential of river systems.

## A1. SOLUTION OF THE NON-LINEAR ALGEBRAIC EQUATION BY NEWTON'S ITERATIVE METHOD

Eqs. 3.16 through 3.24 simulate the water continuity and momentum equations of gradually varied unsteady flow by means of a system of  $2n$  non-linear algebraic equations with  $2n$  unknown. Amein and Fang (1970) suggested a generalised Newton's iteration method for solving equations. For the sake of convenience, the system of equations are arranged as follows:

$$G_0(H_1, Q_1) = 0$$

$$F_1(H_1, Q_1, H_2, Q_2) = 0$$

$$G_1(H_1, Q_1, H_2, Q_2) = 0$$

·  
·  
·

$$F_i(H_i, Q_i, H_{i+1}, Q_{i+1}) = 0$$

$$G_i(H_i, Q_i, H_{i+1}, Q_{i+1}) = 0$$

·  
·  
·

$$F_{n-1}(H_{n-1}, Q_{n-1}, H_n, Q_n) = 0$$

$$G_{n-1}(H_{n-1}, Q_{n-1}, H_n, Q_n) = 0$$

$$F_n(H_n, Q_n) = 0$$

(A1.1)

Application of the generalised Newton's iteration method of the systems of equations(Eq. A1.1) is made by assigning trial values to unknowns. When these trial values are substituted into Eq. A1.1, the right side of the equations may not vanish, but acquire values known as residuals. Solutions are obtained by adjusting the values until each residue vanishes or is reduced to tolerable quantity. The computation may be organised in a series of iteration steps.

To show the procedure, let it be assumed that the computations have been carried through the K-th iteration cycle so the values of the unknowns have been approximated through the (K+1)-th cycle. It is now desired to approximate the values of the 2n unknowns through the (K+1)-th cycle. Let the residuals of Eq. A1.1 evaluated at the K-th iteration cycle be represented by  $R1_{ik}$  and  $R2_{ik}$ , in which R1 is associated with the function F, and R2 is associated with the function G. The value of the residuals at the k-th iteration cycle are:

$$G_0(H_1^k, Q_1^k) = R_{20}^k$$

·  
·  
·

$$F_i(H_i^k, Q_i^k, H_{i+1}^k, Q_{i+1}^k) = R_{1i}^k$$

$$G_i(H_i^k, Q_i^k, H_{i+1}^k, Q_{i+1}^k) = R_{2i}^k$$

·  
·  
·

$$F_n(H_n^k, Q_n^k) = R_{1n}^k$$

(A1.2)

The residuals and the partial derivatives of the system equations are related to the generalised Newton's iteration method as:



$$\frac{\partial G_0}{\partial H_1} dH_1 + \frac{\partial G_0}{\partial Q_1} dQ_1 = -R_{20}^k$$

.

.

.

$$\frac{\partial F_i}{\partial H_i} dH_i + \frac{\partial F_i}{\partial Q_i} dQ_i + \frac{\partial F}{\partial H} dH_{i+1} + \frac{\partial F_i}{\partial Q_{i+1}} dQ_{i+1} = -R_i$$

$$\frac{\partial G_i}{\partial H_i} dH_i + \frac{\partial G_i}{\partial Q_i} dQ_i + \frac{\partial G_i}{\partial H_{i+1}} dH_{i+1} + \frac{\partial G_i}{\partial Q_{i+1}} dQ_{i+1} = -R_2$$

.

.

.

$$\frac{\partial F_n}{\partial H_n} dH_n + \frac{\partial F_n}{\partial Q_n} dQ_n = -R_{1L}^k \tag{A1.3}$$

in which all the partial derivatives are evaluated at the k-th iteration cycle and are known.

Eq. A1.3 is a system of 2n linear equations with 2n unknown of (dH<sub>i</sub>, dQ<sub>i</sub>), (i = 1 . . . n). Any of the standard methods, such as the Gaussian elimination, or matrix methods can be applied for its solution. But in this case, Fread's (1971) direct solution technique has been used to solve this system of linear equations. Its details and advantages are described in Appendix 2

The solution for Eq. A1.3 will provide values of dH and dQ. The values of the unknowns at the (k+1)-th iteration cycle are obtained from:

$$H_i^{k+1} = H_i^k + dH$$

$$Q_i^{k+1} = Q_i^k + dQ \tag{A1.4}$$

The procedure may be repeated until tolerable values are obtained.

In application to problems, it is necessary to evaluate coefficients of the linear system. The expressions for the residuals and the partial derivative terms of Eq. A1.3, which can be obtained by differentiating Eqs. 3.16, through 3.24 are given as follows:

$$R_{1i}^k = \theta \cdot X_4 + 1/2(X_6 - C_9) - C_3$$

$$R_{2i}^k = 1/2(X_2 - C_2) + \theta \cdot X_5 + g/2\theta \cdot X_3 \cdot X_6 - g/2\theta \cdot X_6 \cdot X_8 + g/2\Delta t \cdot X_6 \cdot X_{10}$$

$$R_{1n}^k = H_n^k - H(Q_n^k)$$

$$R_{20}^k = 0$$

$$\frac{\partial F_i}{\partial H_i} = 1/2 T_1^{i+1}$$

$$\frac{\partial F_i}{\partial Q_i} = -\theta$$

$$\frac{\partial F_i}{\partial H_{i+1}} = 1/2 T_{i+1}^{i+1}$$

$$\frac{\partial F_i}{\partial Q_{i+1}} = \theta \frac{\partial G_i}{\partial H_i} = \theta X_{16a} + \frac{g}{2} \cdot \theta \cdot (T_i^k \cdot X_3 - X_6) - \frac{g}{2} \cdot \theta \cdot T_i^k \cdot X_8 + \frac{g}{2} \cdot \Delta t \cdot X_{10} (T_i^k - X_6)$$

$$\frac{\partial G_i}{\partial Q_i} = 1/2 - 2\theta(Q/A)_i^k + \frac{g}{2} \Delta t \cdot X_6 \cdot X_{14a}$$

$$\frac{\partial G_i}{\partial H_{i+1}} = -\theta \cdot X_{16b} + \frac{g}{2} \theta (X_6 + T_{i+1}^k \cdot X_3) - \frac{g}{2} \theta T_{i+1}^k \cdot X_8 + \frac{g}{2} \Delta t \cdot X_{10} (T_{i+1}^k - X_6 \cdot X_{15b})$$

(A1.5)

where:  $\theta = \Delta t / \Delta x$

If the upstream boundary condition is a discharge hydrograph and the down stream boundary condition is a stage-discharge relationship, then:

$$\frac{\partial G_0}{\partial Q_1} = 1$$

$$\frac{\partial G_0}{\partial H_1} = 0$$

$$\frac{\partial F_n}{\partial H_n} = 1$$

$$\frac{\partial F_n}{\partial Q_n} = -\frac{d F_n(Q_n)}{d Q_n}$$

$$C_1 = H_i^j + H_{i+1}^j \quad C_2 = Q_i^j + Q_{i+1}^j$$

$$C_3 = t/2 (q_i^j + q_{i+1}^j)$$

$$C_4 = S_{f_i}^j + S_{f_{i+1}}^j$$

$$C_5 = A_i^j + A_{i+1}^j$$

$$X_1 = H_i^k + H_{i+1}^k$$

$$X_2 = Q_i^k + Q_{i+1}^k$$

$$X_3 = H_{i+1}^k - H_i^k$$

$$X_4 = Q_{i+1}^k - Q_i^k$$



$$X_5 = (Q^2 / A)_{i+1}^k - (Q^2 / A)_i^k$$

$$X_6 = A_{i+1}^k + A_i^k$$

$$X_7 = T_{i+1}^k + T_i^k$$

$$X_8 = Z_i^k - Z_{i+1}^k$$

$$X_9 = C_5(H_i^k - H_i^j)$$

$$X_{10} = (S_{f_i}^k \cdot S_{f_{i+1}}^j)^{1/2}$$

$$X_{11} = C_6(H_{i+1}^k - H_{i+1}^j)$$

$$X_{12} = C_8(Q_{i+1}^k - Q_{i+1}^j)$$

$$X_{13a} = (dT / dH)_i^k$$

$$X_{13b} = (dT / dH)_{i+1}^k$$

$$X_{14a} = X_{10} / Q_i^k$$

$$X_{14b} = X_{10} / Q_{i+1}^k$$

$$X_{15a} = \frac{1}{3A} (5T - 2R \frac{dP}{dH})_i^k$$

$$X_{15b} = \frac{1}{3A} (5T - 2R \frac{dP}{dH})_{i+1}^k$$

$$X_{16a} = (TQ^2 / A^2)_i^k$$

$$X_{16b} = (TQ^2 / A^2)_{i+1}^k \quad (\text{A1.6})$$

The values of the  $C_i$ 's are in terms of the known variables evaluated at time step  $t_j$  and can be determined directly. But  $X_i$  values are functions of the  $k+1$ -th iteration cycle and should be calculated repeatedly in the iteration cycles.

The iteration steps may be summarised as follows:

1. Assume initial trial values:

$$Q_i^k = Q_i^j \text{ and } H_i^k = H_i^j, \quad \text{where } k = 0$$

except  $Q_i^k = Q(t^{j+1})$  or  $H_i^k = H(t^{j+1})$

2. Compute:

$$[R1_i^k, R2_i^k, \frac{\partial F_i}{\partial H_i}, \frac{\partial F_i}{\partial Q_i}, \frac{\partial F_i}{\partial H_{i+1}}, \frac{\partial F_i}{\partial Q_{i+1}}, \frac{\partial G_i}{\partial H_i}, \frac{\partial G_i}{\partial Q_i}, \frac{\partial G_i}{\partial H_{i+1}}, \frac{\partial G_i}{\partial Q_{i+1}}] \text{ from Eq. A1.5 and Eq. A1.6.}$$

3. Compute  $dH_i$  and  $dQ_i$  by applying Fread's technique; and then adjust:

$$H_i^{k+1} = H_i^k + dH \text{ and } Q_i^{k+1} = Q_i^k + dQ$$

4. Compare  $(H_i^{k+1}, Q_i^{k+1})$  with  $(H_i^k, Q_i^k)$ . If they are not comparable, let  $k = k+1$  and repeat steps 2 through 4 until the desired accuracy is obtained.

When the values of the unknown in any two consecutive iterations fall below a tolerable value, let

$$(H_i^{j+1} = H_i^{k+1})$$

and  $(Q_i^{k+1} = Q_i^{k+1})$

and then the computation is carried onto the sedimentation process.

## **A2. SOLUTION OF THE SYSTEM OF EQUATIONS DERIVED FROM THE FULLY IMPLICIT SCHEME BY FREAD'S (1971) TECHNIQUE**

Amein and Fang (1970) related the residual and partial derivatives of the Saint-Venant equations according to Eq. A1.3. They noted that the  $2n$  coefficient matrix associated with the equation had a maximum of only four non-zero elements in any one row and that these elements are banded around the main diagonal. This feature enables a fast matrix solution to be devised. Fread (1971) had encountered this type of matrix and devised a direct solution technique similar to the Gauss elimination method. The technique offers the following advantages:

1. The computations do not involve any of the many zero elements in the coefficient matrix; this saves considerable computation time.
2. The required computer core storage is reduced significantly from that required for a  $2n \times 2n$  matrix to that required for a  $2n \times 4$  matrix. This is a desirable feature of the matrix solution technique when the channel sections under consideration are many and the computer storage capacity is limited.

Fread observed that Eq. A1.3 is a system of  $2n$  linear equations with  $2n$  unknowns of  $(dH_i, dQ_i)$ ,  $i = 1, 2, \dots, n$ . The system of equations is represented as:



$$\frac{\partial G_0}{\partial Q_1} dQ_1 + \frac{\partial G_0}{\partial H_1} dH_1 = -R_{2_0}^k$$

$$\frac{\partial F_1}{\partial Q_1} dQ_1 + \frac{\partial F_1}{\partial H_1} dH_1 + \frac{\partial F_1}{\partial Q_2} dQ_2 + \frac{\partial F_1}{\partial H_2} dH_2 = -R_{1_1}^j$$

$$\frac{\partial G_1}{\partial Q_1} dQ_1 + \frac{\partial G_1}{\partial H_1} dH_1 + \frac{\partial G_1}{\partial Q_2} dQ_2 + \frac{\partial G_1}{\partial H_2} dH_2 = -R_{2_1}^j$$

.

.

.

$$\frac{\partial F_i}{\partial Q_i} dQ_i + \frac{\partial F_i}{\partial H_i} dH_i + \frac{\partial F_i}{\partial Q_{i+1}} dQ_{i+1} + \frac{\partial F_i}{\partial H_{i+1}} dH_{i+1} = -R_{1_i}^j$$

$$\frac{\partial G_i}{\partial Q_i} dQ_i + \frac{\partial G_i}{\partial H_i} dH_i + \frac{\partial G_i}{\partial Q_{i+1}} dQ_{i+1} + \frac{\partial G_i}{\partial H_{i+1}} dH_{i+1} = -R_{2_i}^j$$

.

.

.

$$\frac{\partial F_{n-1}}{\partial Q_{n-1}} dQ_{n-1} + \frac{\partial F_{n-1}}{\partial H_{n-1}} dH_{n-1} + \frac{\partial F_{n-1}}{\partial Q_n} dQ_n + \frac{\partial F_{n-1}}{\partial H_n} dH_n = -R_{1_{n-1}}^k$$

$$\frac{\partial G_{n-1}}{\partial Q_{n-1}} dQ_{n-1} + \frac{\partial G_{n-1}}{\partial H_{n-1}} dH_{n-1} + \frac{\partial G_{n-1}}{\partial Q_n} dQ_n + \frac{\partial G_{n-1}}{\partial H_n} dH_n = -R_{2_{n-1}}^k$$

$$\frac{\partial F_n}{\partial Q_n} dQ_n + \frac{\partial F_n}{\partial H_n} dH_n = -R_{1_n}^k \quad \} \quad (\text{A2.1})$$

where all the residual and differential coefficients can be obtained from Eqs. A1.5 and A1.6. Using matrix notation, Eq. A2.1 takes the form:

$$AX = R \quad (\text{A2.2})$$

in which A = the coefficient matrix with components  $a_{ij}$  and X, R are column vectors having components  $x_i$  and  $r_i$ , respectively, i.e.:

$$\begin{aligned}
 A = & \left[ \begin{array}{cccccccc}
 a_{11} & a_{12} & & & & & & \\
 a_{21} & a_{22} & a_{23} & a_{24} & & & & \\
 a_{31} & a_{32} & a_{33} & a_{34} & & & & \\
 & a_{43} & a_{44} & a_{45} & a_{46} & & & \\
 & a_{53} & a_{54} & a_{55} & a_{56} & & & \\
 & & \cdot & \cdot & \cdot & & & \\
 & & \cdot & \cdot & \cdot & & & \\
 & & \cdot & \cdot & \cdot & & & \\
 & & & a_{2n-2,2n-3} & a_{2n-2,n-2} & a_{2n-2,2n-1} & a_{2n-2,2n} & \\
 & & & a_{2n-1,2n-3} & a_{2n-1,2n-2} & a_{2n-1,2n-1} & a_{2n-1,2n} & \\
 & & & & & a_{2n,2n-1} & a_{2n,2n} & 
 \end{array} \right]
 \end{aligned}
 \tag{A2.3}$$

$$\begin{aligned}
 X = & \left[ \begin{array}{c} x_1 \\ x_2 \\ \cdot \\ \cdot \\ \cdot \\ x_{2N} \end{array} \right] \qquad \text{and} \qquad R = \left[ \begin{array}{c} r_1 \\ r_2 \\ \cdot \\ \cdot \\ \cdot \\ r_{2N} \end{array} \right]
 \end{aligned}
 \tag{A2.4}$$

If the components of A are shifted horizontally such that the relative positions of the components in any one row remain the same, A takes the form of A' with components a'ij. Thus

$$A' = \begin{vmatrix} & & a'_{13} & a'_{14} \\ a'_{21} & a'_{22} & a'_{23} & a'_{24} \\ a'_{31} & a'_{32} & a'_{33} & a'_{34} \\ a'_{41} & a'_{42} & a'_{43} & a'_{44} \\ & \cdot & \cdot & \cdot \\ & \cdot & \cdot & \cdot \\ & \cdot & \cdot & \cdot \\ a'_{2n-2,1} & a'_{2n-2,2} & a'_{2n-2,3} & a'_{2n-2,4} \\ a'_{2n-1,1} & a'_{2n-1,2} & a'_{2n-1,3} & a'_{2n-1,4} \\ a'_{2n,1} & a'_{2n,2} & & \end{vmatrix} \quad (A2.5)$$

and Eq. A2.2 takes the form

$$A' X = R \quad (A2.6)$$

The system of equations (Eq. A2.1) can be efficiently solved by the following technique.

The current formulae, applicable to even-numbered rows, i.e. ( $i = 2, 4, 6, \dots 2n$ ) are:

$$M_{i,2} = -a_{i,1} \frac{M_{i-1,4}}{M_{i-1,3}} + a_{i,2} \quad (A2.7a)$$

$$Z_i = -a_{i,1} \frac{Z_{i-1}}{M_{i-1,3}} + r_i \quad (A2.7b)$$

The current formulae, applicable to the odd-numbered rows, i.e. ( $i = 3, 5, 7, \dots 2n-1$ ) are:

$$M_{i,2} = -a_{i,1} \frac{M_{i-2,4}}{M_{i-2,3}} + a_{i,2} \quad (A2.8a)$$



$$M_{i,3} = -a_{i-1,3} \frac{M_{i,2}}{M_{i-1,2}} + a_{i,3} \quad (\text{A2.8b})$$

$$M_{i,4} = -a_{i-1,4} \frac{M_{i,2}}{M_{i-1,2}} + a_{i,4} \quad (\text{A2.8c})$$

$$Z_i = -M_{i,2} \frac{Z_{i-1}}{M_{i-1,2}} - a_{i,1} \frac{Z_{i-2}}{M_{i-2,3}} + r_i \quad (\text{A2.8d})$$

The computations proceed sequentially from  $i = 2$  to  $i = 2n$ . The components of the solution vector,  $X$ , are obtained by back-substitution commencing at  $i = 2n$  and proceeding sequentially to  $i = 1$ . Thus:

$$X_{2n} = \frac{Z_{2n}}{M_{2n,2}} \quad (\text{A2.9a})$$

and the recurrent formula for ( $i = 2n-1, 2n-3, \dots, 5, 3, 1$ ) is:

$$X_i = \frac{Z_i - M_{i,4} X_{i+3}}{M_{i,3}} \quad (\text{A2.9b})$$

while that for ( $i = 2n - 2, 2n - 4, \dots, 6, 4, 2$ ) is:

$$X_i = \frac{Z_i - a_{i,4} X_{i+2} - a_{i,3} X_{i+1}}{M_{i,2}} \quad (\text{A2.9c})$$

The corresponding terms between Eqs. A2.1 and A2.5 are as follows:

1. When the discharge hydrograph is used as the upstream boundary condition:

$$a_{1,3} = \frac{\partial G_0}{\partial Q_1}, a_{1,4} = \frac{\partial G_0}{\partial H_1}, r_1 = -R_{2,0}^k$$

$$a_{2i,1} = \frac{\partial F_i}{\partial Q_u}, a_{2i,2} = \frac{\partial F_i}{\partial H_i}, a_{2i,3} = \frac{\partial F_i}{\partial Q_{i+1}}, a_{2i,4} = \frac{\partial F_i}{\partial H_{i+1}}, r_{2i} = -R_{i,i}^j$$

$$a_{2i+1,1} = \frac{\partial G_i}{\partial Q_u}, a_{2i+1,2} = \frac{\partial G_i}{\partial H_i}, a_{2i+1,3} = \frac{\partial G_i}{\partial Q_{i+1}}, a_{2i+1,4} = \frac{\partial G_i}{\partial H_{i+1}}, r_{2i+1} = -R_{2,i}^j$$

$$a_{2n,1} = \frac{\partial F_n}{\partial Q_n}, a_{2n,2} = \frac{\partial G_0}{\partial H_1}, I_{2n} = -R_{2,n}^k \quad (\text{A2.10a})$$

where ( $i = 1, 2, \dots, n-1$ )

and all the partial derivative terms and the residuals are formulated in Eq. A1.5 and A1.6. The solutions are then given as:  $dQ_i = x_{2i-1}$  and  $dH_i = x_{2i}$ .

2. When the stage hydrograph is used as the upstream boundary condition:

$$a_{1,3} = \frac{\partial G_0}{\partial H_1}, a_{1,4} = \frac{\partial G_0}{\partial Q_1}, r_1 = -R_{20}^k$$

$$a_{2i,1} = \frac{\partial F_i}{\partial H_i}, a_{2i,2} = \frac{\partial F_i}{\partial Q_i}, a_{2i,3} = \frac{\partial F_i}{\partial H_{i+1}}, a_{2i,4} = \frac{\partial F_i}{\partial Q_{i+1}}, I_{2i} = -R_i^j$$

$$a_{2i+1,1} = \frac{\partial G_i}{\partial H_i}, a_{2i+1,2} = \frac{\partial G_i}{\partial Q_i}, a_{2i+1,3} = \frac{\partial G_i}{\partial H_{i+1}}, a_{2i+1,4} = \frac{\partial G_i}{\partial Q_{i+1}}, I_{2i+1} = -R_i^j$$

$$a_{2n,1} = \frac{\partial F_n}{\partial H_n}, a_{2n,2} = \frac{\partial F_n}{\partial Q_n}, I_{2n} = -R_{11}^k \quad ((2.10b))$$

where ( $i = 1, 2, \dots, n-1$ )

The solutions are then given as  $dH_i = x_{2i-1}$  and  $dQ_i = x_{2i}$ , where ( $i = 1, 2, \dots, n$ )

A computer module for applying this technique to solve Eq. A2.1 has been programmed and given as a subroutine of the main program. In application, the element  $a'_{1,3}$  must have a value other than zero. That is why Eq. A2.10a is rearranged as Eq. A2.10b, depending on whether the upstream condition is a discharge or stage hydrograph.

### A3. SEDIMENT TRANSPORT CALCULATION BY THE ACKERS-WHITE PROCEDURE.

For calculation, the following properties of the system must be known: (1) Particle size,  $D$  ( $D_{35}$  for graded sediments); (2) specific gravity of sediments,  $s$ ; (3) mean velocity of flow,  $V$ ; (4) shear velocity,  $v_*$ , based on measurements of the velocity distribution or the depth/slope relationship ( $v_* = [gdi]^{1/2}$ ); (5) depth of flow,  $d$ ; (6) kinematic viscosity of fluid,  $\nu$ ; and (7) acceleration due to gravity,  $g$ .

The sequence of calculation procedures is as follows:

1, Determine the value  $D_{gr}$ , i.e.

$$D_{gr} = D \left( \frac{g(s-1)}{\nu^2} \right)^{(1/3)}$$

2, Determine values of  $n$ ,  $m$ ,  $A$ , and  $C$  associated with the derived  $D_{gr}$  value, i.e.  
for  $1.0 < D_{gr} \leq 60$

$$n = 1.00 - 0.56 \log D_{gr}$$

$$A = \frac{0.23}{\sqrt{D_{gr}}} + 0.14$$



$$m = \frac{9.66}{D_{gr}} + 1.34$$

$$\log C = 2.86 \log D_{gr} - (\log D_{gr})^2 - 3.53$$

and for coarse sediments,  $D_{gr} > 60$

$$n = 0.00$$

$$A = 0.17$$

$$m = 1.50$$

$$C = 0.025$$

3, Compute the value of the particle mobility,  $F_{gr}$ ;

$$F_{gr} = \frac{V_*^n}{\sqrt{gD(s-1)}} \left[ \frac{V}{\sqrt{32} \log\left(\frac{\alpha d}{D}\right)} \right]^{1-n}$$

4, Determine the value of the sediment transport function,  $G_{gr}$ ;

$$G_{gr} = C \left( \frac{F_{gr}}{A} - 1 \right)^m$$

5, Convert  $G_{gr}$  to sediment flux  $C_s$  (in ppm)

$$C_s = \frac{G_{gr} \cdot S \cdot D}{d \left( \frac{V_*}{V} \right)^n}$$

## **A4. AN ECOLOGICAL VALUATION METHOD FOR CHANNEL SYSTEMS WITH IN-STREAM SAND MINING ACTIVITIES**

### **A4.1 Ecological Valuation on the Kibos**

Going by the prevailing world-wide concern, it is important that river sand mining developments are realised together with the preservation of the environment in a balanced compromise. This is necessary because rivers and their developments are so strongly interconnected with the environment that unless environmental issues are also addressed with the initial river system development plans, subsequent responses could end up conflicting with the very nature they were meant to promote or benefit from.

This assessment has been necessitated noting that river sand is itself a valuable resource in the construction industry and that some hydraulicians have actually supported its practice as a way of clearing and maintaining the capacity of the river channels; yet on the other hand ecologists have labelled it as having land degradation tendencies. The strategy, therefore, is part of the support tools attempting to remit the practice of the damaging tendencies, while at the same time promoting the understanding of conservation of the natural environment along rivers.

The assessment is a follow-up of the previous results from in-stream sand mining on the Kibos River (chapter 3), from which it was concluded that river sand mines can change the landscape and water levels within the vicinity of their practices, unless

appropriate preservative measures were also included. From the observations, and the general knowledge that water and landscape conditions are among the dominant determinants of nature and its ecology, it has been concluded that sand mining can negate ecological qualities unless conservation interventions are also practised.

The data employed were derived from the River Kibos, through visual inspections, measurements, interviews and some historical records. The criterion developed was based on a simple ecological valuation, simple enough to be perceptible to non-biological scientists, but without compromising the index for environmental attributes. The method was based on comparative environmental scores for five areas on the Kibos, measuring 50 m along the river and 50 m inland from the river, located at (1) just upstream of the Kibos bridge, (2) just downstream of the Kibos bridge, (3) in-between the Kibos and Nyamasaria bridge, (4) just upstream of the Nyamasaria bridge and (5) just downstream of the Nyamasaria bridge (Figure 3.2). The upstream reach at Nyamasaria was supported by a grade control weir, and is about 8 km downstream of the Kibos bridge section, which on the other hand is stabilised by side bank gabbions. All of the sections experience sand mining activities, except the third one in between the bridges.

The criterion adopted a system based on 10 parameters which scored on a scale of 0-10 points each for every section. Summation of the scores for all parameters gave the final score for every section. To minimise the biases (professional or cultural preferences in the scores), three people with different backgrounds, a local primary school teacher, a biologist technician and the author, were used to collect the data, after discussions and agreement on how to value the various parameters. The scores were based on the parameter attribution explained in Table A4.1, and then the environmental values were scored independently before they were averaged as given in Table A4.2. The bar chart in Figure A4.1 was hence derived from Table A4.2.



**Table A4.1 Attribution criteria for ecological valuation along River Kibos**

1, Diversity -	Habitats, plants and animals counted, irrespective of their names. The higher the number, the higher the score.
2, Resilience	Ability and speed of regeneration of the vegetation, and multiplication of animals, on the flood plain and in the river, after the dry season.
3, Soil fertility	Vegetation health , cover intensity and soil drainage characteristics favouring agriculture, scored higher.
4, Flood prone	In this case, reaches vulnerable to flooding and water-logging conditions scored less.
5, Land use	Area with higher diversity of usage, agriculture, livestock, settlement, commercial, etc. scored higher.
6, Sand supply	Sand with good mechanical properties, higher demand by contractors and easier to mine meant higher quality.
7, Stability	White wooden blocks on bed were used to measure ease to erode. More landslide marks also implied instability, and scored less.
8, Turbidity	Lowering a reddish wood in water and noting the depth at which its visibility disappeared. Smaller depth meant higher turbidity and therefore low score.
9, Depth of flow	The deeper the flow, the higher the value because it means more room for the aquatic life and recharge capability.
10, Access	Depth, slope and stability of the channel bank indicated how easy it was for locals and their livestock to make use of the river. Easier access scored higher.

---

In the context of the study program, it was found convenient to apply the improvised technique with the assumption that the other underrepresented groups - the microscopic water and soil living communities, river and soil biology and chemistry characteristics, which require high precision and resolution instrumentation - were reflected in the macro-ecological valuation, arguing that requirements by both groups are based on the same environmental qualities.

**Table A4.2 Ecological valuation of 5 locations on a reach along the River Kibos, based on 10 parameters**

PARAMETER	SCORES AT THE FIVE SECTION REACHES				
	Sec.1	Sec.2	Sec.3	Sec.4	Sec.5
Diversity	4	1	5	10	4
Resilience	4	2	6	10	4
Soil fertility	5	4	6	7	6
Flood prone	10	10	9	5	3
Land use	4	2	7	8	5
Sand supply	8	2	2	5	8
Stability	3	2	5	10	4
Turbidity	5	4	5	5	4
Flow depth	4	2	5	8	6
Access	3	1	5	8	5
TOTAL	50	30	55	76	51

Long-term stability, diversity, regeneration, etc., which require long periods of monitoring through a series of regular observations and measurements, or satellite imageries and aerial photograph interpretations, were also assumed to be reflected in the short-term data. It is also noted that since the values were not meant for an absolute ecological scale, but for relative comparisons with certain requirements and preferences, their applications will not be distorted so long as they are limited to the particular purposes and area.



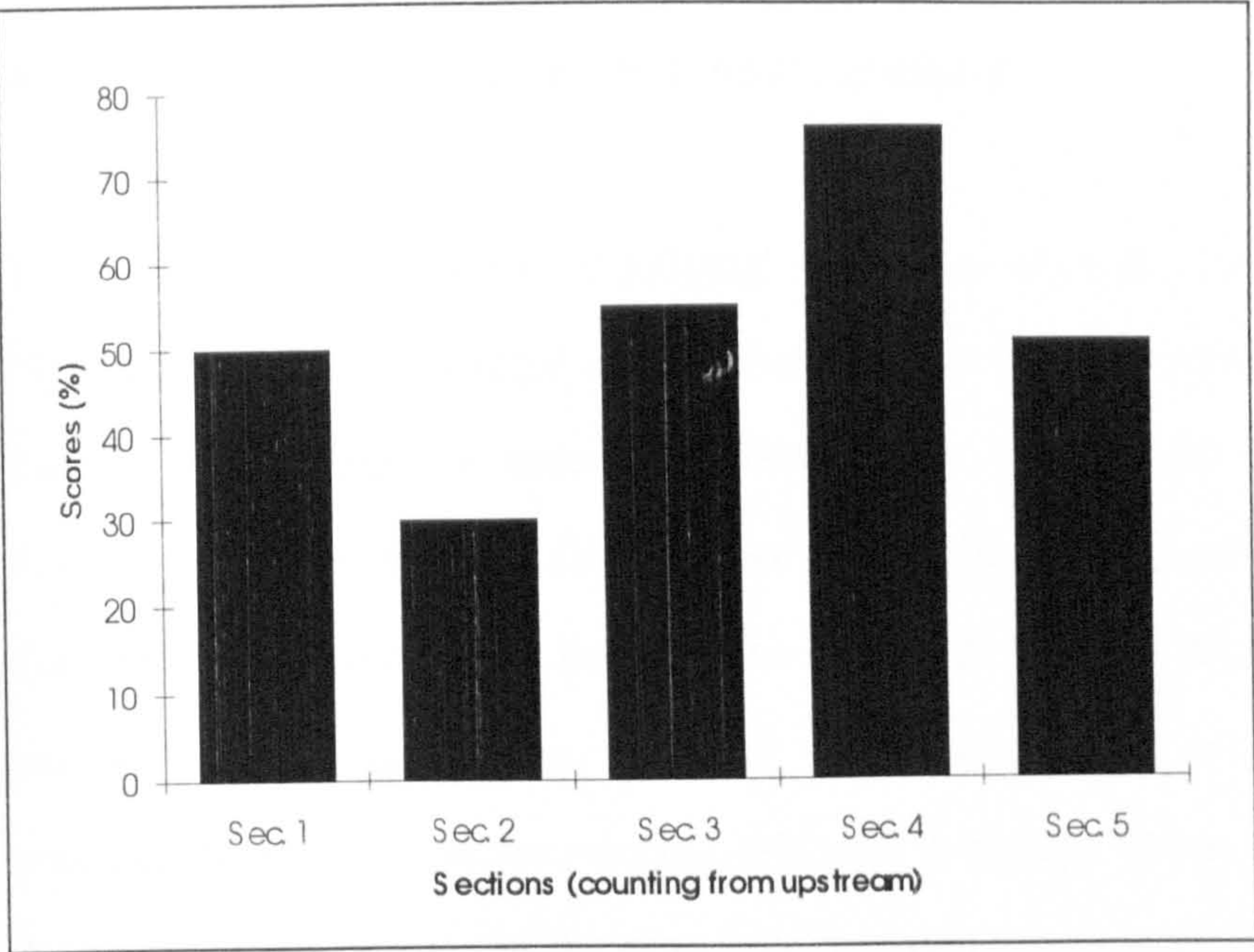


**Fig. A4.1 Relative ecological valuation for five section reaches on the River Kibos.**

Regarding the associated ecological values of the region, as summarised in the attribution list above, the section upstream of the Nyamasaria bridge, section 4, had the best ecological score, 76 %, while the section below the Kibos bridge, section 2, had the least value, scoring 30 %. This is in line with the picture portrayed by the rating curve analysis and photographs (Figs 3.3a and 3.6a). From observation of the results, and with the understanding of the dependence of ecosystems on water table or flood levels and/or frequencies, ( e.g. Hughes, 1984; Pinay and Decamps, 1988; Novak, 1991), a general conceptual ecological model for long term management programmes on particular river systems can be inferred based on the interrelationships between preferred ecological scores and the flooding levels within the reach (or flood prone score). The proposed conceptual model can be useful on river stretches requiring assessment or monitoring programmes to determine the sections that need conservation developments, or need monitoring to indicate trends in the river's ecological richness.



## A4.2 Generalisation of the valuation method

This concept is based on land judging techniques used for land capability mapping (Stalling, 1957) and on some environmental classification method by Jeavons (1994). Taking, for example, the case of the Kibos River stretch, least values were attributed to conditions most prone to flooding because of the destruction and disease outbreaks that are associated with the floods. The effects of flooding are devastating to human health, livestock, agriculture, and even to the aquatic life in that the quality of the water in the river is polluted during this period of high flows. Only at certain flood discharge levels below the flooding level is when the river is devoid of the pollutants from the over-bank flows, and "irrigates" the flood plain such that the conditions are optimal for human health, bank vegetation, bank stability, agriculture, water purification and other ecological potentials. As the flood levels are lowered further, the soil moisture is deplete from the flood plains such that the land is degraded to arid-looking conditions. From this kind of valuation, say for very many section reaches, a plot of the average ecological values against certain flood flow levels (say, 0, 2, 4, 6,... 20 m), is hypothesised to be distributed according to the graph in Figure A4.1. And Figure A4.2 is the conceptual distribution of the ecological values plotted against the full range of the flood flow levels, derived form Figure A4.1

This concept assumes the ecological attribution similar to the ones described for the Kibos river in Table 3.3, so that only those sections with flood flow levels 3-6 m below the flooding level have high environmental values( of more than 70 %). As the depth to the flood flow levels are reduced to zero (water-logging), and then to negative (flooding), the ecological values continue falling towards a minimum. And, on the other hand, as the depth to the flood flow levels are increased beyond 4 m, limiting the bank storage or groundwater reserves in the reach, the ecological value of the reach also starts falling towards a minimum.

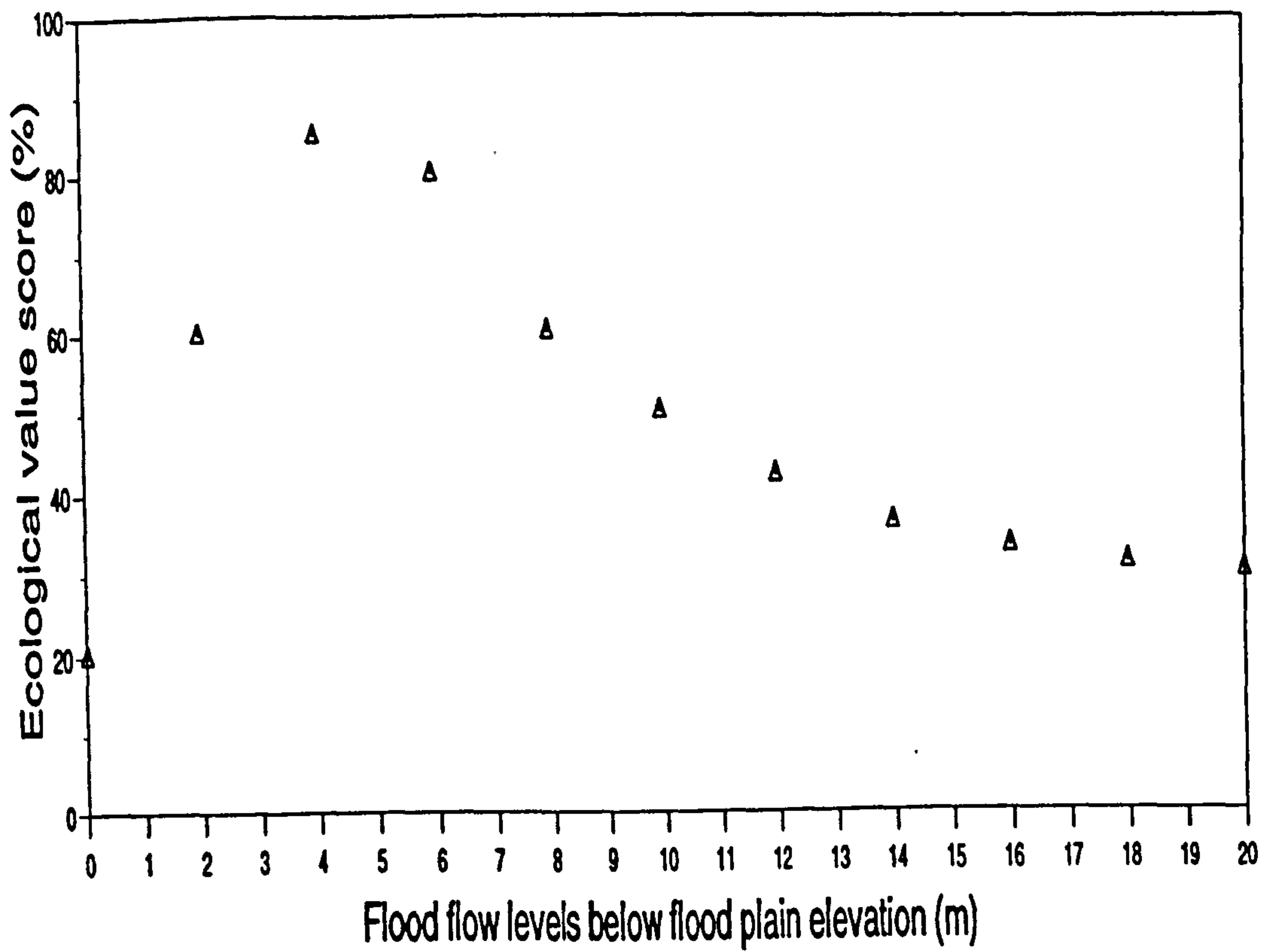


Fig. A4.2 Conceptual ecological values of various flood flow levels

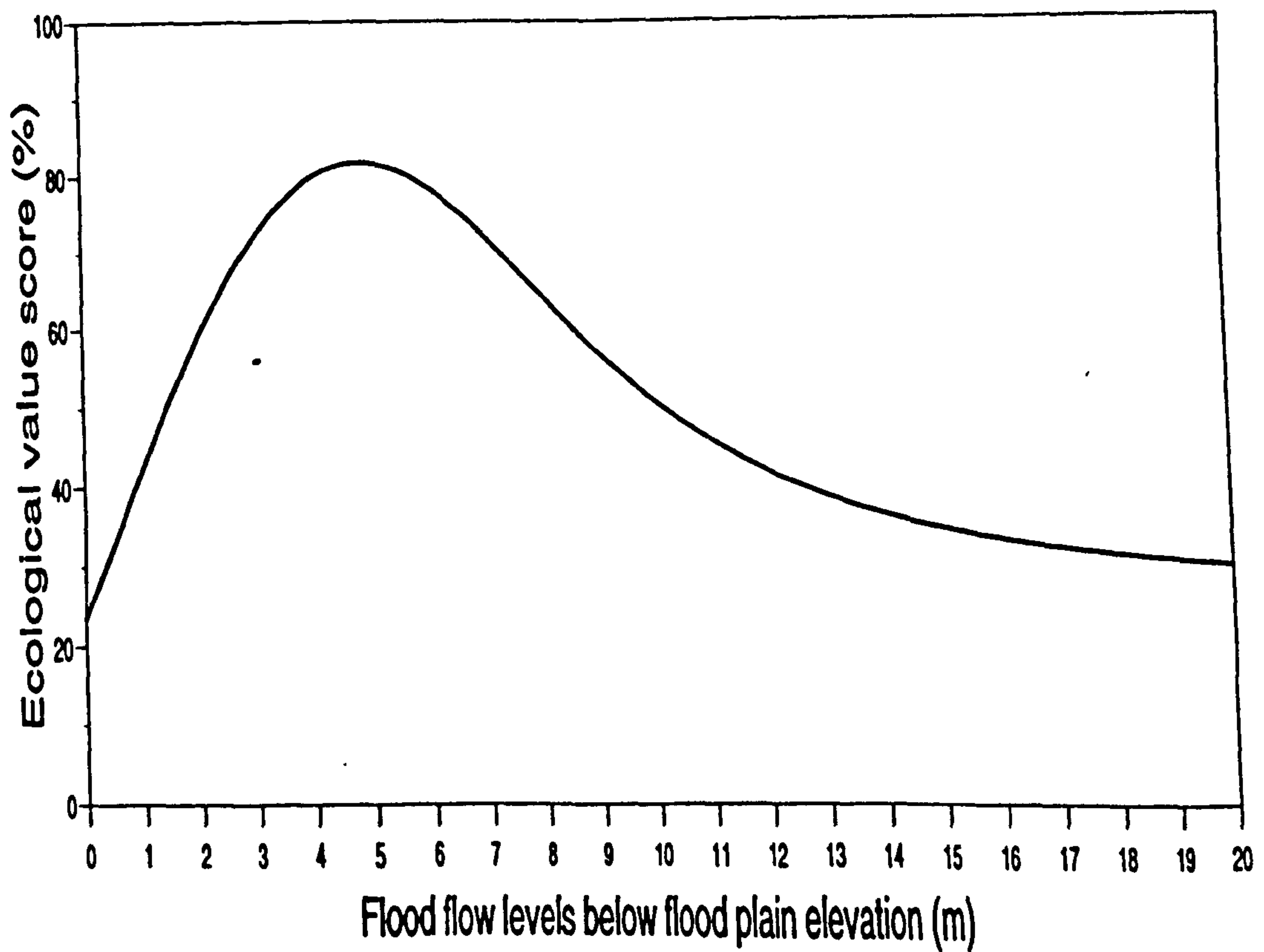


Fig. A4.3 A conceptual distribution of ecological values against the average river stage levels, derived from Fig. 3.16a

It is emphasised that the index for the ecological valuation is relative, depending on different ecosystems-systems, geographical and social-economical preferences, and the personnel and instrumentation available for the valuation computations. It is also possible for the distribution (Figure A4.3) to be normally distributed, or skewed to either side depending on the preferences. For example, whereas Pinay and Decamps (1986) talked of the importance of flooding and water logging conditions for riparian vegetation and de-nitrification processes, Hughes (1984) advocated only seasonal flooding and silt deposition to maintain plain forest regeneration to combat desertification and conserve wildlife primates, while the author, based on the Kibos example, has preferred moderate depth above the flood flow levels (without any flooding) as being the optimal conditions for ecological and human settlement. From the ecological valuation concept (Figure A4.3), different section reaches can then be ecologically placed, by measuring their flood flow levels (or frequency of flooding) and locating them on the x-axis, and then using the score curve to locate the corresponding ecological values on the y-axis. In this way, the whole flood plain can be classified into low, medium and high potential ecological zones. Optimal flow levels are those that result higher ecological values (e.g. 3 - 4 m below the flood plain elevation of the conceptual distribution in Figure A4.3.) Evaluation of specific ecological units (bird species, fish populations, forest regeneration, etc.) can be similarly analysed, in this case by making the species population or health as the y-axis. In this illustration, flood flow levels ( or frequencies or water table) have been selected as the index for valuing ecological potentials because it can be axiomatically stated that water levels are directly affected by sand mining, and river ecosystems, on the other hand are dependant on the water levels.

After deriving the graphical conceptual model, Figure A4.3, it is possible to apply it for detection of sections that are most ecologically sensitive to changes that are bound to alter river levels. These are those sections with flood flow levels at positions on the x-axis corresponding with sections of the curve with highest gradient



slope, for example sections of flood levels between zero and 2 m. What this suggests is that the concept can be applied to indicate section reaches that need urgent conservation measures, or section reaches that are bound to benefit most per unit cost of development, because of their high rate of change with flood flow level variation. For example, the derived conceptual model in Figure A4.3, demonstrates that on this particular stretch, a section of flood flow level of 2 m below flooding level will degenerate in value from about 60% to 40% due to in-stream filling by 1 m, while a section of flood flow level of 7 m will lose the same amount in value after scouring through a depth of up to 2 m

Another possible application of the concept is for monitoring ecological trends. Changes in silt deposition, industrial outflows, upstream land use, etc. may affect the ecological potential of a river system without necessarily showing visible changes in the streamflow hydrographs, water table or channel landscapes levels. Regular ecological valuation, basing on the same scoring index, and then comparison of the temporal valuation curves can detect trends of land deterioration (falling curve), implying need for improvements, or trends in land enrichment (rising curve), implying success of soil and water conservation measures.

Based on the above concept, therefore, sectional flood levels of particular river ecosystems-systems can be used to classify or identify reaches needing conservation attention. Optimal flood levels can also be derived from the same idea so that hydraulic or other control measures can be applied to acquire/maintain ecologically sound flood flow levels. Similarly, the same concept can be applied as a measure to monitor the successes or failures of conservation/development projects. The simplicity of this conceptual model makes it adaptable not only for river sand mining, but also for other various river development schemes, especially those that may affect streamflow levels.

## **A5. AN EXAMPLE OF THE COMPUTER PROGRAM FOR THE MASAI**

This is a simple computer program designed to demonstrate the modelling approach of the MASAI (Model for Alluvial Stream-Aquifer Interaction), to simulate water routing, sediment routing, scour and fill (aggradation and degradation) in channels, and bank storage or stream-aquifer water exchange for an alluvial river system. This is achieved by modelling the interaction between sediment laden steamflows, sediment material forming the river bed and the hydraulics of channel and groundwater flows for a given time period. This example is based on the Nyando River channel reach described in chapter 5.

The source code of the main program is FORTRAN 77, and has been devided into files for a modular approach. The executable program, in DOS, is the 'masai' file; and the data input (supporting) files are:

- (i) CHANEL.DAT, which describes the initial conditions in the channel. It is arranged in seven columns of bed elevation, discharge, flow depth, Manning's  $n$ , lateral inflow per unit width, width of the channel section, and distance between the sections (from left to right), respectively.

And the rows designate the sections, running from upstream to downstream.

- (ii) WTABLE.DAT file gives the initial water levels in the river and the surrounding groundwater. In this example the river levels are in the seventh row, with six

parallel rows of water table levels running on both sides. The streamflow is from left to right. The last row gives the depth of flow in the river.

(iii) SEDIM.DAT file gives the sediment size distribution in five classes. The first column gives the mean diameter of each class; the second gives the percentages of the classes in the mixing zone on the riverbed; and the third column gives the percentages of the sediments already in the flow.

(iv) HYDRO.DAT provides the discharge of the upstream input hydrograph, (at the selected time interval). The discharge values are read in rows from left to right, before moving to the next row.

This computer program (compiled on the Unix-Sun machine) can be run on the main frame computers, or on PC having math chips (such as IBM - PCs). After copying the executable and supporting files onto the hard disk of the computer, all one needs to do to run the model is to **type and enter** the command "**masai**", then everything else follows.

The program generates and displays the water table elevations at every time step, and produces an output file OUTFILE.DAT, for the simulated flow conditions in the river, which **MUST BE DELETED** from the computer memory before the program can be re-run.

The MASAI program is on a floppy disk attached herein.



## REFERENCES

- Abbott, M. B., Bathurst, J. C., Cunge, J. A., O'Connell, P. E., and Rasmussen, J., "An introduction to the European Hydrological System - System Hydrologique Europeen, "SHE", 2: structure of a physically-based, distributed modelling system", J. Hydrol., (87), 1986, pp. 61 - 77.
- Abbot, M. B., "Contributions of Computational Hydraulics to the Foundation of a Computational Hydrology", in Bowles, D. S., and O'Connell, P. E., (eds.), *Recent Advances in the Modeling of Hydrologic Systems*, Kluwer Academic Publishers, London, 1991, pp. 509 - 537.
- Ackers, P. and White, W. R., "Sediment Transport: New Approach and analysis", J. of Hydraulic Div., ASCE, Vol. 99, No. HY11, 1973, pp. 2041 - 2060.
- Alam M. Z. and Kennedy J. F. "Friction factors for flow in sand-bed channels". J. of Hydraulic Division, ASCE, vol. 95 No. HY6, 1969, pp. 1973 - 1993.
- Amein, M. and Fang, S. C. "Implicit flood routing in natural channels." J. of Hydraulic Div., ASCE vol. 96, No. HY12, 1970, pp. 2481 -2501.
- Amein, M. and Chu, H. L. "Implicit numerical modelling of unsteady flows." J. of Hydraulic Div., ASCE vol. 101, No. HY6, 1975, pp 717 -731.
- Bathurst, J. C, "Sensitivity analysis of the Systeme Hydrologique European (SHE) for an upland catchment", J. Hydrol., (87), 1986, pp. 103 -123.
- Bathurst, J. C. and Wicks, J. M. "Framework for Erosion and sediment Yield Modelling" in Bowles, D. S. and O'Connell, P. E. (eds.) *Recent Advances in the Modelling of Hydrologic Systems*, Kluwer Academic Publishers, Dordrecht, 1991, pp. 1 -27..
- Bayazit, N., "Simulation of armour coat formation and destruction", Proc. XVIth. IAHR congress, Sao Paulo, Brazil, 1975, pp. 73-78.
- BBC - Horizon, *After the Floods*, Text adapted from the programme transmitted 18 April 1994, London.
- Bear, J and C Verruijt " *Modelling Ground Water Flow and Pollution*", D Reidel Publishing Company, Dordrecht, 1987.
- Bear, J., *Dynamics of Fluid in Porous Media*, Dover Publications, New York, 1988.

- Bettes, R., "Sediment Transport and Channel Stability", in Calow, P. and Petts, G. E. (eds.), *The Rivers Handbook - Volume 2*, Blackwell Scientific Publications, Oxford, 1994, pp. 227 - 254.
- Beven, K. and O'Connell, P. E. *On the role of physically-based distributed modelling in hydrology*, Institute of Hydrology, Wallingford, Oxford, Rep. No. 81, 1982.
- Borah, D. K.; Alonso, C. V.; and Prasad, S. N. "Routing Grades Sediment in Streams: Formulations" *J. of Hydraulic Div., ASCE* Vol. 108, No. HY12, 1982, pp. 1486 -1503.
- Brookes, A., *Channelised Rivers - Perspective for Environmental Management*, John Wiley and sons, Chichester, 1988.
- Brookes. A., "River Channel Changes", in Calow, P., and Petts, G. E., (eds.), *The Rivers Handbook - Volume 2*, Blackwell Scientific Publications, Oxford, 1994, pp. 55 - 75.
- Calow, P. and Petts, G. E., *The Rivers Handbook - Volume 2*, Blackwell Scientific Publications, Oxford, 1994.
- Chang, F. F. and Richards, D. L. "Deposition of Sediment in transient Flow", *J. of Hydraulic Div., ASCE*. vol. 97, No. HY6, 1971, pp 837 -849.
- Chang, H. H. and Hill, J. C., "Minimum stream power for rivers and deltas." *J. of Hydraulic Div., ASCE* vol. 103, No. HY12, 1977, pp. 1375 -1389
- Chang, H. H. "Mathematical Model for Erodible Channels," *J. of Hydraulic Div., ASCE* Vol. 108, No. HY5, 1982, pp. 678 -689.
- Chang, H. H.; *"Fluvial Processes in River Engineering,"* John Wiley and Sons, New York, 1988a.
- Chang, H. H., "Simulation of river channel changes induced by sand mining." *Intern. Conf. of Fluvial Hydraulics, IAHR, Budapest, Hungary, 1988b*, pp 316 -320..
- Chang, H. H. "Hydraulic design of erodible-bed channels", *J. of Hydraulic Div., ASCE* vol. 116, No. HY1, 1990, pp. 87 -101.
- Chen, Y. H., *Mathematical modelling of water and sediment routing in natural channels*. Ph.D. Thesis, Civil Engineering Dept, Colorado State University, USA., 1973.
- Chen Y. H; Lopez J. L; and Richardson E. V; "Mathematical Modelling of Sediment Deposition in Reservoirs." *J. of Hydraulic Div., ASCE* Vol. 104, No. HY12, 1978, pp. 1605 -1616.

- Chen Y. H; " Water and Sediment Routing in Rivers." in Shen H. W. (ed.), *Modelling of Rivers*, John Wiley and Sons, New York, 1979, pp. 10-1 - 10-97
- Chow, Ven Te, *Open Channel Hydraulics* McGraw-Hill Book Co., New York, 1959.
- Chow, Ven Te, *Handbook of Applied Hydrology*, McGraw-Hill Book Co., New York, 1964.
- Chow, V. T., Maidment, D. R., Mays, L. W., *Applied Hydrology*, McGraw - Hill Book Company, New York, 1988.
- Crane, F. G; *The Effect of Stream flow Variability on Channel Morphology*. Ph.D. Thesis, Civil Engineering Dept. University of Newcastle Upon Tyne, UK. 1980.
- Cunge, J. A., "Feasibility of mathematical modeling of meanders", in River Meandering, *Proceedings of the Conference Rivers '83*, American Society of Civil Engineers, New York, 1983 pp. 794-809.
- Cunningham, A. B., *Modelling and Analysis of Hydraulic Interchange of Surface and Groundwater*. PhD. Dissertation, University of Nevada, Reno, Nev. 1977.
- Cunningham A. B. and Sinclair P.J. "Application and Analysis of a Coupled Surface and Ground water Model." *J. Hydrol*, (43), 1979, pp. 129-148.
- Delie, A., *An outline of flood control measures on Nyando River Basin*, Ministry of Water Development - Irrigation Section, Kenya, 1985.
- Dillon, P. J., " Stream-Aquifer Interaction Models: A review", *Civil Engineering Trans. of Australia*, Vol., 25, 1983, pp -107 -113.
- Dillon, P.J. and Liggett, J. A. "An Ephemeral Stream-Aquifer Interaction Model." *Water Resources Res.*, Vol. 19, No.3, 1983, pp 621 -626.
- Fread, D. L., "Discussion of Implicit Flood Routing in Natural Channels" by Amcin, M and Fang, C. S.", *J. of Hydraulic Div., ASCE*, Vol. 97, No. HY7, 1971, pp. 1156 - 1159.
- Freeze, R. A. and Cherry, J. A. *Groundwater*, Printice-Hall, Inc., Englewood Cliff, N. J, 1979.
- French, R. H., *Open-Channel Hydraulics*, McGraw - Hill Book Company, New York, 1986.
- Gambolati, G. and Galeat, G; "Analysis of Hydrologic Impact of Quarrying System by 3-D Finite Element Model." *J. of Hydraulic Div., ASCE* Vol. 116, No. HY11, 1990, pp. 1388 -1402.



- Garbrecht, G. Hydrologic & hydraulic concepts in antiquity, in Garbrecht, G.(Ed) *Hydraulics and hydraulic Research- A Historical Review.*, IAHR, Jubilee vol., A. A. Balkema, Rotterdam, 1985.
- Genesis, in The Holly Bible, New King James Version, Thomas Nelson Inc., 1982
- Gessler, J., "Aggradation and degradation", in Shen, H. W., (ed.), *River Mechanics*, vol.1, Colorado State University, Ft. Collins, 1971, pp. 8-1 - 8-24.
- Grainger, A., *The Threatening Desert: Controlling Desertification*, Earthscan Publications Ltd., London, 1990.
- Garde, R. J., and Ranga Raju, K.G., *Mechanics of Sediment Transport and Alluvial Stream Problems*, Wiley and Eastern Ltd., New Delhi, 1985.
- Goldman, S. J; Jackson, K; and Bursztynsky, T. A; *Erosion and Sedimentation Control Handbook*. McGraw-Hill Book Co., New York, 1986.
- Gregory, K. J., *River Channel Changes*, John Wiley and sons, Chichester, 1976.
- Hack, J. T. "Studies of Longitudinal Stream Profiles in Virginia and Maryland." USGS Professional Paper 294-B, 1957.
- Hantush, M. S., "Hydraulics of Wells", in Ven Te Chow (ed.), *Advances in Hydrscience*, Vol. 1, Academic Press, New York, NY, 1964.
- Hey, R. D.; "Mathematical Models of Channel Morphology." in Anderson, M. G; (ed.) *Modelling Geomorphological Systems*, John Wiley and Sons, New York, 1988, pp. 99 - 126.
- Hofkes, E. H; (ed.) *Small Community Water Supply - Technology of Small Water Supply Systems in Developing Countries.*" IRC for community Water supply and sanitation, Netherlands, 1983.
- HEC-6, US. Army Corps of Engineers, *Scour and Deposition in Rivers and Reservoirs - Users Manual*. California, 1977.
- Hughes, F. M. R. "A comment on the impact of development schemes on the flood plain forest of the Tana River of Kenya", *The Geographical Journal*, vol. 150 no. 2 1984, pp. 230 -244.
- Hyrni H; "Applied Soil Conservation Research in Ethiopia." in Thomas D. B; Biamah E. K; Kilewe, A. M.; Lundgren, L. L .; Mochoge, B. O; (eds.), *Soil and Water Conservation in Kenya, Proc. of the National Workshop'*, Kabete Campus, Nairobi, 1986.
- Huisman, L. and Oslthoorn, T. R. *Artificial Groundwater Recharge*, Pitman Advanced Pub. Program, Boston, 1982.

- Italconsult, "Pre-Investment Study for Water Management and Development of the Nyando and Nzoia river Basins for MOWD of Kenya", Rome, 1983.
- Jeremiah, in The Holly Bible, New King James Version, Thomas Nelson Inc., 1982
- Kadiro, D., and Santoso, T., *Warujayeng - Kertosono Canal Survey*, Wallingford Hydraulic Research Station, Report Number OD 42, 1982.
- Karim, M. F., and J. F. Kennedy, IALLUVIAL: A computer-based flow-and sediment-routing model for alluvial streams and its application to the Missouri River, *IIHR Rep. 250*, Ia. Inst. of Hydraul. Res., Iowa City, 1982.
- Kirkby, M. J. "Maximum Sediment Efficiency as a Criterion for Alluvial Channels", in Gregory, K. J. (ed.) *River Channel Changes*, John Wiley and Sons, New York, 1980.
- Lane, E. W. "The Importance of Fluvial Geomorphology in Hydraulic Engineering," *J. of Hydraulic Div., ASCE Vol. 81*, Paper 745, 1955.
- Large, A. R. G. and Petts, G. E., "Rehabilitation of River Margins" in Calow, P. and Petts, G. E., (eds.), *The Rivers Handbook - Volume 2*, Blackwell Scientific Publications, Oxford, 1994, pp401 - 418.
- Lee. H. Y. and Odgaard, J. A "Simulation of Bed Armouring in alluvial channels". *J of Hydraulic Div. ASCE. Vol. 112*, no. HY9, 1986, pp .794 - 801.
- Leopold, L. B. and Maddock, T. Jr., "The Hydraulic Geometry of Stream Channels and Physiographic Implications", USGS, Professional Paper 252, 1953.
- Linsley, R. K. and Franzini, J. B., *Water Resources Engineering*, McGraw-Hill, Inc., Stanford, California, 1979.
- Lopes V. L. and L. J. Lane, "Modelling sedimentation processes in small watersheds." *IAHS Publ. No. 174*, Agric. Research Service, USA., 1988, pp. 497 -508.
- Lovera F. and Kennedy J. F. "Friction-factors for flat-bed flows in Sand Channels." *J. of Hydraulic Division, ASCE, Vol. 95 No. HY4*, 1969, pp. 1227 -1234.
- Lu, J. Y., *Mathematical Models for Bed Armouring Channel Degradation and Aggradation*, PhD. Thesis, Colorado State University, Fort Collins, CO, 1984.
- Mackenzie, "Will tomorrow's children starve?" in *New Scientist of the 3rd September 1994*, London, pp 24 - 29.
- Matlock, W. G., *The Effect of Silt-Laden Water on Infiltration in alluvial Channels*. PhD. Thesis, University of Arizona, 1965.

- Medina, J; "Harvesting Surface Runoff and Ephemeral Stream flow in Arid Zones." in *Conservation in Arid and Semi-Arid Zones*, FAO Conservation Guide 3, FAO, Rome, Italy, 1976.
- Nilson, A., *Groundwater dams for rural water supply in developing countries*, Royal Institute of Technology, Meddelande Trita-Kut 1034, Stockholm. 1983.
- Novak, P; Moffat A. I., B; Nalluri, C; and Narayananan, R; "*Hydraulic Structures*." Unwin Hyman, London, 1990.
- Novak, P., (ed.) *Hydraulics and the Environment*, IAHR Extra issue, vol. 29, 1991.
- Pearce, F., "Dam Truths on the Danube" in *New Scientist of the 17th September 1994*, London, pp 27 - 31.
- O'Connell, P. E., "A Historical Perspective", in Bowles, D. S., and O'Connell, P. E., (eds.), *Recent Advances in the Modeling of Hydrologic Systems*, Kluwer Academic Publishers, London, 1991, pp. 3 - 30.
- Parker, G., P.C. Klingeman, and D. L. McLeon, Bedload and size distribution in paved gravel bed streams, *J. Hydraul. Eng.*, 108(HY4), 1982, pp. 544-571.
- Petersen, M. S., "Water for Africa: The human dimension", in Stephenson, D. (ed.) *Water the lifeblood of Africa*, Proceedings, IAHR (ARD), Victoria Falls, Zimbabwe, 1993, pp. 1-1 - 1-31.
- Petts, G., and Foster, I., *Rivers and Landscape*, Edward Arnold, London, 1992.
- Pickup, G; "Hydrology and Sediment Models." in Anderson, A. G; (ed.) *Modelling Geomorphological Systems*, John Wiley and Sons, New York, 1988.
- Pinay, G. and Decamps, H., "The role of riparian woods in regulating Nitrogen fluxes between the alluvial aquifer and surface water: A conceptual model", *Regulated Rivers: Research and management*, Vol. 2, 1988, pp. 507 - 516.
- Pinder, G. F. and Sauer, S. P., "Numerical Simulation of Flood Wave Modification due to bank storage effects". *Water Resour. Res.*, 7(1), 1971, pp. 63 - 70.
- Pogge, E. C., and Chiang, W. L. *Further development and testing stream-aquifer system model*. Kansas Water Resources Research Institute Contribution no. 185. Lawrence, Kansas. 1977.
- Price, R. K., "Comparison of four numerical methods for flood routing." *J. of Hydraulic Div.*, ASCE vol. 100, No. HY7, 1974.
- Pricket, T. A. and Lonquist, C. G. A., *Selected digital computer techniques for groundwater resources evaluation*. Illinois State Water Survey, Bulletin No. 65, Champaign, Illinois, 1981.



- Psalms, in The Holly Bible, New King James Version, Thomas Nelson Inc., 1982
- Quinn, F. H. and Wylie, E. B. "Transient analysis of the Detroit river by the implicit method." *Water Resources Res.*, vol. 8 No. 6, 1972. pp. 1461 - 1469.
- Rahuel, J. L; Holly, F. M; Chollet, J. P; Bellendy, P. J.; and Yang, G; "Modelling of Riverbed Evolution for Bed load Sediment Mixtures." *J. of Hydraulic Div.*, ASCE vol. 115, No. HY11, 1989, pp. 1521 - 1541.
- Rasmussen, J. L., "Management of the Upper Mississippi: A Case History", in Calow, P., and Petts, G. E., (eds.), *The Rivers Handbook - Volume 2*, Blackwell Scientific Publications, Oxford, 1994, pp. 441 -463.
- Richards, K., *Rivers - Form and Process in Alluvial Channels*. Methuen and Company Ltd., London, 1982.
- Ritchie, J. C., Cooper, C. M. and McHenry, J. R., " Sediment accumulation rates in lakes and reservoirs in the Mississippi River Valley", in Wang, S. Y., Shen, H. W., and Ding, L. Z., *River Sedimentation*, Vol. III, Proc. of the Third International Symposium on River Sedimentation, 1986, pp. 1357 - 1368.
- Rovey, C. E. K *Numerical model of flow in a stream-aquifer system*, Colorado State University Hydrology Paper 74. Fort Collins, Colorado, 1975
- Rushton, K. R. and Redshaw S. C., *Seepage and Groundwater Flow*, John Wiley and Sons, Chichester, 1979.
- Schumm, S. A; "The Shape of Alluvial Channels in Relation to Sediment Type", USGS Professional Paper 352-B, 1960.
- Schumm, S. A. "River Adjustment to Altered Hydrologic Regimen-Murrumbidgee River and Paleo channels, Australia," USGS Professional Paper 598, 1968.
- Schumm, S. A; "Fluvial Geomorphology: Historical Perspective." in Shen, H. W; (ed.) *River Mechanics* Vol. 1, Colorado US., 1969.
- Sharp, J. M. Jr., "Limitations of Bank-Storage Model assumptions", *J. of Hydrol.* (35) 1977, pp. 31 -47.
- Simons D. B; "Rivers and canal Morphology." in Shen H. W. (ed.) *Modelling of Rivers*, John Wiley and Sons, New York, 1979, pp. 5-1 - 5-81.
- Singh, K. P., "Some factors affecting baseflow", *Water Resources Res.* Vol. 4, No. 5, 1968, pp. 985 -999.
- Sir, Alexander Gibbs and Partners, *Kenya Nile Water Resources Study*, Ministry of Water, Nairobi, Kenya. 1963.

- Stallings, J. H. *Soil Conservation*, Prentice-Hall, Inc., Englewood Cliffs, N. J 1957
- Storm, B., "Modeling of Saturated Flow and the Coupling of Surface and Subsurface Flow", in Bowles, D. S., and O'Connell, P. E., (eds.), *Recent Advances in the Modeling of Hydrologic Systems*, Kluwer Academic Publishers, London, 1991.
- Strelkoff, T., "The one-dimensional Equation of Open Channel Flow", J. of Hydraulic Div., ASCE, Vol. 95, No. HY3, 1969. pp. 861 - 876.
- Strelkoff, T., "Numerical solution of St. Venant equations." J. of Hydraulic Div., ASCE vol. 96, No. HY1, 1970, pp. 223 -251..
- TAMS Engineers and Architects, *National Master Water Plan Stage I, vol. II, Natural Resources and Potential Projects*, Ministry of Water, Nairobi, Kenya, 1980.
- The Nation Team, "Floods Hit Kano Plains Yet Again", in *The Daily Nation* of the 27th April 1994, Nairobi, pp 2.
- Todd, D. K., "Groundwater flow in relation to a flooding stream", ASCE, Proc. Vol. 81, 1955, pp. 628-1 - 628-20.
- Todini, E, and Bossi, A., "PAB (Parabolic and Backwater) an unconditional stable flood routing scheme particularly suitable for real-time forecasting and control", J of hydraulic Research, Vol. 24, No. 5, 1987.
- Todini, E., "Hydraulic and Hydrologic Flood Routing Schemes", in Bowles, D. S., and O'Connell, P. E., (eds.), *Recent Advances in the Modeling of Hydrologic Systems*, Kluwer Academic Publishers, London, 1991, pp. 389 - 406.
- Troeh, F. R.; Hobbs, J. A; and Donahue, R. L; *Soil and Water Conservation for Productivity and Environmental Protection*. Prentice-Hall, Inc., New Jersey 07632., 1980.
- Vanoni, V. A., "Modeling Alluvial Channels", Water Resources Res., Volume 22, Number 9, 1986, pp 715 - 815.
- Walling, D. E." The sediment delivery problem", J. Hydrol. (65), 1983, pp. 209 -237.
- Walling, D. E, "The sediment yield of African rivers" in UK IAHR (Wallingford HRS Press), *Challenges in African Hydrology and Water Resources*, Proceedings of the Harare Symposium, IAHS Publ. no. 144, 1988, pp. 265 - 283.
- Wang, H. and Anderson M. P. *Introduction to Groundwater modelling: Finite difference and finite element methods*, W. H. Freeman, San Francisco, 1982.

- White, W. R., Bettess, R. and Paris E, "Analytical Approach to River Regime", J. of Hydraulic Div., ASCE vol. 108, No. HY10, 1982, pp. 1179 - 1193.
- Wilson, E. M., *Engineering Hydrology*, Macmillan Education Ltd., 1990.
- WLP Consultants, *Hydrology, Lake Basin River Catchment Development*, United Nations TCD Contract CON 5/83, LBDA, Kisumu, Kenya, 1983.
- Wooldridge, R., *Sedimentation in Reservoirs - Tana River Basin, Kenya*, Wallingford Hydraulic Research Station, Report Number OD 46, 1983.
- WMO (World Meteorological Organisation), *Manual on Stream Gauging - Volume II - Computation of Discharge*, WMO - No. 519, Geneva, 1980.
- Yalin, M. S., "Geometrical properties of sand waves", J. of Hydraulic Div. ASCE, vol. 90, No. HY5, 1964, pp. 105 - 119.
- Yang, C. T., "Incipient Motion and Sediment Transport", J. of Hydraulic Div. ASCE, vol. 99, No. HY10, 1973, pp. 1679 - 1704.
- Yang, C. T., "Minimum Unit stream Power and Fluvial Hydraulics," J. of Hydraulic Div., ASCE, vol. 102, No. HY7, 1976, pp. 919 - 934.
- Yang, C. T., and Song, C.C.S., "Theory of minimum Rate of Energy Dissipation", J. of Hydraulic Div., ASCE, vol. 105, No. HY7, 1979, pp. 769 - 784.
- Younger, P. L., *Stream-Aquifer Interaction - A review*, Department of Civil Engineering, University of Newcastle Upon Tyne, 1987.
- Younger, P. L., *Stream-Aquifer Systems of the Thames Basin: Hydrogeology, Geochemistry and modelling*, PhD Thesis, University of Newcastle Upon Tyne, 1990.
- Younger, P. L.; Mackay R., and Connorton, B. J. "Streambed sediment as a Barrier to Groundwater Pollution; Insights from Fieldwork and Modelling in the River Thames Basin". J. Inst. Wat. Envir. Magnet, vol. 7 no. 6, 1993 , pp. 576 -585.



CONTAINS DISKETTE

UNABLE TO COPY

CONTACT UNIVERSITY

IF YOU WISH TO SEE

THIS MATERIAL